

# Biogeography and biochemistry of bile acid 7-dehydroxylation in the mammalian gut

Présentée le 27 mai 2020

à la Faculté de l'environnement naturel, architectural et construit  
Laboratoire de microbiologie environnementale  
Programme doctoral en génie civil et environnement

pour l'obtention du grade de Docteur ès Sciences

par

**Solenne Anne Marie MARION**

Acceptée sur proposition du jury

Prof. S. Takahama, président du jury  
Prof. R. Bernier-Latmani, K. L. Meibom, directrices de thèse  
Prof. S. Hapfelmeier, rapporteur  
Prof. W.-D. Hardt, rapporteur  
Prof. K. Schoonjans, rapporteuse

# Acknowledgements

This work would not have been possible without the support of many people. First and foremost, I would like to thank my supervisor Rizlan Bernier-Latmani for her guidance and encouragements throughout these 4 years and a half of PhD. She has always been motivated and enthusiastic about the project and has always welcomed and supported my ideas. The skills that I learned during my PhD in her laboratory go well beyond technical proficiencies. I also would like to thank my co-advisor Karin Meibom for her guidance and support, especially for the molecular biology part of the thesis.

Secondly, I would like to thank the members of my committee Kristina Schoonjans, Wolf-Dietrich Hardt, Siegfried Hapfelmeier, and Satoshi Takahama, for their interest in my work and for accepting to review my doctoral dissertation.

I would like to thank all my great colleagues from the Environmental Microbiology Laboratory: Manon, Lyne, Conny, Leia, Mapi, Karin, Luca, Maria, Niels, Karen, Margaux, Zezhen, Ash, Barbora, Matthew Reeves, Edu, Emma, Aislinn, Gabrielle, Yuheng, Carla, Matthew Reid. Special thanks to Lyne for her endless support through the PhD. A lot of ideas and results interpretation were conceived together early morning over breakfast at Arcadie, during breaks under the sun and of course at Satellite! I am grateful for the good time we had together at EPFL and outside. I want to thank my two office mates Conny and Karen for our mutual support during tough times. Special thanks to my ski touring companions Manon, Leia and Meeko for all the great adventures together in altitude! I am also thankful to Matthew and Edu, my Sinergia colleagues, for their support and encouragement in the last year. Finally, I would like to thank Maria for her assistance with the administrative work throughout my time at EML.

I want to thank all my collaborators from the Sinergia Project for their inputs and help over the past few years. I also want to thank the team of the Mass Spectrometry Facility - Laure, Francisco and Daniel – for their support, as well as the PTPSP facility - Kelvin, Amédé, Florence and David - for their guidance and endless support, and for training me in protein purification techniques. It was always a pleasure to work with them at the facility.

I am very thankful for all the wonderful persons that I have met during this journey in Switzerland and that have become my friends. Special thanks to Conny, Dani, Åsa, Robert, Matt, Tomás, Lucía, Niels, Anh Chi, Hugo, Ximena, Manon, Leia, Lyne & Alex and to 'la grande famille des colocs' Fred, Vivi, Inti et Greg. Thank you for your support and for all the amazing time we had together. I also want to thank Pauline and Amélie for their encouragements through the years. Each time we saw each other for a weekend in Lyon or during our vacations in Portugal, Marseille, Paris, it has been real a boost of energy. I am forever grateful for our friendship and for having you by my side since childhood.

I am forever grateful for the support of my family – Papa, Maman, Pierre and Jeanne – for always believing in me and for being there when I needed to be conformed. Special thanks to my grandparents, my aunts and uncles, my cousins – David, Angélique, Laura, Grégoire, Baptiste, Samuel and the young ones Gabriel, Matthieu, Antoine and Lucie – for your endless support and encouragements.

Last but not least, I would like to thank Oscar for being an understanding and supportive partner. Your presence and encouragement have been invaluable to this thesis progression.



# Abstract

Bile acids (BAs) are small molecules synthesized by the host and chemically modified by the microorganisms inhabiting the intestinal tract. It is becoming increasingly apparent that, beyond their ancestral role in lipid digestion, bile acids play a crucial role as signaling molecules. They are metabolized by the gut microbiota and, through enterohepatic recirculation and spill-over into the systemic circulation, reach target metabolic organs and tissues and immune cells. The microbial transformation of BAs in the gut is critical to BA-mediated signaling as it modifies their amount and affinity for specific BA receptors. Bile acid 7-dehydroxylating bacteria are intestinal commensals of particular importance as they catalyze the dehydroxylation of liver-derived (primary) bile acids at the C7 position (i.e., 7-dehydroxylation) and produce secondary bile acids. One of the major receptors for secondary BAs is the G protein-coupled BA receptor 1 (GPBAR1), also known as Takeda G-protein receptor 5 (TGR5), and it is associated with regulation of energy expenditure and glucose management, protection from liver steatosis and inflammation. In addition, 7-dehydroxylated bile acids are also associated with protection from infection by specific intestinal pathogens (i.e., *Clostridioides difficile*). Thus, through their action on primary BAs, 7-dehydroxylating (7-DH-ing) bacteria play an important role in health promotion and in the functioning of major physiological processes in the body such as insulin secretion, thermogenesis and immune responses. On the other hand, excessive abundance of secondary BAs, possibly linked to overabundance of 7-DH-ing bacteria correlates with an increased risk of intestinal cancer and cholesterol gallstone disease. Despite these potentially important roles in the mammalian host, bile acid 7-dehydroxylating bacteria are poorly studied and much remains to be deciphered regarding their metabolism, diversity, abundance in the gut, and colonization dynamics in the host.

Here, we use *Clostridium scindens*, as model organism to study bile acid 7-dehydroxylation *in vitro* and in gnotobiotic mice. We found that *C. scindens* metabolize only human primary bile acids (CA and CDCA). We uncovered the formation of a novel intermediate during CA 7-dehydroxylation by *C. scindens in vitro*: 12-oxoLCA. *In vivo*, we amended *C. scindens* to gnotobiotic mice lacking bile acid 7-dehydroxylating activity. Using NanoSIMS and metabolomic analysis, we demonstrated that the large intestine constitutes *C. scindens* primary ecological niche and, represents the location where it efficiently performs bile acid 7-dehydroxylation in gnotobiotic mice.

Following up on the discovery of the 12-oxoLCA, we hypothesized the existence of another 7-dehydroxylation pathway for cholic acid. We postulated that it may involve the B and C rings of the steroid structure and may entail the oxidation/reduction of the C12-hydroxyl group. Thus, it was dubbed the putative vertical pathway. Conducting *in vitro* enzymatic assays with purified enzymes, we confirmed the existence of this novel vertical biosynthetic 7-dehydroxylation pathway for cholic acid, the most abundant primary bile acid in humans, and identified the core of enzymes necessary and sufficient for CA 7-dehydroxylation.

Furthermore, we used a coupled metabolomic and metaproteomic approach to probe *in vivo* activity of the gut microbial community in a gnotobiotic mouse model. Results revealed the involvement of *Clostridium scindens* in 7 $\alpha$ -dehydroxylation, of the genera *Muribaculum* and *Bacteroides* in deconjugation, and of six additional organisms in oxidation (the genera *Clostridium*, *Muribaculum*, *Bacteroides*, *Bifidobacterium*, *Acutalibacter* and *Akkermansia*). Additionally, we also considered the bile acid profile in mice with more complex microbiota or with no microbiota. By comparing the bile acid profile of the different mice models along with expression of key genes of bile acid synthesis, we emphasized the profound influence of the gut microbial community on BA pool homeostasis.



Altogether, our data provides a significant contribution to our collective understanding of the microbiology of bile acid 7-dehydroxylating bacteria, a group of gut commensals highly relevant to host health but that remains poorly characterized. The discovery of a novel 7-dehydroxylation pathway is a major scientific achievement of this thesis.

## Keywords

*Clostridium scindens*, bile acids, bile acid 7-dehydroxylation, deconjugation, metaproteomic, NanoSIMS, 12-oxoLCA, bile acid signaling, biogeography, bile salt hydrolases, bai operon, hydroxysteroid dehydrogenases, vertical pathway, FXR, Cyp7a1, Sult2a8.

# Résumé

Les acides biliaires (AB) sont des petites molécules synthétisées par l'hôte puis modifiées chimiquement par les micro-organismes de l'intestin. Il est de plus en plus évident qu'au-delà de leur rôle ancestral dans la digestion des lipides, les acides biliaires ont aussi une fonction cruciale en tant que molécule de signalisation. Ils sont métabolisés par le microbiote intestinal, puis au cours de la recirculation entéro-hépatique, se retrouvent en partie éjectés dans la circulation systémique ce qui leur permet d'atteindre de nombreux organes et tissus métaboliques cibles ainsi que des cellules immunitaires. La transformation microbienne des acides biliaires au niveau intestinal est critique pour la signalisation de ces molécules car elle modifie leurs quantités ainsi que leurs affinités pour des récepteurs spécifiques aux acides biliaires. Les bactéries 7-DH sont des bactéries commensales importantes car elles catalysent la déshydroxylation au niveau du groupement hydroxyle C7 des acides biliaires primaires produits par le foie et forment des acides biliaires secondaires. Un des principaux récepteurs aux acides biliaires secondaires est le G protein-coupled bile acid receptor 1 (GPBAR1), aussi connu sous le nom de Takeda G-protein receptor 5 (TGR5). Il est associé à la régulation des dépenses énergétiques, du métabolisme du glucose et de l'inflammation. De plus, les acides biliaires déshydroxylés protègent l'hôte contre l'infection par le pathogène intestinal *Clostridioides difficile*. Par conséquent, par leur action sur les acides biliaires primaires, les bactéries 7-DH ont un rôle important dans la promotion de la santé ainsi que dans le fonctionnement d'important processus physiologiques tels que la sécrétion d'insuline, la thermogenèse et les réponses immunitaires. Par ailleurs, une concentration excessive de ces acides biliaires secondaires, potentiellement liée à une surabondance en bactéries 7-DH, corrèle avec un risque accru de cancers intestinaux et de calculs biliaires. Malgré leur importance pour l'hôte mammifère, les bactéries 7-DH sont peu étudiées et beaucoup d'éléments restent à clarifier en ce qui concerne leur métabolisme, leur diversité, leur abondance dans l'intestin ainsi que leur dynamique de colonisation de l'hôte.

Ici, nous avons utilisé *Clostridium scindens* comme organisme modèle pour étudier la déshydroxylation des AB en position C7 *in vitro* et *in vivo* dans des souris gnotobiotiques. Nous avons observé que *C. scindens* métabolise uniquement les acides biliaires primaires humains (CA et CDCA). Nous avons mis en évidence la formation d'un nouvel intermédiaire lors de la déshydroxylation du cholic acid (CA) par *C. scindens in vitro* : le 12-oxoLCA. *In vivo*, nous avons amendé *C. scindens* aux souris gnotobiotiques n'ayant pas d'activité de déshydroxylation des acides biliaires. En effectuant des analyses NanoSIMS et métabolomiques, nous avons démontré que le gros intestin constitue la niche écologique de *C. scindens* dans lequel il déshydroxyle activement les AB dans les souris gnotobiotiques.

À la suite de la découverte du 12-oxoLCA, nous avons émis l'hypothèse de l'existence d'un autre chemin réactionnel pour la déshydroxylation de l'acide cholique. Nous avons postulé qu'il pourrait impliquer les cycles B et C de la structure stéroïdienne ainsi que l'oxydation/réduction du groupement hydroxyle en position C12. De ce fait, il a été surnommé le chemin réactionnel vertical. En conduisant des essais enzymatiques *in vitro*, nous avons confirmé l'existence d'un nouveau chemin réactionnel vertical de déshydroxylation de l'acide cholique, l'acide biliaire primaire le plus abondant chez l'Homme. De plus, nous avons identifié l'ensemble d'enzymes suffisantes et nécessaires pour la déhydroxylation de l'acide cholique via ce nouveau chemin réactionnel.

En outre, nous avons utilisé une approche couplant analyses métabolomique et métaprotéomique pour sonder l'activité *in vivo* de la communauté microbienne dans un modèle de souris gnotobiotiques. Les résultats obtenus révèlent l'implication de *C. scindens* dans la déshydroxylation, du genre *Muribaculum* et *Bacteroides* dans la déconjugaison et de six autres organismes (appartenant aux genres

*Clostridium*, *Muribaculum*, *Bacteroides*, *Bifidobacterium*, *Acutalibacter* et *Akkermansia*) dans l'oxydation des acides biliaires. De plus, nous avons aussi considéré le profil d'AB de souris avec un microbiote intestinal plus complexe ou plus réduit ou encore en l'absence de microbiote intestinal. En comparant les profils d'AB des différents modèles de souris avec l'expression des gènes clés de la voie de biosynthèse des AB, nous avons souligné l'influence profonde de la communauté microbienne intestinale sur l'homéostasie des acides biliaires.

Ensemble, les données obtenues dans cette thèse contribuent de manière significative à la compréhension collective de la microbiologie des bactéries 7-DH capables de déshydroxyler les AB, un groupe de commensaux très pertinents pour l'hôte, mais qui reste peu caractérisés. La découverte d'un nouveau chemin réactionnel de déshydroxylation est une avancée scientifique majeure de cette thèse.

## Mots-clé

*Clostridium scindens*, acides biliaires, déhydroxylation des acides biliaires en C7, deconjugation, métaprotéomique, NanoSIMS, 12-oxoLCA, signalisation des acides biliaires, biogéographie, hydrolases de sels biliaires, opéron *bai*, hydroxystéroïde déshydrogénase, voie verticale de biosynthèse, FXR, Cpy7a1, Sult2a8.

# Table of Contents

<b>Acknowledgements .....</b>	<b>v</b>
<b>Abstract .....</b>	<b>vii</b>
<b>Keywords.....</b>	<b>viii</b>
<b>Résumé.....</b>	<b>ix</b>
<b>Mots-clé .....</b>	<b>x</b>
<b>Table of Contents.....</b>	<b>xi</b>
<b>List of Figures.....</b>	<b>xiv</b>
<b>List of Tables.....</b>	<b>xvi</b>
<b>Chapter 1     Bile acid 7-dehydroxylating bacteria: key commensals of the gut microbiota. ....</b>	<b>17</b>
1.1    Introduction .....	18
1.2    Bile acid transformation: a collaboration between the host and the gut microbial community.....	18
1.3    Bile acid 7-dehydroxylating bacteria.....	22
1.4    Bile acid 7-dehydroxylation: from a simple transformation to a complex pathway .....	25
1.5    Benefits and limitations for bile acid 7-dehydroxylation in the gut .....	29
1.6    Role of bile acid 7-dehydroxylating bacteria in health and disease. ....	31
1.7    Conclusions .....	36
1.8    Thesis objectives and chapters .....	36
1.8.1    Chapter 2: <i>In vitro</i> and <i>in vivo</i> characterization of <i>Clostridium scindens</i> bile acid transformations...	37
1.8.2    Chapter 3: Two routes are better than one : the bile acid 7-dehydroxylation pathway revamped...	37
1.8.3    Chapter 4: Biogeography of microbial bile acid transformations along the murine gut. ....	37
1.8.4    Chapter 5: Conclusion and future perspectives.....	37
<b>Chapter 2     <i>In vitro</i> and <i>in vivo</i> characterization of <i>Clostridium scindens</i> bile acid transformations .....</b>	<b>39</b>
<b>Abstract .....</b>	<b>40</b>
2.1    Introduction .....	40
2.2    Material and Methods.....	43
2.2.1    Oligo-MM12 Microbiota and gnotobiotic sDMDMm2 mice.....	43
2.2.2    Bacterial strains and culture conditions .....	43
2.2.3    Impact of bile acids on bacterial growth .....	43
2.2.4    Bile acid transformations experiments.....	43
2.2.5    Cell-free extract (CFE) experiment .....	44
2.2.6    Preparation of Standard Solutions .....	44
2.2.7    Bile Acid Extraction from cell cultures .....	44
2.2.8    Isotopic labeling of <i>C. scindens</i> cells .....	45
2.2.9 <i>In vitro</i> experiment: dilution of <i>C. scindens</i> isotopic labeling in unlabeled medium. ....	45
2.2.10    Animal experiment.....	45
2.2.11    NanoSIMS sample preparation and analysis .....	45
2.2.12    Bile acid extraction from intestinal content.....	46
2.2.13    UHPLC-HRMS Analyses.....	46
2.2.14    Statistical analysis .....	47

<b>2.3 Results .....</b>	<b>48</b>
2.3.1 <i>Clostridium scindens</i> growth in the presence of human and murine bile acids <i>in vitro</i> . ....	48
2.3.3 <i>In vitro</i> bile acid transformations by <i>Clostridium scindens</i> .....	49
2.3.4 <i>Clostridium scindens</i> colonization and bile acid transformation in the murine intestinal tract. ....	51
<b>2.4 Discussion .....</b>	<b>55</b>
<b>2.5 Conclusion .....</b>	<b>60</b>
<b>Chapter 3 Two routes are better than one: the bile acid 7-dehydroxylation pathway revamped. ....</b>	<b>61</b>
<b>Abstract .....</b>	<b>62</b>
<b>3.1 Introduction .....</b>	<b>62</b>
<b>3.2 Material and Methods.....</b>	<b>65</b>
3.2.1 Bacterial strains and culture conditions .....	65
3.2.2 <i>In vitro</i> 7-dehydroxylation of CA and CDCA by <i>C. scindens</i> .....	65
3.2.3 Cloning of <i>bai</i> genes into <i>E. coli</i> .....	65
3.2.4 Protein expression and purification.....	65
3.2.5 Bile acid standards.....	66
3.2.6 Bile acid pathway <i>in vitro</i> reconstruction .....	66
3.2.7 Specificity of 12 $\alpha$ -HSDH and BaiA.....	66
3.2.8 Identifying key enzymes of the bile acid 7-dehydroxylation pathways .....	66
3.2.9 LC/MS analysis of bile acid metabolites .....	67
<b>3.3 Results and Discussion .....</b>	<b>68</b>
3.3.1 Biochemical reconstruction of two 7-dehydroxylation pathways .....	68
3.3.2 Time-dependent CA 7-dehydroxylation via the two pathways. ....	68
3.3.3 12 $\alpha$ -HSDH and BaiA2 initiating the vertical and horizontal pathway are highly specific. ....	71
3.3.4 Identifying key enzymes of the vertical and horizontal 7-dehydroxylation pathway.....	72
<b>Chapter 4 Biogeography of microbial bile acid transformations along the murine gut .....</b>	<b>77</b>
<b>Abstract .....</b>	<b>78</b>
<b>4.1 Introduction .....</b>	<b>78</b>
<b>4.2 Material and Methods.....</b>	<b>81</b>
4.2.1 Animal experiments.....	81
4.2.2 Quantitative Real-Time PCR.....	81
4.2.3 Preparation of bile acid standard solutions.....	81
4.2.4 Bile acid extraction .....	81
4.2.5 Ultra-High-Pressure Liquid Chromatography-High Resolution Mass Spectrometry.....	82
4.2.6 Bile acid-metabolizing enzyme database.....	82
4.2.7 Metaproteome analysis.....	82
<b>4.3 Results and Discussion .....</b>	<b>84</b>
4.3.1 Mapping bile acid transformations in gnotobiotic mice.....	84
4.3.2 The microbiota shapes the bile acid pool composition .....	89
4.3.3 Microbiota-host interactions regulate the bile acid pool size .....	93
4.3.4 Bile acid detoxification .....	95
<b>4.4 Conclusion .....</b>	<b>96</b>
<b>Chapter 5 Conclusions and perspectives .....</b>	<b>97</b>
<b>References.....</b>	<b>103</b>

---

<b>Annex 1   Supplementary information for Chapter 1. ....</b>	<b>113</b>
<b>Annex 2   Supplementary information for Chapter 2. ....</b>	<b>115</b>
<b>Annex 3   Supplemental information of Chapter 3.....</b>	<b>119</b>
<b>Annex 4   Supplemental information for Chapter 4 .....</b>	<b>123</b>

# List of Figures

Figure 1.1  Bile acid structure and diversity.....	19
Figure 1.2  Bile acid metabolism. ....	20
Figure.1.3  First model of bile acid 7-dehydroxylation pathway proposed by Samuelsson in 1960. ....	25
Figure 1.4  The Hylemon model of the bile acid 7-dehydroxylation pathway.....	27
Figure 1.5  Most recent model of the bile acid 7-dehydroxylation pathway proposed by Funabashi <i>et al</i> (2019). ....	28
Figure 1.6  Bile acid 7-dehydroxylating bacteria synthesize secondary bile acid DCA and LCA which are ligands of the bile acid receptor TGR5. ....	33
Figure 1.7  Bile acid 7-dehydroxylation protects against <i>C. difficile</i> infection.....	35
Figure 2.1  Structure of selected human and murine bile acids.....	42
Figure 2.2  Impact of primary and secondary bile acids on <i>C. scindens</i> growth. ....	48
Figure 2.3  Bile acid transformations by <i>Clostridium scindens</i> <i>in vitro</i> . ....	50
Figure 2.4  Secondary bile acid transformations by <i>Clostridium scindens</i> <i>in vitro</i> (whole cell and cell-free extract). ....	51
Figure 2.5  <i>Clostridium scindens</i> colonizes the large intestine of the murine gut. ....	52
Figure 2.6 Luminal bile acid composition along the intestinal tract of sDMDMm2 mice colonized with <i>C. scindens</i> (sDMDMm2 + Cs) compared to sDMDMm2 control mice.....	53
Figure 2.7  Secondary bile acid composition along the intestinal tract of sDMDMm2 mice colonized with <i>C. scindens</i> compared to control sDMDMm2 mice. ....	54
Figure 2.8  Deoxycholic acid (DCA) formation <i>in vivo</i> as a function of time.....	54
Figure 2.9  Cholic acid (CA) transformations carried out by <i>Clostridium scindens</i> <i>in vitro</i> and <i>in vivo</i> . ....	57
Figure 2.10  Chenodeoxycholic acid (CDCA) transformations carried out by <i>Clostridium scindens</i> <i>in vitro</i> and <i>in vivo</i> . ....	57
Figure 3.1  Bile acid 7-dehydroxylation of the human primary bile acids. ....	64
Figure 3.2  7-dehydroxylation of CA with the VP and HP enzyme mix. ....	68
Figure 3.3  Time-dependent cholic acid 7-dehydroxylation.....	70
Figure 3.4  BaiCD and BaiH do not have activity on the vertical pathway intermediate m/z 387.....	71
Figure 3.5  Conversion of the vertical pathway intermediate m/z 387 to 12-oxoLCA by BaiI and BaiO. ....	71
Figure 3.6  Conversion of 12-oxoLCA to DCA with 12 $\alpha$ -HSDH with NADH or NADPH as cofactor. ....	71
Figure 3.7  Specificity of 12 $\alpha$ -HSDH, BaiA1/3 and BaiA2.....	72
Figure 3.8  Identifying essential enzymes for the vertical pathway.....	73
Figure 3.9  Identifying essential enzymes for the horizontal pathway. ....	73
Figure 3.10  Proposed vertical CA 7-dehydroxylation pathway in <i>C. scindens</i> ATCC 35704 based on the intermediates detected in the enzymatic assays with purified enzymes.....	75
Figure 3.11  Proposed horizontal CA 7-dehydroxylation pathway in <i>C. scindens</i> ATCC 35704 based on the intermediates detected in the enzymatic assays with purified enzymes.....	76
Figure 4.1  Microbial bile acid transformations.....	79
Figure 4.2  Protein abundance along the intestinal tract of sDMDMm2 and <i>C. scindens</i> -colonized sDMDMm2 gnotobiotic mice based on the metaproteomic analysis of intestinal content.....	84

---

Figure 4.3  Bile acid composition along the intestinal tract of sDMDMm2 and <i>C. scindens</i> -colonized sDMDMm2 gnotobiotic mice based on LC-MS/MS analysis. ....	87
Figure 4.4  Biogeography of specific bile acid transformation enzymes and the associated microorganisms based on metaproteomic analysis. ....	87
Figure 4.5  Bile acid composition along the intestinal tract in germ-free, SPF, and clindamycin-treated SPF mice based on LC-MS/MS analysis. ....	91
Figure 4.6  Bile acid pool composition along the intestinal tract of the mouse models based on LC-MS/MS. ....	92
Figure 4.7  Probing the influence of the gut microbiota on BA synthesis and detoxification. ....	94
Figure 5.1  Structure of cholic acid and 7 $\alpha$ , 12 $\alpha$ -cholanic acid and Norcholic acid. ....	99
Figure 5.2  Bile acid 7 $\beta$ -dehydroxylation. ....	100



# List of Tables

**Table 1.1| Classification of common bile acid species. .... 21**

**Table 1.2| Major bile acid 7-dehydroxylating bacteria isolated from human feces. .... 23**

# Chapter 1 Bile acid 7-dehydroxylating bacteria: key commensals of the gut microbiota.

This first chapter consists of a general introduction on bile acid microbial transformations and in particular the bile acid 7-dehydroxylation and the microorganisms catalyzing this transformation. Parts of this chapter constitute a review article that will be submitted to FEMS Microbiology Reviews in the near future. The latter has been written by Solenne Marion under the supervision of Rizlan Bernier-Latmani.

## 1.1 Introduction

Bile acids (BAs) are amphipathic steroid molecules synthesized from cholesterol in the hepatocytes and stored in the gallbladder. Post-prandium, they are released in the gut where they promote lipid digestion. Due to their structure, bile acids form micelles with which lipids and lipid-soluble vitamins associate, in effect promoting their solubilization and absorption<sup>1</sup>. This detergent property is also responsible for their toxicity due to the solubilization of bacterial and host cell membranes; in fact, their cytotoxicity correlates positively with their hydrophobicity<sup>2</sup>. Bile acids are actively reabsorbed in the ileum, and passively along the gut and return to the liver through the portal vein. This cycle is referred to as enterohepatic circulation of the bile acids and occurs several times per day. During this cycle, a small fraction of bile acids escapes re-uptake by the liver and is released into the systemic circulation.

In addition to their local action in the intestine, bile acids reach other organs of the human body (i.e., via systemic circulation). Bile acid receptors are found in many organs and tissues, as well as on immune cells, suggesting the broad field of action of these compounds in humans<sup>3,4</sup>.

In the intestinal tract, the two liver-derived primary bile acids, conjugated cholic acid (CA) and chenodeoxycholic acid (CDCA), undergo several transformations mediated by gut microbes, leading to a large diversity of secondary bile acids. The microbial transformation of BAs in the gut is critical to bile acid signaling as it modifies their affinity for host receptors<sup>5</sup>. Bile acid 7-dehydroxylating (7-DH-ing) bacteria are a group of commensals of particular importance as they catalyze the dehydroxylation of liver-derived (primary) BA at the C7 position (i.e., 7-dehydroxylation) and produce 7-dehydroxylated BAs, which represent a large fraction of the secondary BA pool in the large intestine. 7-dehydroxylated bile acids are strong agonists for a major BA receptor, the G protein-coupled BA receptor 1 (GPBAR1), also known as Takeda G-protein receptor 5 (TGR5). TGR5 is associated with regulation of metabolism and energy expenditure as well as inflammation<sup>3,6</sup>. In addition, BAs lacking the 7-hydroxyl group are also associated with protection from infection by intestinal pathogens (i.e., *Clostridioides difficile*<sup>7,8</sup>) and parasites (i.e., *Entamoeba histolytica*<sup>9</sup>).

The microbial transformations undergone by bile acids in the gut play an important role in maintaining host health, and modulation of the composition of the bile acid pool represents a promising avenue for the prevention of several diseases. Changes of the bile acids pool is linked to major metabolic diseases (e.g., obesity, type 2 diabetes, non-alcoholic fatty liver disease<sup>10</sup>), cardiovascular diseases (e.g., atherosclerosis), inflammatory diseases (e.g., inflammatory bowel disease), gastrointestinal cancers<sup>11,12</sup>, as well as infectious disease (i.e., *Clostridioides difficile* infection<sup>13</sup>). Collectively, these diseases exact a heavy socio-economic toll due their increasing occurrence and severity in first world countries<sup>14–16</sup>.

The action of bile acid 7-dehydroxylating bacteria on primary BAs makes them a promising target for the therapeutic modulation of bile acid metabolism. However, they require much more attention before their biochemical activity can be harnessed. In fact, much remains to be deciphered regarding their metabolism, diversity, abundance in the gut, and colonization dynamics in the host. This review aims at providing a condensed overview of the current knowledge on the microbiology of bile acid 7-dehydroxylating organisms and their importance for host health.

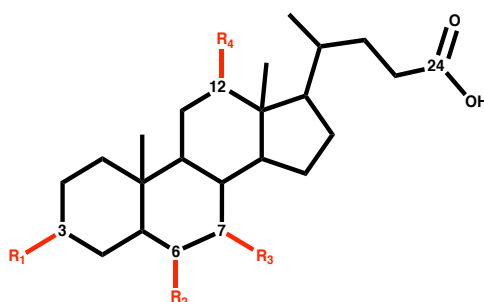
## 1.2 Bile acid transformation: a collaboration between the host and the gut microbial community

Bile acids are amongst the most abundant and diverse microbiota-derived metabolites<sup>17</sup>. Primary bile acids, synthesized in the liver, are conjugated to either taurine or glycine (at the C24 position, Figure 1.1) and represent the main component of bile. Conjugated primary bile acids are often referred to as bile salts. Post-prandium, bile salts are released into the intestinal tract where they will undergo successive microbial transformations. In the small intestine, bile salts are rapidly deconjugated by bile salts hydrolases (BSH) produced by deconjugating bacterial species. These enzymes are widespread in commensal bacteria that inhabit both the small and large intestine<sup>1,18</sup>. The major unconjugated primary bile acids, which are cholic acid (CA) and chenodeoxycholic acid (CDCA) in humans (Figure 1.1, Table 1.1), undergo several bacterial transformations including oxidation of the C3, C7, C12 hydroxyl groups,

epimerization of the C3 and C7 hydroxyl groups, epimerization of the 5-H, and dehydroxylation of the C7 (7-dehydroxylation) and C12 hydroxyl groups<sup>19</sup>. Side chain conjugation blocks 7-dehydroxylation and highlights the crucial role of the deconjugating bacteria prior to 7-dehydroxylation<sup>20</sup>. Similarly, sulfation of bile acid precludes 7-dehydroxylation<sup>21</sup>. Desulfating bacteria inhabit the intestinal tract and have the potential to release desulfated bile acid that can be further 7-dehydroxylated (Figure 1.2, Table 1.1).

Deoxycholic acid (DCA) and lithocholic acid (LCA) resulting from microbial 7-dehydroxylation (7-DH-ion) of CA and CDCA, respectively are the most abundant secondary bile acids, accounting for approximately 50% of the fecal bile acid pool in humans<sup>22</sup>. Furthermore, these compounds are not the end product of the bile acid metabolism. They can be further metabolized into a series of 7-dehydroxylated secondary bile acids. Most notably, 3 $\beta$ -epimers of DCA (iso-deoxycholic acid (isoDCA)) and of LCA (iso-lithocholic (iso-LCA)) are reported to be the third and fourth most abundant bile acids in the healthy gut, accounting for about 15% of the cecal BA pool<sup>23,24</sup> (Figures 1.1 and 1.2, Table 1.1).

The mouse primary BA pool includes additional specific murine BA, that are also hydroxylated at the C6 position:  $\alpha$ -muricholic acid ( $\alpha$ -MCA) and  $\beta$ -muricholic acid ( $\beta$ -MCA)<sup>6</sup>. The BAs undergo the same transformations as CA and CDCA, resulting in the formation of additional 7-dehydroxylated BAs: hyodeoxycholic acid (HDCA) and murideoxycholic acid (MDCA) (Figure 1.1, Table 1.1).



Bile Acid Name	Abbreviations	R1	R2	R3	R4
Cholic acid	CA	$\alpha$ -OH		$\alpha$ -OH	$\alpha$ -OH
Chenodeoxycholic acid	CDCA	$\alpha$ -OH		$\alpha$ -OH	
$\alpha$ -Muricholic acid	$\alpha$ MCA	$\alpha$ -OH	$\beta$ -OH	$\alpha$ -OH	
$\beta$ -Muricholic acid	$\beta$ MCA	$\alpha$ -OH	$\beta$ -OH	$\beta$ -OH	
Ursodeoxycholic acid	UDCA	$\alpha$ -OH		$\beta$ -OH	
Deoxycholic acid	DCA	$\alpha$ -OH			$\alpha$ -OH
Lithocholic acid	LCA	$\alpha$ -OH			
Isodeoxycholic acid	isoDCA	$\beta$ -OH			$\alpha$ -OH
Isolithocholic acid	isoLCA	$\beta$ -OH			
Hyocholic acid	HCA ( $\gamma$ MCA)	$\alpha$ -OH	$\alpha$ -OH	$\alpha$ -OH	
$\omega$ -Muricholic acid	$\omega$ -MCA	$\alpha$ -OH	$\alpha$ -OH	$\beta$ -OH	
Hyodeoxycholic acid	HDCA	$\alpha$ -OH	$\alpha$ -OH		
Murideoxycholic acid	MDCA	$\alpha$ -OH	$\beta$ -OH		

**Figure 1.1 | Bile acid structure and diversity.** Bile acids are steroid end products of cholesterol metabolism. They differ by the number and position of hydroxyl groups (C3, C6, C7, C12). The substituent at C6 (R2) is specific of murine bile acids. Substituents at C3, C6 and C12 are present on both human and murine bile acid. Bile acids are conjugated at C24 to glycine or taurine in the liver. List of major primary and secondary bile acids found in humans and rodents. 7-dehydroxylated secondary BAs are annotated in red.

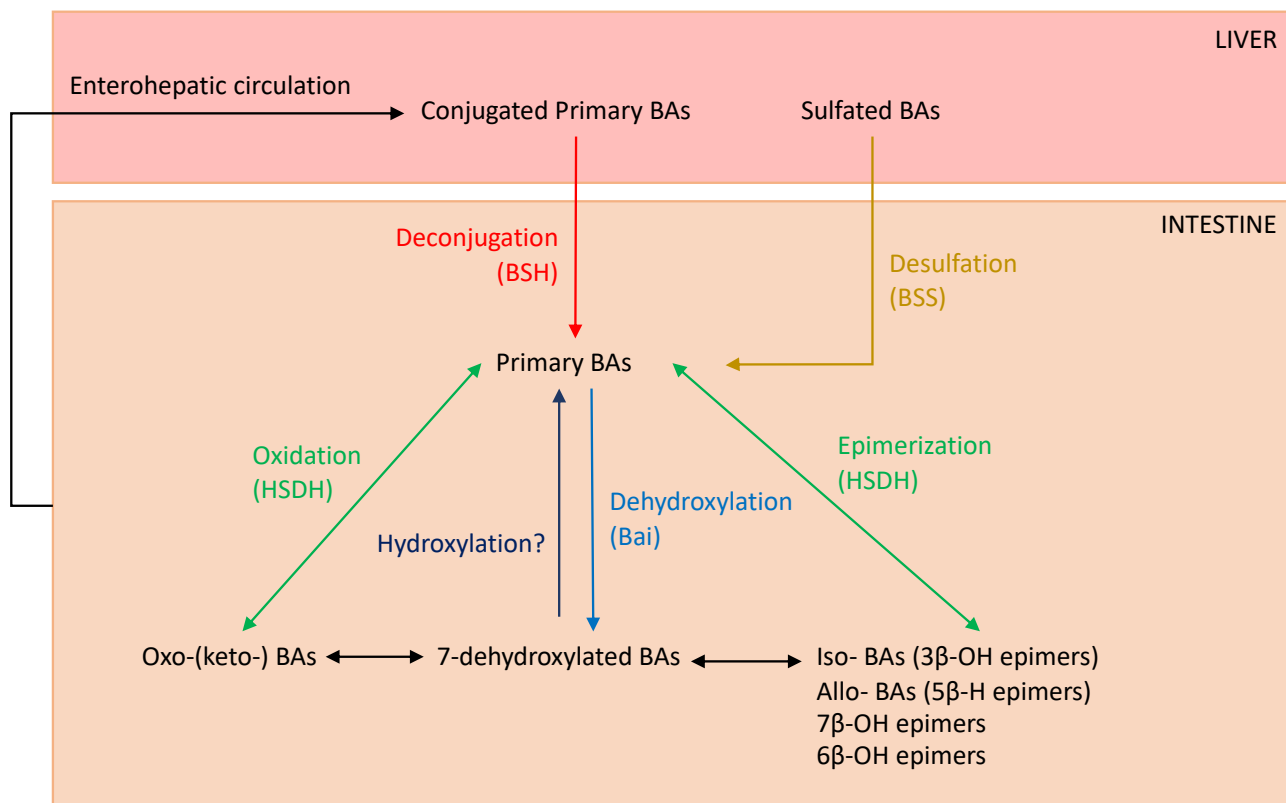


**Figure 1.2| Bile acid metabolism.** Bile acid transformations occurring in the liver are in the red box and the ones occurring in the intestinal tract are in the brown one. Taurine- and glycine- conjugated primary bile acids are deconjugated in the gut and undergo 7-dehydroxylation, oxidation and epimerization subsequently. In addition, 95% of the bile acids are recycled back to the liver where they can be sulfonated and re-conjugated before re-release. In humans, BAs are conjugated to glycine, while in rodents, they are conjugated to taurine. When known, the bacterial enzymes catalysing the transformation are indicated with parentheses. BSH, Bile salt hydrolase; HSDH, Hydroxysteroid dehydrogenase; BSS, Bile acid sulfate sulfatase; Bai, Bile acid inducible enzymes involved in the 7-dehydroxylation pathway. In the mouse, dehydroxylated BAs can be re-hydroxylated in the liver.

**Table 1.1 | Classification of common bile acid species.**

Class	Metabolic Conversions	Bile Acids
Primary bile acids		
	<b>From cholesterol by hepatic classical (neutral) or alternative (acidic) pathways</b>	CA, CDCA in humans CA, CDCA, UDCA, $\alpha$ MCA, $\beta$ MCA in mice
Secondary bile acids		
	<b>From primary bile acids</b>	
	Through microbial 7-dehydroxylation	DCA, LCA in both humans and mice MDCA, HDCA in mice
	<b>From primary or secondary bile acids</b>	
	Through microbial 7 $\alpha$ / $\beta$ -epimerization	UDCA in humans
	Through microbial 6 $\alpha$ / $\beta$ -epimerization	HCA, $\omega$ MCA in mice
	Through microbial 3 $\alpha$ / $\beta$ -epimerization	Iso- bile acids
	Through microbial 5 $\alpha$ / $\beta$ -epimerization	Allo- bile acids
	Through microbial oxidation	Oxo- (keto-) bile acids

Enterohepatic recirculation of bile acids back to the liver enables liver-mediated modifications of bile acids such as re-conjugation, sulfonation<sup>25</sup> and 3 $\beta$ -epimerization<sup>26</sup>, further expanding the diversity of the bile acid pool. Furthermore, rehydroxylation of secondary BAs at C7 position occurs in the mouse but not the human liver<sup>27</sup>. Thus, bile acid homeostasis represents a tight collaboration between the host and gut commensals leading to the wide variety of secondary bile acids present in the human (and murine) gut.

The formation of 7-dehydroxylated (7-DH-ed) BAs illustrates this collaborative network between the host and the gut microbes. The 7-DH-ing bacteria rely on other gut commensals to produce the proper bile acid substrate that can undergo 7-dehydroxylation. Bile acids that can be dehydroxylated must have a free-hydroxyl group at the position C7 and are not conjugated<sup>20</sup>. Thus, conjugated liver-derived, primary bile acids require deconjugation by bacteria synthesizing bile salt hydrolases (BSH) prior to 7-dehydroxylation. Furthermore, gut microbes metabolizing bile acids release secondary bile acids (such as oxo-bile acids) with a 7-hydroxyl group that can be further 7-dehydroxylated by 7-DH-ing bacteria. In a recent paper, Doden *et al.* (2018) illustrate how 7-dehydroxylating organisms can use multiple oxo-bile acids as substrates for 7-dehydroxylation<sup>28</sup>.

7-dehydroxylated bile acids can also be further metabolized by bacteria. As a consequence, it is crucial that studies investigating the extent of 7-DH-ion, quantify not only DCA and LCA but also other 7-dehydroxylated species. In a recent study from our group, we observed that 12-oxoLCA was another major 7-DH-ed secondary bile acid of the 7-DH-ion of CA by *C. scindens* *in vitro*<sup>29</sup>.

Bile acid transformations have been mostly studied in bacteria but fungi also metabolize bile acids and are even capable of 7-hydroxylation<sup>30,31</sup>. Unfortunately, the contribution of the gut mycobiota to the secondary bile acid pool remains understudied.

### 1.3 Bile acid 7-dehydroxylating bacteria

Bile acid 7-dehydroxylating bacteria are gut commensals found in vertebrates including mammals. The presence of 7-dehydroxylated bile acids in reptiles, birds and fishes suggests their colonization of a wide range of vertebrates<sup>32,33</sup>. These bacteria colonize and perform BA 7-dehydroxylation primarily in the large intestine of the gastrointestinal tract<sup>29,34</sup>. The predominance of deconjugated bile acids and the anaerobic environment make the large intestine a favorable environment for bile acid 7-DH-ing bacteria to inhabit. The small intestine contains high levels of conjugated primary bile acids that cannot be 7-dehydroxylated<sup>20</sup>. Bile acid 7-dehydroxylating bacteria have been typically isolated from healthy and diseased human feces<sup>35,36</sup> (Table 1.2), mouse<sup>37</sup>, rat<sup>38,39</sup>, rabbit feces<sup>40</sup> (Table S1). In a single instance, 7-DH-ing strains were isolated from municipal sewage samples<sup>41</sup>.

Furthermore, by screening the NCBI database for *bai* homologous nucleotide and protein sequences, we identified two new potential 7-DH-ing strains: *Africanella massiliensis* P-2538<sup>42</sup>, isolated from a fecal sample of a healthy 44-month old Nigerian girl, and *Proteocatella sphenisci* DSM 23131 isolated from guano of Magellanic penguins<sup>43</sup>.

Bile acid 7-DH-ing bacteria are all anaerobic, Gram-positive, rod-shaped bacteria and some are endospores formers<sup>41,44,45</sup> (Table S2). Most are fermenters and can use diverse carbohydrates as carbon and energy sources to grow. However, several strains, including the two 'Eggerthella lenta-like' strains b-8 and c-25<sup>46</sup> and 4 strains isolated from gallstone patients<sup>36</sup>, were unable to ferment any of the carbohydrates tested. The majority of 7-DH-ing species were attributed to the genus *Clostridium* (*Clostridiaceae* family) but this represents a mis-assignment, which, regrettably, is a common occurrence<sup>47</sup>. In fact, *C. scindens* and *C. hylemonae* pertain to the family *Lachnospiraceae*, *C. sordellii* to *Peptostreptococcaceae*, and *C. leptum* to *Ruminococcaceae*<sup>48</sup>. *C. hiranonis* was recently reported as a misnamed member of the *Peptostreptococcaceae* family and still remains to be properly classified<sup>49</sup>. 'Eggerthella lenta-like' strains c-25 and b-8<sup>50</sup> have been mis-assigned to this species. A recent study showed that *Eggerthella lenta* type strain (DSM 2243) is not capable of bile acid 7-dehydroxylation<sup>51</sup>. *Africanella massiliensis* pertain to the *Lachnospiraceae*<sup>42</sup>. Many others 7-DH-ing strains were isolated through the years but they were not further characterized and were classified either as *Eubacterium sp.* or *Clostridium sp.* or unclassified<sup>36,44,52</sup> (Tables S1 et S2). Recently, Vital *et al.* (2019) screened metagenome-assembled genomes (MAGs) derived from human stool samples for the presence of a gene cluster, the *bai* (bile acid inducible) gene cluster, characteristic of 7-DH-ing species. The majority of *bai* gene-containing MAGs were found to belong to the *Ruminococcaceae*, whereas fewer MAGs were associated with *Lachnospiraceae* and even fewer with the *Peptostreptococcaceae*<sup>53</sup>.

While 7 $\alpha$ -dehydroxylation has been the focus of research, 7 $\beta$ -dehydroxylation could potentially also occurs in the gut<sup>54,55</sup>. 7 $\beta$ -dehydroxylating strains have been isolated from humans (Table 1.2) and from rats (strain HDCA-1)<sup>39</sup>. Not all 7 $\alpha$ -DH-ing strains can use 7 $\beta$ -bile acids (e.g., UDCA,  $\omega$ MCA) as substrates (Tables 1.2). However, the isolated 7 $\beta$ -dehydroxylating strains also perform 7 $\alpha$ -dehydroxylation. The only enzyme shown to have specificity for 7 $\beta$ -bile acids is BaiH<sup>56</sup>. BaiI is predicted to be a 7 $\beta$ -dehydratase but this remains to be confirmed<sup>56</sup>. One alternative hypothesis is that what has been reported to be 7 $\beta$ -dehydroxylation is rather a two-step process including first an epimerization of the 7 $\beta$ - hydroxyl group, followed by a 7 $\alpha$ -dehydroxylation. In that case, 7 $\beta$ -dehydroxylating strains should carry a gene encoding a 7 $\beta$ -HSDH and the *bai* operon. The fact that all 7 $\beta$ -DH-ing strains show 7 $\alpha$ -DH-ion activity supports the latter hypothesis.

**Table 1.2| Major bile acid 7-dehydroxylating bacteria isolated from human feces.**

A green cell indicates that the strain could 7-dehydroxylate the bile acid substrate tested. A red cell indicates that the strain was unable to 7-dehydroxylate the bile acid substrate tested. If bile acid 7-dehydroxylation was not tested, the cell is blank. All strains except *C. scindens* VPI 12708 were isolated from feces or intestinal content of healthy humans.

\* *C. scindens* VPI 12708 was isolated from a colon cancer patient. Bile acid 7-dehydroxylating bacteria isolated from other hosts are detailed in Table S1.

\*\* Strains b-8 and c-25 were initially assigned to the *Eubacterium* genus<sup>50</sup> (as *E. lentum* like sp.). Later *E. lentum* was renamed as *Eggerthella lenta* based on phylogenetic analysis<sup>57</sup>. However, this assignment is likely incorrect because a recent study showed that *Eggerthella lenta* type strains are incapable of bile acid 7-DH-ion. .

\*\*\* *Africanella massiliensis* P-2538 is suspected to be a 7-dehydroxylating strain after mining the NCBI database using BLAST with the *bai* nucleotide and protein sequences.

Organism	Strain	Family	7 $\alpha$ -dehydroxylation		7 $\beta$ -dehydroxylation		References
			CA	CDCA	$\alpha$ -MCA	UDCA	
<i>Clostridium scindens</i>	ATCC 35704	Lachnospiraceae					29,58
	VPI 12708*						44,45,54,58
	Y-1113						44,45,58
	I-10						45,58
	M-18						44,45,58
	365						44,45,58
	TH-82						45,58
<i>Clostridium hiranonis</i>	TO-931	Peptostreptococcaceae					58–60
	HD-17						41,44,58,61
<i>Clostridium hylemonae</i>	TN-271	Lachnospiraceae					58,59
	TN-272						
<i>Clostridium sordellii</i>	Y-67	Peptostreptococcaceae					44,58
	ATCC 9714						58
	4709						41
<i>Clostridium leptum</i>	ATCC 29065	Ruminococcaceae					58
	VPI 10900						62
Mis-assigned to ' <i>Eggerthella lenta</i> like sp'***	c-25	Mis-assignment					41,44,55,63
	b-8						41
<i>Africanella massiliensis</i>	P-2538***	Lachnospiraceae					42

#### • Abundance of the 7-DH-ing bacteria in the gut

Early studies reported that bile acid 7-DH-ing bacteria were rare and detected in low numbers in the feces, when cultivation methods were utilized. For instance, no 7-DH-ing organisms were found among 124 strains isolated from rat intestinal tracts<sup>64</sup> and only one 7-DH-ing strain (HD-17, later characterized as *Clostridium hiranonis*) was found out of 75 isolated strains from healthy human feces<sup>61</sup>. Fecal levels of 7-dehydroxylating bacteria ranging from approximately  $10^4$  to  $10^6$  per gram of feces in humans have been proposed<sup>44,62</sup>, which remain very low in comparison to the total abundance of bacteria in human feces:  $\sim 10^{11}$  / g in stool<sup>65</sup>. But these estimates may be of limited value due to the inherent limitations of cultivation approaches. More recent studies have used qPCR to quantify 7-DH-ing bacteria in biological samples. Kitahara *et al.* (2004) reported concentrations of  $10^3$ - $10^7$  *C. scindens* cells/g of wet feces<sup>66</sup>.



It is estimated that 400-800 mg of BA enters the large intestine per day<sup>24</sup>. Thus, the *in vivo* activity of 7-DH-ing bacteria must be sufficiently high to transform 400-800 mg of BA a day, which requires, a specific activity on the order of ~0.6-1.3 nmol cholic acid transformed per hour and per mg 7-DH-ing biomass. This is clearly within the range of *in vitro* specific activities of 'high activity' strains<sup>35</sup> but represents about 10 times more rapid activity than that of the 'low activity' strains. It is unlikely that gut microorganisms would routinely achieve the highest specific activity obtained *in vitro* in pure culture, thus it is reasonable to hypothesize that bile acid 7-DH-ing bacteria represent a larger fraction of the microbiota than reported in the literature.

Two major gut microbiome metagenome projects, Human Microbiome project (HMP) and MetaHIT (Metagenome of the Human Intestinal Tract), seem to favor this hypothesis. Two of the 7-DH-ing bacteria, *Clostridium scindens* and *Clostridium leptum*, were amongst the 57 most abundant microorganisms in the feces of healthy humans<sup>67</sup>. Another 7-DH-ing bacterium, *C. hylemonae*, was detected by BlastP in HMP metagenomes, suggesting that it is abundant enough to be identified by sequencing. Furthermore, Kurakawa *et al.* investigated the abundance of several species of the *Clostridium* cluster XIVa, which is a major contributor to the microbial population of the large intestine and included *C. scindens* and *C. hylemonae* in their study. RT-qPCR analysis of fecal samples from 96 volunteers (32 children, 32 adults and 32 elderly) revealed that *C. scindens* was more frequent than *C. hylemonae* in general and that the prevalence of these two bile acid 7-DH-ing organisms was significantly greater in the elderly than in children and adults. Concentrations of these organisms ranged within  $10^6$ - $10^8$  / g of feces for *C. scindens* and  $10^6$  / g of feces for *C. hylemonae*<sup>68</sup>.

So far the BA 7-DH-ing strains seem to be phylogenetically monolithic as all known strains belong to families within the Class *Clostridia* (Table 1.2)<sup>53</sup>. The only exception is *Eggerthella lenta*, but the corresponding strains are likely mis-assigned to this genus and species. Most of the research has focused on *C. scindens*, *C. hylemonae* and *C. hiranonis*. However, many more 7-DH-ing strains have been isolated in the past 50 years but were not further characterized (Table S2). These may represent greater phylogenetic diversity than currently described. Thus, there are several lines of evidence indicating that bile acid 7-DH-ing organisms might be more diverse and more abundant than previously thought.

Diverse methods have been used to isolate bile acid 7-dehydroxylating organisms from feces. Most are tedious and consist of serial dilutions of the fecal sample on plates (with or without a pretreatment with heat, chloroform, or a bile solution), pooling colonies and testing them for their 7-DH-ing activity. The active pooled colonies are then streaked again and individual colonies tested for 7-DH-ing activity<sup>36,41,44,52,59</sup>. Less tedious approaches are emerging that do not require individual testing of each colony for 7-DH-ing activity but rather rely on use of PCR amplification of target genes associated with the 7-dehydroxylation pathway (see next section) to identify candidate 7-DH-ing bacteria<sup>69</sup>.

- *Acquisition and transmission of the 7-DH-ing organisms.*

Unlike for pathogens, the acquisition and transmission cycles of intestinal commensals remains unappreciated and poorly understood<sup>70</sup>. Jönsson *et al.* (1995) investigated the microbial bile acid transformation in 3 infants from birth up to 24 months of age. They reported that bile acid 7-dehydroxylation was a late event and started at different age (6, 12 and 21 months)<sup>71</sup>. This suggests an environmental acquisition of bile acid 7-dehydroxylating bacteria rather than direct vertical transmission from the mother to the child during birth. Firmicutes (including *Clostridia*) are not part of the newborn microbiota; they are acquired later after weaning when solid food is introduced to the infant<sup>72</sup>.

In recent review from Browne *et al.* (2017), a model was proposed for the inter-host transmission dynamics of intestinal bacteria distinguishing the transmission of spore and non-spore forming bacteria. The non-spore-forming bacteria rely on the close proximity between individuals whereas the spore-forming bacteria have an increased spatial and temporal distance for transmission as spores are resistant to environmental stresses and remain viable for extended period of time<sup>70</sup>.

The acquisition and transmission of these organisms as well as of most of the commensals is unknown. Considering that bile acid 7-dehydroxylating bacteria pertain to families of spore-formers (*Lachnospiraceae*, *Ruminococcaceae*, *Peptostreptococcaceae*)<sup>70</sup>, we could argue that the acquisition and transmission of these commensals may occur via spores.

However, for surprisingly many of the 7-dehydroxylating strains isolated, sporulation was not observed<sup>39,44,45,52</sup> (Table S2). For instance, Kitahara *et al.* (2000) observed sporulation for only 1 out of 7 strains of *C. scindens*<sup>45</sup>. Thus, there is a discrepancy between their assignment to families pertaining the class *Clostridia* (spore-formers) and the absence of sporulation. One possible explanation is a poor sporulation efficiency of those strains. Indeed, Kitahara *et al.* (2000) reported that spores of *C. scindens* ATCC 35704 were very difficult to demonstrate microscopically<sup>45</sup>.

Several questions remain unanswered at present: are all 7-DH-ing strains capable of sporulation? Is the transmission of these commensals occurring via spores or/and vegetative cells? What is the reservoir? Does the gut constitute a reservoir or is there an environmental reservoir?

Further research should be undertaken to understand the transmission cycle of these commensals.

This could be particularly relevant for the clinical management of *Clostridioides difficile* infections (CDI). In 2015, Buffie *et al.* demonstrated that the 7-DH-ing bacterium *C. scindens* is crucial for colonization resistance against the intestinal pathogen<sup>7</sup>. Recently, Solbach *et al.* (2018) confirmed that the abundance of 7-DH-ing bacteria is negatively correlated with *C. difficile* infection<sup>73</sup>. Thus, a better understanding of the transmission of these important commensals could help identify new strategies for the prevention and clinical management of CDI. Fecal transplantation, which constitutes an active transmission of these commensals, is an effective treatment for patients suffering from recurrent *C. difficile* infections<sup>8</sup>.

## 1.4 Bile acid 7-dehydroxylation: from a simple transformation to a complex pathway

Bile acid 7-dehydroxylation consists in the removal of a hydroxyl group at the C7 position on the steroid nucleus of the bile acid structure (Figure 1.1). This microbial transformation, which may seem simple at first sight (removal of a hydroxyl group on the bile acid molecule), is the result of a complex 8-step transformation pathway. The pathway has evolved through the years from the simple Samuelsson model, to the Hylemon pathway. Recently, Funabashi *et al.* (2019), identified 6 enzymes sufficient to carry out bile acid 7-dehydroxylation. Of note, Funabashi *et al.* (2019) is a preprint and therefore has not been peer-reviewed.

- **Samuelsson's pathway**

The first model of the cholic acid 7-dehydroxylation pathway was proposed by Samuelsson in 1960<sup>74</sup>. His 7-dehydroxylation pathway consisted of a diaxial *trans* elimination of water (6 $\beta$ H, 7 $\alpha$ OH) followed by reduction of the  $\Delta^6$ -intermediate (Figure 1.3).

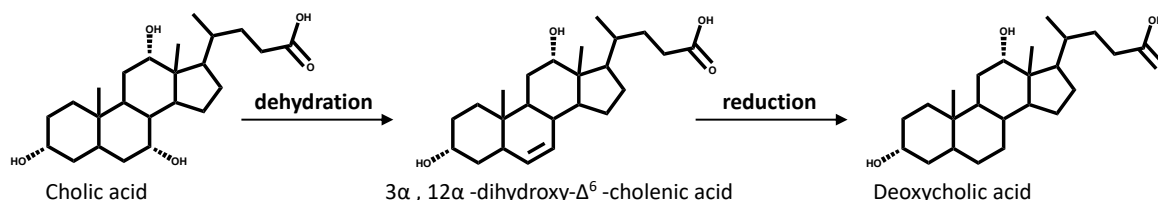


Figure.1.3| First model of bile acid 7-dehydroxylation pathway proposed by Samuelsson in 1960.

- **The Hylemon pathway**

The bile acid 7-dehydroxylation pathway described by Hylemon and colleagues is a complex 8-step transformation pathway involving gene products of the bile acid inducible (*bai*) operon (Figure 1.4). This pathway was elucidated by the cloning and expression of the corresponding genes from *C. scindens* strain VPI 12708 into *Escherichia coli*<sup>75–84</sup>.

The unconjugated primary bile acid is first transported into the cell by a proton-dependent active transporter (BaiG) encoded by the *baiG* gene<sup>78</sup>. Once in the cytosol, coenzyme A is ligated to a free carboxyl group by the action of a bile acid CoA ligase (BaiB)<sup>76</sup>. This ligation step is thought to commit the BA to 7-dehydroxylation by trapping the CoA conjugate inside the cell<sup>22</sup>. Oxidation of the 3-hydroxyl group of the bile acid CoA conjugate is catalyzed by a 3 $\alpha$ -hydroxysteroid dehydrogenase (BaiA)<sup>85</sup>. Two separate *baiA* genes (*baiA1/3* and *baiA2*) are present in *C. scindens*, on the polycistronic *bai* operon. These two genes encode for 3 $\alpha$ -hydroxysteroid dehydrogenases that have specificity for CoA conjugates. These 3 $\alpha$ -HSDHs utilize NAD<sup>+</sup> and NADP<sup>+</sup> as electron acceptors in this oxidation step of the pathway, resulting in the production of a 7-hydroxy, 3-oxo-bile acid CoA ester<sup>86</sup>.

The ensuing step involves oxidation of the 7 $\alpha$ -hydroxy CoA conjugates at the C4 position by an NADH:flavin-dependent oxidoreductase (BaiCD) and by a homologous enzyme (BaiH) encoded by the *baiH* gene for the 7 $\beta$ -hydroxy CoA conjugates<sup>56</sup>. The next step is a 7 $\alpha$ / $\beta$ -dehydration catalyzed by a 7 $\alpha$ -dehydratase encoded by *baiE*<sup>81,87</sup>. The gene *baiI* is hypothesized to encode a 7 $\beta$ -dehydratase<sup>56</sup>. This series of transformations catalyzed by BaiB, BaiA, BaiCD and BaiE represent the oxidative arm of the BA 7-DH-ion pathway and results in an intermediate 3-oxo- $\Delta$ 4,6-bile-acid-CoA ester<sup>87</sup>.

The secondary bile acid is then formed from the intermediate through three reductive steps along with a CoA removal step. Two CoA transferases encoded by *baiF* and *baiK*, catalyze the removal of the CoA moiety<sup>79,88</sup>. The first two reductive steps are catalyzed by BaiN, a  $\Delta$ 4,6-reductase identified in *C. scindens* ATCC 35704<sup>89</sup>. The enzyme catalyzing the last reductive step remains unknown but is likely to involve one of the *baiA* genes encoding 3 $\alpha$ -HSDH<sup>86</sup>. The secondary BA product is then presumed to be effluxed out of the cell via an unknown transporter.

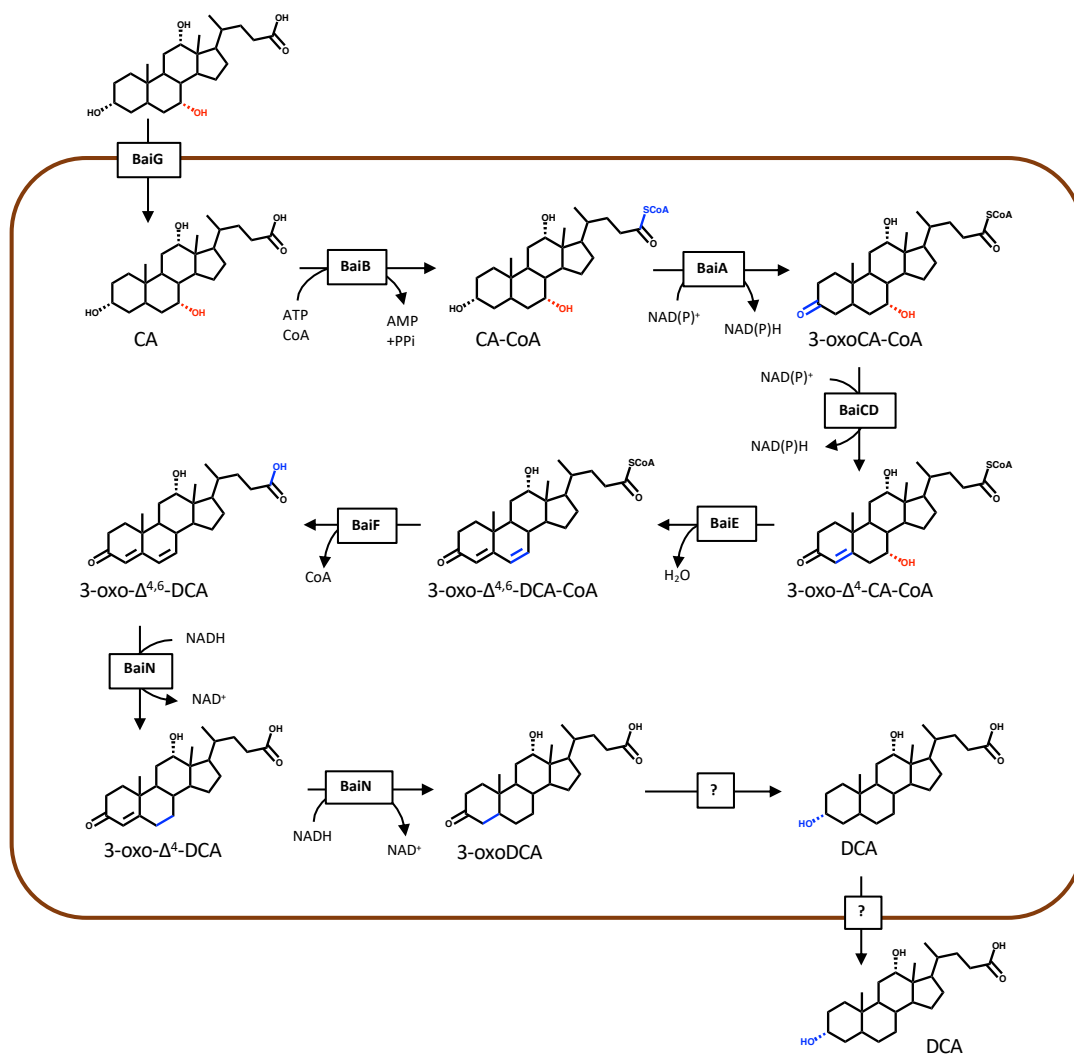


**Figure 1.4 | The Hylemon model of the bile acid 7-dehydroxylation pathway.** The C7-hydroxyl group is highlighted in red. Structural changes on the bile acid molecule at each enzymatic step are indicated in blue.

### • The Funabashi pathway

Recently, Funabashi *et al.* (2019) completed the 7-dehydroxylation pathway, particularly the reductive arm (Figure 1.5). They demonstrated that BaiH, BaiCD and BaiA2 catalyzed the three reductive steps of the pathway. Performing *in vitro* anaerobic assays, they established a set of six enzymes necessary and sufficient for the 8-step conversion of CA to DCA. This set of enzymes includes BaiB, BaiA2, BaiCD, BaiE, BaiF and BaiH. Then, they engineered the pathway into *Clostridium sporogenes*, a commensal incapable of carrying out bile acid 7-dehydroxylation and demonstrated the production of DCA and LCA with the engineered strain<sup>90</sup>.

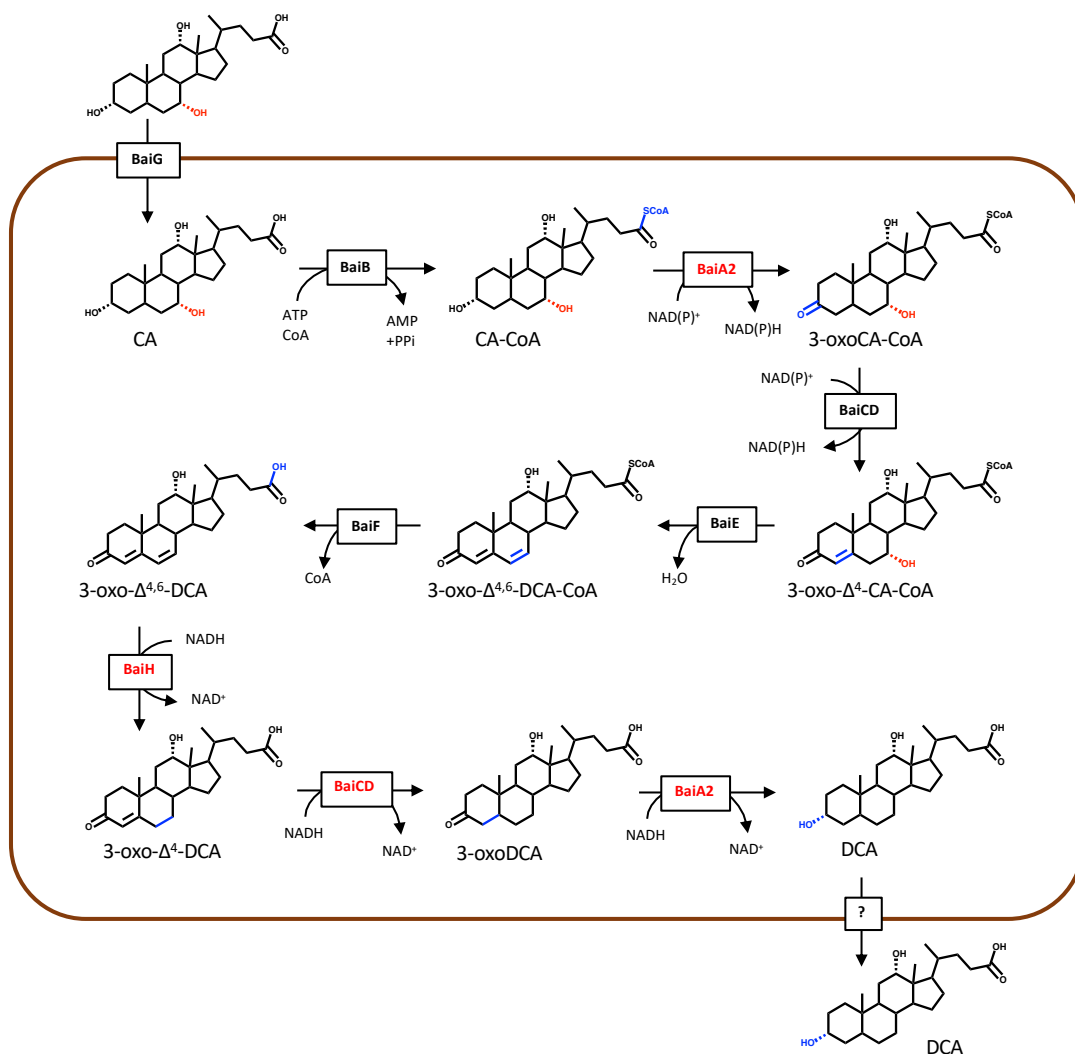


**Figure 1.5 | Most recent model of the bile acid 7-dehydroxylation pathway proposed by Funabashi *et al* (2019).** The enzymes highlighted in red indicate novel findings relative to the Hylemon pathway. The C7-hydroxyl group is highlighted in red. Structural changes on the bile acid molecule at each enzymatic step are indicated in blue.

The function of the enzymes encoded by the genes *bail*, *bailj*, and *bailk* from the *baiBCDEAFGHI* and *baiJKL* operons as well as *baiO* and *baiP*<sup>91</sup> remains to be elucidated. The gene *bailj* is predicted to encode a flavoprotein, possibly involved in C-C double bond oxidation/reduction<sup>1</sup>. BaiP is predicted to be a transporter<sup>91</sup>.

There is variability in terms of substrate specificity amongst the enzymes of the 7-DH-ion pathway. Some enzymes, such as BaiF and BaiK, the two bile acid CoA transferases, or the CoA ligase BaiB show broad substrate specificity while other enzymes (such as BaiCD

and BaiH) are substrate-specific<sup>56,76,88</sup>. For instance, the oxidoreductase BaiCD recognizes only bile acids with 7 $\alpha$ -hydroxyl group (CA and CDCA) and the oxidoreductase BaiH recognizes specifically the 7 $\beta$ -hydroxyl group of UDCA<sup>56</sup>. The bile acid transporter BaiG seems to have higher affinity for BAs with a free 7-hydroxyl group because DCA and 7-oxoCA were transported less efficiently<sup>78</sup>. At present, it is not well established whether murine primary bile acids ( $\alpha$ MCA and  $\beta$ MCA) can be transformed by enzymes of this pathway. A single study explored this point by showing that the two CoA transferases BaiF and BaiK could use  $\beta$ MCA as substrate<sup>88</sup>. However, CoA transferases generally have broad substrate specificity. The ability of other, more substrate-specific enzymes (such as BaiCD, BaiH, BaiE), to transform the 6-hydroxylated murine BAs remains to be investigated.

## 1.5 Benefits and limitations for bile acid 7-dehydroxylation in the gut

Bile acids are generally toxic to bacterial cells because of their detergent effect on the membrane<sup>2</sup>. In the small intestine, the high concentration of bile salts controls microbial growth<sup>92</sup>. The genetics of bile acid resistance are poorly understood, particularly in Gram-positive organisms, which seem to be more sensitive to the deleterious effects of bile acids than Gram-negative bacteria. Furthermore, the ability to withstand bile acids varies amongst bacterial species, and proteins that take up or extrude bile acids, or enzymes that modify and transform the structure of bile salts are likely to play an important role in bile acid resistance. Therefore, the ability to metabolize bile acids might confer the bacteria resistance towards their detergent action.

Hence, bile acid 7-DH-ion could be a detoxification process. As dehydroxylated bile acids have low solubility, these molecules could precipitate at moderately acidic pH<sup>93</sup>. For instance, the solubility of cholic acid in water (pH=7) is 273  $\mu$ M while the solubility of deoxycholic acid is 28  $\mu$ M (10-fold lower)<sup>94</sup>. The precipitation of secondary bile acids in the large intestine may mitigate their toxicity to bacterial cell.

Another hypothesis is that bile acid 7-DH-ion provides a growth and competitive advantage relative to bacteria unable to catalyze this transformation. The 7 $\alpha$ / $\beta$ -DH-ion pathway results in the net consumption of 2 electrons (one NADH) suggesting that BAs are used as electrons acceptors. However, it remains unclear whether this transformation provides a metabolic benefit to the organism. It has been shown that exogenous electron acceptors can serve as sinks for excess electrons derived from fermentation, allowing continued oxidation of the substrate<sup>95</sup>, but this has not been demonstrated for bile acids<sup>22</sup>.

Secondary bile acids are more hydrophobic than primary bile acids and indeed have greater cytotoxicity. Therefore, the synthesis of secondary BA could function to exclude certain bacteria sensitive to these hydrophobic molecules and control the surrounding gut microbial community<sup>22</sup>. By modulating the microbial community through the cytotoxic activity of secondary bile acids, the 7-DH-ing bacteria could create their own niches and thus improve their colonization and survival in the gut.

Several factors influence bile acid 7-dehydroxylation including the host, the bile acid pool, the 7-dehydroxylating bacteria and the gut microbial community.

First, the formation of 7-oxo BAs (with a carbonyl group at C7 position) by 7-dehydroxylating bacteria seems to influence the formation of 7-dehydroxylated secondary bile acid<sup>44,50,96</sup>. High levels of 7-DH-ed bile acids are usually associated with low level of 7-oxo BA intermediates<sup>50</sup>. Hirano *et al.* (1981) isolated 4 strains (I-55, I-102, H-B6, II-27) lacking 7 $\alpha$ -HSDH (enzyme responsible for the formation of 7-oxo groups) and these strains show higher levels of LCA compared to strains carrying a 7 $\alpha$ -HSDH<sup>41</sup>. It is possible that 7-hydroxyl oxidation is a competing transformation with 7-DH-ion. Unraveling the role of the 7-oxo bile acids and their link with 7-DH-ion requires further investigation.

Bile acids induce the *bai* operon but it is not well-established which bile acids participate in the induction. The presence of the 12 $\alpha$ -hydroxyl group in CA (absent in CDCA) increases 7-dehydroxylation activity 5-fold relative to the saturated C12<sup>97</sup>. Additionally, both 5 $\beta$ -H and 5 $\alpha$ -H (allo- bile acids) primary bile acid can induce 7-dehydroxylation activity<sup>98</sup>. Thus, it appears as though several regions of the bile acid structure are recognized by the proteins involved in regulating the expression of the genes encoding the oxidative

branch of the bile acid 7-DH-ion pathway<sup>98</sup>, suggesting that the diversity of BAs produced by the microbiota may regulate 7-DH-ion activity.

Additionally, bile acid competition for the enzymes encoded by the *bai* genes is also likely to modulate bile acid 7-dehydroxylation. *In vitro*, several authors showed that 7-DH-ion is impacted in the presence of additional bile acids. In general, CA either enhances or only slightly reduces the rate of conversion of less abundant BAs such as CDCA, while addition of CDCA significantly decreases the rate of CA conversion<sup>62</sup>. For instance, an increasing concentration of CDCA caused a large decrease in the conversion rate of CA to DCA. In contrast, an increasing concentration of CA caused only a slight decrease in the initial rate of CDCA conversion to LCA<sup>62</sup>. Unraveling the regulation of the enzymes in the 7-DH-ion pathway as well as the competition between distinct bile acids for enzyme active sites will likely be important for our understanding of the difference in 7-DH-ion activity amongst strains *in vitro*<sup>58</sup> as well as between *in vitro* and *in vivo* conditions.

Several studies suggest the cooperative work of two or more microorganisms for the synthesis of 7-dehydroxylated secondary BAs<sup>39,50,59,60,99</sup>. In a minimal consortium of two strains including a 7 $\alpha$ -dehydroxylating *Clostridium* strain 9/1 and a deconjugating *Bacteroides* strain R1, the growth of strain 9/1 depended on the reduction of taurine to H<sub>2</sub>S by the deconjugating strain. The reduced S compound served as a necessary growth factor for the 7-dehydroxylating strain<sup>99</sup>. Similarly, an unknown growth factor secreted by *Ruminococcus productus* was essential for the growth of the rat 7-DH-ing bacterium HDCA-1<sup>39</sup>. This strain could grow in pure culture only if the supernatant of a 48h-culture of *R. productus* was added to liquid medium or streaked on plates<sup>39</sup>. Further, Hirano and Masuda reported an enhancement of 7-DH-ing activity of the '*E. lenta*-like' strain c-25 specifically in mixed culture with *Bacteroides*<sup>50</sup>. The mechanism of enhancement is unclear as the *Bacteroides* strains tested were free of any bile acid activity precluding the potential formation of an intermediate bile acid used preferentially as a substrate. The mechanism likely involves an unidentified metabolite that is primarily intracellular but partially released into the medium (presumably through cell lysis) as the 7-DH-ion enhancement was reproduced by adding cell extract of *Bacteroides* to the growth medium<sup>50</sup>. In both cases, the unknown metabolite (produced by *Ruminococcus productus* and *Bacteroides*) might be a flavin. Addition of flavins to a growth medium *in vitro* enhanced bile acid 7 $\alpha$ -dehydroxylation activity by the 7-DH-ing strain c-25 but not growth (precluding a nutritional role)<sup>100</sup>. Flavins are involved in the bile acid 7-DH-ion pathway: *baiCD* and *baiH* genes encode NADH:flavin dependent oxidoreductases, *baiN* encodes a flavoprotein and the *baiJ* gene is also predicted to encode a flavoprotein<sup>1,56,88</sup>. Another group reported the enhancement of bile acid 7-DH-ion by riboflavin<sup>99</sup>. Similarly, pantothenic acid, which is a precursor of coenzyme A, stimulated 7-dehydroxylation by *C. scindens* VPI 12708. It was proposed that the stimulatory effect was due to the conversion of CA to its CoA-ester, which is used for the initial step of the dehydroxylation pathway<sup>76</sup>. In contrast, the flavin analog acriflavin and ATPase inhibitors (such as N,N-dicyclohexylcarbodiimide, o-phenanthroline) as well as EDTA inhibit bile acid 7-DH-ion<sup>62,84</sup>.

Interestingly, a number of Actinobacteria and fungi capable of 7 $\alpha$ - and 7 $\beta$ -hydroxylating the secondary bile acids DCA and LCA to the 7 $\alpha$ - and 7 $\beta$ -hydroxylated primary bile acids CA/UCA and CDCA/UDCA *in vitro* were identified recently<sup>30,31</sup>. The mycobiota, referring to the fungal community in the human gut, represents approximately 0.03–2% of total gut microorganisms. Studies have shown that the human gut is home to more than 66 genera and 184 species of fungi<sup>101</sup>. 7-hydroxylation of secondary bile acids has never been demonstrated *in vivo* but the potential role of fungi in this process remains a tantalizing possibility that requires further investigation. The *in vivo* 7-hydroxylation of bile acids would clearly influence the 7-dehydroxylated bile acid pool.

There remains much to decipher regarding the interactions of 7-DH-ing organisms with the rest of the gut microbiota. Previous work offers precious few glimpses of potential syntrophic interactions that could alter our view of this microbial group. In particular, inhibition of 7-DH-ion induced by antibiotics or other treatments may in fact be due to the inhibition of the partner strains of 7-DH-ing bacteria rather than to that of 7-DH-ing strains themselves.

## 1.6 Role of bile acid 7-dehydroxylating bacteria in health and disease.

Over the past few decades, it has become clear that bile acid-metabolizing bacteria in the gut are crucial for host health<sup>4,6,102,103</sup>. An important function of bile acids is their role as signaling molecules targeting metabolic organs and tissues as well as immune cells (Figure 1.6). Gut microbial transformations of bile acids are essential as they modify their amount and composition and thus their affinity for the major bile acids receptors, the nuclear Farnesoid X receptor (FXR) and the membrane Takeda G-protein receptor 5 (TGR5). Bile acid 7-DH-ing bacteria are of particular importance as the 7-dehydroxylated secondary bile acids DCA and LCA and their conjugated form are potent activators of TGR5<sup>3</sup> and also agonists of FXR<sup>102</sup>. The gut microbiome and particularly the bile acid 7-dehydroxylating bacteria constitute a target to modulate TGR5 and FXR activity. A shift in microbiome composition, especially in bile acid-metabolizing bacteria could stimulate or protect the host from multiple diseases.

The bile acid-responsive membrane receptor TGR5 is involved in the regulation of host metabolism and inflammation. TGR5 is expressed in a wide variety of metabolic tissues (brown adipose tissue, skeletal muscle, enteroendocrine cells in the intestine, pancreas) but also in immune cells (Kupffer cells, T lymphocytes, monocytes, macrophages) and in neurons and astrocytes<sup>3,6,104</sup>. Conjugated and unconjugated BAs are endogenous TGR5 agonist with LCA, DCA, CDCA and CA being the most potent activators, in descending order<sup>3</sup>.

Another major bile acid receptor is the nuclear receptor FXR. FXR is predominantly expressed in organs that constitute the entero-hepatic circulation (liver and intestine), but is expressed at lower levels in many other organs, tissues and immune cells<sup>6,105</sup>. Bile acids, including the 7-dehydroxylated secondary bile acids, activate FXR according to the following ranking from highest to lowest potency: CDCA > DCA = LCA > CA<sup>102,106</sup>.

Herein, we detail the cases in which bile acid 7-DH-ing bacteria could be involved in the maintenance of the host health.

- *Bile acid homeostasis*

Bile acid synthesis is under a negative feedback loop control through FXR in the ileum<sup>107</sup>. Activation of this nuclear receptor by BAs in ileal enterocytes results in upregulation of fibroblast growth factor 15 (fgf15), which suppresses expression of CYP7A1, the rate-limiting enzyme in the synthesis of bile acids in the liver<sup>108,109</sup>. A recent study demonstrated the role of the microbiota in the regulation of bile acid synthesis and maintenance of a normal bile acid pool<sup>5</sup>. By re-deriving FXR-deficient mice as germ-free, the authors showed that  $\alpha$ -MCA and  $\beta$ -MCA were antagonists for FXR<sup>5</sup>. Indeed, upon deconjugation, primary bile acids undergo 7-dehydroxylation to DCA, LCA, HDCA and MDCA. Thus, by lowering levels of  $\alpha$ -MCA and  $\beta$ -MCA and producing FXR agonists (CDCA > DCA = LCA > CA), deconjugating bacteria and 7-DH-ing bacteria may be involved in the regulation of bile acid synthesis and, more generally, in bile acid homeostasis in the host.

- *Gut mucus homeostasis*

Bile acids may also contribute to homeostasis of the gut mucus layer by stimulating the production of mucus by goblet cells. The mucus layer, composed of mucins secreted by goblet cells, covers the surface of the intestinal epithelium and acts as a physical barrier, protecting the gastrointestinal mucosa<sup>110</sup>. DCA, produced by 7-DH-ing bacteria, was shown to induce mucus secretion, while CA and UDCA had no impact<sup>111</sup>. Another study reported enhanced mucus secretion with DCA compared to that of the primary bile acid CA and CDCA<sup>112</sup>. This finding suggests an indirect role for bile acid 7-DH-ing bacteria in mucus layer homeostasis<sup>111</sup>. Interestingly, Van Den Abbeele (2013), observed that *Clostridium* cluster XIVa, which include the bile acid 7-DH-ing bacteria *C. scindens* and *C. hylemonae*, account for almost 60% of the mucin-adhered gut microbiota in an *in vitro* gut model (colon tissues coated with mucins). These findings suggest that bile acid 7-DH-ing bacteria are in close contact with the mucus layer and consequently could interact



more closely with the epithelium (and goblet cells). Furthermore, it supports a possible role of bile acid 7-DH-ing bacteria in gut mucosa homeostasis<sup>113</sup>.

- *Inflammatory diseases*

Recent work has investigated the impact of secondary bile acids on the colonic mucosa at physiological concentrations and showed, using colon-relevant concentrations, that LCA exerts a protective anti-inflammatory action in the colon<sup>114</sup>. *In vitro*, LCA efficiently prevented the release from colonic epithelial cells of TNF- $\alpha$ , Tumor necrosis factor alpha, a signaling molecule (cytokine) involved in systemic inflammation. Additionally, when administered to mice, LCA was also effective in inhibiting epithelial cytokine release and protected against dextran sodium sulfate (DSS)-induced inflammation<sup>114</sup>. Thus, the activity of 7-DH-ing bacteria (i.e., the production of LCA) can be linked indirectly to mitigation of colon inflammation.

Ulcerative colitis and Crohn's disease are the two main inflammatory bowel diseases (IBD) and are characterized by a chronic and relapsing inflammation of the gastrointestinal tract<sup>115</sup>. It is likely linked to the activation of the mucosal immune system in the intestine and to dysbiosis (deviation from a normal gut microbiota). 7-dehydroxylated secondary BAs (DCA and LCA) were found to be significantly lower in feces of IBD patients relative to healthy individuals<sup>115</sup>. Several studies have described the under-representation of *Clostridium* cluster XIVa (which include the BA 7-DH-ing bacteria) in IBD patients<sup>116</sup>. Recently, Wang *et al.* (2019), showed that diet-induced remission in chronic enteropathy in the dog is associated with increased levels of the secondary bile acids DCA and LCA. Performing metagenomic analysis, they observe an elevation of 7-DH-ing bacterium *C. hiranonis* following dietary therapy. Further, they induced colitis with DSS and gavaged specific-pathogen-free (SPF) mice with either *C. hiranonis* or a PBS vehicle. They showed that mice that received *C. hiranonis* had preserved levels of DCA and an improvement of colitis. Finally, by mining public data they found that the bile acid 7-DH-ing bacterium *C. scindens* was associated with diet-induced remission in human pediatric Crohn's disease cohort<sup>117</sup>.

- *Liver disease*

In cirrhosis, inflammation represses bile acid synthesis via the down regulation of the cholesterol 7 $\alpha$ -hydroxylase CYP7A1 (rate-limiting enzyme in BA synthesis) by pro-inflammatory cytokines<sup>118–120</sup>. As a consequence, there is an approximate 5-fold decrease in the total bile acid pool, and the ratios of DCA/CA and LCA/CDCA are also reduced significantly. Cirrhosis has been correlated with a reduction of the *Clostridium* cluster XIVa concentrations and *Lachnospiraceae*, which include bile acid 7-dehydroxylating bacteria<sup>119,121</sup>. Secondary bile acid, which are produced by these microorganisms, are less abundant in cirrhotic patients than in healthy patients.

Non-alcoholic fatty liver disease (NAFLD) is a spectrum of liver diseases, culminating in non-alcoholic steatohepatitis (NASH)<sup>122</sup>. These diseases are characterized by a dysbiosis that alters the size and composition of the bile acid pool, resulting in impaired signaling to the bile acid receptors FXR and TGR5. NAFLD is often associated with an overrepresentation of *Lachnospiraceae*<sup>123,124</sup> (which include 7-DH-ing bacteria) and elevated levels of secondary bile acids<sup>125</sup>. Hence, the production of secondary 7-dehydroxylated BAs by 7-DH-ing bacteria, may play an indirect role in the development of NAFLD.

- *Glucose metabolism and energy expenditure*

TGR5 activation influences energy expenditure and glucose homeostasis<sup>6</sup>. Activation of TGR5 by secondary BAs triggers the secretion of GLP1 by enteroendocrine cells<sup>105,126,127</sup>. GLP1 stimulates insulin secretion in pancreatic beta cells, thus increasing glucose tolerance (Figure 1.6). Additionally, TGR5 receptors present in brown adipose tissue (BAT) and skeletal muscle cells are activated in response to 7-dehydroxylated BAs which results in increased transcription of type II iodothyronine deiodinase (Dio2) and an increased

conversion of thyroid hormone T4 to T3, ultimately stimulating thermogenesis (Figure 1.6). Thus, activation of TGR5 has the general effect of modulating glucose metabolism and energy expenditure, with a beneficial impact on obesity and diabetes<sup>3,105</sup>. Because they produce the two strongest TGR5 agonists, BA 7-DH-ing bacteria are very likely to play a role in glucose homeostasis and energy expenditure but this link has not been shown and the potential intricacies of host-mediated regulation of abundance of 7-DH-ing bacteria has not been explored.

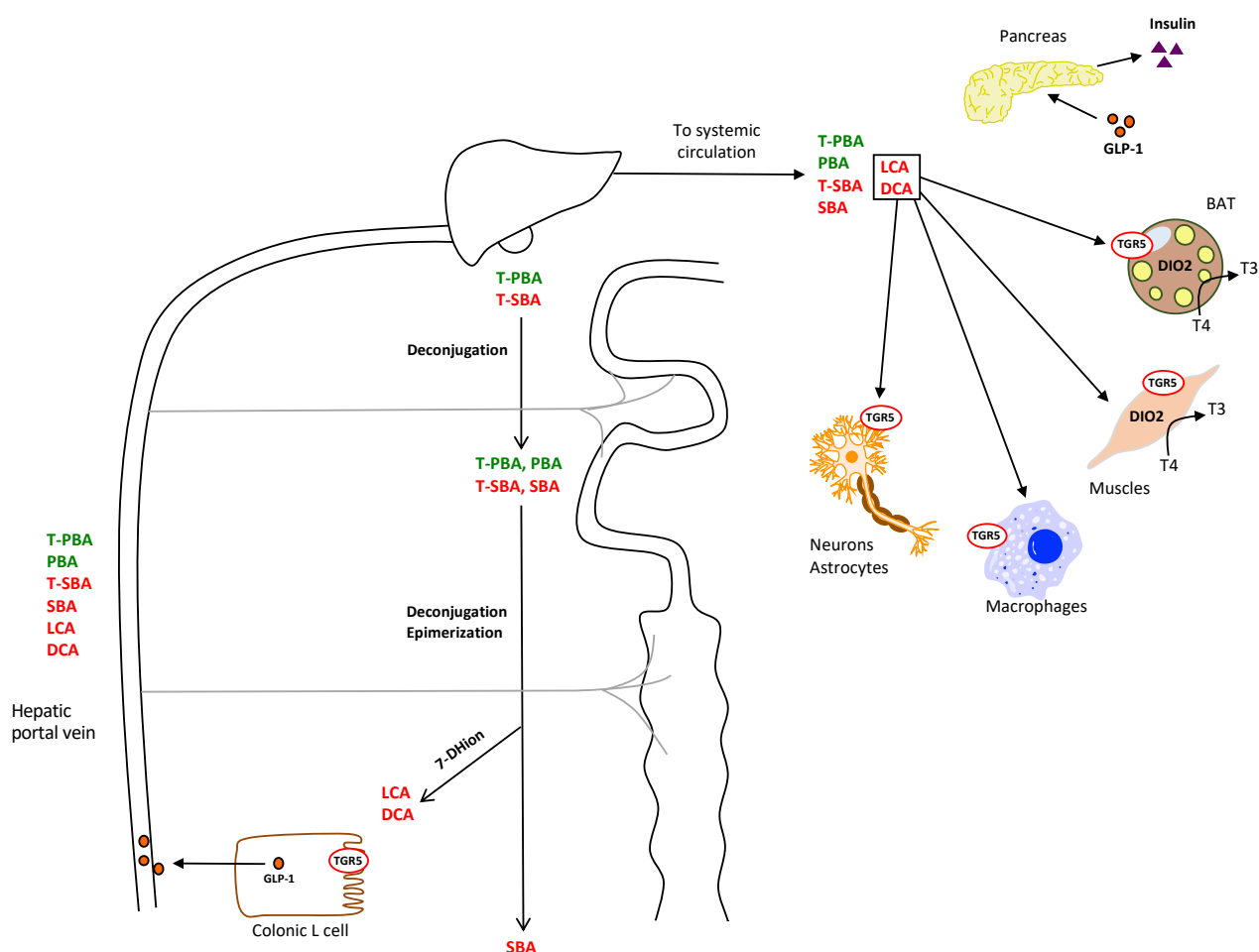


**Figure 1.6| Bile acid 7-dehydroxylating bacteria synthesize secondary bile acid DCA and LCA which are ligands of the bile acid receptor TGR5.** Activation of TGR5 on neurons, neuroglial cells and immune cells leads to reduced inflammation. Targeting the immunomodulatory effect of TGR5 via BA 7-DH-ing bacteria appears a promising avenue for the treatment of inflammation-associated diseases (hepatic encephalopathy, inflammatory bowel diseases, atherosclerosis, NAFLD). TGR5 activation also influences energy expenditure and glucose homeostasis. In the gut, activation of TGR5 on enteroendocrine L-cells triggers the release of glucagon-like peptide 1 which further stimulate insulin release from pancreatic  $\beta$  cells thus influencing glucose metabolism. Activation of TGR5 on brown adipose tissues and skeletal muscles generates an up-regulation of Dio2 and an increased conversion of thyroid hormone T4 to T3, which subsequently stimulate thermogenesis. The effect of 7-DH-ing bacteria-mediated activation of TGR5 on insulin secretion and energy expenditure could be beneficial for the treatment of obesity, type 2 diabetes and NAFLD. T-PBA, tauro-conjugated primary bile acids; T-SBA, tauro-conjugated secondary bile acids; PBA, primary bile acids; SBA, secondary bile acids; DCA, deoxycholic acid; LCA, lithocholic acid

- *Clostridioides difficile* infection

*Clostridioides difficile* infection (CDI) is one of the major hospital-acquired infections linked to antibiotic use in developed countries<sup>128</sup>. The infection is thought to occur through the loss of specific bacterial taxa as a result of the antibiotic treatment. One particular organism associated with resistance to CDI was identified to be *Clostridium scindens*, one of the 7-DH-ing bacteria<sup>7</sup>. DCA and LCA produced by *C. scindens* protect the host against CDI by inhibiting *C. difficile* life cycle (spore germination, cell outgrowth) The presumed mechanism of the loss of colonization resistance is that bile acid 7-DH-ing bacteria are inhibited by antibiotic treatment preceding the onset of CDI, leading to a bile acid pool deficient in secondary BA and indeed, decreased resistance to *C. difficile* germination and colonization (Figure 1.7).

A study investigated the role of secondary bile acids in the colonization resistance against CDI in a simplified gnotobiotic mouse model including a single dehydroxylating species, *C. scindens* ATCC 35704<sup>129</sup>. It was observed that the pool of secondary BAs produced by *C. scindens* delayed the onset of CDI but could not prevent the infection completely<sup>129</sup>. Comparing the secondary BA pool of the gnotobiotic mouse model (SDMDMm12+*C. scindens*) and of specific pathogen free mice (SPF), the authors observed a major difference in the level of  $\omega$ MCA, the 6 $\beta$ -epimer of the primary BA,  $\beta$ MCA. Because  $\omega$ MCA is a potent inhibitor of *C. difficile* spore germination<sup>130,131</sup>, they hypothesized that this low  $\omega$ MCA concentration may have limited the CDI-inhibitory effect of the human derived-*Clostridium scindens* in the gnotobiotic mouse model<sup>129</sup>. The authors concluded that more complete gnotobiotic mouse microbiota are needed to be representative of this pathogen inhibition effect.

Indeed, as reported earlier, the pool of secondary BA is the result of a dynamic collaborative network amongst numerous bile acid-metabolizing commensals. Furthermore, not only are the 7-dehydroxylated DCA and LCA involved in the colonization resistance against *C. difficile*, but other secondary BA also inhibit *C. difficile* spore germination, cell outgrowth and toxin activity<sup>130</sup> (Figure 1.7). The loss of colonization resistance against *C. difficile* leading to infection is likely to be the result not only of the loss of 7-DH-ing organisms but also others commensals metabolizing the bile acid pool.

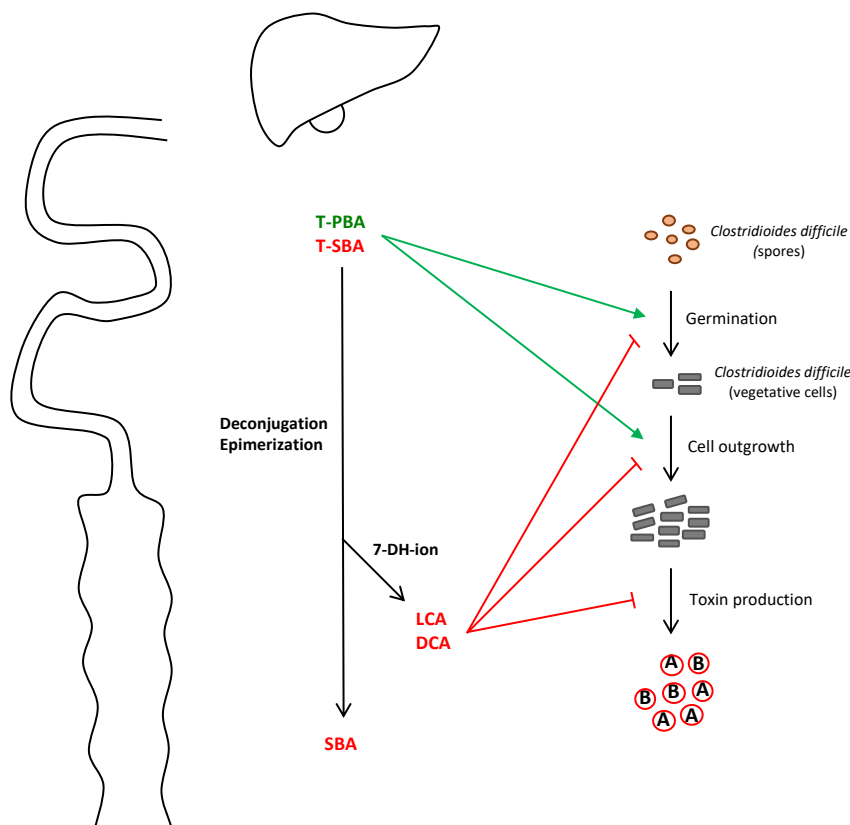


**Figure 1.7 | Bile acid 7-dehydroxylation protects against *C. difficile* infection.** Bile acid 7-DH-ing bacteria play a role in the colonization resistance against *Clostridioides difficile*. The dehydroxylated secondary bile acids DCA and LCA produced by these commensals inhibit the germination of *C. difficile* spores as well as the outgrowth of *C. difficile* cells and toxin production, thus preventing the onset of the disease. They counteract the stimulatory effect of conjugated primary bile acids (e.g., TCA) on spore germination and outgrowth of the pathogen. T-PBA, tauro-conjugated primary bile acids; T-SBA, tauro-conjugated secondary bile acids; SBA, secondary bile acids; DCA, deoxycholic acid; LCA, lithocholic acid.

- **Amebiasis**

Amebiasis is a major cause of diarrhea in developed countries and is triggered by the protozoan parasite *Entamoeba histolytica*. Recently, Burgess *et al.* (2019) presented a novel mechanism by which the bile acid 7-DH-ing bacteria protect the host from this infectious disease. They observed that colonization with the 7-DH-ing bacterium *Clostridium scindens* protected mice against infection by *Entamoeba histolytica* via a neutrophil-mediated response. Transfer of bone-marrow from *C. scindens*-colonized animals into naive mice protected against infection and increased intestinal neutrophils. Administration of DCA alone also protected mice against amebiasis, suggesting that this 7-DH-ed secondary bile acid, produced by *C. scindens*, triggers the immune response protecting the host against infection by the parasite. Finally, in a human cohort, they found that DCA was elevated in the sera of children protected from amebiasis. These findings suggest that the gut microbiota signals to the bone marrow via the production of 7-DH-ed secondary bile acids to foster an innate immune response and provide a non-antigen-specific protection from amebiasis<sup>9</sup>.

Hence, 7-DH-ing bacteria, that produce agonists for TGR5 and FXR receptors, represent a particularly relevant group of microorganisms. Targeting the interplay between microbiota, bile acids, FXR and TGR5 signaling appears to be a particularly promising avenue for the treatment of various metabolic, inflammatory and infectious diseases.<sup>3,4,6,10,105,132</sup>. One could imagine, that by shifting the microbiome composition, especially in bile acid-metabolizing bacteria, we could stimulate or protect the host from multiple diseases. A good example is the fecal microbiota transplantation (FMT) to treat recurrent CDI. Weingarden *et al.* reported that changes in colonic bile acid following FMT is sufficient to restore colonization resistance against the pathogen<sup>8</sup>. 7-DH-ion is intricately dependent on deconjugation by microbes producing BSH (deconjugating enzymes). Therefore, BSH inhibitors<sup>133</sup> represent a promising strategy

to treat diseases associated with an abnormally high secondary bile acid pool such as NAFLD and gastrointestinal cancers. For diseases associated with an abnormally low secondary bile acid pool, stimulating 1) BSH or/and 7-DH-ing activity *in vivo*, and/or 2) stimulating FXR and TGR5 signaling with synthetic agonists (e.g., obeticholic acid, INT-777) constitute also promising approaches to restore impaired BA signalling. Obeticholic acid has been approved by FDA for the treatment of primary biliary cholangitis and is currently under investigation for the treatment of NASH.

## 1.7 Conclusions

The human body is a complex ecosystem where prokaryotic cells interact with host eukaryotic cells. Bile acid signaling illustrates this complex and dynamic interplay between the host and its microorganisms. The maintenance of the bile acid pool is crucial for the host. Therefore, bile acid 7-dehydroxylating bacteria are key commensals of the gut microbiota as they catalyze the transformation of primary bile acid to 7-dehydroxylated bile acid accounting for the majority of the secondary bile acid pool. It is conceivable that considerable diversity and abundance of 7-DH-ing strains has been overlooked due to the primarily cultivation-based approaches for identifying these organisms. In the future, PCR-based identification might be the key to identify new 7-DH-ing organisms.

The picture that emerges from the current state-of-the-art is that the activity of this functional group of organisms plays an important role in health and disease but that these interactions remain poorly explored. It is likely that the size of the population or the activity of these organisms must be tightly regulated by the host in order to prevent accumulation or depletion of the secondary BA pool. Many fundamental questions remain about these organisms, their diversity and abundance *in vivo*, their biogeography and transmission/acquisition, and their impact on host metabolism.

Ultimately, bile acid 7-DH-ing bacteria have the potential for use in prophylactic or therapeutic applications but a more robust understanding of their *in vivo* behavior in health and disease must first be obtained.

## 1.8 Thesis objectives and chapters

The human microbiota refers to the vast array of microorganisms that live on and inside the human body. The highest density of these microorganisms is found in the gut, which is home to trillions of bacteria. Collectively, gut microbes interact with one another and with the host, and contribute to numerous aspects of host health, including nutrient metabolism, homeostasis of intestinal tissues, development of the innate and adaptive immune responses and more generally, defense against intestinal infection by pathogens. The influence of gut microbes on host metabolism and physiology is so essential that a disruption of the normal composition of the microbiota- called dysbiosis- by environmental factors such as diet change or antibiotic treatment, has been associated with many metabolic, immune and infectious diseases. The role of the gut microbiota in host health has been extensively studied and it is now clear that gut microbes are important to maintain intestinal homeostasis. However, the contribution of individual microbial functional groups is poorly understood.

This work aims to investigate bile acid 7-dehydroxylating bacteria – a small group of commensals inhabiting our gut, which play a fundamental role in the maintenance of the host health. These bacteria are involved in bile acid metabolism and produce secondary bile acid metabolites that act as hormones activating host receptors and consequently regulating various metabolic pathways. Furthermore, secondary bile acid produced by these commensals trigger colonization resistance against pathogenic agents such as *Clostridioides difficile* or *Entamoeba histolytica*.

Despite their importance for the host health, bile acid 7-dehydroxylating bacteria remain overlooked. **The objective of my PhD thesis is to provide a better understanding of bile acid 7-dehydroxylation and the microbiology of the organisms carrying out this transformation.** My thesis is divided into five chapters, where the first chapter constitutes this thesis introduction. The following chapter aims to characterize *in vitro* and *in vivo* 7-dehydroxylating activity of *Clostridium scindens* and its colonization dynamics in the mouse

gut. The third chapter of my thesis focuses on bile acid 7-dehydroxylation at the molecular level and probe the existence of a novel biosynthetic pathway. In the fourth chapter, we assess the impact of different microbial communities on the murine bile acid pool. Finally, the fifth chapter is a conclusion of the thesis along with future perspectives for this research.

### 1.8.1 Chapter 2: *In vitro* and *in vivo* characterization of *Clostridium scindens* bile acid transformations

This chapter delineates all the bile acid transformations carried out by the well-known 7-dehydroxylating bacterium *Clostridium scindens*. *In vitro*, microbial transformation of both human (CA, CDCA) and murine primary bile acids was assessed. *In vivo*, we amended gnotobiotic mice lacking 7-dehydroxylating activity with *C. scindens*. We analyzed the bile acid profile along the intestinal tract to locate 7-DH-ing activity in the gut. Finally, using Nanoscale Secondary Ion Mass Spectrometry (NanoSIMS), we identify the ecological niche of *C. scindens* in the murine gut.

### 1.8.2 Chapter 3: Two routes are better than one : the bile acid 7-dehydroxylation pathway revamped.

In this chapter, we investigate a putative vertical bile acid 7-dehydroxylation pathway for the conversion of CA to DCA. By cloning genes from *C. scindens* and purifying individual enzymes suspected to play a role in the pathway, we aim to reconstruct this novel pathway *in vitro* and to identify the core of enzymes involved in this novel pathway.

### 1.8.3 Chapter 4: Biogeography of microbial bile acid transformations along the murine gut.

This fourth chapter focuses not only on 7-dehydroxylation but also on other bile acid transformations including deconjugation, dehydrogenation and epimerization. Using metaproteomics, we characterize the biogeography of these diverse transformations and identify the bacterial species responsible for each transformation in gnotobiotic mice. Furthermore, we analyze the bile acid profile of mice lacking microbes (germ-free mice), with a reduced microbiota (gnotobiotic and antibiotic-treated SPF mice) or a more diverse microbiota (SPF mice). Finally, we quantify expression of genes involved in FXR signaling (*fgf15*), bile acid synthesis (*cyp7a1*) and bile acid detoxification (*sult2a8*) for the different mice models.

### 1.8.4 Chapter 5: Conclusion and future perspectives

The fifth chapter is a summary of the achieved results and presents an outlook for future research.



# Chapter 2 *In vitro* and *in vivo* characterization of *Clostridium scindens* bile acid transformations

Chapter 2 investigates the bile acid transformations carried out by the bile acid 7-dehydroxylating organisms *Clostridium scindens* *in vitro* and *in vivo* and the biogeography of this organism in the murine gut. This work is published as follows:

Solenne Marion, Nicolas Studer, Lyne Desharnais, Laure Menin, Stéphane Escrig, Anders Meibom, Siegfried Hapfelmeier & Rizlan Bernier-Latmani (2018)

*In vitro* and *in vivo* characterization of *Clostridium scindens* bile acid transformations, Gut Microbes, 10:4, 481-503

DOI: [10.1080/19490976.2018.1549420](https://doi.org/10.1080/19490976.2018.1549420).

## Author contributions:

SM carried out the experimental work and wrote the manuscript under the supervision of RBL. NS helped with the animal experiments under the supervision of SH. LD carried out the bile acid analysis at the Mass Spectrometry Facility managed by LM. SE carried out the NanoSIMS analysis under the supervision of AM. NS, LD, LM, SE, AM, SH and RBL gave feedback on the manuscript.



## Abstract

The human gut hosts trillions of microorganisms that exert a profound influence on human biology. Gut bacteria communicate with their host by secreting small molecules that can signal to distant organs in the body. Bile acids are one class of these signaling molecules, synthesized by the host and chemically transformed by the gut microbiota. Among bile acid metabolizers, bile acid 7-dehydroxylating bacteria are commensals of particular importance as they carry out the 7-dehydroxylation of liver-derived primary bile acids to 7-dehydroxylated bile acids. The latter represents a major fraction of the secondary bile acid pool. The microbiology of this group of gut microorganisms is understudied and warrants more attention. Here, we detail the bile acid transformations carried out by the 7-dehydroxylating bacterium *Clostridium scindens* *in vitro* and *in vivo*. *In vitro*, *C. scindens* exhibits not only 7 $\alpha$ -dehydroxylating capabilities but also, the ability to oxidize other hydroxyl groups and reduce ketone groups in primary and secondary bile acids. This study revealed 12-oxolithocholic acid as a major transient product in the 7 $\alpha$ -dehydroxylation of cholic acid. Furthermore, the *in vivo* study included complementing a gnotobiotic mouse line (devoid of the ability to 7-dehydroxylate bile acids) with *C. scindens* and investigating its colonization dynamics and bile acid transformations. Using NanoSIMS (Nanoscale Secondary Ion Mass Spectrometry), we demonstrate that the large intestine constitutes a niche for *C. scindens*, where it efficiently 7-dehydroxylates cholic acid to deoxycholic acid. Overall, this work reveals a novel transient species during 7-dehydroxylation as well as provides direct evidence for the colonization and growth of 7-dehydroxylating bacteria in the large intestine.

## 2.1 Introduction

Bile acids (BAs) are endogenous molecules synthesized from cholesterol in the liver and stored in the gall bladder. Upon meal stimulation, they are released into the duodenum to facilitate the solubilization and absorption of lipids and lipid-soluble vitamins<sup>2</sup>. A major fraction of the BA pool (>95%), actively reabsorbed in the terminal ileum and passively along the entire intestinal tract, returns to the liver through the hepatic portal vein. Only a small proportion of the BA pool (5%) enters the large intestine. This cycle is referred to as the enterohepatic circulation of BAs and occurs several times per day. During the cycle, a small fraction of BAs escapes hepatic uptake and reaches the systemic circulation.

Bile acids act as signaling molecules and are thought to play a key role in the maintenance of the host's health. In addition to their local action in the intestine, they are proposed to reach other organs in the human body (via the systemic circulation)<sup>134</sup>. Bile acid receptors are found on many organs and tissues (e.g., liver, pancreas, intestine, brown adipose tissue), as well as on immune cells, suggesting the broad field of action of these compounds<sup>3</sup>. Bile acids also act indirectly when they activate receptors that induce the release of other signaling molecules. For instance, the activation of the BA receptor Takeda G-protein receptor 5 (TGR5) induces Glucagon-Like Peptide-1 (GLP-1) production by entero-endocrine L-cells, which subsequently potentiates  $\beta$ -cell glucose-induced insulin secretion in the pancreas<sup>4</sup>.

In the human intestinal tract, the two liver-derived primary BAs (Figure 2.1), conjugated cholic acid (CA) and chenodeoxycholic acid (CDCA), undergo several transformations mediated by gut microbes, leading to a large diversity of secondary bile acids. The microbial transformation of BAs in the gut is critical to BA-mediated signaling as it modifies their affinity for specific BA receptors<sup>135</sup>. Bile acid 7-dehydroxylating bacteria are a group of gut commensals of particular importance as they catalyze the dehydroxylation of liver-derived (primary) BAs at the C7 position (i.e., 7-dehydroxylation) and produce 7-dehydroxylated BAs, which represent a large fraction of the secondary BA pool in the large intestine. Bile acids transformed by these bacteria are agonists for TGR5, which is involved in

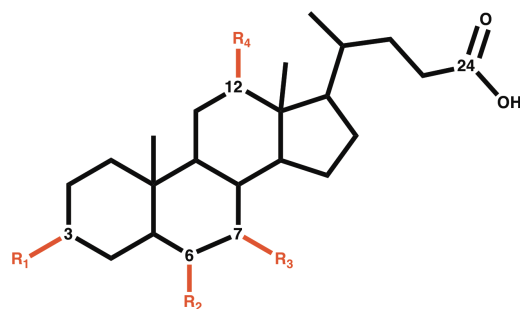
the regulation of metabolism and energy expenditure as well as inflammation<sup>105</sup>. In addition, BAs lacking the 7-hydroxyl group are also associated with protection from infection by a specific intestinal pathogen, *Clostridium difficile*<sup>136</sup>.

The microbial transformations undergone by BAs in the gut play an important role in health<sup>135</sup>, and modulation of the bile acid pool composition represents a promising avenue for the prevention and treatment of various diseases<sup>102</sup>. Perturbation of the bile acid pool is linked to major metabolic diseases (e.g., obesity, type 2 diabetes, non-alcoholic fatty liver disease)<sup>10</sup>, cardiovascular diseases (e.g., atherosclerosis)<sup>10</sup>, inflammatory diseases (e.g., inflammatory bowel disease), gastrointestinal cancers<sup>137</sup>, as well as *Clostridium difficile* infection<sup>136</sup>. Collectively, these diseases exact a heavy socio-economic toll due to their increasing occurrence and severity in first-world countries. Bile acid metabolizing bacteria, particularly 7-dehydroxylating organisms, represent a promising target to modulate the bile acid pool and consequently host physiology<sup>138</sup>. However, much remains to be deciphered about this group of microorganisms, including their metabolism, diversity, abundance in the gut, and colonization dynamics in the host.

The spatial organization of the gut microbial community is suggested to be linked to their function within the host<sup>92,139</sup>. Only one study, conducted by Midvedt and Norman (1968), has explored the distribution of bile acid-metabolizing bacteria along the intestinal tract (in this case in rats)<sup>34</sup>. They pointed out that the organisms responsible for the elimination of the 7 $\alpha$  hydroxyl of bile acids are found in the cecum and feces of rats. Other studies have probed the bile acid composition longitudinally along the intestinal tract and observed the formation of deoxycholic acid (DCA) and lithocholic acid (LCA), the products of 7 $\alpha$ -dehydroxylation of CA and CDCA, respectively, mainly in the cecum and colon<sup>5</sup>, suggesting the large intestine is a colonization site for 7-dehydroxylating bacteria. However, concluding the presence or absence of certain microorganisms only based on the *in vivo* bile acid composition lacks rigor since it does not link specific organisms with their *in vivo* activity. Several studies reported discrepancies in bile acid transformations by bacteria *in vitro* or *in vivo*. For instance, Narushima *et al.* (1999), observed that *Clostridium* sp. TO-931 (now known as *Clostridium hiranonis*<sup>140</sup>) did not deconjugate tauro-conjugated bile acids in germ-free mice, although its ability to deconjugate taurocholic acid (TCA) was shown *in vitro*<sup>60</sup>. Furthermore, side chain conjugation of bile acids precludes 7-dehydroxylation<sup>20</sup>. Thus, if the 7-dehydroxylating bacteria does not synthesize bile salts hydrolases (deconjugating enzymes), they will rely on deconjugating bacteria to perform 7-dehydroxylation. *Clostridium hiranonis* is a known 7 $\alpha$ -dehydroxylating and deconjugating species, but it did not perform deconjugation nor 7 $\alpha$ -dehydroxylation *in vivo* even in the presence of an additional deconjugating strain (*Bacteroides diastonis* K-5)<sup>60</sup>. Bile acid 7 $\alpha$ -dehydroxylation *in vivo* is likely to be influenced by various factors including pH, oxygen partial pressure<sup>62</sup>, enzymatic co-factors (e.g., flavins)<sup>100</sup>, the bile acid pool, and gut microbes. Examples of intestinal bacteria influencing bile acid 7 $\alpha$ -dehydroxylation include *Bacteroides* sp. and a *Ruminococcus* strain. *Bacteroides* sp. enhances bile acid 7 $\alpha$ -dehydroxylation by *Eubacterium* sp strain c-25 via an unknown mechanism<sup>50</sup>. The *Ruminococcus* strain secretes a soluble factor necessary for the growth of the 7 $\alpha$ -dehydroxylating strain HDCA-1<sup>39</sup>. Hence, the production of 7-dehydroxylated secondary bile acid results from complex interactions between the host, the 7-dehydroxylating species and the gut microbial community.

The model organism used in this study, *Clostridium scindens*, is one of the major 7-dehydroxylating bacteria found in humans<sup>45,141</sup> and rodents<sup>38</sup>. This bacterium was first isolated from feces of a patient with colon cancer and characterized by Holdeman and Moore in 1973<sup>97</sup>. Forty-two years later, *C. scindens* was identified as a potential protective gut commensal against *Clostridium difficile* infection<sup>136</sup>. The 7-dehydroxylated secondary bile acids (e.g., DCA and LCA) produced by bile acid 7-dehydroxylating bacteria impact *C. difficile* spore germination and outgrowth, thus preventing the onset of disease<sup>142,143</sup>.

The objectives of the study are 1) to investigate the bile acids transformations performed by *Clostridium scindens* *in vitro*, and *in vivo* in a gnotobiotic mouse model, and 2) to explore its colonization dynamics in the murine intestinal tract using Nanoscale Secondary Ion Mass Spectrometry (NanoSIMS)<sup>144</sup>. This study provides a better understanding of the microbiology of 7-dehydroxylating organisms, and is motivated by the fact that these commensals constitute a direct link between bile acids and host health.



Bile Acid Name	Abbreviations	R1	R2	R3	R4	ketone group
Cholic acid	CA	3 $\alpha$		7 $\alpha$	12 $\alpha$	-
Chenodeoxycholic acid	CDCA	3 $\alpha$		7 $\alpha$		-
$\alpha$ -Muricholic acid	$\alpha$ MCA	3 $\alpha$	6 $\beta$	7 $\alpha$		-
$\beta$ -Muricholic acid	$\beta$ MCA	3 $\alpha$	6 $\beta$	7 $\beta$		-
Ursodeoxycholic acid	UDCA	3 $\alpha$		7 $\beta$		-
Deoxycholic acid	DCA	3 $\alpha$			12 $\alpha$	-
Lithocholic acid	LCA	3 $\alpha$				-
3-oxodeoxycholic acid	3-oxoDCA				12 $\alpha$	R1
3-oxocholic acid	3-oxoCA			7 $\alpha$	12 $\alpha$	R1
7-oxodeoxycholic acid	7-oxoDCA	3 $\alpha$			12 $\alpha$	R3
7-oxolithocholic acid	7-oxoLCA	3 $\alpha$				R3
12-oxolithocholic acid	12-oxoLCA	3 $\alpha$				R4

**Figure 2.1 | Structure of selected human and murine bile acids.** Bile acids differ by the position of the hydroxyl groups on the molecule. CA and CDCA are found both in humans and rodents, while UDCA and the muricholic acids are primary BAs synthesized only in rodents. In humans, UDCA is produced from CDCA by microbial enzymes and therefore, is considered as a secondary bile acid. The full list of BAs considered in this study and their structures is included in supplemental information (Table S1).

## 2.2 Material and Methods

### 2.2.1 Oligo-MM12 Microbiota and gnotobiotic sDMDMm2 mice

The sDMDMm2 gnotobiotic mouse model was used in this study. sDMDMm2 mice are colonized with a mouse-intestine derived 12-species mouse microbiota (Oligo-MM12) consisting of the following bacterial species: *Acutalibacter muris* sp. nov. KB18 (DSM 26090), *Flavonifractor plautii* YL31 (DSM 26117), *Clostridium clostridioforme* YL32 (DSM 26114), *Blautia coccoides* YL58 (DSM 26115), *Clostridium innocuum* I46 (DSM 26113), *Lactobacillus reuteri* I49 (DSM 32035), *Enterococcus faecalis* KB1 (DSM 32036), *Bacteroides caecimuris* sp. nov. I48 (DSM 26085), *Muribaculum intestinale* sp. nov. YL27 (DSM 28989), *Bifidobacterium longum* subsp. *animalis* YL2 (DSM 26074), *Turicimonas muris* sp. nov. YL45 (DSM 26109) and *Akkermansia muciniphila* YL44 (DSM 26127). A detailed description of the Oligo-MM12 consortium species and description of novel taxa are provided by Brugiroux *et al.*, (2016)<sup>145</sup> and Lagkouvardos *et al.*, (2016)<sup>37</sup>. A group of seven sDMDMm2 mice (6–12 week-old males) was used for the experiment. Gnotobiotic sDMDMm2 mice (Brugiroux *et al.*, 2016) were established and maintained at the Clean Mouse Facility (CMF) of the Department of Clinical Research of the University of Bern. All animal experiments were performed in accordance with the Swiss Federal and the Bernese Cantonal regulations and were approved by the Bernese Cantonal ethical committee for animal experiments under license number BE 82/13.

### 2.2.2 Bacterial strains and culture conditions

*Clostridium scindens* ATCC 35704 (Morris *et al.*, 1985)<sup>141</sup> was grown in BHIS-S medium, which contains 37g brain heart infusion (BHI), 5 g yeast extract, 40 mL salts solution (0.2 g CaCl<sub>2</sub>, 0.2 g MgSO<sub>4</sub>, 1 g K<sub>2</sub>HPO<sub>4</sub>, 1g KH<sub>2</sub>PO<sub>4</sub>, 10g NaHCO<sub>3</sub>, and 2g NaCl in 1 L ddH<sub>2</sub>O), 1g L-cysteine and 2 g fructose per L ddH<sub>2</sub>O or on BHIS-S agar (BHIS-S + 15g/L agar). The *in vitro* experiments were conducted in an anaerobic chamber (Coy Laboratory Products, 95% N<sub>2</sub>, 5% H<sub>2</sub>) at 37°C. For the *in vivo* experiments, erythromycin (10 µg/mL) was added to BHIS-S agar in order to select for *C. scindens* ATCC 35704 from mice intestinal content samples for quantification purposes. The selective plates (BHIS-S + erythromycin) were incubated in an anaerobic chamber (Don Whitley A45 HEPA, 10% CO<sub>2</sub>, 10% H<sub>2</sub>, 80% N<sub>2</sub>) for 72 h at 37°C.

### 2.2.3 Impact of bile acids on bacterial growth

We assessed the impact of human (CA and CDCA) and murine (αMCA, βMCA, UDCA) primary and secondary (3-oxoDCA, 12-oxoLCA, DCA) bile acids on *C. scindens* growth *in vitro*. Cholic acid (CA, ref. A11257) was purchased from VWR, ursodeoxycholic acid (UDCA, ref. U5127) from Sigma-Aldrich, chenodeoxycholic acid (CDCA, ref. C0940-000), alpha-muricholic acid (αMCA, ref. C1890-000), beta-muricholic acid (βMCA, ref. C1895-000), deoxycholic acid (DCA, ref. C1070-000), 3-oxodeoxycholic acid (3-oxoDCA, ref. C1725-000) and 12-oxolithocholic acid (12-oxoLCA, ref. C1650-000) from Steraloids. These bile acids were dissolved in 100% ethanol and then, added to Erlenmeyer flasks with autoclaved and anoxic 150mL BHIS-S liquid medium (final concentration of ethanol in the medium ≤ 1%) to a final concentration of 100 µM. The concentration of 100 µM was chosen based on other studies investigating bile acid transformations *in vitro* but also to ensure the detection of minor transformation products<sup>44,46</sup>. An additional condition (CDCA at a concentration of 200 µM) was included as this concentration was also used for the bile acid transformation experiments *in vitro*. A control without bile acid (but with the ethanol vehicle) and a sterile control were prepared in parallel. For each bile acid condition or the controls, cultures were prepared in triplicate. Samples were taken regularly and OD<sub>600</sub> was immediately measured with a V-1200 spectrophotometer (VWR).

### 2.2.4 Bile acid transformations experiments

Bile acid containing media and the controls (without bile acid) were inoculated with *C. scindens* to an initial OD<sub>600</sub> value of 0.050. Bile acids were probed at a concentration of 100 µM albeit a higher concentration was used for CDCA (200 µM) because of the low

conversion to LCA and the attendant detection issues. This experiment was done in triplicates. A sterile control and an additional control without bile acid (but with the ethanol vehicle) were prepared in triplicates.

The tubes were incubated in an anaerobic chamber (Coy Laboratory Products, 95% N<sub>2</sub>, 5% H<sub>2</sub>) at 37°C. Samples were collected periodically and OD<sub>600</sub> was measured immediately after sampling. Each sample (1 mL) was centrifuged at 4°C for 5 minutes at 16,000 x g. The supernatant (SUP) was separated from the pellet (PEL) and placed in a new epitube. For experiments with DCA, 12-oxoLCA and 3-oxoDCA, an additional 1 mL of culture was collected. This sample containing both supernatant and biomass was named 'Total' (TOT). Samples (pellets, supernatants, total) were stored at -20°C to await bile acid analysis.

An additional experiment was conducted on a few PEL samples to determine whether the bile acids present in the pellet (biomass) are located intracellularly (in the cytoplasm) or are bound to the cell envelope. The selected pellets (CA t=68 h, CDCA t=44 h) were resuspended in sterile water containing lysozyme (1 mg/mL) and incubated for 1 h at 37°C. After cell lysis, samples were ultra-centrifuged (20,000 x g) at 4°C, for 30 min. The supernatant (corresponding to the cytoplasmic fraction) was collected in another epitube. The pellet (representing the cell envelope fraction) was also retained. All samples were stored at -20°C to await bile acid analysis.

## 2.2.5 Cell-free extract (CFE) experiment

This experiment was designed to test whether the lack of intracellular transport of bile acids was responsible for the limited transformation of 3-oxoDCA and DCA by *C. scindens*. As a positive control, we also included 12-oxoLCA. This experiment was performed under anaerobic conditions, as bile acid 7-dehydroxylation is sensitive to oxygen<sup>62</sup>. *C. scindens* was grown in BHIS-S medium. When bacterial growth reached mid-exponential phase (OD<sub>600</sub>=0.7), CA was added to the culture to a final concentration of 100 µM, in order to induce the synthesis of bile acid inducible (bai) enzymes. After 90 min of incubation with CA, the culture was centrifuged and the supernatant (containing CA) removed. The pellets of *C. scindens* cells were resuspended in BHIS-S containing 2 mg/mL lysozyme and incubated at 37°C for 90 min. After cell lysis, 3-oxoDCA, DCA, or 12-oxoLCA were added separately to the medium (Cf=100 µM). This experiment was done in triplicates and samples were collected every 2 h during 10 h. Samples were stored at -20°C to await bile acid analysis.

## 2.2.6 Preparation of Standard Solutions

Stock solutions [10 mM] of each internal and external BA standard were prepared in methanol. Deuterated LCA, DCA, CDCA, CA, TUDCA and TCA (Table S2) were used as internal standards (ISTD). Individual standard solutions [100 µM] were mixed together and diluted with ammonium acetate [5 mM] – methanol (50:50, v/v) to construct external standard curves between 1 and 10,000 nM. Each calibration level was spiked with the mixed ISTD solution [4 µM] for a final concentration of 500 nM. Additionally, 50 µL of BHIS-S medium was added to each calibration level of the standard curves used for quantification of *in vitro* supernatant samples (SUP) to account for matrix effects.

## 2.2.7 Bile Acid Extraction from cell cultures

Supernatants (SUP) from *in vitro* experiments were spiked with the mixed ISTD solution [4 µM] and diluted with ammonium acetate [5 mM] – methanol (50:50, v/v) to obtain the same final concentration of ISTD [500 nM].

BAs contained in pellets (PEL), in total (TOT) and cell-free extract (CFE) samples were extracted with the following protocol. Freeze-dried samples were first spiked with 100 µL of mixed ISTD solution [100 µM] and then extracted with 500 µL of ice-cold alkaline acetonitrile in 2 mL tubes filled with 0.5 mm glass beads using an automated Precellys 24 Tissue Homogenizer (Bertin Instruments) at 6,500 rpm for 3x30 s with a 30 s break. Samples were vigorously vortexed, and continuously shaken for 1 h at room temperature. The mixtures were centrifuged at 16,000 x g for 10 min and the supernatants collected and lyophilized in a rotational vacuum

concentrator (Christ) before reconstitution in 1 mL of ammonium acetate [5mM] – methanol (50:50, v/v) pH 6. The reconstituted samples were further diluted 20 times in the same solution prior to LC-MS injection.

### 2.2.8 Isotopic labeling of *C. scindens* cells

*C. scindens* was serially grown ( $\geq 50$  generations) in medium composed of a 9:1 ratio of Celtone Complete Medium (CCM -  $^{13}\text{C}$ , 98%+,  $^{15}\text{N}$ , 98%+) to BHIS-S1/2 medium. BHIS-S1/2 corresponds to a 1:1 mixture of BHIS-S medium and sterile ddH<sub>2</sub>O amended with 5 g/L of Celtone Base Powder (CBP -  $^{13}\text{C}$ , 98%+,  $^{15}\text{N}$ , 98%+). *C. scindens* did not grow in the CCM alone and required the amendment of a small volume of BHIS-S1/2. The final labeled medium contained only a small amount of unlabeled nutrients (coming from BHIS-S).

An unlabeled culture of *C. scindens* (control) was prepared following the same protocol but with unlabeled CCM and unlabeled CBP. Labeled CCM (ref. CGM-1040-CN-0.1) and CBP (ref. CGM-1030P-CN-PK), as well as unlabeled CCM (ref. CGM-1040-U-0.1) and CBP (ref. CGM-1030P-U-PK) were purchased from Cambridge Isotope Laboratories.

### 2.2.9 *In vitro* experiment: dilution of *C. scindens* isotopic labeling in unlabeled medium.

*C. scindens* was labeled *in vitro* according to the procedure described above. The labeled cells were transferred into BHIS-S medium (lacking labeled nutrient) and incubated anaerobically at 37°C for 24 h while sampling periodically. Growth was quantified using OD<sub>600</sub> measurement. All the samples were fixed in 2.5% glutaraldehyde and rinsed at least three times with sterile ddH<sub>2</sub>O. Samples were stored at 4°C to await NanoSIMS analysis.

### 2.2.10 Animal experiment

Cultures of isotopically labeled and unlabeled (control) *C. scindens* were centrifuged and washed in PBS-1X prior to mouse gavage. A total of seven SDMDMm2 mice were included in our study. Four mice were inoculated with  $10^9$  labeled *C. scindens* cells (L-mice) and two mice with  $10^9$  unlabeled *C. scindens* cells (U-mice). A sample of the inoculum was kept for NanoSIMS analysis. One additional mouse was used as a control and was gavaged only with PBS-1X. Only for bile acid analysis, two additional control mice were included in the study to have an equal number of mice in the two groups compared (Figures 2.6, 2.7 and 2.8). Six and twenty-four hours after inoculation, 2 'L-mice' and 1 'U-mice' were sacrificed. The control mouse was sacrificed at the end of the experiment ( $t_{24\text{h}}$ ). The content of four intestinal compartments were collected: two parts of the small intestine (jejunum and ileum), the cecum and the colon. For each sample, the intestinal content was divided into 3 tubes for the different analyses. The samples for NanoSIMS (intestinal contents samples and *C. scindens* inoculum) were fixed with 2.5% glutaraldehyde (for a minimum of 3 h). The fixed samples were rinsed (at least 3 times) with sterile ddH<sub>2</sub>O and stored at 4°C to await NanoSIMS analysis. The samples for bile acid analysis were stored at -20°C. The samples for *C. scindens* quantification were directly plated on a selective medium (BHIS-S + erythromycin) and incubated in an anoxic chamber at 37° for 72 h. In the results part, *C. scindens* counts are expressed as colony-forming unit (CFU) per gram of fecal content. The values indicated in the paper represent the mean  $\pm$  standard deviation.

### 2.2.11 NanoSIMS sample preparation and analysis

Two types of samples were analyzed by NanoSIMS: the *in vitro* samples (*C. scindens* culture), and the *in vivo* samples (mouse intestinal contents). Regarding the *in vivo* experiment, samples of one L-mouse per time point were chosen for the analysis.

The fixed samples (from the *in vitro* and *in vivo* experiments) were mounted on silicon wafers: for each sample, 5 to 10  $\mu\text{L}$  of bacterial suspension was deposited in the center of the silicon wafers and dried at 37°C. The silicon wafers were then coated with 10 nm of gold to avoid charging effects. The distribution of the secondary ions species  $^{12}\text{C}^{15}\text{N}^-$ ,  $^{12}\text{C}^{14}\text{N}^-$ ,  $^{12}\text{C}^{13}\text{C}^-$ , and  $^{12}\text{C}^{12}\text{C}^-$  on bacterial cells was mapped with a NanoSIMS 50L (Cameca) operating at a mass resolution of  $>9000$  (Cameca definition), sufficient to resolve these

masses from potential mass interferences. Images of typically 30x30µm<sup>2</sup> with a resolution of 256x256 pixels and a primary beam diameter of about 120 nm were collected across the samples. Each NanoSIMS image consists of 5 sequential images that were drift corrected, and accumulated using the software L'IMAGE (developed by Dr. Larry Nittler, Carnegie Institution of Washington, USA). Nitrogen and carbon isotopes ratio images were obtained by taking the ratio between the cumulated <sup>12</sup>C<sup>15</sup>N<sup>-</sup>, <sup>12</sup>C<sup>14</sup>N<sup>-</sup> and <sup>12</sup>C<sup>13</sup>C<sup>-</sup>, <sup>12</sup>C<sup>12</sup>C<sup>-</sup> images, and reported in the delta notation against a control sample of normal isotopic composition measured several times during the same run:  $R \text{ (in ‰)} = \left( \frac{R_{\text{sample}}}{R_{\text{control}}} - 1 \right) \times 1000$ , where R represents either <sup>15</sup>N/<sup>14</sup>N or <sup>13</sup>C/<sup>12</sup>C, respectively.

Regions of interest (ROIs) were drawn around single *C. scindens* cells or small cluster of cells with the software L'IMAGE to quantify mean δ<sup>15</sup>N enrichments of the *C. scindens* cells along the intestinal tract or in BHIS-S medium (for the *in vitro* experiment).

## 2.2.12 Bile acid extraction from intestinal content

Approximately 10 milligrams of freeze-dried intestinal contents were homogenized with 200 µL of ISTD solution ([1mM or 25µM] depending on the intestinal compartment) in 2 mL tubes filled with 2.8 mm zirconium oxide beads. Homogenization was performed using an automated Precellys 24 Tissue Homogenizer (Bertin Instruments) at 5000 rpm for 1x20 s. Mixed samples were equilibrated on ice for 1 h. An amount of 500 µL of ice-cold alkaline acetonitrile (5% ammonia in acetonitrile) was added to the homogenates, which were then vigorously vortexed, and continuously shaken for 1 h at room temperature. The mixtures were centrifuged at 16,000 x g for 10 min and the supernatants collected. The pellets were extracted with another 500 µL of ice-cold alkaline acetonitrile. Supernatants from the two extractions steps were pooled and lyophilized in a rotational vacuum concentrator (Christ) before reconstitution in 100 µL of ammonium acetate (5 mM) – methanol (50:50, v/v) pH 6 and stored at -20°C. Supernatants were diluted according to the intestinal compartment (4000 times for the small intestine samples and 100 times for the cecum and colon samples) for LC-MS injection.

## 2.2.13 UHPLC-HRMS Analyses

Both qualitative and quantitative analyses were conducted on an Agilent 6530 Accurate-Mass Q-TOF LC/MS mass spectrometer coupled to an Agilent 1290 series UHPLC system (Agilent Technologies). The separation was achieved using a Zorbax Eclipse-Plus C18 column (2.1 × 100 mm, 1.8 µm; Agilent Technologies) heated at 50°C. A binary gradient system consisted of ammonium acetate [5 mM] pH 6 in water as eluent A and acetonitrile as eluent B. The sample separation was carried out at 0.4 mL/min over a 22 min total run time using the following program: 0–5.5 min, isocratic 21.5% B; 5.5–6 min, 21.5–24.5% B; 6–10 min, 24.5–25% B; 10–10.5 min, 25–29% B; 10.5–14.5 min, isocratic 29% B; 14.5–15 min, 29–40% B; 15–18 min, 40–45% B; 18–20.5 min, 45–95% B, 20.5–22 min, isocratic 95%. The system was re-equilibrated in initial conditions for 3 min. The sample manager system temperature was maintained at 4°C and the injection volume was 5 µL. Mass spectrometer detection was operated in negative ionization mode using the Dual AJS Jet stream ESI Assembly. The QTOF instrument was operated in 4 GHz high-resolution mode (typical resolution 17,000 (FWHM) at m/z 1000) in profile mode and calibrated in negative full scan mode using ESI-L solution (Agilent Technologies). Internal calibration was performed during acquisition via continuous infusion of a reference mass solution [5 mM purine, 1 mM HP-921 (Agilent reference mass kit, Agilent Technologies) in 95% MeOH acidified with 0.1% formic acid] and allowed to permanently achieve a mass accuracy better than 5 ppm. HR mass spectra were acquired over the range of m/z 100–1700 at an acquisition rate of 5 spectra/s. AJS settings were as follows: drying gas flow, 8 L/min; drying gas temperature, 300°C; nebulizer pressure, 35 psi; capillary voltage, 3500 V; nozzle voltage, 1000 V; fragmentor voltage, 175 V; skimmer voltage, 65 V; octopole 1 RF voltage, 750 V. Data were processed using the MassHunter Workstation (Agilent Technologies). According to this method, 40 bile acids (SI Table 2) were quantified by external calibration curves and corrected with internal standards. Extracted ions chromatograms (EIC) were based on a retention time (RT) window of ±0.5 min with a mass-extraction-windows (MEW) of ±30 ppm centered on m/z theor of each bile acid. For each BA, the

limits of detection (LODs) were estimated by using the signal-to-noise ratio (S/N) equal to or over 3, values calculated automatically by the program after injection of serially diluted calibration standard solutions (Table S2).

#### 2.2.14 Statistical analysis

All statistical analyses were performed using GraphPad Prism 7 software (GraphPad Software). The statistical tests used are indicated in the figure legends. P values < 0.05 were considered statistically significant.



## 2.3 Results

### 2.3.1 *Clostridium scindens* growth in the presence of human and murine bile acids *in vitro*.

OD<sub>600</sub> measurements were used to quantify the growth of *Clostridium scindens* as a function of time and to assess the impact of primary bile acids on the growth of this organism (Figure 2.2a). The primary bile acids CA, UDCA, αMCA and βMCA had no significant effect on *C. scindens* *in vitro* compared to the control cultures without bile acids. The biomass was maximal after 24 h of incubation in media containing CA (OD<sub>max</sub> ≈ 1.32 ± 0.015), UDCA (1.38 ± 0.025), αMCA (1.35 ± 0.015) and after 28 h of incubation in βMCA medium (1.43 ± 0.060). In the absence of bile acids (i.e., the control), a peak cell density of OD<sub>600</sub>=1.40 ± 0.021 was reached at 24 h of incubation. Of all the primary bile acids tested, only CDCA had a significant impact on *C. scindens* growth, resulting in a slower growth rate, a reduced peak cell density and a lower end point cell density in a dose-dependent manner. The maximal cell density was reached after 24 h and 28 h of incubation in the media containing CDCA 100μM (1.16 ± 0.016) and CDCA 200μM (1.03 ± 0.023), respectively. Overall, *C. scindens* is resistant to most primary bile acids *in vitro*. Additionally, we also investigated the impact of selected secondary bile acids (DCA, 12-oxoLCA and 3-oxoDCA) on the growth of *C. scindens*. These compounds did not exhibit any evidence of toxicity at a concentration of 100 μM (Figure 2.2b). Next, we investigated the bile acid transformations performed by *C. scindens* *in vitro*.

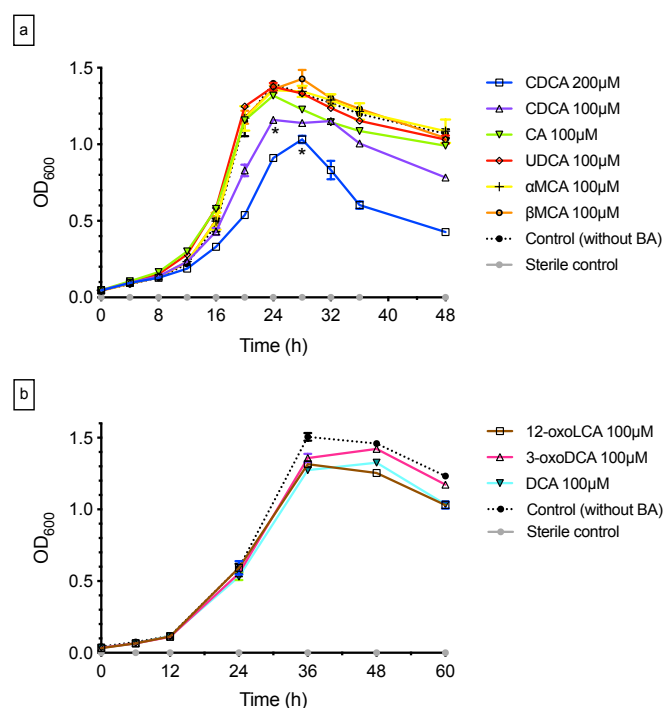


**Figure 2.2| Impact of primary and secondary bile acids on *C. scindens* growth.** *C. scindens* was grown in BHIS-S medium containing a) one primary bile acid (CA, CDCA, UDCA, α-MCA, β-MCA) or b) one secondary bile acid (DCA, 3-oxoDCA, 12-oxoLCA). A control without bile acids and one sterile control were prepared in parallel. For each bile acid condition or the controls, cultures were prepared in triplicate. Growth of *C. scindens* was quantified with OD<sub>600</sub> measurements of samples collected from triplicate cultures of *C. scindens*. Each symbol indicates the mean and the standard deviation. Statistical analysis used the Holm-Sidak test to compare the maximal cell density mean of each bile acid condition to the maximal cell density mean of the control without bile acid. The absence of a symbol under the maximal density time point indicates that there was no statistically significant difference ( $p>0.05$ ) relative to the control group (\*= $p<0.05$ ).

### 2.3.3 *In vitro* bile acid transformations by *Clostridium scindens*

In order to investigate *C. scindens* bile acid transformations *in vitro*, bile acid analyses were performed on the culture supernatants (representing dissolved BAs (SUP)) and pellets (representing cell-associated BAs (PEL)). Furthermore, in order to discriminate between BAs in the cytoplasm from those bound to the cell envelope, we separated the cytoplasmic and cell envelope fraction of the biomass by ultracentrifugation after cell lysis for selected pellet samples, and analyzed the bile acids in both fractions.

We observed that *C. scindens* removes the C7-hydroxyl group from CA and CDCA. CA is partially 7 $\alpha$ -dehydroxylated to DCA, as reported previously<sup>146</sup>, and 12-oxoLCA is also produced (Figure 2.3a). Overall, about 83% of the CA is converted to 7-dehydroxylated bile acid species (DCA and 12-oxoLCA) after a 24 h incubation. In contrast, *C. scindens* converted only 10% of CDCA to LCA after 52 h of incubation (Figure 2.3d), presumably partly due to the toxicity of this compound. The major 7-dehydroxylated secondary bile acids of CA include DCA and 12-oxoLCA, and those from CDCA include LCA and 3-oxoLCA. The 3 $\beta$ -epimer of LCA (isoLCA) was also detected (Figure 2.3d and 2.3e) but only in a minor amount (<1 $\mu$ M).

In addition to 7 $\alpha$ -dehydroxylation, *C. scindens* oxidized hydroxyl groups at the C3 and C7 positions on CA and CDCA molecules and additionally at the C12 position for CA (Figure 2.3). The oxidized secondary BAs produced include 3-oxoCA, 3-oxoCDCA, 3-oxoLCA, 7-oxoDCA, 7-oxoLCA, and 12-oxoLCA. Some of these secondary bile acid species, such as 12-oxoLCA (a product of CA transformation) are found in large quantities. 12-oxoLCA is formed rapidly and abundantly: at 24 h of incubation, 36% of CA was converted into 12-oxoLCA (Figure 2.3a). It represents the major cell-associated bile acid during CA transformation (Figure 2.3b) and is located in the cytoplasmic fraction (Figure 2.3c). Furthermore, between 24 h and 48 h of incubation, 12-oxoLCA decreased while DCA concentrations increased (Figure 2.3a).

In studies assessing bile acid transformations *in vitro*, the BA mass balance is not always achieved when measuring solution bile acids<sup>44</sup>. Hence, we quantified BAs in solution as well as associated with the cells. We found that about 10% and 5% of the CA- and CDCA-derived secondary bile acids are cell-associated, respectively (Figure 2.3b, 2.3e). After fractionation of the biomass, we observed that LCA was the only cell-associated BA that was primarily bound to the cell envelope (Figure 2.3f). *C. scindens* ATCC 35704 did not metabolize UDCA nor the two murine primary bile acids  $\alpha$ MCA and  $\beta$ MCA (Figure S1). In the experiments with CA, UDCA,  $\alpha$ MCA and  $\beta$ MCA (Figure 2.3a and S1), we noticed a decrease in the total bile acid concentration over time, both in the experimental and sterile control tubes. This decrease might be due to the adsorption of bile acids from the sample to walls of the epitube. In further experiments, all samples were extracted with alkaline acetonitrile, circumventing this experimental problem.

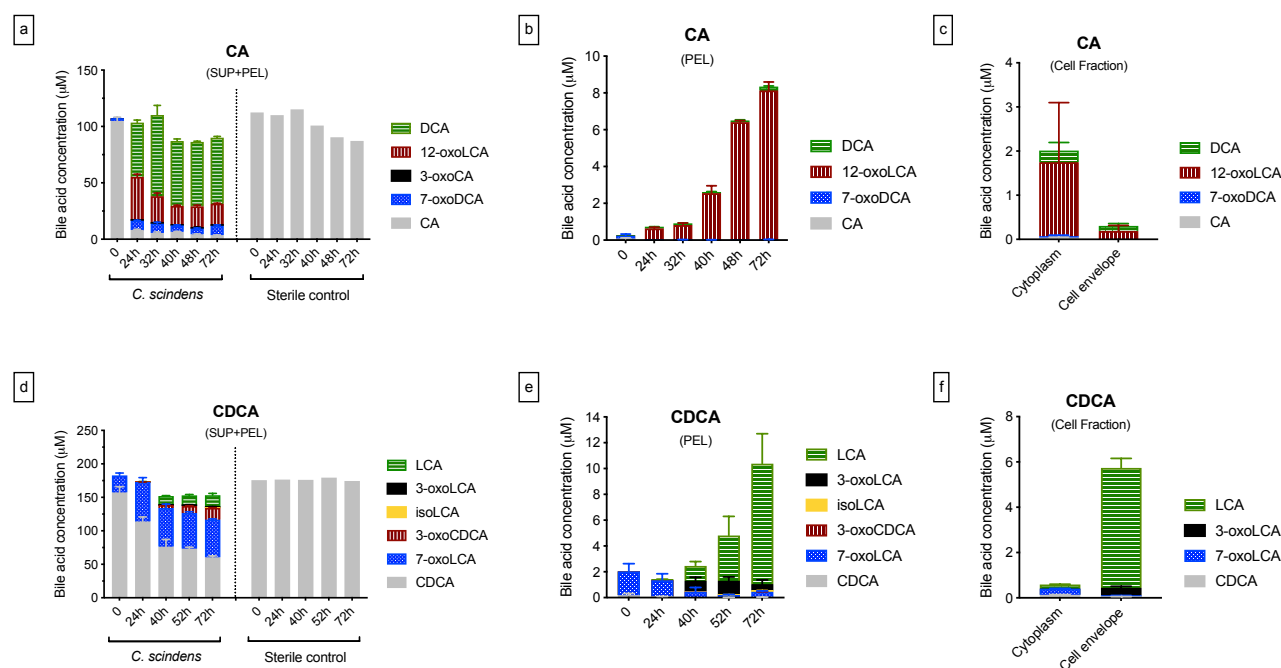


**Figure 2.3| Bile acid transformations by *Clostridium scindens* in vitro.** *C. scindens* was grown in triplicate in BHIS-S containing either CA or CDCA. Cultures were sampled and the pellet (PEL) separated from the supernatant (SUP) by centrifugation. Selected pellets were further fractionated into cytoplasmic and cell envelope fractions. Bile acids quantification is reported for the combined supernatant and pellet (SUP+PEL) (a,d), for pellets (PEL) (b,e), and for the cytoplasmic and cell envelope fraction of the biomass (c,f). The analyses were carried out in triplicate, collected from triplicate cultures of *C. scindens*. Histograms indicate the mean and one standard deviation. Time zero represents the minimal amount of time needed to sample the culture, post bacterial amendment.

The formation of 12-oxoLCA and its accumulation intracellularly was unexpected as it is not an intermediate of the 7-dehydroxylation pathway<sup>1</sup> but rather described as an oxidized form of DCA<sup>30,61,147,148</sup>. In contrast, a known intermediate of the 7-dehydroxylation pathway, 3-oxoDCA, was not detected in the experiments (Figure 2.3). In order to better understand the formation of 12-oxoLCA, we performed additional *in vitro* experiments to investigate the transformation products of DCA, 3-oxoDCA, and 12-oxoLCA (Figure 2.4). We observed the oxidation of a small fraction of DCA (~11%) to 12-oxoLCA after 30 min followed by the reduction of 12-oxoLCA back to DCA within 36 h (Figure 2.4a). Regarding 3-oxoDCA, only a small fraction (~7%) was converted to DCA and this transformation was extremely slow (Figure 2.4b). In contrast, 12-oxoLCA was rapidly and extensively converted to DCA (Figure 2.4c). After 6h of incubation, the majority of 12-oxoLCA (~91%) was converted to DCA.

Bile acid 7-dehydroxylation is an intracellular process. In order to assess whether the limited transformation of DCA and 3-oxoDCA (Figures 2.4a and 2.4b) by *C. scindens* were due to inefficient transport of these BAs inside the cells, we performed an additional experiment using *C. scindens* cell-free extract (CFE) induced with CA before lysis and exposed to DCA or 3-oxoDCA (Figures 2.4d and 2.4e). CA is a known inducer of the expression of the *bai* operon encoding the 7-dehydroxylating enzymes<sup>149</sup>. The transformation of 12-oxoLCA by the CA-induced CFE was also assessed (Figure 2.4f). We observed that the CFE was more efficient at reducing 3-oxoDCA to DCA as compared to *C. scindens* whole cells (Figures 2.4b and 2.4e) despite corresponding to half the cell concentration ( $OD_{600} \sim 0.7$  instead of  $\sim 1.4$ ). The maximal DCA concentration with CFE was about 35  $\mu$ M after 10 h as compared to 5  $\mu$ M DCA after 60 h incubation with *C. scindens* whole cells. Interestingly, we detected a small fraction ( $\approx 1.35 \pm 0.06$   $\mu$ M after 10 h) of isoDCA, thus demonstrating the potential of *C. scindens* to epimerize the C3-hydroxyl group. Furthermore, another product of transformation of 3-oxoDCA was detected on the chromatogram with a  $m/z$  of 387.2523 [M-H]<sup>-</sup>, which could correspond to the elemental composition  $C_{24}H_{36}O_4$ , so a

loss of two H atoms from 3-oxoDCA. Unfortunately, we did not have an appropriate standard to definitively identify and quantify this product based on its retention time, accurate mass and fragmentation pattern. This unknown product of 3-oxoDCA transformation could be 3,12-dioxoDCA, but further experiments will be needed to confirm this assignment.

The transformation of DCA by cell-free extract is similar to that with *C. scindens* whole cells. We observed the formation of a maximum of  $13.3 \pm 1.5$   $\mu\text{M}$  12-oxoLCA with the CFE compared to  $12.8 \pm 1.2$   $\mu\text{M}$  with the whole cells (despite the factor of  $\sim 2$  less protein in the CFE system). However, the 12-oxoLCA formed by CFE remained in the medium and was not reduced back to DCA as observed with *C. scindens* whole cells (Figures 2.4a and 2.4d). Furthermore, we detected the formation of a small amount of 3-oxoDCA ( $3.5 \pm 0.1$   $\mu\text{M}$  after 10 h of incubation) with CFE, which was not observed in the whole cell experiment (Figures 2.4a and 2.4d).

CFE reduced 12-oxoLCA rapidly and almost completely to DCA, similarly to our observation with *C. scindens* whole cells. In less than 30 minutes, almost all 12-oxoLCA ( $\sim 95\%$ ) was converted to DCA (Figure 2.4f).

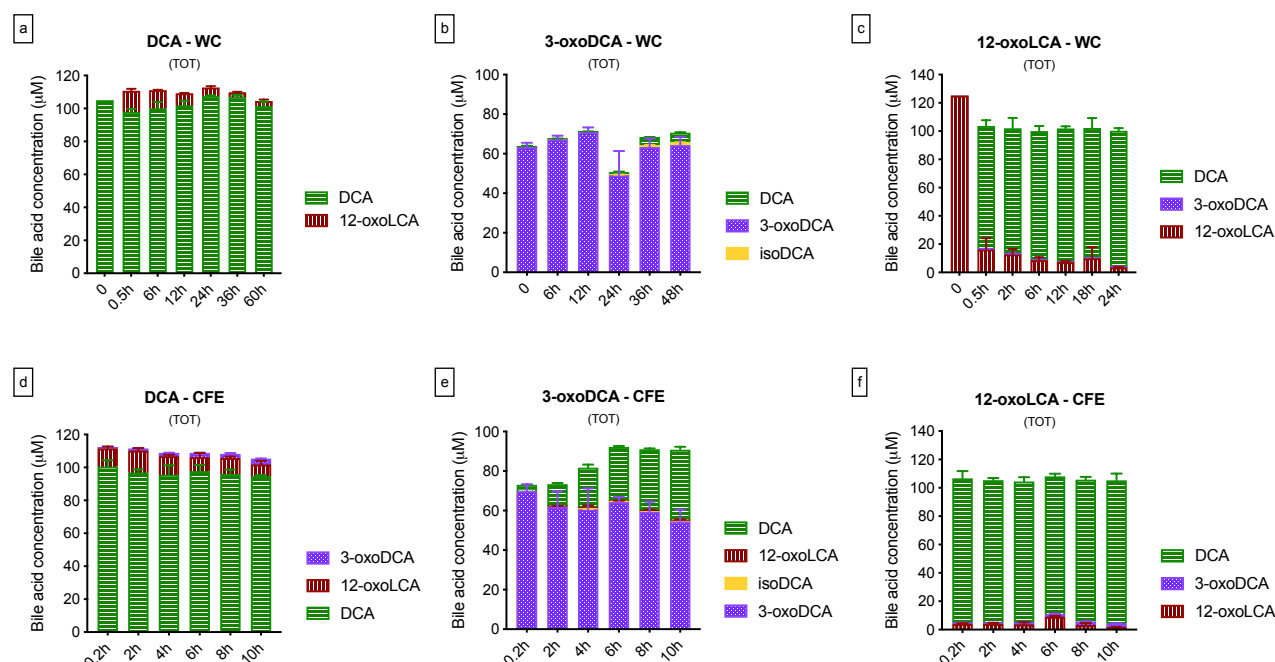


**Figure 2.4 | Secondary bile acid transformations by *Clostridium scindens* in vitro (whole cell and cell-free extract).** Transformation products of the secondary bile acids DCA, 3-oxoDCA and 12-oxoLCA by whole *C. scindens* cells (WC) (a, b, and c). *C. scindens* was grown in BHIS-S containing one secondary bile acid (DCA, 3-oxoDCA, or 12-oxoLCA) in triplicate. Transformation products of the secondary bile acids DCA, 3-oxoDCA and 12-oxoLCA by CA-induced *C. scindens* cell-free extract (CFE) (d, e, and f). The synthesis of Bai enzymes was induced by the amendment of CA to a growing culture of *C. scindens*. The CA-induced cells were lysed and the cell-free extracts were amended with DCA, 3-oxoDCA or 12-oxoLCA. Each experiment was carried out in triplicates. Bile acids were extracted directly from the culture/CFE (supernatant and biomass), representing the total bile acids ('TOT'). Histograms indicate the mean and one standard deviation.

### 2.3.4 *Clostridium scindens* colonization and bile acid transformation in the murine intestinal tract.

In order to investigate BA 7-dehydroxylation by *C. scindens* in vivo and its colonization dynamics, we used  $^{15}\text{N}$  and  $^{13}\text{C}$  labeled cells of *C. scindens*. We calibrated the decrease in  $\delta^{15}\text{N}$  and  $\delta^{13}\text{C}$  isotopic ratio as a function of division cycle by growing labeled *C. scindens* cells in unlabeled medium and monitoring the change in isotopic ratio (Figure S2). As expected, the isotopic ratios ( $^{13}\text{C}/^{12}\text{C}$  and  $^{15}\text{N}/^{14}\text{N}$ ) of individual *C. scindens* cells are halved at each cell division as individual cells undergo symmetric division taking up normal composition N and C from the medium. Once the stationary phase is reached and the cells stop dividing, the isotopic ratios remain

quasi constant (Figure S2). The nitrogen isotopic ratio is 3 times greater than the carbon ratio and was selected for further analyses because it affords greater resolution of bacterial division.

The  $^{15}\text{N}$  isotopically labeled *C. scindens* cells were used to complement the intestinal microbial community of mice from a gnotobiotic mouse line (sDMDMm2) devoid of 7-dehydroxylating strains<sup>129,145</sup>. Six hours after inoculation by gavage of  $10^9$  cells, *C. scindens* was already detectable in the distal intestinal tract (Figure 2.5). *C. scindens* concentrations were low in the jejunum and ileum compared to the large intestine. In the small intestine, *C. scindens* numbers were below detection by cultivation at 6 h. At 24 h, there was on average of  $6.5 \pm 5.7 \times 10^2$  CFU of *C. scindens* per g of intestinal content in the ileum only. In contrast, the cell counts were  $6.1 \pm 8.6 \times 10^5$  and  $3.2 \pm 4.9 \times 10^5$  CFU of *C. scindens* per g of intestinal content at 6 h and 24 h, respectively for the cecum. In the colon, the cell counts were  $4.6 \pm 6.4 \times 10^6$  at 6 h and at 24 h they were comparable to those in the cecum ( $7.2 \pm 11.5 \times 10^5$ ).

The nitrogen isotopic ratio of the *C. scindens* gavage culture equaled 420,600 (Figure S3). Thus, within the gut microbial community of sDMDMm2 mice, *C. scindens* cells, were readily detected using the NanoSIMS-generated  $^{12}\text{C}^{15}\text{N}^-$  and  $^{12}\text{C}^{13}\text{C}^-$  images (Figure S4).

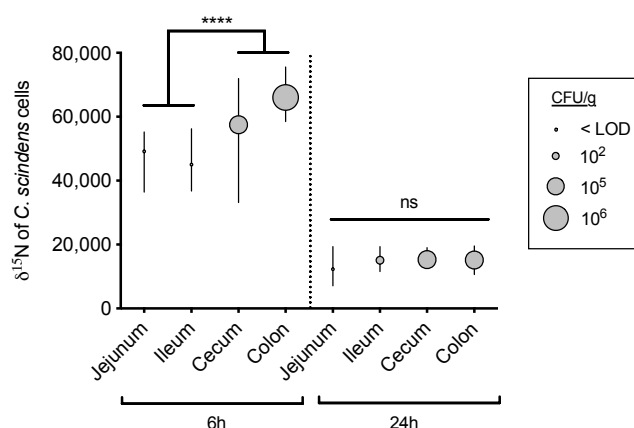


**Figure 2.5 | *Clostridium scindens* colonizes the large intestine of the murine gut.** *C. scindens* was grown *in vitro* in a medium with  $^{15}\text{N}$ -labeled nutrients and gavaged into sDMDMm2 mice. A control culture was obtained in a medium lacking labeled compounds (unlabeled). The nitrogen isotopic ratio of *C. scindens* along the intestinal tract was quantified from NanoSIMS images. Samples from two mice (one per time point) were analyzed. *C. scindens* concentration (CFU/g of intestinal content) were determined by plating on selective medium. The y-axis indicates  $^{15}\text{N}$  isotopic ratio of *C. scindens* cells. The bubble centers indicate medians and the vertical bars the interquartile range. The size of the bubbles indicates *C. scindens* concentrations. Statistical analysis used Mann-Whitney-U tests to compare the *C. scindens* isotopic ratios in the small and large intestine. Ns, not statistically significant ( $p \geq 0.05$ ), \*\*\*\* $p < 0.0001$ . <LOD implies that the value is below the limit of detection.

The nitrogen isotopic ratio of *C. scindens* cells decreased rapidly overtime in the intestinal tract (Figure 2.5). After 6 h, the ratios were significantly lower in the small intestine compared to the large intestine, suggesting that cells in the large intestine underwent fewer bacterial divisions than those in the small intestine. Twenty-four hours after gavage, the isotopic ratios were lower than at 6 h, suggesting that cells continued to divide in all intestinal compartments. There is no statistically significant difference among the compartments at 24 h indicating that *C. scindens* cells underwent a similar number of bacterial divisions. However, only considering the nitrogen isotope ratios provides an incomplete view of the process because it does not take into account the fact that the number of cells present in the ileum is three orders of magnitude smaller than that in the cecum or colon. Hence, while the small number of cells present in the ileum (and to a lesser extent, the jejunum) divides at the same rate as those in the cecum and colon, they represent a small population. Thus, the great majority of *C. scindens* cells have colonized the large intestine and are dividing and growing in that compartment.

We analyzed the bile acid profile along the intestinal tract of sDMDMm2 mice and sDMDMm2 mice colonized with *C. scindens* to explore the impact of *C. scindens* on the bile acid metabolome. Figure 2.6 shows that the luminal bile acid concentrations vary greatly

along the murine intestinal tract. The bile acid pool in the large intestine represents about 5% of that in the small intestine. In the small intestine, the bile acid composition is largely accounted for by conjugated species: TCA, T $\beta$ MCA, as well as tauro-conjugated cholic acid sulfated at the C7 position (TCA7S). In the large intestine, we observe the efficient deconjugation of bile acids, with the major remaining species consisting mainly of sulfated cholic acids (CA7S and TCA7S) and  $\beta$ MCA.

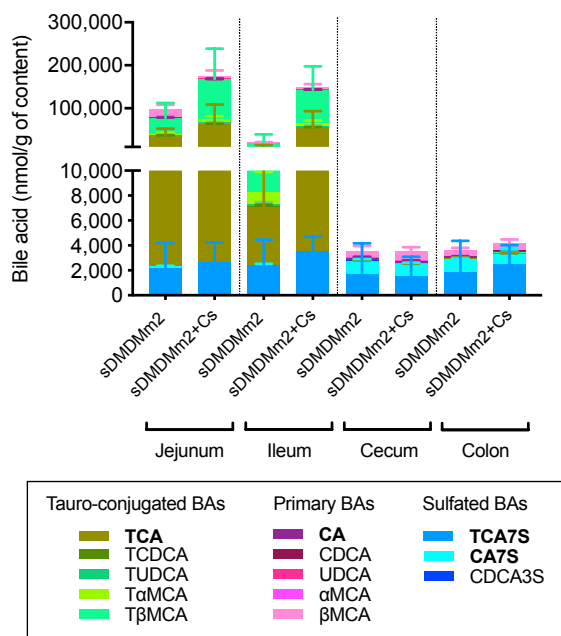


**Figure 2.6 Luminal bile acid composition along the intestinal tract of sDMDMm2 mice colonized with *C. scindens* (sDMDMm2 + Cs) compared to sDMDMm2 control mice.** Bile acids were analyzed with UHPLC-HRMS in four intestinal compartments collected from sDMDMm2 mice colonized with *C. scindens* for 24h (n=3, sDMDMm2+Cs) and a control group (n=3, sDMDMm2) that received a PBS vehicle. The legend indicates the bile acids detected. The ones abundant enough to be visible on the graph are in bold in the legend. The secondary bile acids are depicted in Figure 2.7 and 2.8.

The presence of these unconjugated bile acids in the large intestine allows further transformations, including the epimerization of the hydroxyl group at the C6 position (producing  $\omega$ MCA), and the oxidation of the hydroxyl groups at the C3 and C7 positions (producing 3-oxoCA, 3-oxoCDCA, 7-oxoDCA, and 7-oxoLCA) (Figure 2.7)<sup>20</sup>. These transformations occur in the presence and absence of *C. scindens*, suggesting that members of the sDMDMm2 microbial community are responsible. Furthermore, the concentrations of these unconjugated secondary BAs are not significantly different in the large intestine of *C. scindens*-colonized sDMDMm2 mice relative to control mice (sDMDMm2) (Figure 2.7).

There is one bile acid species that is only present in the mouse with the *C. scindens*-amended microbiota: DCA (Figure 2.8). This is the 7-dehydroxylated form of CA. This result is consistent with the 7-dehydroxylating activity of *C. scindens* and confirms the colonization data. The amount of DCA is stable over time in the cecum and colon (Figure 2.8).

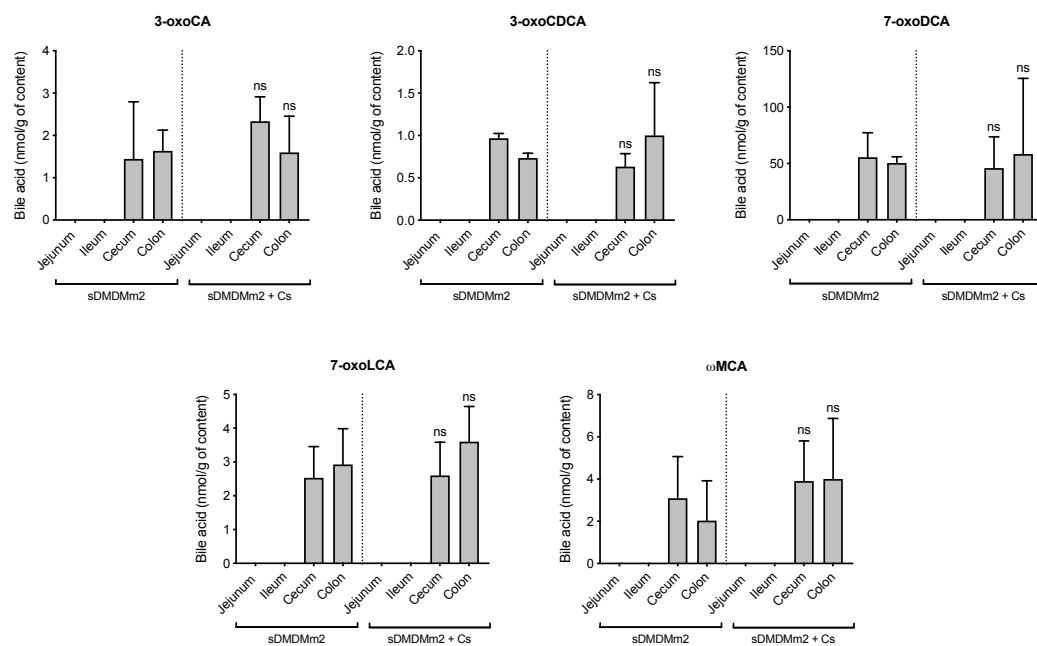


**Figure 2.7| Secondary bile acid composition along the intestinal tract of sDMDMm2 mice colonized with *C. scindens* compared to control sDMDMm2 mice.** Bile acids were analyzed with UHPLC-HRMS in four intestinal compartments collected from sDMDMm2 mice colonized with *C. scindens* for 24h ( $n=3$ , sDMDMm2+Cs) and a control group ( $n=3$ , sDMDMm2) that received PBS vehicle. Statistic analysis used the Mann-Whitney-U tests to compare the secondary bile acid concentrations in mice colonized with *C. scindens* to a control sDMDMm2 mouse. Histograms indicate the mean with the standard deviation. ns, not statistically significant ( $p \geq 0.05$ ). A value of zero indicates that the concentration is below the limit of detection.

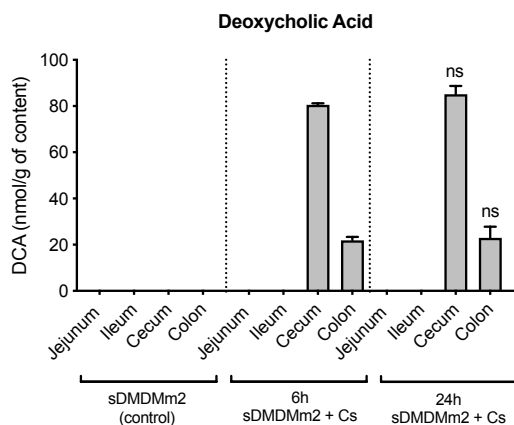


**Figure 2.8| Deoxycholic acid (DCA) formation *in vivo* as a function of time.** DCA was quantified with UHPLC-HRMS in four intestinal compartments (jejunum, ileum, cecum and colon) collected from sDMDMm2 mice colonized with *C. scindens* for 6h ( $n=3$ , sDMDMm2+Cs) and 24h ( $n=3$ , sDMDMm2+Cs) and a control group ( $n=3$ , sDMDMm2) that received PBS vehicle. Histograms indicate the mean with the standard deviation. Mann-Whitney-U tests were performed to compare DCA levels between T6h and T24h. ns, not statistically significant ( $p \geq 0.05$ ). A value of zero indicates that the concentration is below the limit of detection.

## 2.4 Discussion

Bile acids exhibit detergent properties. In the small intestine, they form micelles and promote dietary lipid solubilization and absorption. When present at high concentrations, bile acids can be cytotoxic to the bacteria and the host. The intestinal bile acid pool (size and composition) is known to structure the microbial community along the intestinal tract and therefore plays an important role in maintaining the intestinal barrier function<sup>150–152</sup>.

Bile acid 7-dehydroxylating bacteria represent an important functional group amongst bile-transforming gut bacteria. They produce 7-dehydroxylated secondary bile acids, which represent a major fraction of the secondary bile acids pool (~64% in the cecum of the *C. scindens*-colonized sDMDMm2 mice). 7-dehydroxylated bile acids, such as DCA and LCA, are potent activators of the bile acid receptor TGR5, and consequently are involved in the regulation of glucose homeostasis, energy expenditure and inflammation<sup>3,4,153</sup>. Bile acid 7-dehydroxylating bacteria thus may represent a critical link between bile acids and host health<sup>135</sup>. As such, they could be a target for the prevention and treatment of various metabolic diseases<sup>10</sup>, as well as *Clostridium difficile* infections (CDI)<sup>136</sup> and some gastrointestinal cancers, which are associated with increased levels of 7-dehydroxylated bile acids<sup>12</sup>. Using 7-dehydroxylating bacteria for therapeutic or preventative applications requires a better understanding of their microbiology *in vivo* as well as their interactions with the host. In the present study, we explored the bile acid metabolism of *C. scindens*, a known 7-dehydroxylating bacterium, both *in vitro* and *in vivo* and investigated its colonization dynamics in the murine intestinal tract.

The growth of *C. scindens* ATCC 35704 was not impacted by the primary or secondary bile acids tested *in vitro* (Figure 2.2a, 2.2b). A notable exception is CDCA, which revealed a toxic effect (Figure 2.2a), as is expected because it is a hydrophobic bile acid.

*C. scindens* metabolized CA and CDCA *in vitro* and the products of their transformation were primarily recovered from solution. LCA is the exception as it was associated with the cell envelope, underscoring its hydrophobicity. Another is 12-oxoLCA, which was recovered from the cytoplasm, suggesting it is not effectively effluxed by the cell (Figure 2.3). CA was more efficiently dehydroxylated than CDCA (Figure 2.3), as was previously reported for *C. hiranonis*<sup>44</sup> and *C. scindens* VPI 12708<sup>146</sup>.

In contrast, the murine primary bile acids  $\alpha$ MCA and  $\beta$ MCA remained unchanged (Figure S1), confirming previous reports that human intestinal bacteria are unable to metabolize muricholic acids<sup>60,154</sup>. A possible explanation for this is host specificity as *C. scindens* may have evolved in the human gut in the absence of murine primary bile acids. However, *C. scindens* may not be an exclusively human commensal as a new strain (strain G10) was recently isolated from rat feces<sup>38</sup>. The 7 $\beta$ -dehydroxylation of UDCA was also tested *in vitro*. This transformation was previously reported for several 7-dehydroxylating organisms including several *C. scindens* strains (VPI 12708, 36S, M-18, Y-98, Y-1112, Y-1113) and *Eubacterium* strain C-25<sup>44,54</sup>. The gene *bail* is predicted to encode a 7 $\beta$ -dehydratase<sup>98</sup> but this remains to be confirmed as this process could also occur via a 7 $\beta$ -epimerization to CDCA followed by 7 $\alpha$ -dehydroxylation. Here, we did not observe any conversion of UDCA by *C. scindens* ATCC 35704 *in vitro* (Figure S1), consistent with previous reports<sup>155</sup>.

*In vitro*, *C. scindens* also oxidized the C3 and C7 hydroxyl groups in CA and CDCA, yielding 3-oxoCA and 7-oxoDCA (for CA) and 3-oxoCDCA and 7-oxoLCA (for CDCA) (Figure 2.3). In addition, 7-dehydroxylation was combined with oxidation, to produce 12-oxoLCA for CA and 3-oxoLCA for CDCA, and with epimerization to produce isoLCA. Oxidation at C3, C7 and C12, as well as 7 $\alpha$ - and 7 $\beta$ -dehydroxylation of the C7 hydroxyl group by various *C. scindens* strains have all been previously reported<sup>1,44,46,54,141,146,155</sup>. Thus, these findings are in line with the expected composition of the products of CA and CDCA incubations with *C. scindens*. In contrast, it is the first time that epimerization of the C3-hydroxyl of LCA to isoLCA (3 $\beta$ ) is reported for *C. scindens* perhaps due to its presence at a low concentration ( $\leq 2\mu\text{M}$ ). While *Clostridium scindens* carries several 3 $\alpha$ -hydroxysteroid dehydrogenase (3 $\alpha$ -HSDH) on the *bai* operon (*BaiA* enzymes)<sup>86</sup>, 3 $\beta$ -HSDH has never been characterized for this organism.



The BA 7-dehydroxylation pathway invokes the oxidation of the C3 hydroxyl, followed by the oxidation of the C4-C5 bond, the dehydration at the C7 hydroxyl, the reduction of the C4-C5 and C6-C7 bonds, and finally the reduction of the C3 ketone group<sup>1</sup>. Thus, a 3-oxoDCA intermediate is involved in the pathway<sup>89</sup>. However, we did not detect it in our experiment (Figure 2.3) nor is it reported as a product of CA transformation by *C. scindens* in a recent study, while it is detected during CA 7-dehydroxylation by *C. hiranonis*<sup>28</sup>. In the same study, no transformation of 3-oxoDCA into DCA (as would be expected based on the pathway) is detected in any of the 7-dehydroxylating strains considered<sup>28</sup>. Similarly, our results show that *C. scindens* converted a minor part of 3-oxoDCA (7%) to DCA (Figure 2.4b). *C. scindens* has several copies of the *baiA* gene encoding 3 $\alpha$ -HSDH enzymes<sup>86</sup>, thus it is unclear whether the lack of 3-oxoDCA reduction is due to limited expression of the 3 $\alpha$ -HSDHs or to the lack of transport of 3-oxoDCA into the cell. To circumvent these possible confounding effects, we used CA-induced *C. scindens* CFE to interrogate 3-oxoDCA transformation. Reduction of 3-oxoDCA ensued (39% at 10 h), resulting in increased production of DCA compared to that with whole cells (Figure 2.4e). These results confirm that 3-oxoDCA is a likely intermediate in the formation of DCA and that its intracellular intake is limited.

An unanticipated finding was the transformation of CA into 12-oxoLCA (Figure 2.3a). This secondary bile acid has not been reported in previous CA 7-dehydroxylation experiments with *C. scindens*<sup>28</sup>. We observed a transient accumulation of this bile acid in the biomass during CA transformation *in vitro* (Figure 2.3b). Interestingly, this bile acid species accumulated in the cytoplasm of the cells (Figure 2.3c). In the literature, this secondary bile acid is described as a product of the oxidation of DCA<sup>30,61,96,147,148</sup>.

We investigated the transformation of 12-oxoLCA by *C. scindens* to determine whether 12-oxoLCA may be reduced to DCA. The transformation of 12-oxoLCA to DCA by both whole cells and CFE was very rapid (86% in 2 h and 95% in less than 30 minutes, respectively), suggesting high 12 $\alpha$ -HSDH activity (Figure 2.4c and 2.4f). Similarly, Doden *et al.* (2018) report complete conversion of 12-oxoLCA to DCA by the three major 7-dehydroxylating species *C. scindens*, *C. hylemonae* and *C. hiranonis*<sup>28</sup>.

In contrast, DCA transformation to 12-oxoLCA by *C. scindens* whole cells was slow (11.5% in 30 minutes) and the 12-oxoLCA produced was converted back to DCA (<3% remaining at 36 h) (Figure 2.4a). This is consistent with previous work by Winter *et al.* (1984) and Doden *et al.* (2018)<sup>28</sup> who reported no conversion of DCA by *C. scindens* strain ATCC 35704<sup>155</sup>. To address the possible confounding issues of expression of the 12 $\alpha$ -HSDH in the presence of DCA and of the potentially limited uptake of DCA by cells, CA-induced *C. scindens* CFE was exposed to DCA and a minor transformation of DCA to 12-oxoLCA (11.8% in 12 min) was observed, similar to that with *C. scindens* whole cells after 30 minutes. However, the 12-oxoLCA formed by CFE was not converted back to DCA over time (Figure 2.4d). These results suggest that 12-oxoLCA could be a transient species during CA 7-dehydroxylation to DCA, which is incompatible with the 7-dehydroxylation pathway<sup>1</sup>. Further investigations are needed to elucidate the occurrence of this secondary bile acid species, its connection with the 7-dehydroxylation pathway, and its role on host physiology.

Overall, the *in vitro* transformation of CA by *C. scindens* involves BA 7-dehydroxylation to both reduced (DCA and isoDCA) and oxidized (12-oxoLCA, 3-oxoDCA) secondary BAs as well as oxidation of primary BAs (7-oxoDCA, 3-oxoCA) (Figure 2.9). Similarly, for CDCA, reduced (LCA and isoLCA) and oxidized (3-oxoLCA) 7-dehydroxylated species are formed along with oxidized primary BAs (7-oxoLCA, 3-oxoCDCA) (Figure 2.10). The 3-oxo, 7-dehydroxylated species (3-oxoDCA and 3-oxoLCA) are intermediates in the known 7-dehydroxylation pathway, whereas the 12-oxo, 7-dehydroxylated species (12-oxoLCA) is likely to be a transient species formed during CA 7-dehydroxylation. The 7-oxo species are not substrates for 7-dehydroxylation<sup>1</sup> and require reduction back to the primary BA for further transformation by *C. scindens* (Figures 2.9 and 2.10).

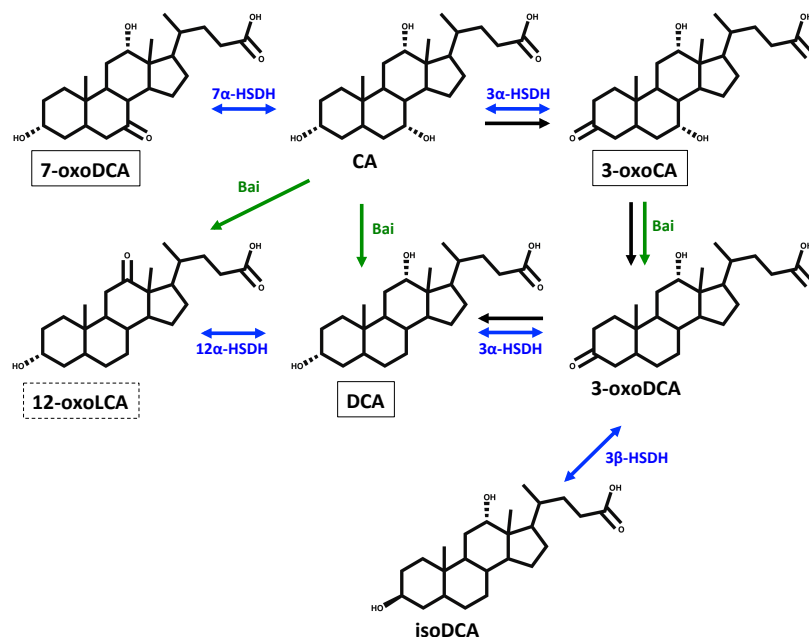


**Figure 2.9 | Cholic acid (CA) transformations carried out by *Clostridium scindens* *in vitro* and *in vivo*.** The secondary bile acids produced by *C. scindens* *in vitro* are indicated and those that were also detected *in vivo* are in boxes. The dashed boxes indicate those reported *in vivo* in the study from Studer *et al.* (2016), using the same gnotobiotic mouse model (sDMMDm2 + *C. scindens*)<sup>129</sup>. The black arrows indicate the 7-dehydroxylation pathway and its BA intermediates. The green arrows depict bile acid 7-dehydroxylation and the blue bidirectional arrows show the oxidation/reduction transformations. Enzymes catalyzing these transformations are indicated next the arrows. Bai stands for the enzymes of the bai operon involved in the 7-dehydroxylation.

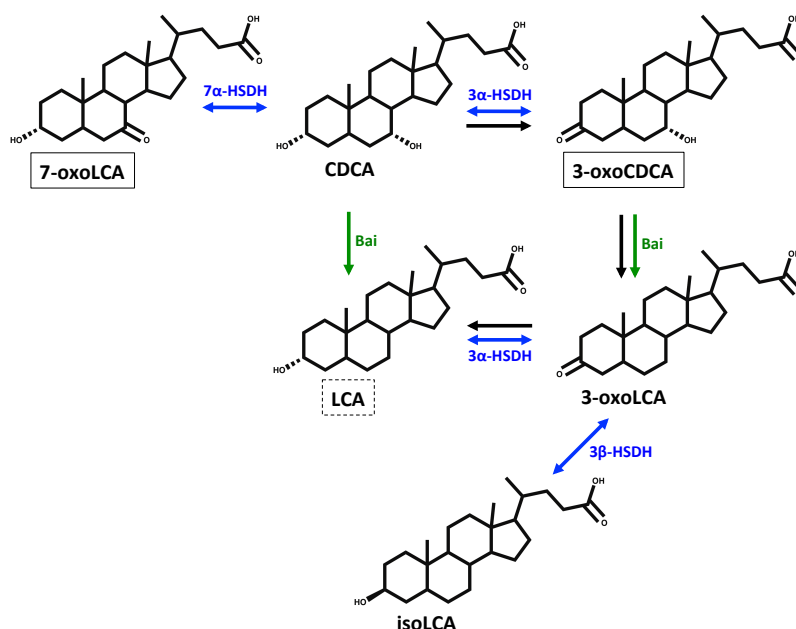


**Figure 2.10 | Chenodeoxycholic acid (CDCA) transformations carried out by *Clostridium scindens* *in vitro* and *in vivo*.** The secondary bile acids produced by *C. scindens* *in vitro* are indicated and those that were also detected *in vivo* are in boxes. The dashed boxes indicate those reported *in vivo* in the study from Studer *et al.* (2016), using the same gnotobiotic mouse model (sDMMDm2 + *C. scindens*)<sup>129</sup>. The black arrows indicate the 7-dehydroxylation pathway and the bile acid 7-dehydroxylation and the blue bidirectional arrows show the oxidation/reduction transformations. Enzymes catalyzing these transformations are indicated next the arrows. Bai stands for the enzymes of the bai operon involved in the 7-dehydroxylation.

In order to evaluate the relevance of *C. scindens* *in vitro* bile acid transformations *in vivo*, we amended a gnotobiotic mouse model with  $^{15}\text{N}$ - and  $^{13}\text{C}$ -labeled *C. scindens* cells and analyzed the bile acid metabolome along the intestinal tract. In parallel, we probed the *in vivo* colonization behavior of *C. scindens* by following the cell isotopic ratios in the mouse intestine using NanoSIMS. The selected gnotobiotic mouse model (sDMDMm2) is associated with a stable, low-complexity microbiota consisting of 12 species belonging to the main phyla of the murine gut microbiota and devoid of 7-dehydroxylation capability<sup>145</sup>. Thus, by amending the model microbiota with *C. scindens*, we aimed to restore bile acid 7-dehydroxylation. This complemented mouse model (sDMDMm2 + *C. scindens*) was previously reported by our group<sup>129</sup>. However, it is the first time the bile acid profile along the intestinal tract (jejunum, ileum, cecum and colon) of this mouse model is documented.

The bile acid composition along the gut in mice colonized with *C. scindens* and in the control mouse confirms previous observations that approximately 95% of the bile acid pool is reabsorbed into the distal ileum as part of the enterohepatic recirculation and that only 5% enters the large intestine (Figure 2.6)<sup>156</sup>. Additionally, we observe a rapid conversion of CA to DCA in the mice colonized with *C. scindens* (Figure 2.8) while, as expected, DCA is absent in mice that are not colonized with *C. scindens*. Hence, the amendment of *C. scindens* to the sDMDMm2 mice microbial community partly restores the expected bile acid composition by allowing 7 $\alpha$ -dehydroxylation, as previously shown<sup>129</sup>. As expected, all the secondary bile acid detected *in vivo* (Figure 2.7 and 2.8) were not detected in germ-free mice<sup>129</sup>, highlighting the role of microorganisms in the synthesis of secondary bile acids.

Interestingly, in contrast to our observations *in vitro* (Figure 2.3d) and the study from Studer *et al.* (2016)<sup>129</sup>, there was no evidence of LCA, suggesting that *C. scindens* did not 7-dehydroxylate CDCA *in vivo* (Figure 2.6). This discrepancy could be attributed to the short colonization time with *C. scindens* (24 h). Studer *et al.* (2016) colonized the mice with *C. scindens* for 7 days. Similarly, 12-oxoLCA was reported in the cecum of sDMDMm2 mice colonized with *C. scindens* for 7 days but not detected in this study. A longer colonization time (>24 h) with *C. scindens* might be required for the production of certain secondary bile acids (e.g., LCA and 12-oxoLCA). Other secondary bile acids formed from CDCA (e.g., 3-oxoCDCA and 7-oxoLCA) were detected in the cecum and colon of the mice and taken together, these secondary bile acids are found at the same concentration as CDCA, suggesting that half of the CDCA bile acid pool was oxidized (at C3 and C7). Oxidation of CDCA was also found to exceed 7-dehydroxylation *in vitro* (Figure 2.3d). A possible explanation for this might be that the enzymes oxidizing bile acids (HSDH) are more abundantly expressed than the 7-dehydroxylating enzymes (encoded by *bai* genes) within the gut microbial community<sup>22</sup>. Further, consistent with the *in vitro* data (Figure S1), *C. scindens* did not use muricholic acids as substrates for 7-dehydroxylation *in vivo* (Figure 2.6). In contrast to the *in vitro* data, iso-secondary bile acids were not detected in the mice. The concentrations of isoLCA and isoDCA detected *in vitro* were low (<2 $\mu\text{M}$ ), thus the epimerization of C3-hydroxyl is a minor transformation of *C. scindens*. In humans, other bacteria, such as *Eggerthella lenta* and *Ruminococcus gnavus*, likely contribute to the formation of iso (3 $\beta$ -hydroxyl) bile acids which are reported to be the second most abundant class of bile acids in the gut<sup>24</sup>.

*In vivo*, we observed that the concentrations of secondary bile acids (3-oxoCA, 3-oxoCDCA, 7-oxoDCA, 7-oxoLCA and  $\omega$ MCA) were comparable between *C. scindens*-colonized sDMDMm2 mice and the control sDMDMm2 mice (Figure 2.7). Thus, in the large intestine, *C. scindens* restores bile acid 7-dehydroxylation without affecting the rest of the bile acid pool. In line with this observation, our group recently reported that *C. scindens* association had only a minor impact on the composition of the sDMDMm2 microbiota<sup>129</sup>.

To explore the colonization dynamics of this 7-dehydroxylating bacterium in the murine intestinal tract, mice were inoculated with isotopically labeled *C. scindens* cells (with  $^{15}\text{N}$  and  $^{13}\text{C}$ ) and their isotopic signatures along the gut were measured with NanoSIMS (Figure S4). As bacteria grow, the N or C isotopic ratio of *C. scindens* cells decreases because C and N with normal isotopic composition is taken up, diluting the isotopic signature (Figure S2). Thus, based on the cell isotopic ratios, we can infer the average number of cell divisions and hence, determine whether the cells present at that location have grown relative to previous time point. Given that the cells were delivered in a single gavage, we surmise that to remain in the intestinal tract, their growth rate must exceed the rate of

cell death and loss through feces. Hence, only cells that colonize the intestine should be able to divide once the bolus has passed through the intestinal tract (< 6 h). We found that cell growth was detectable in all compartments, suggesting colonization throughout the intestinal tract but cell numbers were vastly different in the small and large intestines. In the small intestine, *C. scindens* numbers were below detection limit by cultivation at 6 h. At 24 h, there was about  $10^2$ - $10^3$  CFU of *C. scindens* per g of intestinal content in the ileum only. In contrast, the cell counts ranged between  $10^4$ - $10^7$  CFU of *C. scindens* per g of intestinal content at 6 h and 24 h, for the cecum and colon (Figure 2.5).

Interestingly, the isotopic ratios of *C. scindens* cells were lower in the small intestine than in the large intestine at 6 h, suggesting that cells underwent more bacterial divisions in the small than in the large intestine (Figure 2.5). Thus, there are fewer cells colonizing the small intestine than the cecum or colon but those that have colonized appear to divide more rapidly at the initial time point. Considering the large inoculum administered into the mice and intestinal motility, we interpret these results as representing the arrival of cells from the inoculum (with high isotopic values, Figure S3) to the large intestine. It is common that large inocula undergo a 'lag phase' *in vivo* following administration before colonization starts. The bolus, dominated by slowly proliferating bacteria, transits through the gastrointestinal tract and seeds bacteria that start to genuinely colonize and proliferate. The bacteria in the small intestine at 6 h arrived a few hours earlier than those in the large intestine, thus have undergone more bacterial division and have lower isotopic ratios. We hypothesize that colonization of the small intestine is generally unfavorable but that there are microenvironments in which the 7-dehydroxylating cells live and divide, particularly in the ileum. After 24 h, the isotopic ratio is similar across the entire intestinal tract reflecting the steady-state colonization of the gut but the overwhelming majority of the 7-dehydroxylating biomass remains in the large intestine. This study also demonstrates the potential of NanoSIMS technology to track a bacterium of interest in a host<sup>157-159</sup>.

We demonstrated that *C. scindens* could divide in the small intestine and persist in small numbers (Figure 2.5). However, the large intestine is its primary ecological niche, and it is where *C. scindens* efficiently performs CA 7-dehydroxylation to DCA *in vivo* (Figure 2.8). DCA was not detected in the small intestine despite the presence of actively growing *C. scindens* 6 h after gavage, based on NanoSIMS analysis (Figure 2.5). Several factors may have impacted bile acid 7-dehydroxylation in the small intestine. The most parsimonious explanation is that bile acids in the small intestine are conjugated (Figure 2.6), which precludes 7-dehydroxylation<sup>20</sup>. The gnotobiotic sDMDMm2 mice have an efficient deconjugating community in the large intestine, as most bile acids are deconjugated (Figure 2.6). Thus, *C. scindens* cells have access to unconjugated primary BAs that can be dehydroxylated, which is not the case in the small intestine.

Interestingly, the majority of the primary BAs in the cecum and colon are sulfated (76% in *C. scindens*-colonized sDMDMm2 mice) while only a small fraction (3% in *C. scindens*-colonized sDMDMm2 mice) of the small intestine BAs exhibits this modification (Figure 2.6). Bile acid sulfation at the C3 and C7 positions has been suggested to represent a detoxification strategy<sup>25</sup> as it effectively increases their solubility, decreases the intestinal reabsorption and consequently promotes their elimination in feces and urine<sup>25</sup>. However, it has been shown that this modification precludes 7-dehydroxylation if the sulfate group is associated with the hydroxyl group at the C7 position<sup>21</sup>.

Thus, the colonization dynamics appear to confirm the work by Midvedt and Norman (1968) where they considered the spatial distribution of the bile acid transformations along the rat intestinal tract. Bile acid 7-dehydroxylating bacteria were found in the cecum but not in the ileum of three conventional rats<sup>34</sup>. Fifty years later, we confirm that the bile acid 7-dehydroxylating bacterium *C. scindens* colonizes primarily the large intestine of gnotobiotic mice but we also report limited colonization of the ileum (Figure 2.5). However, it is clear that the activity of 7-dehydroxylating bacteria is only detectable in the large intestine, presumably due to the exclusive availability of deconjugated bile acids in that intestinal compartment.

## 2.5 Conclusion

This study provides insight into the microbiology of 7-dehydroxylating organisms. First, the detailed analysis of bile acid transformations catalyzed by *C. scindens* allowed the uncovering of a novel intermediate, 12-oxoLCA. It is unclear how this intermediate fits into the well-established 7-dehydroxylation pathway. Further investigations are required to further unravel the role of this compound in 7-dehydroxylation. Furthermore, we have shown that DCA and LCA are products of primary bile acid metabolism by *C. scindens* (as expected) but also that other 7-dehydroxylated species form (e.g., 3-oxoLCA, 12-oxoLCA, isoDCA and isoLCA) and should be accounted for in the pool of 7-dehydroxylated product. The partitioning of bile acids into the cell envelope occurs for the more hydrophobic species and should also be considered for bile acid mass balance purposes. Finally, investigation of the dynamics of colonization of *C. scindens* in the gut using NanoSIMS has confirmed the primarily cecal and colonic localization of 7-dehydroxylating bacteria but has also evidenced the colonization of the ileum by a small number of *C. scindens* cells. There is no evidence of bile acid 7-dehydroxylation in that compartment but growth can clearly take place fuelled by fermentative processes.

# Chapter 3 Two routes are better than one: the bile acid 7-dehydroxylation pathway re-vamped.

Chapter 3 probes the existence of a novel bile acid 7-dehydroxylation pathway for the conversion of CA to DCA. By cloning genes from *Clostridium scindens* and purifying individual enzymes suspected to play a role in the pathway, we aim to define this novel pathway *in vitro* and identify the core of enzymes involved in this pathway.

## Authors:

S. Marion<sup>1</sup>, M. Reeves<sup>1</sup>, K. Meibom<sup>1</sup>, K. Lau<sup>2</sup>, F. Pojer<sup>2</sup>, L. Menin<sup>3</sup>, R. Bernier-Latmani<sup>1</sup>

## Author information:

<sup>1</sup>*Environmental Microbiology Laboratory, École Polytechnique Fédérale de Lausanne (EPFL), Lausanne, Switzerland*

<sup>2</sup>*Protein Production and Core Facility, École Polytechnique Fédérale de Lausanne (EPFL), Lausanne, Switzerland*

<sup>3</sup>*Institute of Chemical Sciences and Engineering, École Polytechnique Fédérale de Lausanne (EPFL), Lausanne, Switzerland*

## Author contributions:

SM carried out all the experimental work and wrote the manuscript under the supervision of RBL. MR assisted with the bile acid analysis at the Mass Spectrometry Facility supervised by LM. KL and FP provided advice and training for protein purification and provided as well as all the materials needed.

## Abstract

Symbiotic relationships are ubiquitous in nature and often relies on molecular interactions between the symbiotic partners. The microbial community inhabiting the human body synthesizes hundreds of small molecules that impact host physiology. Amongst these microbially-derived metabolites, the 7-dehydroxylated secondary bile acids deoxycholic acid (DCA) and lithocholic acid (LCA), which represent the major fraction of the large intestine bile acid pool, protect the host against *Clostridioides difficile* infections, and modulate several metabolic pathways by activating host receptors. Despite their importance for host health, incomplete knowledge of their biosynthetic pathway and the absence of genetic tools for their indigenous producers preclude designing therapeutic approach for diseases caused by bile acid pool abnormalities. Here, we uncover the co-existence of two bile acid 7-dehydroxylation pathways involving different region on the primary bile acid molecule. Using purified enzymes, we identified individual steps and bile acid intermediates of the two biosynthetic pathways. Furthermore, we established a set of enzymes necessary and sufficient for the 7-dehydroxylation of CA for the two pathways. These data illustrate a remarkable strategy – two pathways working simultaneously – developed by microorganisms likely to improve the synthesis capacity of two major component of the bile acid pool and key signaling molecules with broad impact on the host health.

## 3.1 Introduction

The human body is colonized by microorganisms from all three domains of life, with the gastrointestinal tract exhibiting the greatest microbial density and diversity. These microorganisms collectively produce thousands of small molecules and metabolites with local and systemic effects on host physiology. Identifying the active microorganisms that causally affect host phenotype and deciphering the underlying molecular mechanisms have become a major focus in microbiome research and have begun to enable the development of microbiota-based therapeutics.

Among these microbially-derived metabolites, bile acids are of particular interest as they constitute a direct link between the host and its microbiota. Primary bile acids, cholic acid (CA) and chenodeoxycholic acid (CDCA), are synthesized by the host hepatocytes and chemically modified by the gut microbial community. Bile acid 7 $\alpha$ -dehydroxylation is a microbial transformation of prime importance as 7-dehydroxylated secondary bile acids represent the major fraction of the bile acid pool in the large intestine<sup>22</sup>. Bile acid 7-dehydroxylating species are all classified as belonging to the genus *Clostridia*. The most studied are *C. scindens*<sup>29</sup>, *C. hylemonae*<sup>160</sup> and *C. hiranonis*<sup>140</sup>. They are very low abundance species – reported by some to represent 0.0001% of the colonic microbiota<sup>161</sup> – and remarkably manage to convert hundreds of mg of primary bile acids daily. Another intriguing aspect of bile acid 7-dehydroxylation is the different efficiency of transformation of the two primary bile acids CA and CDCA, which differ only by the presence of one hydroxyl group at the C12 position in CA. Bile acid 7-dehydroxylation in a pure culture of *C. scindens* converts about 80% of CA to deoxycholic acid (DCA) and derivatives. In contrast, only 10 % of CDCA is 7-dehydroxylated to lithocholic acid (LCA) and derivatives (Figures 3.1a and 3.1b). This difference was first reported by White *et al.* forty years ago<sup>97</sup> but the underlying mechanism has not yet been elucidated.

In their pioneering work, Hylemon and colleagues showed that the intestinal bacterium *Clostridium scindens* VPI 12708 carries out the 7 $\alpha$ -dehydroxylation of CA to produce DCA. They observed that CA induces 7 $\alpha$ -dehydroxylation, which involved the expression of a bile acid-inducible operon (referred to as *bai*) containing eight genes (*baiBCDEAFGHI*)<sup>1</sup>. Later, another operon *baiJKL* was identified and is also thought to be involved in bile acid transformations<sup>1</sup> (Figure 3.1c). However, this second operon is not conserved amongst all 7-dehydroxylating species. The pathway proposed by Hylemon and colleagues (Chapter 1, Figure 1.4) consists of an oxidative arm, where CA is first ligated to CoA by BaiB, followed two oxidation steps by BaiA2 and BaiCD forming a 3-oxo- $\Delta^4$ -CA-CoA intermediate. The next step is a dehydration step catalyzed by BaiE forming the 3-oxo- $\Delta^4,6$ -DCA-CoA intermediate. Then, the CoA

moiety is removed by BaiF prior to the reductive arm of the pathway involving 3 reductive steps to DCA. While, Harris *et al.*, identified BaiN<sup>89</sup> as the reductase catalyzing the two first reductive steps, Funabashi *et al.*, report that the oxido-reductases BaiCD and BaiH<sup>90</sup> are the ones involved in the reduction of the 3-oxo- $\Delta$ 4,6-DCA intermediate to 3-oxoDCA (Chapter 1, Figure 1.5). Furthermore, they also identified BaiA2 as the enzyme catalyzing the last reductive step to DCA<sup>90</sup>. Despite their interesting data, it is worth mentioning that the Funabashi's study has been released on bioRxiv but has not yet been peer-reviewed.

In a previous study, we identified 12-oxoLCA as a transient intermediate formed during CA 7-dehydroxylation *in vitro* (Chapter 2)<sup>29</sup>. This finding led us to the hypothesis of the existence of an alternative 7-dehydroxylation pathway which would involve the oxidation of the C12-hydroxyl group and formation of 12-oxoLCA as an intermediate. To probe this hypothesis, we cloned and purified 12 enzymes known to be involved in the current model of 7-dehydroxylation pathway (BaiA1/3, BaiA2, BaiCD, BaiH, BaiB, BaiF, BaiE, BaiN), or characterized and expected to be involved in the alternative pathway (12 $\alpha$ -HSDH). Finally, we also included other enzymes not yet characterized but thought to carry out bile acid transformations (BaiI, BaiJ, BaiO).

Using purified enzymes and conducting enzymatic assays under anoxic conditions, we demonstrate the co-existence of two 7-dehydroxylation pathways: a horizontal pathway (the Hylemon pathway) and a vertical pathway. The vertical pathway is novel and could explain why CA which carries a hydroxyl group at C12 is dehydroxylated to greater extent than CDCA which lacks that hydroxyl group.



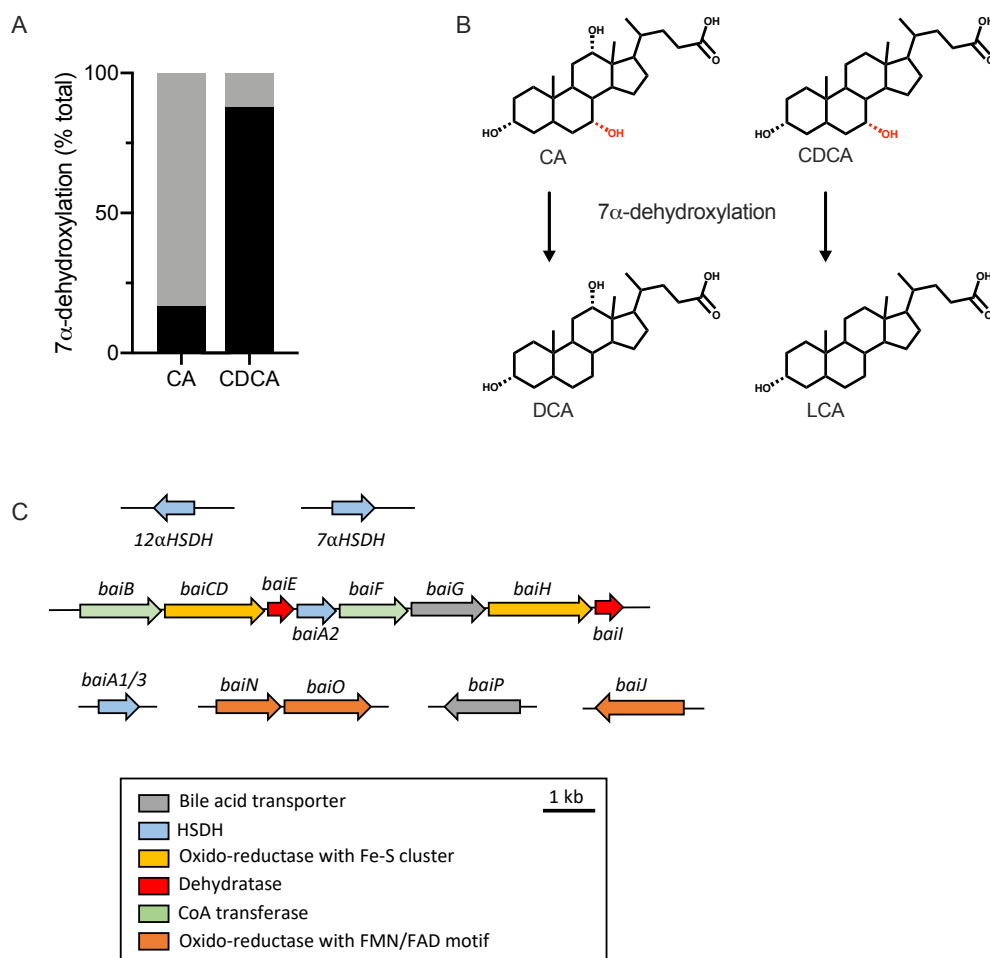


**Figure 3.1 | Bile acid 7-dehydroxylation of the human primary bile acids.** A) Extent of bile acid 7-dehydroxylation of CA compared to CDCA from an *in vitro* experiment with a pure culture of *C. scindens* ATCC 35704 after 24 hours incubation. The fraction in grey indicates the fraction of 7-dehydroxylated secondary bile acid formed from CA (DCA, 12oxoLCA) and CDCA (LCA, IsoLCA, 3-oxoLCA). B) Structure of CA, CDCA and their 7-dehydroxylated derivatives DCA and LCA respectively. C) *bai* operon along with other genes known or suspected to be involved in bile acid transformations in *C. scindens* ATCC 35704.

## 3.2 Material and Methods

### 3.2.1 Bacterial strains and culture conditions

Bacterial strains and plasmids used in this study are listed in Supplementary Table S1. *Clostridium scindens* ATCC 35704 (Morris et al., 1985) was grown in BHSS medium as previously reported (Marion et al. 2018) in an anaerobic chamber (Coy Laboratory Products, 95% N<sub>2</sub>, 5% H<sub>2</sub>) at 37°C.

The *E. coli* strains TOP10 and BL21-CodonPlus(DE3)-RIPL (Agilent) used for cloning and protein expression purposes were grown in LB medium or TB medium at 37°C supplemented with ampicillin (100 µg/mL) or kanamycin (50 µg/mL), spectinomycin (50 µg/mL) and chloramphenicol (25 µg/mL) when indicated.

### 3.2.2 *In vitro* 7-dehydroxylation of CA and CDCA by *C. scindens*

*C. scindens* ATCC 35704 was grown in BHSS medium containing 100 µM cholic acid or chenodeoxycholic acid. Samples were collected after 24h. Bile acid metabolites were analyzed from supernatant with an Agilent 6530 Accurate-Mass Q-TOF Ultra-High Pressure liquid chromatography mass spectrometer (heretofore LC/MS).

### 3.2.3 Cloning of *bai* genes into *E. coli*

Genes encoding 12 $\alpha$ -HSDH, BaiA1/3, BaiA2, BaiCD, BaiH, BaiB, BaiF, BaiE, BaiI, BaiJ, BaiO, BaiN from *Clostridium scindens* ATCC 35704 were amplified by PCR using primers listed in Supplementary Table 1. Each PCR-amplified gene was cloned into a modified pET28b+ vector (m-PET28b+) using Gibson Assembly (New England BioLabs) according to manufacturer's instructions. The modified pET28b+, provided by the Protein Purification and Core Facility of EPFL, carries both a His-Tag and a Strep-Tag sequence (unpublished). Restriction sites used for plasmid digestion are indicated in Supplementary Table 1. The recombinant plasmid pET51b+ containing the 12 $\alpha$ -HSDH<sup>28</sup> was kindly provided by Heidi Doden and Jason Ridlon (University of Illinois Urbana-Champaign, USA). Recombinant plasmids were transformed into *E. coli* TOP10 (One Shot™ TOP10 Chemically Competent *E. coli*, Invitrogen). All plasmid constructs were verified by sequencing. One clone for each gene was selected and the plasmid further transformed into the expression strain *E. coli* BL21-CodonPlus(DE3)-RIPL.

### 3.2.4 Protein expression and purification

Recombinant *E. coli* BL21-CodonPlus(DE3)-RIPL were grown on LB agar plate containing kanamycin (for recombinant m-pET28b+) or ampicillin (for recombinant pET51b+) and spectinomycin and chloramphenicol. A single colony was used to start an overnight culture in 100mL LB containing the antibiotics mentioned above. The overnight culture was used to inoculate 2 L of TB or TB autoinduction medium (for BaiO). Cultures were kept at 37°C under constant agitation for two hours until OD<sub>600</sub> reached 0.5. Then, for protein expression in TB, 0.5 mM IPTG was added to the medium to induce protein expression and cultures were transferred to 20°C. Cultures (TB and autoinduced TB) were grown for approximately 18h before being harvested by centrifugation at 15 000 x g. Cells pellets were stored at -20°C until purification.

In a typical purification, the cell pellet was resuspended in 30mL lysis buffer (20mM Hepes, pH 7.5, 300mM NaCl) supplemented with 10% v/v glycerol, 5µL Benzonase® nuclease (Merck), and 1 Protease inhibitor Cocktail tablet (Roche). For the purification of the flavoproteins (BaiJ, BaiO) 500µM of FAD and FMN were also added to cells prior lysis. Cells lysis was performed with a French Press Emulsiflex-C3 (Avestin). The lysate was removed by centrifugation at 4°C for 40 min at 20,000 x g. Supernatant was filtered through a 0.45 µm filter and subsequently loaded onto a 5mL HisTrap™ excel column (GE Healthcare Life Sciences) or 5mL Strep-Tactin® XT Superflow® column (Iba) for the purification of His-tagged protein and Strep- tagged proteins respectively, using an ÄTKA Purifier (GE Healthcare Life Sciences). The column was washed with 10 column volumes of lysis buffer before elution. The elution buffer for His-

tagged proteins contained 500mM NaCl, 10mM HEPES pH 7.5, 500mM imidazole pH 7.5. The elution buffer for purification of Strep-tagged proteins contained 60mM Hepes pH 7.5, 30mM Tris, 250mM NaCl, 50mM Biotin. Samples from the lysate, the column flow-through and the eluted fractions were run on a NuPAGE™ 4-12% Bis-Tris gel (Invitrogen) to verify the size of the purified protein and the purity of the eluted fractions. The fraction(s) containing the protein, based on absorbance at 280 nm, were pooled together and dialyzed overnight in 2L of dialysis buffer (20mM HEPES pH 7.5, 150mM NaCl). After dialysis, proteins were concentrated with Amicon® Ultra-15 Centrifugal Filter Units (Merck). The final protein concentration was estimated using absorbance measurement at 280 nm and the extinction coefficient calculated with ExPASy ProtParam tool<sup>162</sup> based on its amino acid sequence. Figure S1 shows a gel with all the purified enzymes.

### 3.2.5 Bile acid standards

Bile acid standards were either purchased or synthesized. All CoA conjugates were synthesized using the following procedure: 100μM bile acid standard, 250 μM CoA, 500 μM ATP and 100 μg of purified BaiB (CoA ligase) were mixed and reactions were incubated for 2h at 37°C in oxic conditions. All information regarding the bile acid standards used in the study are provided in Supplementary Table S2.

### 3.2.6 Bile acid pathway *in vitro* reconstruction

Assays were performed in buffer (50 mM HEPES pH 7.5, 50 mM KCl, 0.5 mM TCEP) containing 500μM NAD, 500 μM NADP, 500 μM FMN, 500 μM FAD, 500 μM CoA, 500 μM ATP and 100 μM of cholic acid. Buffer and enzymes (kept on ice) were purged under N<sub>2</sub> flow for 1h. All subsequent steps were carried out in an anoxic chamber (Coy Laboratory Products, 95% N<sub>2</sub>, 5% H<sub>2</sub>) at 37°C.

10 μg of each enzyme were pooled together in a tube. The horizontal pathway (HP) mix includes BaiA1/3, BaiA2, BaiCD, BaiH, BaiB, BaiF, BaiE, BaiI, BaiO, BaiN. The vertical pathway (VP) mix includes 12α-HSDH, BaiCD, BaiH, BaiB, BaiF, BaiE, BaiI, BaiO, BaiN. Reactions were initiated by addition of the HP or VP enzyme mix and incubated at 37°C. Samples (10μL) were collected and mixed with 50% v/v of methanol/eluent A (water with 5mM ammonium acetate). Each assay was performed in triplicates. Metabolites were analyzed with LC/MS.

### 3.2.7 Specificity of 12α-HSDH and BaiA

Assays were conducted in buffer (50 mM HEPES pH 7.5, 50 mM KCl) containing 500μM NAD, 500 μM NADP, 500 μM FMN, 500 μM FAD and 100 μM cholic acid. In addition, each assay contained 100 μg of one of the following enzymes: 12α-HSDH, BaiA1/3, or BaiA2. As mentioned above, both buffer and enzymes were purged with N<sub>2</sub> on ice for 1h. Reactions were initiated by amendment of the enzymes and incubated at 37°C for 24h. Samples (10μL) were collected and mixed with 50% v/v of methanol/eluent A (water with 5mM ammonium acetate). Each assay was performed in triplicates. As above, metabolites were analyzed with LC/MS.

### 3.2.8 Identifying key enzymes of the bile acid 7-dehydroxylation pathways

Assays were performed in buffer (50 mM HEPES pH 7.5, 50 mM KCl, 0.5 mM TCEP) containing 500μM NAD, 500 μM NADP, 500 μM FMN, 500 μM FAD, 500 μM CoA, 500 μM ATP and 100 μM of cholic acid. Buffer and enzymes (kept on ice) were purged under N<sub>2</sub> flow for 1h. All subsequent steps were carried out in an anoxic chamber (Coy Laboratory Products, 95% N<sub>2</sub>, 5% H<sub>2</sub>) at 37°C.

For each assay, one or two enzyme(s) were removed from the VP and HP mix of enzymes to identify the key enzymes necessary for each pathway. The enzymes thought to be homologous were removed at the same time (e.g., the two dehydratases BaiE and BaiI). Reactions were initiated by addition of the enzyme mix and incubated at 37°C. Samples (10μL) were collected and mixed with 50%

v/v of methanol/eluent A (water with 5mM ammonium acetate). Each assay was performed in triplicates. Metabolites were analyzed with LC/MS.

### 3.2.9 LC/MS analysis of bile acid metabolites

Bile acid metabolites were analyzed using an Agilent 6530 Accurate-Mass Q-TOF LC/MS mass spectrometer coupled to an Agilent 1290 series UHPLC system with a Zorbax Eclipse-Plus C18 column (2.1 × 100 mm, 1.8 μm; Agilent) heated at 50°C. Water with 5 mM ammonium acetate pH 6 (eluent A) and acetonitrile (eluent B) was used as mobile phase at a flow rate of 0.4 mL/min over a 22 min gradient: 0–5.5 min, isocratic 21.5% B; 5.5–6 min, 21.5–24.5% B; 6–10 min, 24.5–25% B; 10–10.5 min, 25–29% B; 10.5–14.5 min, isocratic 29% B; 14.5–15 min, 29–40% B; 15–18 min, 40–45% B; 18–20.5 min, 45–95% B, 20.5–22 min, isocratic 95%. The system was re-equilibrated to initial conditions for 3 min. The sample manager system temperature was maintained at 4°C and the injection volume was 5 μL. Mass spectrometer detection was operated in negative ionization mode using the Dual AJS Jet stream ESI Assembly. The QTOF instrument was operated in the 4 GHz high-resolution mode (typical resolution 17,000 (FWHM) at m/z 1000) in profile mode and calibrated in negative full scan mode using ESI-L solution (Agilent, Santa Clara, CA, USA). Internal calibration was performed during acquisition via continuous infusion of a reference mass solution [5 mM purine, 1 mM HP-921 (Agilent reference mass kit, Agilent, Santa Clara, CA, USA) in 95% MeOH acidified with 0.1% formic acid] and allowed to permanently achieve a mass accuracy better than 5 ppm. HR mass spectra were acquired over the range of m/z 300– 700 at an acquisition rate of three spectra/s. AJS settings were as follows: drying gas flow, 8 L/min; drying gas temperature, 300°C; nebulizer pressure, 35 psi; capillary voltage, 3500 V; nozzle voltage, 1000 V; fragmentor voltage, 175 V; skimmer voltage, 65 V; octopole 1 RF voltage, 750 V. Data was processed using the MassHunter Workstation (Agilent, Santa Clara, CA, USA). Extracted ions chromatograms (EIC) were based on a retention time (RT) window of ±0.5 min with a mass- extraction-windows (MEW) of ±30 ppm centered on m/z<sub>theor</sub> of each bile acid.

### 3.3 Results and Discussion

#### 3.3.1 Biochemical reconstruction of two 7-dehydroxylation pathways

Previous studies of the Bai enzymes were conducted with cell extract of *E. coli*-expressing the enzyme or directly with a single purified enzyme, considering a single step of the pathway<sup>28,76,81,84,85,88,89,163</sup>. We chose an alternative approach in which purified enzymes were pooled and assayed *in vitro* for the multi-step process of cholic acid 7-dehydroxylation. We believe that this approach would not only delineate the set of enzymes sufficient for the horizontal and the presumed pathway and also identify specific enzymes involved in the vertical pathway. We focused our efforts on all the genes shared amongst 7-dehydroxylating strains including genes of the *bai* operon (*baiB*, *baiCD*, *baiE*, *baiA2*, *baiF*, *baiH*, *baiI*), other genes reported to be involved in bile acid transformations (*baiA1/3*, *12 $\alpha$ -HSDH*, *baiN*) and yet uncharacterized genes but suggested to be involved in bile acid transformation (*baiJ*, *baiO*). We cloned each gene from *C. scindens* ATCC 35704, a well-studied 7-dehydroxylating strain, expressed them individually in *E. coli* and purified them as His<sub>6</sub> or Streptavidin fusions.

The horizontal pathway (HP) enzyme mix include the two 3 $\alpha$ -HSDH (BaiA1/3, BaiA2), the CoA ligase BaiB, the CoA transferase BaiF, the two dehydratases (BaiE and BaiI), and the oxidoreductases (BaiCD, BaiH, BaiJ, BaiO, BaiN). The vertical pathway (VP) enzyme mix is similar except for the two 3 $\alpha$ -HSDH (BaiA1/3, BaiA2) enzymes that are replaced by the 12 $\alpha$ -HSDH. When we incubated the mix of purified Bai enzymes (VP and HP) with CA, cofactors (NAD, NADP, FAD, FMN), CoA and ATP under anaerobic conditions and monitored the reaction by LC-MS, we observed a time-dependent conversion of CA to 3-oxoDCA with the horizontal pathway mix and of CA to a yet unknown 7-dehydroxylated bile acid with a m/z of 387.2548 with the vertical pathway mix (Figure 3.2).

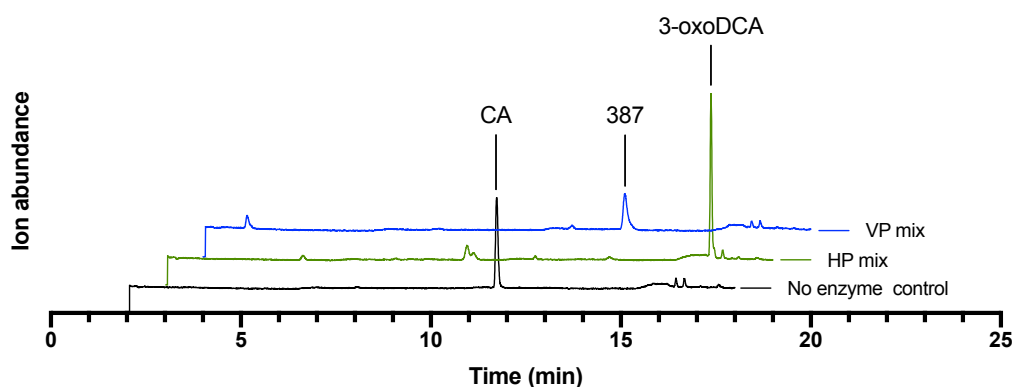


**Figure 3.2 | 7-dehydroxylation of CA with the VP and HP enzyme mix.** Cholic acid was incubated with the vertical pathway (VP) or the horizontal pathway (HP) enzyme mix for 20h at 37°C in anoxic condition.

#### 3.3.2 Time-dependent CA 7-dehydroxylation via the two pathways.

In a time-course experiment, we investigated the formation of the bile acid intermediates in the two pathways (Figure 3.3). We observed that the first step is the oxidation of the C12 and C3 hydroxyl groups (in the VP and HP respectively) followed by the CoA ligation. This contrasts with the reports from the previous models which propose CoA ligation as the first step of the horizontal pathway (Chapter 1, Figure 1.4, 1.5)<sup>1,90</sup>. Rapidly, we see formation of a transient intermediate with a m/z (mass over charge ratio) of 1,152 which indicates an oxidation step from (putatively) 12-oxoCDCA-CoA to 12-oxo- $\Delta^9$ -CDCA-CoA and from 3-oxoCA-CoA to 3-oxo- $\Delta^4$ -CA-CoA. In absence of standards, we cannot confirm these assignments. For both pathways, we observe that, at 3 hours, an intermediate with a mass of 1,134 is formed, suggesting a dehydration (loss of 18 m/z, corresponding to the H<sub>2</sub>O molecule) as third step.

Unfortunately, we do not yet have standards to confirm the structure of these 1,134 m/z intermediates but we hypothesize that they correspond to 12-oxo- $\Delta$ 7,9-LCA-CoA and 3-oxo- $\Delta$ 4,6-DCA-CoA for the vertical and horizontal pathway respectively. Subsequently, the dehydroxylated intermediates are reduced. The first reductive step leads to the formation of a m/z 1,136 product which we detect in the vertical pathway. We hypothesize this intermediate to be 12-oxo- $\Delta$ 7-LCA-CoA. The first reductive step may be extremely rapid, explaining the absence of the m/z 1,136 intermediate in the horizontal pathway. The second reductive step is illustrated by the formation of 12-oxoLCA-CoA and 3-oxoDCA-CoA. This suggests that the CoA conjugates can undergo the reductive steps in contrast with the current model of the pathway which reports that CoA removal precedes the reductive steps for the horizontal pathway (Chapter 1, Figure 1.4, 1.5)<sup>1,90</sup>. However, in the vertical pathway, the major end product (m/z 387) has lost the CoA moiety before the second reductive step, suggesting that for the vertical pathway two routes co-exist: 1) reduction of CoA conjugates or/and 2) CoA removal prior to the second reductive step.

For the horizontal pathway, we observe the last reductive step converting 3-oxoDCA to DCA. However, this last reduction is not very efficient in our system. The major peak remains 3-oxoDCA after 5 days of incubation (Figure 3.3b). Similarly, for the vertical pathway, the major peak corresponds to the m/z 387 intermediate after 5 days of incubation, suggesting that the two last reductive steps are not efficient in our system (Figure 3.3a). We hypothesized that our system is missing a reduced cofactor (such as NADH and NADPH) needed for the reductive step. To investigate this hypothesis, we removed all enzymes from the reaction after the formation of the m/z 387 compound and amended the reaction with NADH and one of the oxidoreductases: BaiCD, BaiH, BaiJ or BaiO. BaiCD and BaiH did not reduce the m/z 387 intermediate to 12-oxoLCA (Figure 3.4) but BaiJ and BaiO did after 20h of incubation (Figure 3.5). The last reductive step converting 12-oxoLCA to DCA is very efficient in *C. scindens* and required 12 $\alpha$ -HSDH and NADPH or NADH as a cofactor (Chapter 2, Figure 3.6)<sup>29</sup>. Interestingly, BaiJ and BaiO, which are not involved in the current model of the horizontal pathway, catalyze at least one reductive step in the vertical pathway (Figures 3.5 and 3.10).

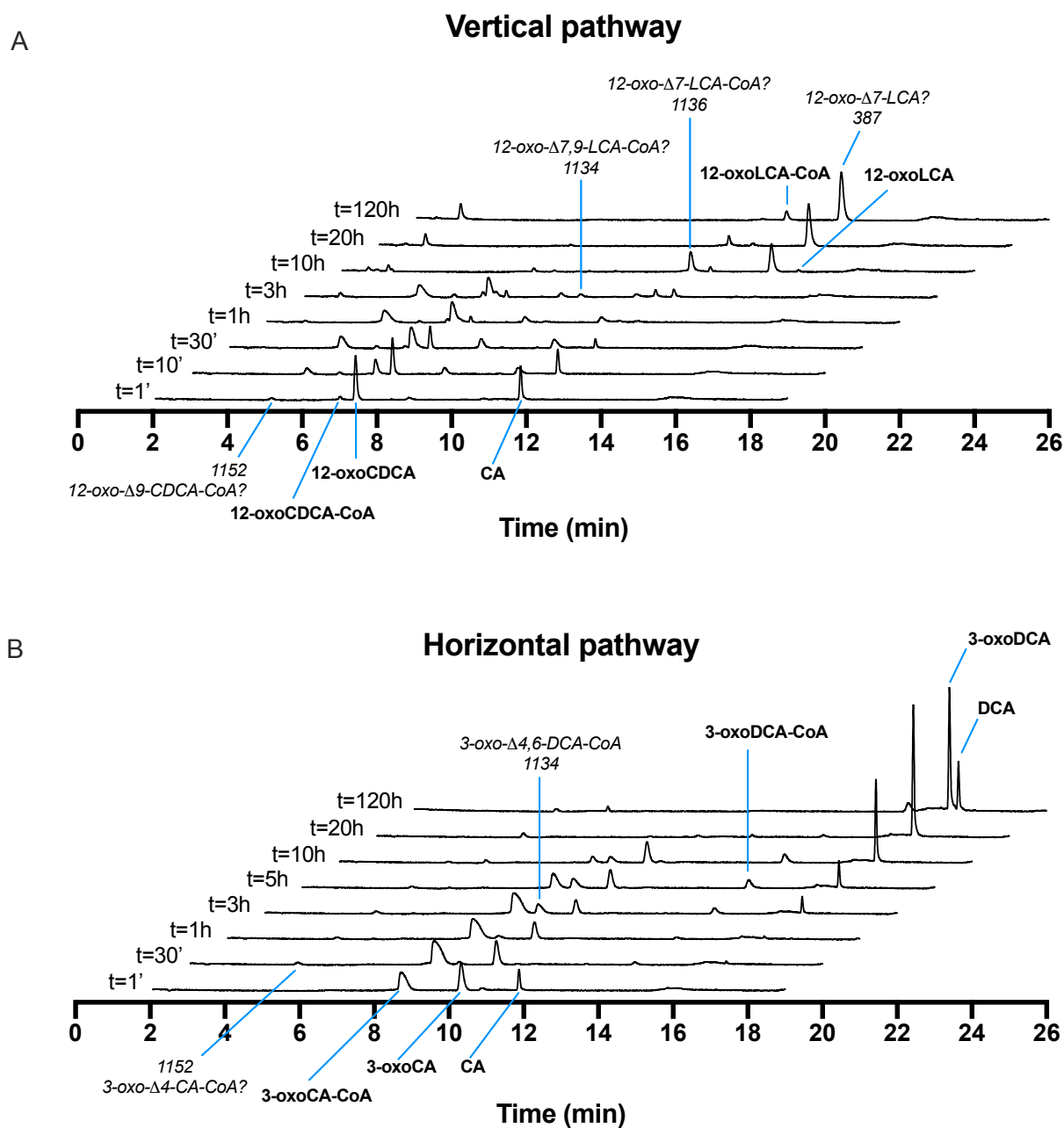


**Figure 3.3 | Time-dependent cholic acid 7-dehydroxylation.** Cholic acid was incubated with A) the vertical pathway or B) the horizontal pathway enzyme mix. Samples were taken as a function of time and bile acid intermediates analyzed by LC-MS. Intermediates in bold were confirmed by comparing masses and retention times with a standard. Intermediates in *italics* indicate that the structure as not been yet confirmed because appropriate standards are unavailable.

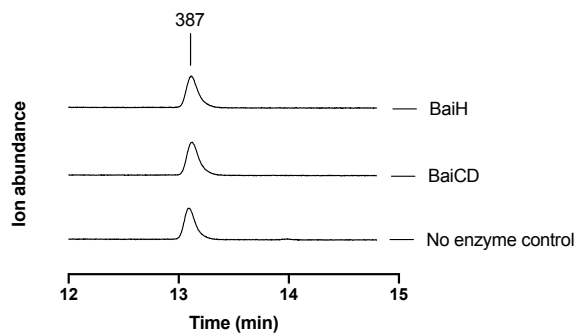


**Figure 3.4| BaiCD and BaiH do not have activity on the vertical pathway intermediate m/z 387.**  
Reactions were incubated for 20 hours in anoxic conditions.

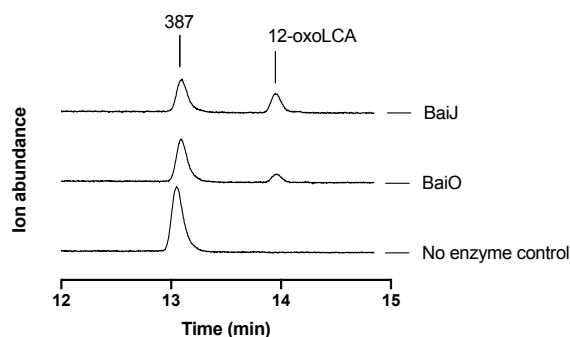


**Figure 3.5| Conversion of the vertical pathway intermediate m/z 387 to 12-oxoLCA by BaiJ and BaiO.**  
Reactions were incubated for 20 hours in anoxic conditions.

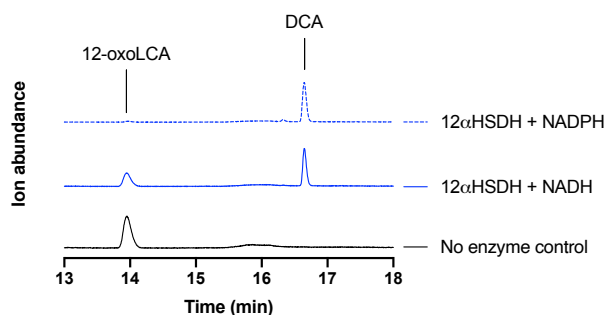


**Figure 3.6| Conversion of 12-oxoLCA to DCA with 12α-HSDH with NADH or NADPH as cofactor.**  
Reactions were incubated for 20 hours in anoxic conditions.

### 3.3.3 12α-HSDH and BaiA2 initiating the vertical and horizontal pathway are highly specific.

Hydroxysteroid dehydrogenases (HSDH) are central in the bile acid 7-dehydroxylation pathway. They initiate the first oxidative step (Figures 3.10 and 3.11). In order for the vertical pathway to be truly distinct from the horizontal pathway, it must not involve any 3-HSDH activity. Thus, the 12α-HSDH enzyme must be highly specific to oxidize and reduce the hydroxyl at the C12 position rather than at the C3 position. To confirm the specificity of the 12α-HSDH and BaiA2 or BaiA1/3 for the vertical and horizontal pathway respectively, we incubated CA with one of the three HSDHs: 12α-HSDH, BaiA1/3, or BaiA2. After a 3-hour incubation, we observed that 12α-



HSDH fully converted CA to 12-oxoCDCA (Figure 3.7). Similarly, BaiA2 fully converted CA to 3-oxoCA. This finding demonstrates that these enzymes have high specificity for the two pathways. In contrast, BaiA1/3 showed less specificity. It oxidizes both C3 and C7-hydroxyl groups forming 3-oxoCA, 7-oxoDCA and 3,7-dioxoCA (Figure 3.7).

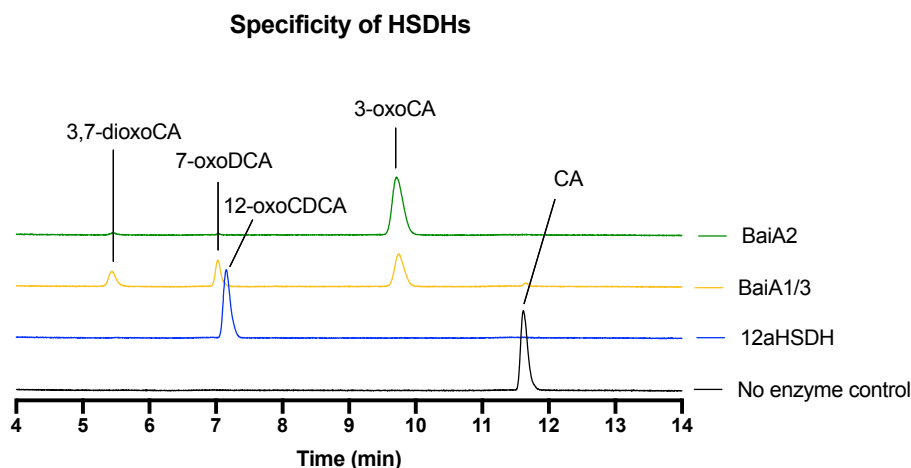


**Figure 3.7 | Specificity of 12 $\alpha$ -HSDH, BaiA1/3 and BaiA2.** CA was incubated with one of the three HSDH (12 $\alpha$ -HSDH, BaiA2 and BaiA1/3) for 3 hours. Metabolites were analysed by LC-MS.

### 3.3.4 Identifying key enzymes of the vertical and horizontal 7-dehydroxylation pathway.

To identify the enzymes involved in the vertical and horizontal 7-dehydroxylation pathway and those which are not involved in the transformation, we set up systematic assays where we removed enzymes from the full mix one at a time (Figures 3.8 and 3.9). Only for homologous enzymes (e.g., the dehydratases BaiE and BaiI), we did remove two enzymes from the mix at a time.

For both the vertical and the horizontal pathways, we observe that the CoA ligase BaiB, the CoA transferase BaiF and the reductase BaiN are not required for the 7-dehydroxylation to occur. When they are absent, CA is converted to the as-of-yet unidentified 7-dehydroxylated m/z 387 intermediate and to 3-oxoDCA for the vertical and horizontal pathways, respectively (Figure 3.8 and 3.9). Interestingly, in absence of 12 $\alpha$ -HSDH in the vertical pathway mix, CA 7-dehydroxylation occurs via the horizontal pathway as the final product is 3-oxoDCA (Figure 3.8). This suggests that another enzyme in the mix harbors 3 $\alpha$ -HSDH activity. In favor of this hypothesis, when BaiA1/3 and BaiA2 are lacking in the horizontal pathway mix, 7-dehydroxylation still occurs via the horizontal pathway leading to the formation of 3-oxoDCA (Figure 3.9). The enzymes required for the vertical pathway 7-dehydroxylation are 12 $\alpha$ -HSDH, BaiCD/BaiH, BaiE/BaiI and BaiJ/BaiO. The enzymes required for the horizontal pathway 7-dehydroxylation are BaiCD/BaiH, BaiE/BaiI and BaiJ/BaiO.

Regarding the CoA ligases/transferases BaiB and BaiF, it is likely that one or the other is required for both pathways. This is because when only one of the two is removed (Figures 3.8 and 3.9), the other was present and 7-dehydroxylation is reported.

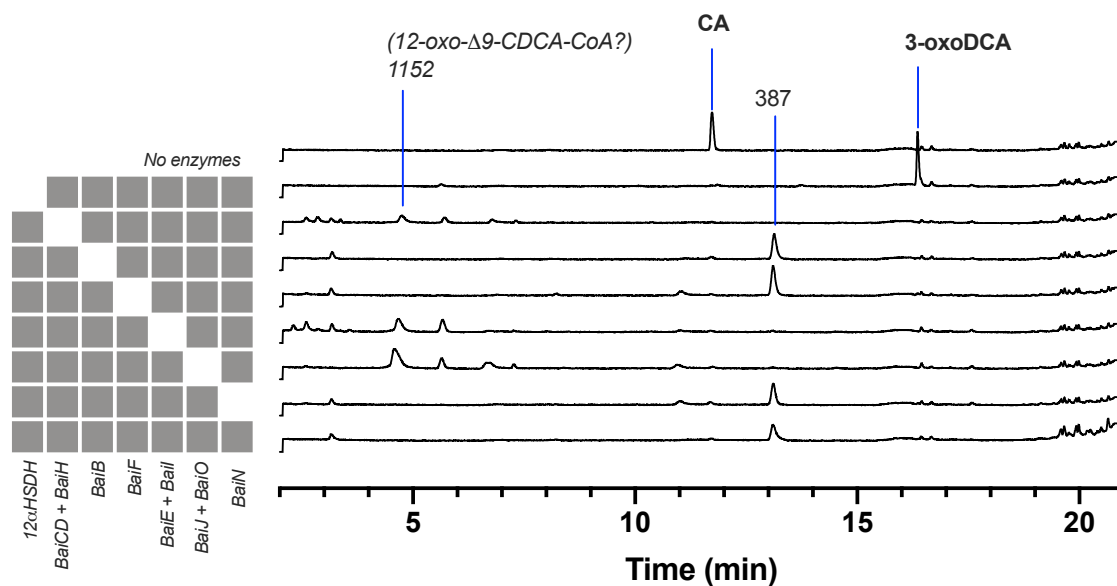


**Figure 3.8 | Identifying essential enzymes for the vertical pathway.** 100μM CA was incubated with the various enzyme mix. Samples were taken after 20h of incubation at 37 °C and analyzed on the LC-MS. Chromatograms show the bile acid intermediates detected with LC-MS.

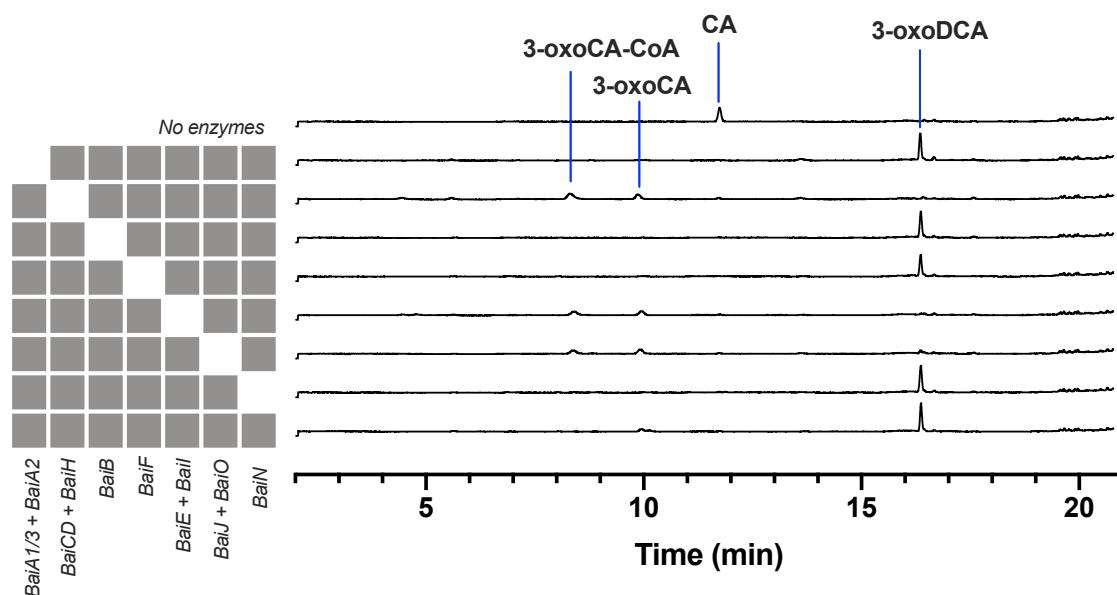


**Figure 3.9 | Identifying essential enzymes for the horizontal pathway.** 100μM CA was incubated with the various enzyme mix. Samples were taken after 20h of incubation at 37 °C and analyzed on the LC-MS. Chromatograms show the bile acid intermediates detected with LC-MS.

Our findings demonstrate the co-existence of two 7-dehydroxylation pathways involving different regions of the cholic acid molecule (Figures 3.10 and 3.11). The horizontal pathway has been characterized by Hylemon and colleagues in their pioneering work<sup>1</sup>. Recently, Funabashi *et al.* reported to have completed the horizontal pathway by identifying enzymes catalyzing the reductive arm of the pathway<sup>90</sup>. In spite of the previous characterization, some of our findings differ from the current knowledge on the horizontal

pathway. For instance, we report that BaiA2, and BaiB or BaiF are not required for the 7-dehydroxylation via the horizontal pathway while Funabashi *et al.* include them in the core set of six enzymes necessary and sufficient for CA 7-dehydroxylation<sup>90</sup>. Furthermore, we demonstrate that oxidation of C3 precedes CoA ligation by BaiB and not the opposite as previously reported<sup>1,90</sup> (Figures 3.11, 1.4, 1.5). Finally, we observe that the CoA conjugate undergoes the two reductive steps, which contrasts with the current model in which the CoA moiety is removed prior to the reductive steps (Figures 3.11, 1.4, 1.5).

A major achievement of this study is the discovery of a novel pathway: the vertical 7-dehydroxylation pathway (Figure 3.10). This pathway involves the oxidation of C12-hydroxyl group by the 12 $\alpha$ -HSDH, followed by CoA ligation with BaiB or BaiF, oxidation forming a double bond between C9 and C11, then the dehydration step by a dehydratase (BaiE or BaiI). The dehydrated intermediate is suspected to be 12-oxo- $\Delta$ 7,9-LCA-CoA. The reductive step would first remove the double bond between C9-C11 forming 12-oxo- $\Delta$ 7-LCA-CoA. From this point on, we observed two routes. A minor one, which includes a reduction of the C7-C8 double bond to 12-oxoLCA-CoA prior to CoA removal. In contrast, the main route involves removal of the CoA moiety forming the m/z 387 compound (possibly 12-oxo- $\Delta$ 7-LCA) prior to the reductive step carried out by BaiJ and BaiO and generating 12-oxoLCA (Figure 3.4). The last reductive step, converting 12-oxoLCA to DCA, is carried out by 12 $\alpha$ -HSDH (Figure 3.6).

Experiments are being conducted to identify the specific enzyme (BaiCD, BaiH, BaiJ or BaiO) catalyzing the second oxidative step and the reductive steps in the two pathways (Figures 3.10 and 3.11). NMR analysis will be performed to confirm the structure of the m/z 387 intermediate of the vertical pathway.

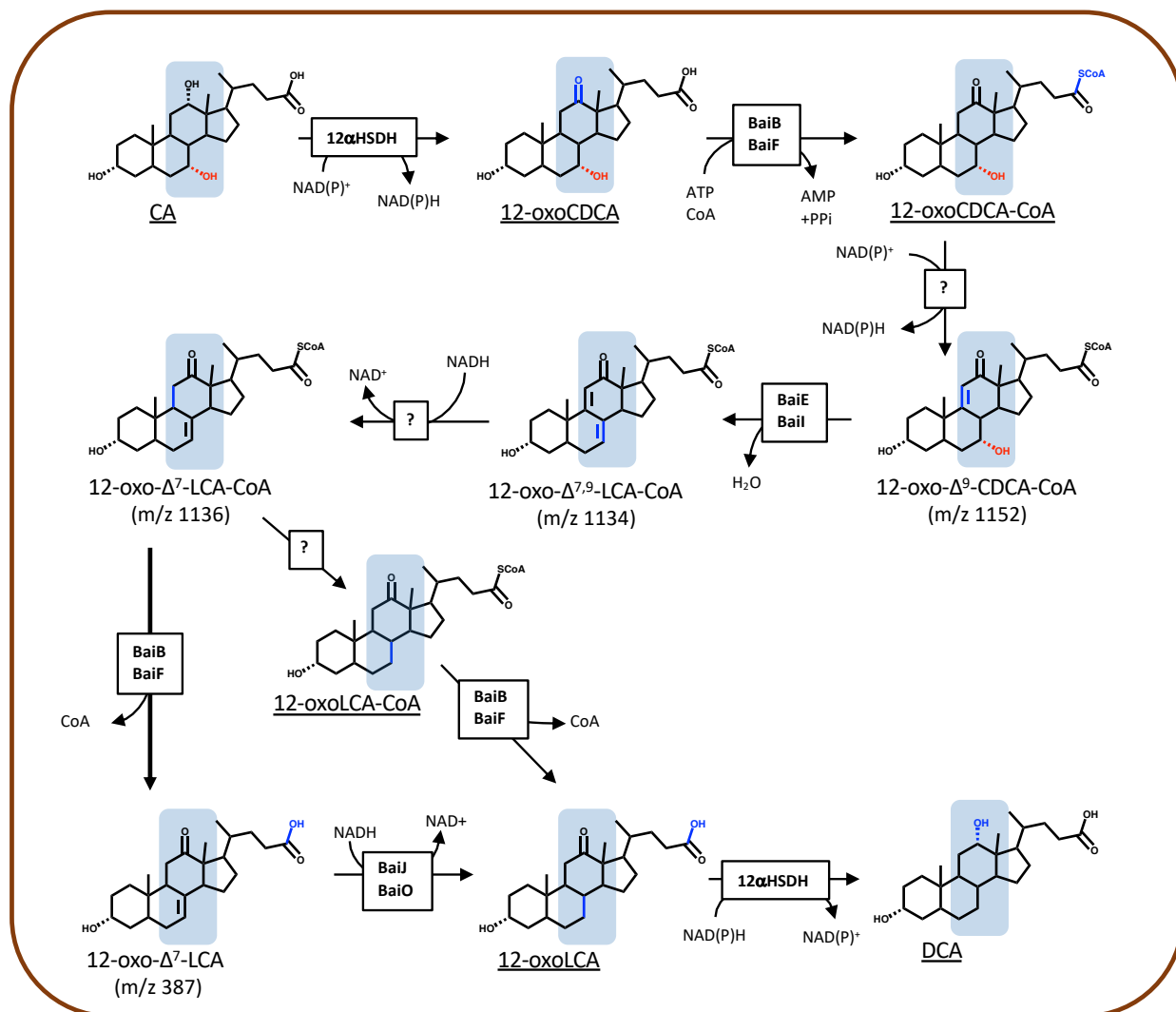


**Figure 3.10 | Proposed vertical CA 7-dehydroxylation pathway in *C. scindens* ATCC 35704 based on the intermediates detected in the enzymatic assays with purified enzymes.** Bile acid intermediates underlined indicate that the structure was confirmed by comparing mass and retention time with a known standard. Box with a question mark indicates that the enzyme is not defined yet but we know that is one of the oxidoreductases (BaiCD, BaiH, BaiI or BaiO). The C7-hydroxyl group is highlighted in red. Changes on the cholic acid structure at each step are indicated in blue.

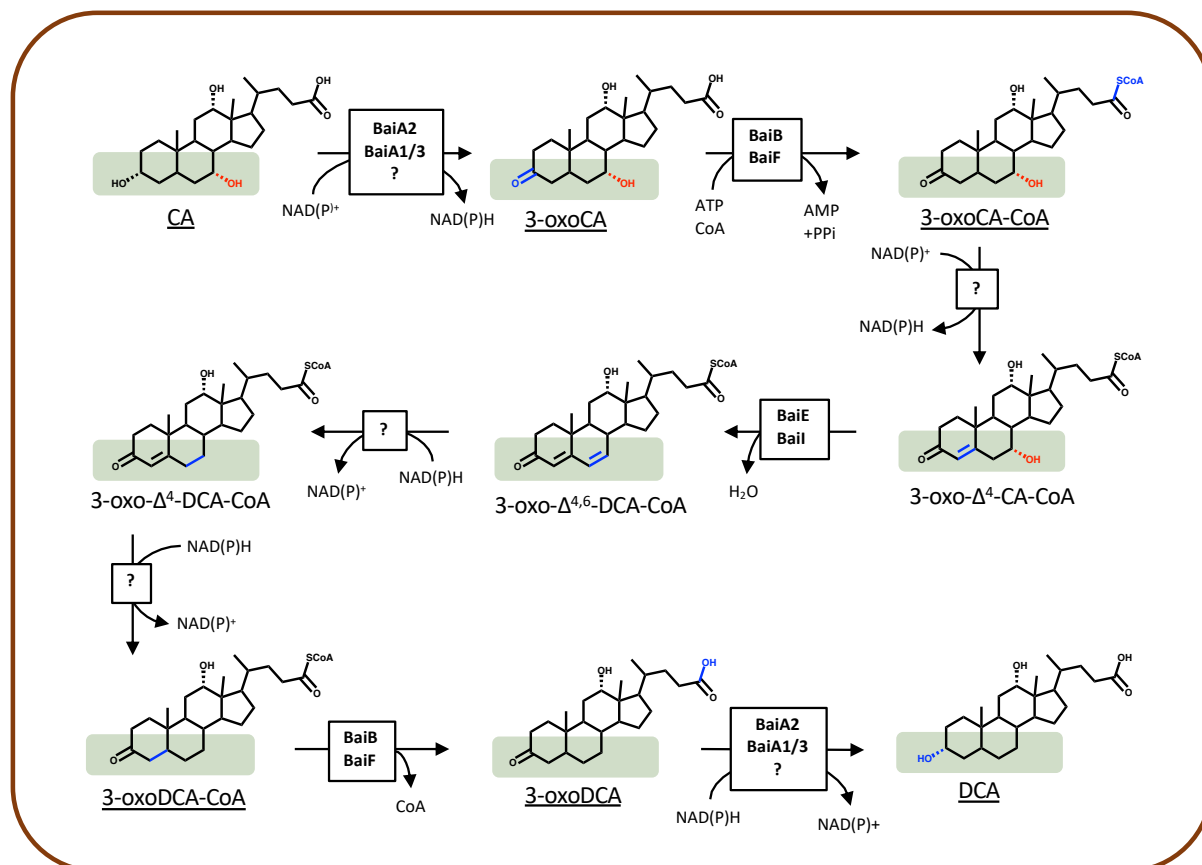


**Figure 3.11 | Proposed horizontal CA 7-dehydroxylation pathway in *C. scindens* ATCC 35704 based on the intermediates detected in the enzymatic assays with purified enzymes.** Bile acid intermediates underlined indicate that the structure was confirmed by comparing mass and retention time with a known standard. Box with a question mark indicates that the enzyme is not defined yet but we know that is one of the oxidoreductases (BaiCD, BaiH, BaiI or BaiO). The C7-hydroxyl group is highlighted in red. Changes on the cholic acid structure at each step is indicated in blue.

Steroid molecules are a class of secondary metabolites widely found in nature (in plants, in microorganisms, vertebrates and invertebrates) where they act as hormones and antimicrobial agents<sup>164,165</sup>. This class of molecules is extensively used in human medicine as contraceptive drug (e.g., estrogen, progesterone), cardiovascular agent (e.g., digoxin), anti-cancer (e.g., formestane), anti-inflammatory drug (e.g., cortisone) and anti-asthmatic agent (e.g., prednisone). Discovery of new biosynthetic pathways and new enzymes active on the steroid core is of interest for a broad range of scientific disciplines. In this study, we demonstrate the co-existence of two pathways transforming the steroid core of bile acid. The underlying rationale for the presence of redundant pathways remains to be elucidated. Multiple pathways found in nature are the result of an evolutionary advantage: either the generation of more metabolites to adapt to environmental variations or an increase in the efficiency of product formation<sup>166</sup>. In the case of bile acid 7-dehydroxylation, one could hypothesize that these dual pathways have been developed to cope with the low abundance of these microorganisms in the gut and to enhance the rate of CA conversion to DCA.

# Chapter 4 Biogeography of microbial bile acid transformations along the murine gut

Chapter 4 investigates the biogeography of microbial bile acid transformations along the murine gut and identifies the microorganisms responsible for these transformations in a gnotobiotic mouse model. This work has been submitted to *Journal of Lipid Research* and is currently under revision.

## Authors:

Solenne Marion<sup>1</sup>, Lyne Desharnais<sup>1</sup>, Nicolas Studer<sup>2</sup>, Yuan Dong<sup>2</sup>, Matheus D. Notter<sup>2</sup>, Suresh Poudel<sup>3</sup>, Laure Menin<sup>4</sup>, Andrew Janowczyk<sup>5</sup>, Robert L. Hettich<sup>3</sup>, Siegfried Hapfelmeier<sup>2</sup>, Rizlan Bernier-Latmani<sup>1</sup>

## Author information:

<sup>1</sup>*Environmental Microbiology Laboratory, École Polytechnique Fédérale de Lausanne (EPFL), Lausanne, Switzerland*

<sup>2</sup>*Institute for Infectious Diseases, University of Bern, Bern, Switzerland*

<sup>3</sup>*Chemical Sciences Division, Oak Ridge National Laboratory, Oak Ridge, TN, United States*

<sup>4</sup>*Institute of Chemical Sciences and Engineering, École Polytechnique Fédérale de Lausanne (EPFL), Lausanne, Switzerland*

<sup>5</sup>*Bioinformatics Core Facility, Swiss Institute of Bioinformatics, Lausanne, Switzerland*

## Author contributions:

SM wrote the manuscript under the supervision of RBL. LD carried out the bile acid analysis at the Mass Spectrometry Facility supervised by LM. SM, NS, YD and MDN carried out the animal experiments in Bern under the supervision of SH. SP carried out the metaproteomic analysis under the supervision of RH. AJ performed the bioinformatic analysis. All co-authors (LD, NS, YD, MDN, SP, LM, AJ, RH, SH) provided feedback on the manuscript.

## Abbreviations

BA, bile acid; CA, cholic acid; CDCA, chenodeoxycholic acid; UDCA, ursodeoxycholic acid; MCA, muricholic acid; DCA, deoxycholic acid; LCA, lithocholic acid; MDCA, murideoxycholic acid; HCA, hyocholic acid; HDCA, hyodeoxycholic acid; TGR5, Takeda G-protein receptor 5; FXR, farnesoid X receptor; Fgf15, fibroblast growth factor 15; BSH, bile salt hydrolase; HSDH, hydroxysteroid dehydrogenase; SPF, specific pathogen-free; GF, germ-free; CDI, *Clostridioides difficile* infection;

## Abstract

Bile acids, synthesized from cholesterol by the liver, are chemically transformed along the intestinal tract by the gut microbiota and the products of these transformations signal through host receptors, impacting overall host health. These transformations include bile acid deconjugation, oxidation, and 7 $\alpha$ -dehydroxylation. An understanding of the biogeography of bile acid transformations in the gut is critical because deconjugation is a prerequisite for 7 $\alpha$ -dehydroxylation and because most gut microorganisms harbor bile acid transformation capacity. Here, we used a coupled metabolomic and metaproteomic approach to probe the *in vivo* activity of the gut microbial community in a gnotobiotic mouse model. Results revealed the involvement of *Clostridium scindens* in 7 $\alpha$ -dehydroxylation, of the genera *Muribaculum* and *Bacteroides* in deconjugation, and of six additional organisms in oxidation (the genera *Clostridium*, *Muribaculum*, *Bacteroides*, *Bifidobacterium*, *Acutalibacter* and *Akkermansia*). Furthermore, the bile acid profile in mice with a more complex microbiota, with a dysbiosed microbiota or with no microbiota was considered. For instance, conventional mice harbor a large diversity of bile acids, but treatment with an antibiotic such as clindamycin results in complete inhibition of 7 $\alpha$ -dehydroxylation, underscoring the strong inhibition of organisms able to carry out this process by this compound. In this study, bile acid transformations were mapped to the associated active microorganisms, offering a systematic characterization of the relationship between microbiota and bile acid composition.

### Keywords

Bile acids and salts, Bile acids and salts/Biosynthesis, Bile acids and salts/Metabolism, Animal models, Gut microbiome, Mass spectrometry, Metabolomics, Proteomics

## 4.1 Introduction

The gut is a complex ecosystem hosting a wide diversity of microorganisms. The gut microbiome is sometimes referred to as the forgotten endocrine organ because of its profound influence on host physiology. Gut microbes convert dietary and other exogenous molecules into signaling metabolites to communicate with the host<sup>17</sup>. Bile acids (BAs) are one of these microbiota-derived signaling metabolites.

Primary bile acids are synthesized in the liver from cholesterol (dietary or endogenous). In the hepatocytes, they are conjugated to glycine or taurine and stored continuously in the gall bladder as the main component of bile. The human liver synthesizes only two primary bile acids: cholic acid (CA) and chenodeoxycholic acid (CDCA), while the rodent liver synthesizes five: CA, CDCA, two muricholic acids ( $\alpha$ MCA and  $\beta$ MCA) and ursodeoxycholic acid (UDCA), the 7 $\beta$  epimer of CDCA<sup>135</sup>. After food intake, the presence of fat molecules in the duodenum stimulates the release of a hormone, cholecystokinin, which triggers the contraction of the gall bladder and the relaxation of the Oddi sphincter, leading to the release of bile into the small intestine<sup>2</sup>. Along the intestinal tract, primary bile acids undergo several chemical transformations that are catalyzed by gut microorganisms, leading to the formation of secondary bile acids. Thus, the activity of the gut microbiota increases the diversity of the bile acid pool. The microbial transformation of the bile acid pool is essential as it modifies their detergent properties (i.e., their cytotoxicity) and also their affinity for host bile acid receptors<sup>135</sup>. For instance, the secondary bile acids deoxycholic acid (DCA) and lithocholic acid (LCA), resulting from microbial 7 $\alpha$ -dehydroxylation of CA and CDCA, have a higher affinity for the membrane receptor Takeda G-protein receptor 5 (TGR5) compared to the host liver-derived primary bile acids<sup>6,167</sup>.

Gut microorganisms act on the side chain, the hydroxyl groups, as well as the cyclohexane rings in the bile acid structure. Thus, microbial bile acid transformations include deconjugation or hydrolysis (i.e., the removal of the taurine/glycine moiety on the side chain), oxidation and epimerization of hydroxyl groups (at the C3, C7, and C12 positions) and of the C5-hydrogen, reduction of ketone

groups, dehydroxylation at C7 and C12<sup>168</sup>, desulfation<sup>169</sup>, esterification of hydroxyl groups<sup>170</sup>, and the oxidation of a steroid ring to form unsaturated bile acids<sup>171,172</sup> (Figure 4.1). Recently, a new microbial bile acid transformation was identified in both humans and mice: reconjugation. After being deconjugated by bacteria carrying bile salt hydrolase (BSH), the unconjugated bile acid can be reconjugated by bacteria with amino acids such as tyrosine, phenylalanine, leucine forming tyroscholeic acid, phenylalaninocholeic acid, and leucocholeic acid respectively<sup>173</sup>.

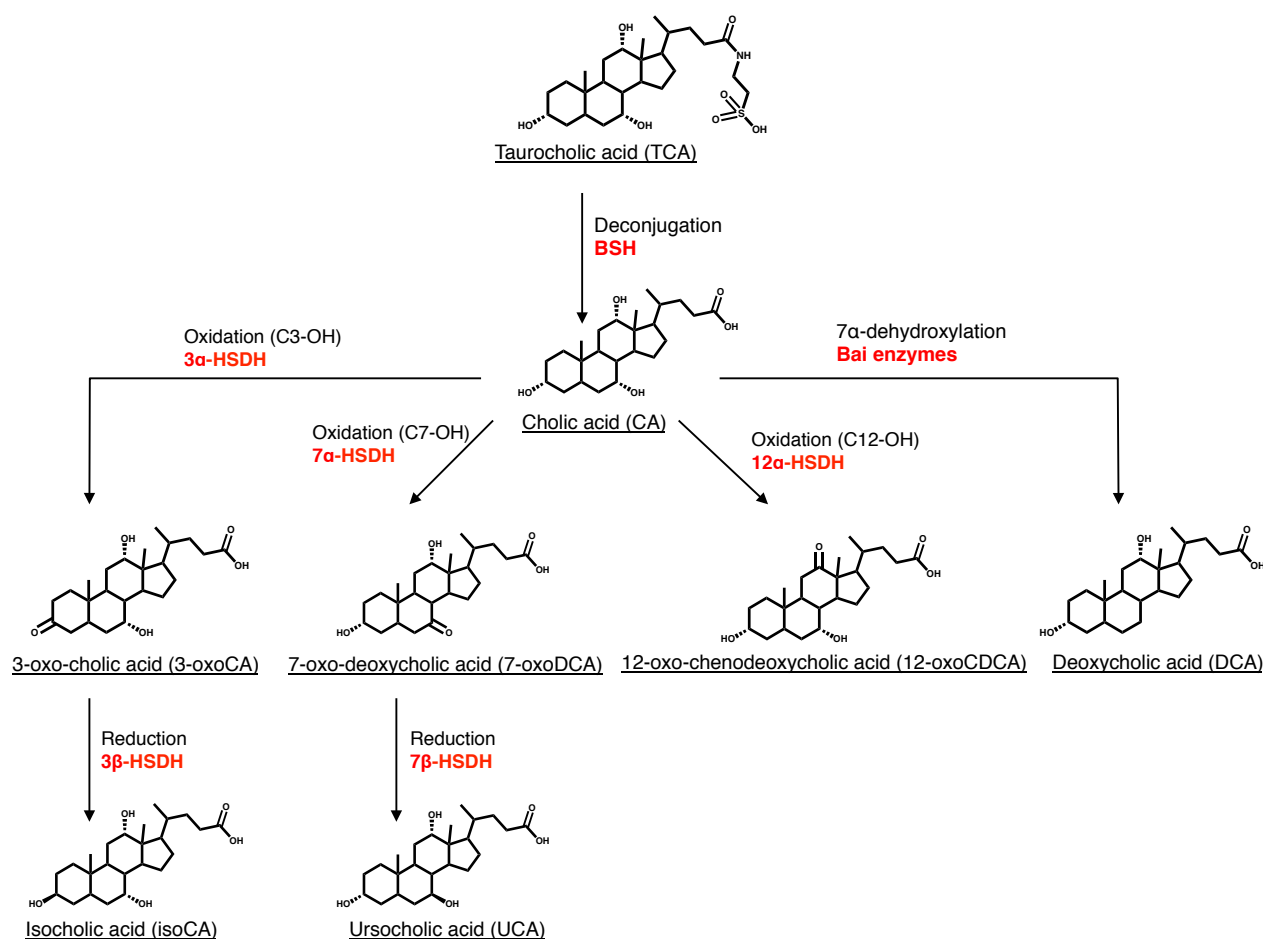


**Figure 4.1 | Microbial bile acid transformations.** Deconjugation (bile salt hydrolysis), oxidation of hydroxyl groups, reduction of ketone group and bile acid 7 $\alpha$ -dehydroxylation are major bile acid transformations occurring in the intestinal tract and are those on which we focused in this study. The enzymes catalyzing each transformation are indicated in red. Other microbial bile acid transformations (such as desulfation<sup>174</sup>, reconjugation<sup>173</sup>, the oxidation of C12-hydroxyl group on taurocholic acid by 12 $\alpha$ -HSDH<sup>28,175</sup>) are not presented in this figure for the sake of clarity. BSH, bile salt hydrolase; HSDH, hydroxysteroid dehydrogenase.

The abundance and diversity of bacteria carrying out the various bile acid transformations vary enormously. Deconjugating bacteria, synthesizing BSH, are reported to be abundant in the gut and widespread across bacterial phyla<sup>18,176,177</sup>. Similarly, oxidation of the hydroxyl groups in bile acids is also a common activity in gut microorganisms and is catalyzed by hydroxysteroid dehydrogenases (HSDHs)<sup>28</sup>. In contrast, 7 $\alpha$ -dehydroxylating bacteria are considered as rare organisms in the gut and so far, only belong to the order Clostridiales<sup>22</sup>. The 7 $\alpha$ -dehydroxylation reaction is catalyzed by a series of proteins (Bai proteins) encoded by genes belonging to the *bai* operon<sup>1</sup>. However, deconjugation is a prerequisite for bile acid 7 $\alpha$ -dehydroxylation, thus the importance of considering the relative localization of these two bile acid transformations<sup>20,178</sup>.



Connecting the spatial organization of the gut microorganisms to biological function remains challenging because of the high diversity of the microbial community<sup>139</sup>. For bile acid transformations, this difficulty is compounded by the large number of bile acid chemical species that can be generated by the gut microbiota. The original study of microbial bile acid transformation biogeography dates back to 1968, when Midtvedt and Norman sampled luminal content along the intestinal tract of three rats and probed *in vitro* for bile acid transformations in each sample<sup>34</sup>. First, they noticed variability in the distribution of microbial bile acid transformations amongst the three rats. For instance, one rat had very little deconjugating activity in the small intestine (ileum) compared to the two other rats. Two rats showed 7 $\alpha$ -HSDH activity (oxidation of the 7 $\alpha$ -hydroxyl) in the ileum while the third rat did not. Since then, other studies have investigated bile acid profiles longitudinally<sup>5,179</sup>. However, probing for the presence/absence of specific bile acids may not accurately reflect the *in vivo* microbial bile acid transformation activity nor the presence/absence of the organisms responsible for the synthesis of that particular bile acid. For instance, it was recently observed that bile acid 7 $\alpha$ -dehydroxylation activity was absent in the ileum of gnotobiotic mice despite colonization of the 7 $\alpha$ -dehydroxylating organism, *Clostridium scindens*<sup>29</sup>. It was hypothesized that the high level of tauro-conjugated bile acids in the ileum likely precluded bile acid 7 $\alpha$ -dehydroxylation<sup>29</sup>. Furthermore, the ability to transform bile acids *in vitro* does not necessarily reflect the *in vivo* activity. For instance, Narushima *et al.* (1999) reported that the 7 $\alpha$ -dehydroxylating bacterium *Clostridium hiranonis* (formerly *Clostridium strain TO-931*), known to 7 $\alpha$ -dehydroxylate cholic acid *in vitro* did not show 7 $\alpha$ -dehydroxylating activity in gnotobiotic mice<sup>60</sup>. Thus, *in vivo* studies are needed to identify organisms active in bile acid metabolism within the microbial community of the gut.

In this study, we explored the longitudinal distribution of bile acid transformations in gnotobiotic mouse models and identified the microorganisms responsible for these transformations using a combined metabolomic and metaproteomic approach. Bile acid 7 $\alpha$ -dehydroxylation was a transformation of particular interest because of its connection to TGR5 signaling. We contrasted gnotobiotic mice lacking bile acid 7 $\alpha$ -dehydroxylating activity with gnotobiotic mice containing the same base microbiota but complemented with the 7 $\alpha$ -dehydroxylating organism *Clostridium scindens* ATCC 35704. Finally, for comparison, we considered the bile acid profile in mice with either a complex microbiota (conventional, specific pathogen-free (SPF) mice), a reduced microbiota (antibiotic-treated SPF mice), or no microbiota (germ-free).

## 4.2 Material and Methods

### 4.2.1 Animal experiments

Groups of age-matched C57BL/6 mice (6–12 weeks old) were used. Germ-free (GF) and gnotobiotic sDMDMm2 mice were established and maintained at the Clean Mouse Facility of the Department of Clinical Research of the University of Bern. sDMDMm2 mice were colonized with a mouse-intestine derived 12-species mouse microbiota (Oligo-MM12) (Table S1). All Oligo-MM12 strains are available at <http://www.dsmz.de/miBC>. In-depth description of the Oligo-MM12 consortium species and description of novel taxa are provided elsewhere<sup>37,145,180</sup>. SPF mice were purchased from Envigo (formerly Harlan) and acclimatized to the local animal facility for 7 days before the start of experiments. SPF mice were pretreated with the antibiotic clindamycin (100 µL by intra-peritoneal injection, 2 mg/mL in PBS) or streptomycin (100 µL by gavage, 200 mg/mL in PBS) 24h before sacrifice. sDMDMm2 mice were inoculated with *C. scindens* ATCC 35704 by gavage of  $10^{7-9}$  CFU of *C. scindens* and colonized for 7 days before sacrifice. *C. scindens* pre-colonization was performed in flexible film isolators. These mice are denoted sDMDMm2+Cs.

All animals were sacrificed inside a sterile laminar flow hood and aseptic technique was used to collect the specific tissues and contents (liver, terminal ileum tissue, distal duodenum content, ileum content, cecum content and colon content). The collected samples were flash-frozen in liquid nitrogen and kept at -80°C to await subsequent analyses. All animal experiments were performed in accordance with the Swiss Federal and the Bernese Cantonal regulations and were approved by the Bernese Cantonal ethical committee for animal experiments under the license number BE 82/13.

### 4.2.2 Quantitative Real-Time PCR

Liver (30 mg of the caudate lobe) and terminal ileum tissue were lysed and homogenized in tubes filled with 2.8 mm zirconium oxide beads using a Precellys 24 Tissue Homogenizer (Bertin Instruments) at 6,500 rpm for 3x10 sec. Total RNA was isolated with the RNeasy Plus Mini Kit (QIAGEN). QuantiTect Reverse Transcription Kit (QIAGEN) was used to synthesize 20 µL cDNA templates from 1 µg of purified RNA. cDNA templates were diluted 10x before use in subsequent reactions. SensiFAST SYBR No-ROX Kit (Bioline) was used for quantitative real-time PCR with a final reaction volume of 10 µL (7.5 µL of mix and 2.5 µL of diluted cDNA template). Gene-specific primers (400nM) were used in each reaction and all results were normalized to the ribosomal protein L32 mRNA (primer sequences can be found in Table S7). PCR product specificity was verified by performance of a melting curve for each primer set. Assays were performed using Mic qPCR Cycler (Bio Molecular Systems) with a three-step program (2 min 95°C, followed by 40 cycles of 95°C for 5 s, 60°C for 10 s and 72 °C for 10 s). Four replicates of each sample for each primer set were performed, as well as negative controls (no reverse transcription and no template controls). Relative Quantification analysis using the REST method was performed with the Mic qPCR analysis software (Bio Molecular Systems).

### 4.2.3 Preparation of bile acid standard solutions

Stock solutions (10 mM) of each BA standard were prepared in methanol (Table S2). Deuterated CDCA and DCA were used as recovery standards. Individual standard solutions (100 µM) were mixed together and diluted with a 50:50 (v/v) mix of ammonium acetate (5 mM) and methanol to construct external standard curves between 1 and 10,000 nM.

### 4.2.4 Bile acid extraction

Approximately 10 mg of freeze-dried intestinal sample was homogenized with 150 µL of H<sub>2</sub>O and spiked with 40 µL of recovery standard (100 µM) in 2 mL tubes filled with 2.8 mm zirconium oxide beads. Homogenization was performed using an automated Precellys 24 Tissue Homogenizer (Bertin Instruments) at 5,000 rpm for 20 s. Mixed samples were equilibrated on ice for 1 h. A volume of 500 µL of ice-cold alkaline acetonitrile (5% ammonia in acetonitrile) was added to the homogenates, which were then vigorously

vortexed, and continuously shaken for 1 h at room temperature. The mixtures were centrifuged at 16,000 x g for 10 min and the supernatants collected. The pellets were extracted with another 500 µL of ice-cold alkaline acetonitrile. Supernatants from the two extractions steps were pooled and lyophilized in a rotational vacuum concentrator (Christ) before reconstitution in 100 µL of a 50:50 (v/v) mix of ammonium acetate [5 mM] and methanol at pH 6, and stored at -20°C. Supernatants were diluted according to the intestinal compartment (4,000-fold for the small intestine and liver samples and 100-fold for the cecum and colon samples) before LC-MS injection. The extraction recovery ratios ranged between 75 and 85%.

#### 4.2.5 Ultra-High-Pressure Liquid Chromatography-High Resolution Mass Spectrometry

Both qualitative and quantitative analyses were conducted on an Agilent 6530 Accurate-Mass Q-TOF LC/MS mass spectrometer coupled to an Agilent 1290 series UHPLC system (Agilent). The separation was achieved using a Zorbax Eclipse-Plus C18 column (2.1 × 100 mm, 1.8 µm; Agilent) heated at 50°C. A binary gradient system consisted of 5 mM ammonium acetate pH 6 in water as eluent A and acetonitrile as eluent B. The sample separation was carried out at 0.4 mL/min over a 22 min total run time using the following program: 0–5.5 min, isocratic 21.5% B; 5.5–6 min, 21.5–24.5% B; 6–10 min, 24.5–25% B; 10–10.5 min, 25–29% B; 10.5–14.5 min, isocratic 29% B; 14.5–15 min, 29–40% B; 15–18 min, 40–45% B; 18–20.5 min, 45–95% B, 20.5–22 min, isocratic 95%.

The system was re-equilibrated to initial conditions for 3 min. The sample manager system temperature was maintained at 4°C and the injection volume was 5 µL. Mass spectrometer detection was operated in negative ionization mode using the Dual AJS Jet stream ESI Assembly. The QTOF instrument was operated in the 4 GHz high-resolution mode (typical resolution 17,000 (FWHM) at m/z 1000) in profile mode and calibrated in negative full scan mode using ESI-L solution (Agilent). Internal calibration was performed during acquisition via continuous infusion of a reference mass solution [5 mM purine, 1 mM HP-921 (Agilent reference mass kit, Agilent) in 95% MeOH acidified with 0.1% formic acid] and allowed to permanently achieve a mass accuracy better than 5 ppm. HR mass spectra were acquired over the range of m/z 300–700 at an acquisition rate of three spectra/s. AJS settings were as follows: drying gas flow, 8 L/min; drying gas temperature, 300°C; nebulizer pressure, 35 psi; capillary voltage, 3500 V; nozzle voltage, 1000 V; fragmentor voltage, 175 V; skimmer voltage, 65 V; octopole 1 RF voltage, 750 V. Data was processed using the MassHunter Workstation (Agilent). According to this method, 42 bile acids (Table S2) were quantified by external calibration curves. Extracted ions chromatograms (EIC) were based on a retention time (RT) window of ±0.5 min with a mass-extraction-windows (MEW) of ±30 ppm centered on m/z theor of each bile acid.

#### 4.2.6 Bile acid-metabolizing enzyme database

Whole genomes for the 12 Oligo-MM12 species<sup>180</sup> and *C. scindens* ATCC 35704<sup>178</sup> were obtained from the NCBI and EBI. Sequences were processed by Prodigal<sup>181</sup> to produce the gene sequences forming the BLASTP search database. Reference protein sequences for BSH, 3α-HSDH, 3β-HSDH, 7α-HSDH, 7β-HSDH, 12α-HSDH proteins were obtained from NCBI via the accession numbers presented in Table S3. These sequences were subsequently blasted against the produced protein database. The top 5 matches, as identified by bit score were selected for manual review. The final sequences with the highest scores were selected and are presented in Table S4.

#### 4.2.7 Metaproteome analysis

Proteins were extracted from small intestine, cecum and colon content samples of sDMDMm2 (n=3) and sDMDMm2+Cs mice (n=3) at the Oak Ridge National Laboratory (Oak Ridge, TN, United States). Protein extraction and digestion followed by LC-MS/MS analysis were performed as described previously<sup>182</sup> with slight modifications. Briefly, intestinal content samples were suspended in SDS lysis buffer (4% SDS, 100 mM Tris-HCl, 10 mM dithiothreitol, pH 8.0) and subjected to bead-beating. The proteins were isolated by chloroform-methanol extraction and resuspended in 4% sodium deoxycholate (SDC) in 100 mM ammonium bicarbonate (ABC) buffer. The crude protein concentration was estimated using a Nanodrop (Thermo Fisher Scientific). Protein samples (250 µg) were then

transferred to a 10 kDa MWCO spin filter (Vivaspin 500, Sartorius), washed with ABC buffer, and digested with sequencing-grade trypsin.

After proteolytic digestion, the tryptic peptide solution was adjusted to 1% formic acid to precipitate the remaining SDC. The precipitated SDC was removed using water-saturated ethyl acetate. For each sample, 9 µg of peptides were analyzed by automated 2D LC-MS/MS using a Vanquish UHPLC with autosampler plumbed directly in-line with a Q Exactive Plus mass spectrometer (Thermo Fisher Scientific) across three successive salt cuts of ammonium acetate (35, 100 and 500 mM), each followed by a 155-minute organic gradient. Eluting peptides were measured and sequenced by data-dependent acquisition on the Q Exactive Plus as described earlier<sup>183</sup>.

Peptide identification and protein inference were performed as follows: MS raw data files were searched against the protein database of 12 bacterial species genomes published by Garzetti *et al.* (2017)<sup>180</sup> and the *C. scindens* ATCC 35704 genome published by Devedran *et al.* (2019)<sup>178</sup> along with common contaminants (e.g., trypsin, human keratin) appended with a decoy database consisting of reverse protein sequences to control the false-discovery rate (FDR) to 1% at the spectral level<sup>184</sup>. MS/MS spectra were searched using Tide-search<sup>185</sup>. For Tide-search, default settings were used except for the following parameters: allowed clip n-term methionine, a precursor mass tolerance of 10 parts per million (ppm), a static modification on cysteines (iodoacetamide; +57.0214 Da), and dynamic modifications on methionine (oxidation; +15.9949). The obtained search result was processed by Percolator<sup>186</sup> to estimate q values using default parameters. MS1-level precursor intensities were derived from moFF<sup>187</sup> using default parameters along with match between runs features from biological replicates. The peptides ranked in the bottom 1% were removed prior to analysis. Protein intensities were calculated by summing together quantified peptides and normalized by performing LOESS and median central tendency procedures on log2-transformed values by InfernoRDN<sup>188</sup>. All proteins that had at least one unique peptide sequence were retained for biological interpretation.

All raw mass spectra for the proteome measurements have been deposited into the ProteomeXchange repository with the following accession numbers: (MassIVE Accession: MSV000084484, ProteomeXchange: PXD015971, FTP link to files: <ftp://MSV000084484@massive.ucsd.edu>, Reviewer password: 'abcd1234')

## 4.3 Results and Discussion

### 4.3.1 Mapping bile acid transformations in gnotobiotic mice

The first goal of this study was to explore, using a combined metabolomic and metaproteomic approach, the longitudinal distribution of bile acid transformations in gnotobiotic mouse models (sDMDMm2 and sDMDMm2 + *C. scindens*) and to identify the microorganisms responsible for these transformations.

#### 4.3.1.1 Bile salt deconjugation is an active transformation in the large intestine

Bile salt deconjugation (hydrolysis) constitutes the first step in the microbial bile acid metabolism (Figure 4.1)<sup>177</sup>. For instance, 7 $\alpha$ -dehydroxylation requires unconjugated bile acids<sup>20</sup>, while other processes such as dehydrogenation (oxidation) have been reported to occur with conjugated bile acid<sup>28,175</sup>.

In the small intestine, the amendment of *C. scindens* to the Oligo-MM12 microbial community led to a decrease in deconjugating activity. Indeed, in the jejunum of *C. scindens*-colonized gnotobiotic mice, not only was the concentration of the dominant unconjugated primary BA ( $\beta$ MCA) 8-fold lower as compared to that in the sDMDMm2 cohort in absolute terms, but also, the ratio of  $\beta$ MCA to its conjugated counterpart (T $\beta$ MCA) was 16-fold lower than in the microbiota lacking *C. scindens* (Figure 4.3). Accordingly, bile salt hydrolase (BSH) peptides were not detected in the small intestine of *C. scindens*-colonized gnotobiotic mice (Figure 4.4). In contrast, BSH expression was detected in all compartments in the sDMDMm2 cohort. Together, the bile acid profile and the BSH protein expression data suggest decreased BSH activity in the small intestine in presence of *C. scindens* (Figures 4.3 and 4.4). This could be due either to differences in microbiota colonization of the gut or more directly to changes in the expression of the BSH enzymes. In line with the first hypothesis, notable differences are observed in the protein composition in the small intestine between the two gnotobiotic mouse models (Figure 4.2). For instance, protein abundance from the BSH-producing *Muribaculum intestinale* YL27 is 2-fold lower in the *C. scindens*-colonized cohort than in control mice (Figure 4.2).

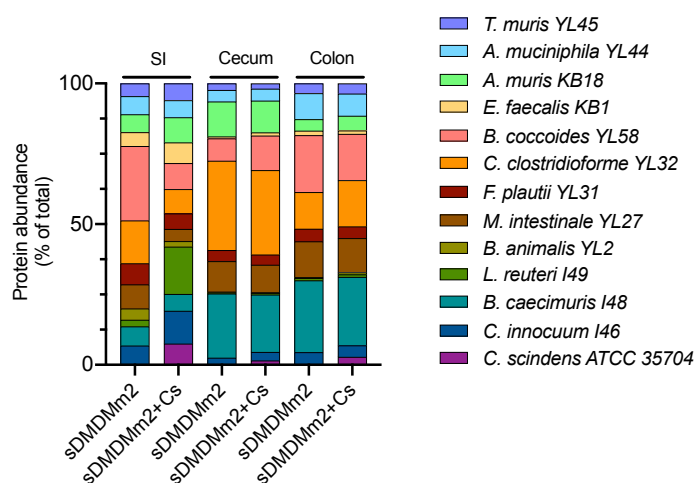


**Figure 4.2| Protein abundance along the intestinal tract of sDMDMm2 and *C. scindens*-colonized sDMDMm2 gnotobiotic mice based on the metaproteomic analysis of intestinal content.** sDMDMm2 mice (n=3) and sDMDMm2 mice pre-colonized 7 days with *C. scindens* (n=3) were sacrificed and intestinal content samples were harvested and processed for metaproteomic analysis.

In the large intestine of the two gnotobiotic mouse models, deconjugated bile acids predominate and BSH are detected, suggesting active bile salt hydrolysis in this compartment (Figures 4.3 and 4.4). In contrast to the small intestine, the protein abundance composition is comparable between the two gnotobiotic mouse models in the cecum and colon (Figure 4.2)

While seven of the twelve organisms in the Oligo-MM12 microbiota harbor BSH-encoding genes (Table S4), BSHs from only two organisms, *Muribaculum intestinale* YL27 and *Bacteroides caecimuris* I48, were detected in the metaproteome (Figure 4.4 and Table S5). Thus, we propose that these two organisms are the main bile salt hydrolyzing strains in this mouse model. The BSH of *M. intestinale* YL27 is highly expressed along the entire intestinal tract of sDMDMm2 animals, while the BSH of *B. caecimuris* I48 was detectable only in the colon in both types of gnotobiotic mice (Figure 4.4).

Thus, based on the bile acid profile and the metaproteomic data of gnotobiotic mice (both sDMDMm2 and *C. scindens*-colonized sDMDMm2), we show that bile salt hydrolysis activity is mainly extant in the large intestine (Figures 4.3 and 4.4).



**Figure 4.3| Bile acid composition along the intestinal tract of sDMDMm2 and *C. scindens*-colonized sDMDMm2 gnotobiotic mice based on LC-MS/MS analysis.** sDMDMm2 mice (n=5) and sDMDMm2 mice pre-colonized 7 days with *C. scindens* (n=5) were sacrificed and intestinal content samples were harvested and processed for bile acid LC-MS/MS measurements. Values indicate measured bile acid concentrations in nmol / g of tissue or intestinal content. Black bars indicate primary conjugated bile acids, teal bars secondary conjugated BAs, gray bars primary deconjugated BAs, yellow bars secondary BAs (all but 7- dehydroxylated), and blue bars represent 7-dehydroxylated BAs.

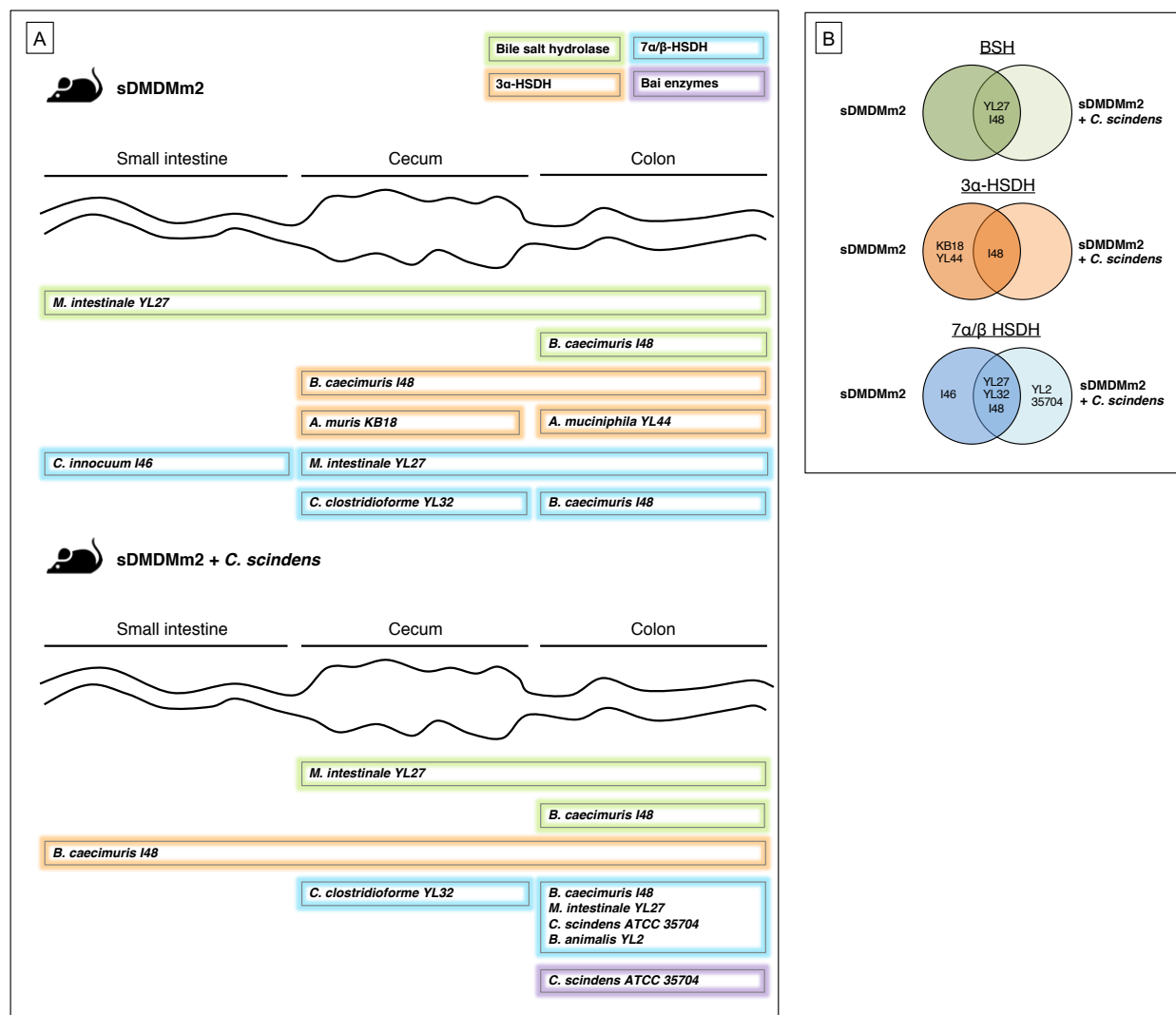


**Figure 4.4| Biogeography of specific bile acid transformation enzymes and the associated microorganisms based on metaproteomic analysis.** sDMDMm2 mice (n=3) and sDMDMm2 mice pre-colonized 7 days with *C. scindens* (n=3) were sacrificed and intestinal content samples were harvested and processed for metaproteomic analysis. Metaproteomes were mined to find homologous sequences of known bile salt hydrolases (BSH), 3α/β-HSDH, 7α/β-HSDH and 12α-HSDH as well as *C. scindens* bai genes. A) Scheme illustrating where bile salt hydrolases, 3α-, 7α- and 7β-hydroxysteroid dehydrogenase (HSDH) and Bai enzymes are expressed in the gut and which are the bacterial species producing these enzymes. 12α-HSDH and 3β-HSDH were not detected in the metaproteome, and therefore are not presented on this figure. B) Venn diagrams summarizing the bile acid metabolizing enzymes detected in sDMDMm2 mice and *C. scindens*-colonized sDMDMm2 mice metaproteomes. For each enzyme detected, the strain producing the enzyme is indicated on the diagram, on the left or right circle if the enzyme was detected in sDMDMm2 mice or *C. scindens*-colonized sDMDMm2 mice respectively. If an enzyme was found in both sDMDMm2 and *C. scindens* colonized-sDMDMm2 mice, the producing-strain is indicated in the middle overlapping part of the two circles.



#### 4.3.1.2 Bile acid oxidation is the most widespread transformation in the intestinal tract

Another common microbial bile acid transformation is oxidation (dehydrogenation), producing bile acids such as 3-oxoCA or 7-oxoDCA (Figure 4.1). There are several hypotheses regarding the role of bile acid oxidation. First, it increases the hydrophilicity of the bile acid pool, and consequently reduces its toxicity for the host and the microbiota<sup>189</sup>. Thus, it could be considered a detoxification process. Second, it is also hypothesized that oxo- groups could serve as electron sinks<sup>28</sup>. Reduction of these oxo- groups would result in a net consumption of two electrons which would be favorable for fermenting bacteria in the anoxic environment of the large intestine, which is lacking in electrons acceptors<sup>190</sup>.

Hydroxysteroid dehydrogenases (HSDH) catalyze the oxidation and epimerization of hydroxyl groups in the bile acid structure (Figure 4.1). Thirty-two predicted HSDHs were found in the genomes of the Oligo-MM12 species and *C. scindens*. They include 3 $\alpha$ -HSDH (oxidation of 3 $\alpha$ -OH and reduction of 3-oxo group), 3 $\beta$ -HSDH (oxidation of 3 $\beta$ -OH and reduction of 3-oxo group), 7 $\alpha$ -HSDH (oxidation of 7 $\alpha$ -OH and reduction of 7-oxo group), 7 $\beta$ -HSDH (oxidation of 7 $\beta$ -OH and reduction of 7-oxo group) and 12 $\alpha$ -HSDH (oxidation of 12 $\alpha$ -OH and reduction of 12-oxo group) (Figure 4.1 and Table S4). Only 9 out of 32 predicted HSDHs were detected with the metaproteomic analysis (Figure 4.4, Tables S4 and S5) and corresponded exclusively to 3 $\alpha$ -HSDH, 7 $\alpha$ -HSDH, and 7 $\beta$ -HSDH (thus missing 3 $\beta$ -HSDH and 12 $\alpha$ -HSDH). Furthermore, the bile acid profiles of gnotobiotic mice suggest that microbial oxidation of BAs is only taking place in the large intestine (Figure 4.3).

Indeed, oxo- bile acids were not detected in the small intestine despite the presence of 7 $\beta$ -HSDH from *C. innocuum* I46 in sDMDMm2 mice and of 3 $\alpha$ -HSDH from *B. caecimuris* I48 in *C. scindens*-colonized sDMDMm2 mice (Figures 4.3, 4.4, Table S5). The gradient of oxygen along the intestinal tract may explain these observations<sup>92</sup>. Hirano and Masuda (1981) reported that oxygen inhibited the activity of the 7 $\alpha$ -HSDH of *Eubacterium lentum*<sup>148</sup>. Thus, if the *C. innocuum* 7 $\alpha$ -HSDH is oxygen-sensitive, the higher oxygen level in the small intestine might inactivate its activity, precluding the formation of 7-oxo bile acids. However, oxygen sensitivity has never been reported for 3 $\alpha$ -HSDH.

The metaproteomic analysis revealed that 7 species of the Oligo-MM12 as well as *C. scindens* were producers of 3 $\alpha$ -HSDH and 7 $\alpha/\beta$ -HSDH in the intestinal tract of the gnotobiotic mice (Figure 4.4, Table S5). Interestingly, the amendment of *C. scindens* clearly decreased the expression of 3 $\alpha$ -HSDH *in vivo*. In the original gnotobiotic mice, 3 $\alpha$ -HSDH from *Acutalibacter muris* KB18, *Akkermansia muciniphila* YL44 and *B. caecimuris* I48 were present in the large intestine, while in the mice amended with *C. scindens*, only the one from *B. caecimuris* I48 was detected (Figure 4.4). In contrast, the amendment of *C. scindens* enhanced the expression of 7 $\alpha/\beta$ -HSDHs. The 7 $\beta$ -HSDH from *Bifidobacterium animalis* YL2 and the 7 $\alpha$ -HSDH from *C. scindens* were observed only in the metaproteome of *C. scindens*-colonized animals. Additionally, in both cohorts, the 7 $\alpha$ -HSDHs from *M. intestinale* YL27 and *B. caecimuris* I48, as well as the 7 $\beta$ -HSDH from *C. clostridioforme* YL32 were encountered. These findings demonstrate that a single strain can profoundly alter the bile acid composition and expression of bile acid-metabolizing enzymes within a given microbial community. Whether *C. scindens* affected the expression of enzymes directly or it impacted the abundance of certain species is difficult to deconvolute. Previously, Studer *et al.* (2016) observed only minor changes in the fecal Oligo-MM12 microbiota composition following the addition of *C. scindens*<sup>129</sup>. These minor changes included a decrease in abundance of *A. muris* KB18 that could explain the absence of 3 $\alpha$ -HSDH from this species in *C. scindens*-colonized cohort (Figure 4.4). However, protein abundance of the 12 Oligo-MM12 species is comparable in the large intestine of the two gnotobiotic mouse model suggesting that the amendment of *C. scindens* has little impact on the large intestine microbial community (Figure 4.2). Furthermore, Devendran and colleagues (2019) reported a downregulation, by the secondary bile acid DCA, of many genes encoding bile acid-transforming enzymes in *C. scindens*<sup>178</sup>. Amongst them, *baiA2* (HDCHBGLK\_01433) encodes a 3 $\alpha$ -HSDH<sup>86</sup>. We hypothesize that *C. scindens*-specific metabolites, such as 7-dehydroxylated secondary bile acids (e.g., DCA), may affect the expression of bile acid-metabolizing enzymes by other bacteria of the Oligo-MM12

consortium. The non-detection of 3 $\alpha$ -HSDH associated with *A. muris* KB18 and *A. muciniphila* YL44 in gnotobiotic mice colonized with *C. scindens* (Figure 4.4) supports this hypothesis. Interestingly, 3 $\beta$ -HSDH were entirely absent in the metaproteome. Consistent with this result, iso-bile acids were not detected in the gnotobiotic animals (Figures 4.1 and 4.3). 12 $\alpha$ -HSDH were also lacking in the metaproteome despite the presence of 12-oxoLCA in *C. scindens*-colonized mice (Figure 4.3). *C. scindens* is known to carry a gene encoding a 12 $\alpha$ -HSDH and could be an active producer of 12-oxoLCA *in vivo*. Marion *et al.* (2018) reported the formation of 12-oxoLCA *in vitro* and proposed it as a transient intermediate of CA 7 $\alpha$ -dehydroxylation by *C. scindens*<sup>29</sup>. Here, we hypothesize that 12 $\alpha$ -HSDH from *C. scindens* is present in too low an abundance to be detected with metaproteomic analysis. In line with this hypothesis, the other enzymes of the 7 $\alpha$ -dehydroxylation pathway were absent in the metaproteome despite the clear presence of 7 $\alpha$ -dehydroxylated secondary bile acids (Figure 4.3).

#### 4.3.1.3 Bile acid 7 $\alpha$ -dehydroxylation is restricted to the large intestine

The bile profile in the large intestine is very similar for mice models with and without *C. scindens*, with the exception of the presence of 7 $\alpha$ -dehydroxylated species in the model including *C. scindens* (Figure 4.3). The 7 $\alpha$ -dehydroxylated species detected include LCA, DCA and MDCA (murideoxycholic acid), the conjugated form of the latter two (TDCA and TMDCA), as well as 7 $\alpha$ -dehydroxylated and oxidized species (6-oxoLCA, 6-oxo-alloLCA, 12-oxoLCA).

Amongst enzymes of the 7 $\alpha$ -dehydroxylation pathway, only the 7 $\alpha$ -hydroxy-3-oxo- $\Delta$ 4-cholenoic acid oxidoreductase (BaiCD)<sup>163</sup> was detected in the colon of *C. scindens*-colonized cohort. None of the Bai enzymes were detected in the small intestine samples of these mice (Figure 4.4, Table S5). Based on the metaproteomic and metabolomic data, we show that bile acid 7 $\alpha$ -dehydroxylation occurs only in the large intestine of mice colonized with *C. scindens* (Figures 4.3 and 4.4). This observation supports an earlier study in which the large intestine was demonstrated to be the ecological niche of *C. scindens* in the gnotobiotic sDMDMm2 mouse model<sup>29</sup>.

While all 12 microorganisms within the Oligo-MM12 microbiota harbor bile acid-modifying enzymes (Table S4), peptides from only 7 of them were detected that mapped onto bile acid-related enzymes (Figure 4.4, Table S5). Because the metaproteomic approach is limited in measurement dynamic range, we cannot rule out the activity of the 5 other strains but can conclude that these 7 are the most active in bile acid transformations.

The second goal of the study was to assess the impact of the microbiota on the bile acid pool. To tackle this, we compared the bile acid pools of gnotobiotic mice to ones of mouse models with various gut microbiota complexities: a very complex microbiota (SPF), a reduced microbiota (antibiotic-treated SPF), or the absence of microbiota (germ-free).

#### 4.3.2 The microbiota shapes the bile acid pool composition

Germ-free mice are devoid of microbial bile acid transformations. Thus, their bile acid pool is exclusively composed of liver-derived tauro-conjugated primary bile acids (Figure 4.5). TCA and T $\beta$ MCA dominate the bile acid pool in all compartments (i.e., they represent  $\approx$ 94% of the liver BA pool). Smaller contributions from TCDCA, TUDCA and T $\alpha$ MCA are also observed. In the liver, a small fraction of unconjugated  $\beta$ MCA (836 $\pm$ 544 nmol/g of tissue) is also noted along with very minor contributions (<10nmol/g of content) of the  $\alpha$ MCA and  $\beta$ MCA in some intestinal compartments (ileum, cecum and colon). These observations support an earlier study from Sayin *et al.* (2013)<sup>5</sup> who also observed minor fractions of unconjugated MCAs in germ-free mice. We hypothesize that the high bile acid synthesis activity in the liver does not allow for conjugating enzymes to act on all of the newly synthesized BA, resulting in the release into the intestine of a fraction of not-yet conjugated bile acids. As expected, secondary bile acids are altogether absent in the GF mouse intestine due to the dearth of microorganisms.

For comparison, we also considered SPF animals with or without antibiotic treatment. As expected, SPF mice exhibited the highest bile acid diversity (Figure 4.5). Secondary bile acids in SPF mice are present in the small intestine, while in *C. scindens*-bearing gnotobiotic animals, they were detected only in the large intestine (Figures 4.3 and 4.5). As the liver is able to re-conjugate deconjugated BA, tauro-conjugated 7 $\alpha$ -dehydroxylated bile acids (TMDCA, THDCA, TDCA, TwMCA) are observed in the upper intestinal tract. Thus, it is not possible to determine whether the 7 $\alpha$ -dehydroxylated bile acids DCA and HDCA in the small intestine come from 7 $\alpha$ -dehydroxylation of CA and HCA (the 6 $\alpha$  epimer of  $\alpha$ MCA) or from the deconjugation of TDCA and THDCA in that compartment (Figure 4.5).

In contrast to the other models, secondary bile acids represent more than half of the bile acid pool in the large intestine of SPF mice and the conjugated bile acids are quasi nonexistent (Figure 4.5). Additionally, 7 $\alpha$ -dehydroxylated secondary bile acids, comprising the 7-dehydroxylated form of the primary bile acids (DCA, LCA, MDCA, HDCA), the oxidized species (12-oxoLCA, 3-oxoLCA, 6-oxoLCA, 6-oxo-alloLCA) and the epimerized species (isoLCA, alloLCA), represents 57% of the pool of secondary BA (Figure 4.5). Finally, SPF mice are the only mice to produce iso-bile acid (3 $\beta$ -epimers), allo-bile acids (5 $\alpha$ -epimers), and 6 $\beta$ -epimers (e.g., HCA) in the large intestine (Figure 4.5).

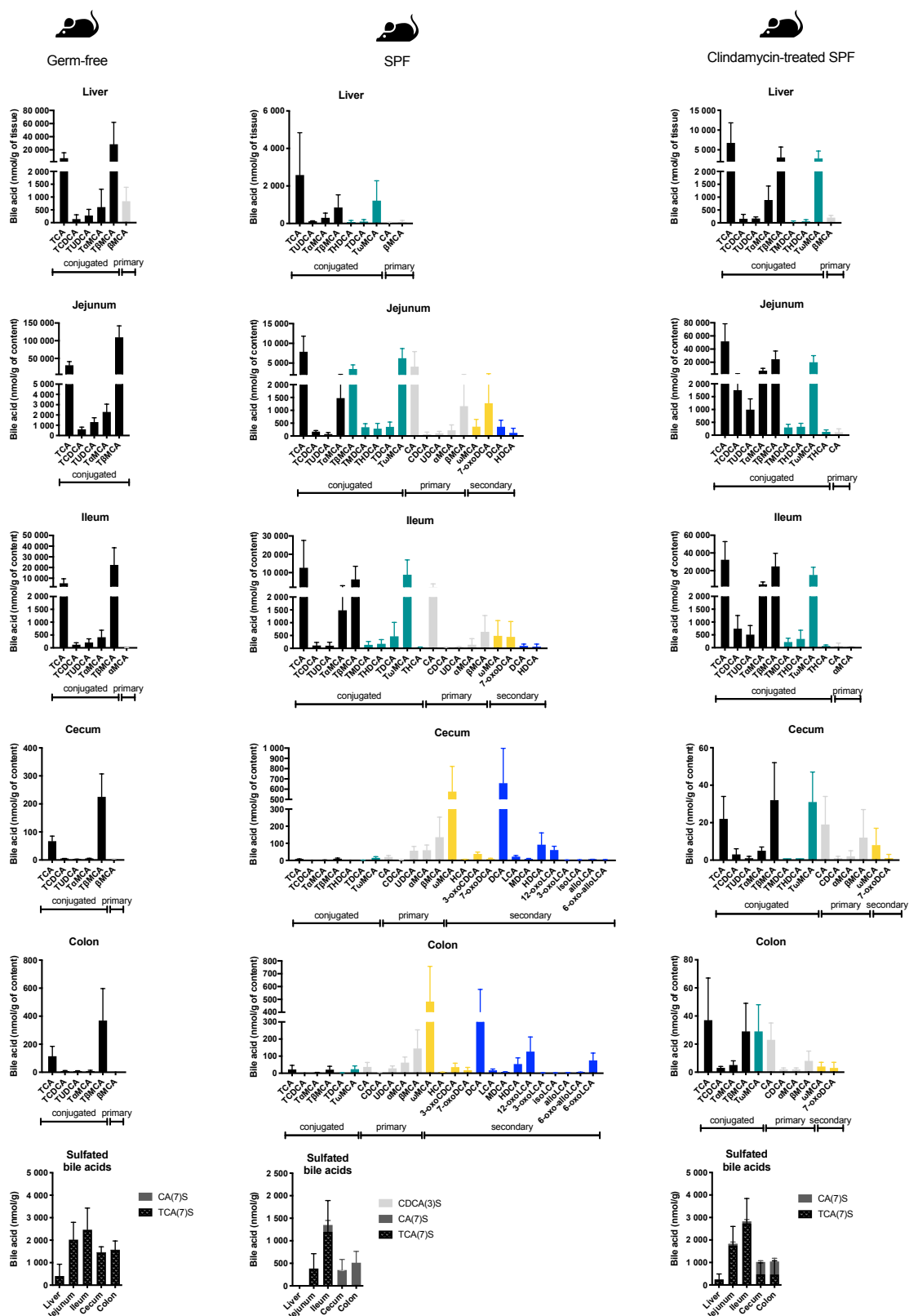


**Figure 4.5 | Bile acid composition along the intestinal tract in germ-free, SPF, and clindamycin-treated SPF mice based on LC-MS/MS analysis.** SPF mice were pre-treated with clindamycin 24h before sacrifice. Intestinal content samples were harvested from GF mice (n=5), SPF mice (n=5), clindamycin-treated SPF mice (n=5). Samples were processed for bile acid LC-MS/MS measurements. Values indicate measured bile acid concentrations in nmol / g of tissue or intestinal content. Black bars indicate primary conjugated bile acids, teal bars secondary conjugated BAs, gray bars primary deconjugated BAs, yellow bars secondary BAs (all but 7-dehydroxylated), and blue bars represent 7-dehydroxylated BAs.

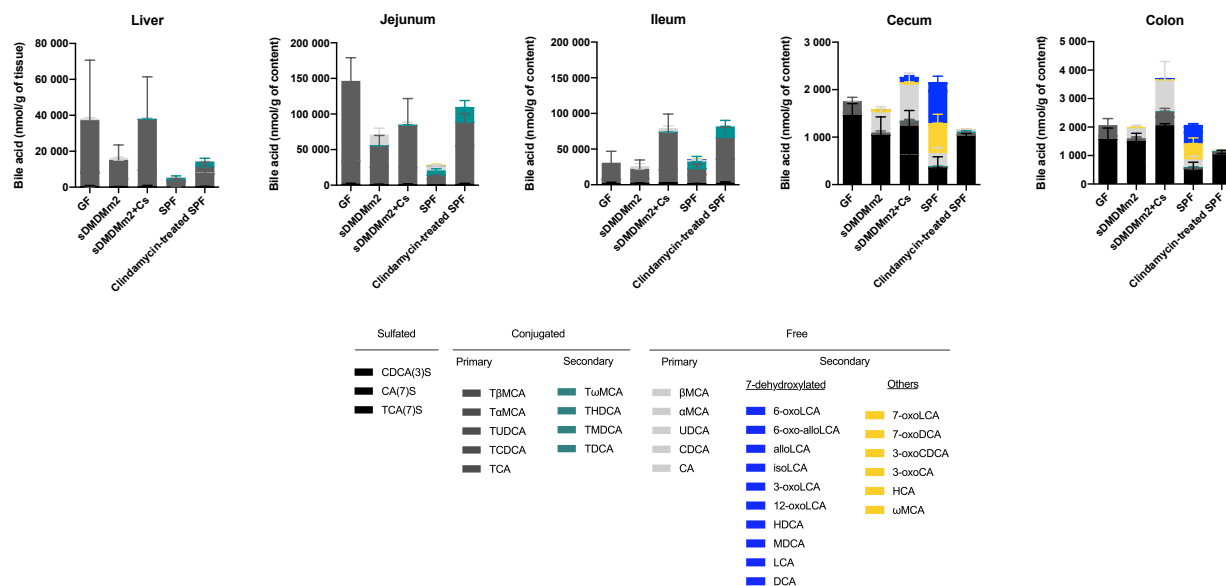


**Figure 4.6] Bile acid pool composition along the intestinal tract of the mouse models based on LC-MS/MS.** For each mouse model, the samples were collected from n=5 animals. Samples were processed for bile acid LC-MS/MS measurements. Values indicate measured bile acid concentrations in nmol / g of tissue or intestinal content.

Antibiotic treatment had a tremendous impact on bile acid transformation throughout the intestinal tract. In the small intestine, bile acid diversity was extremely reduced compared to that in untreated SPF mice (Figure 4.5). The most salient impacts are the suppression of bile acid deconjugation in the small intestine and the complete abolition of 7 $\alpha$ -dehydroxylation by the clindamycin treatment (Figure 4.5). Streptomycin-treated animals exhibited decreased amounts of 7 $\alpha$ -dehydroxylated species but this antibiotic was not as efficient as clindamycin at inhibiting 7 $\alpha$ -dehydroxylation, suggesting the survival of 7 $\alpha$ -dehydroxylating bacteria to streptomycin treatment (Figure S1). Interestingly, tauroconjugated 7 $\alpha$ -dehydroxylated species (TMDCA and THDCA) were detected in the small intestine (Figure 4.5). We attribute the presence of those species to the 7-dehydroxylation of MCAs ( $\alpha$ -,  $\beta$ -,  $\omega$ -MCA) and HCA prior to the antibiotic treatment, followed by recycling via the enterohepatic circulation and re-conjugation in the liver before release into the small intestine.

7 $\alpha$ -dehydroxylated bile acids have been linked to protection against *Clostridioides difficile* infections (CDI) through the inhibitory role of 7-dehydroxylated BAs in *C. difficile* spore germination and outgrowth<sup>7,142</sup>. Based on the bile acid profile of clindamycin- and streptomycin-treated mice (Figures 4.5 and S1), it would be predicted that treatment with streptomycin is less of a risk factor for CDI as compared to that with clindamycin, and that 7 $\alpha$ -dehydroxylating organisms are sensitive to clindamycin but not streptomycin.

In accordance with these hypothesis, Slimings and Riley (2014) reported no association between the use of aminoglycosides (an antibiotic class that includes streptomycin) and CDI, while clindamycin was the antibiotic most frequently associated with CDI (both hospital-acquired and community-acquired) in patient meta-analyses<sup>191–193</sup>. Additionally, two of the major bile acid 7 $\alpha$ -dehydroxylating organisms, *C. scindens* and *C. hylemonae*, are sensitive to clindamycin (Table S6). Furthermore, two studies observed that restricting the use of clindamycin led to a sustained decrease in CDI<sup>194,195</sup>. Buffie *et al.* (2015), observed that the cecal microbiota of SPF mice treated with clindamycin underwent profound losses of *Lachnospiraceae*, a family that includes several 7 $\alpha$ -dehydroxylating strains (e.g., *C. scindens* and *C. hylemonae*)<sup>196</sup>. These observations are all consistent with clindamycin effectively inhibiting BA 7-dehydroxylation and thus, creating conditions propitious for the germination and outgrowth of *C. difficile* spores.

### 4.3.3 Microbiota-host interactions regulate the bile acid pool size

Supporting earlier research<sup>5</sup>, our data show that germ-free mice harbor an abundant bile acid pool (Figures 4.5, 4.6). Here, we also observed that mouse models with a reduced microbiota (gnotobiotic and antibiotic-treated mice) have an increased hepatic bile acid pool compared to conventional mice (SPF), harboring a more diverse microbiota (Figure 4.7a). Furthermore, we noted a large inter-individual variability of the hepatic BA pool in GF and gnotobiotic mice cohorts compared to that in SPF and antibiotic-treated SPF mice (Figure 4.7a). This clearly indicates that BA synthesis is more tightly regulated in hosts with more complex microbial communities (e.g., SPF). In mammals, the nuclear receptor farnesoid X receptor (FXR), highly expressed in the ileum<sup>197</sup>, controls hepatic bile acid synthesis through a negative feedback loop<sup>198</sup>. The activation of FXR by bile acids induces the release of fibroblast growth factor 15 (Fgf15) in the intestine, which reaches the liver via portal vein circulation and inhibits the expression of the hepatic enzyme Cyp7a1 (cholesterol 7 $\alpha$ -hydroxylase), responsible for catalyzing the rate-limiting step in bile acid synthesis<sup>5</sup>.

The tauro-conjugated murine primary BAs are strong antagonists of FXR<sup>199</sup>, while CDCA, and the 7 $\alpha$ -dehydroxylated species DCA and LCA are potent FXR agonists<sup>200</sup>, thus acting as repressors of bile acid synthesis. Gut microbes are important actors in FXR-mediated regulation of bile acid synthesis because they decrease the concentration of FXR antagonists (e.g., T $\beta$ MCA, T $\alpha$ MCA) and produce unconjugated bile acids and secondary bile acids, which activate FXR<sup>5</sup>. The role of the deconjugating microbial community is particularly important as deconjugation contributes to a decrease in the concentration of the FXR antagonists TMCAs<sup>201</sup> and allows further transformation such as 7 $\alpha$ -dehydroxylation<sup>20</sup>. Germ-free mice, devoid of microbial bile acid transformations, have the largest bile acid pool size compared to that of other mice models harboring a microbial community (Figure 4.5). As previously demonstrated<sup>5</sup>, we observed that the concentration of T $\beta$ MCA was high in germ-free mice, resulting from the absence of microbial deconjugation (Figure 4.5).

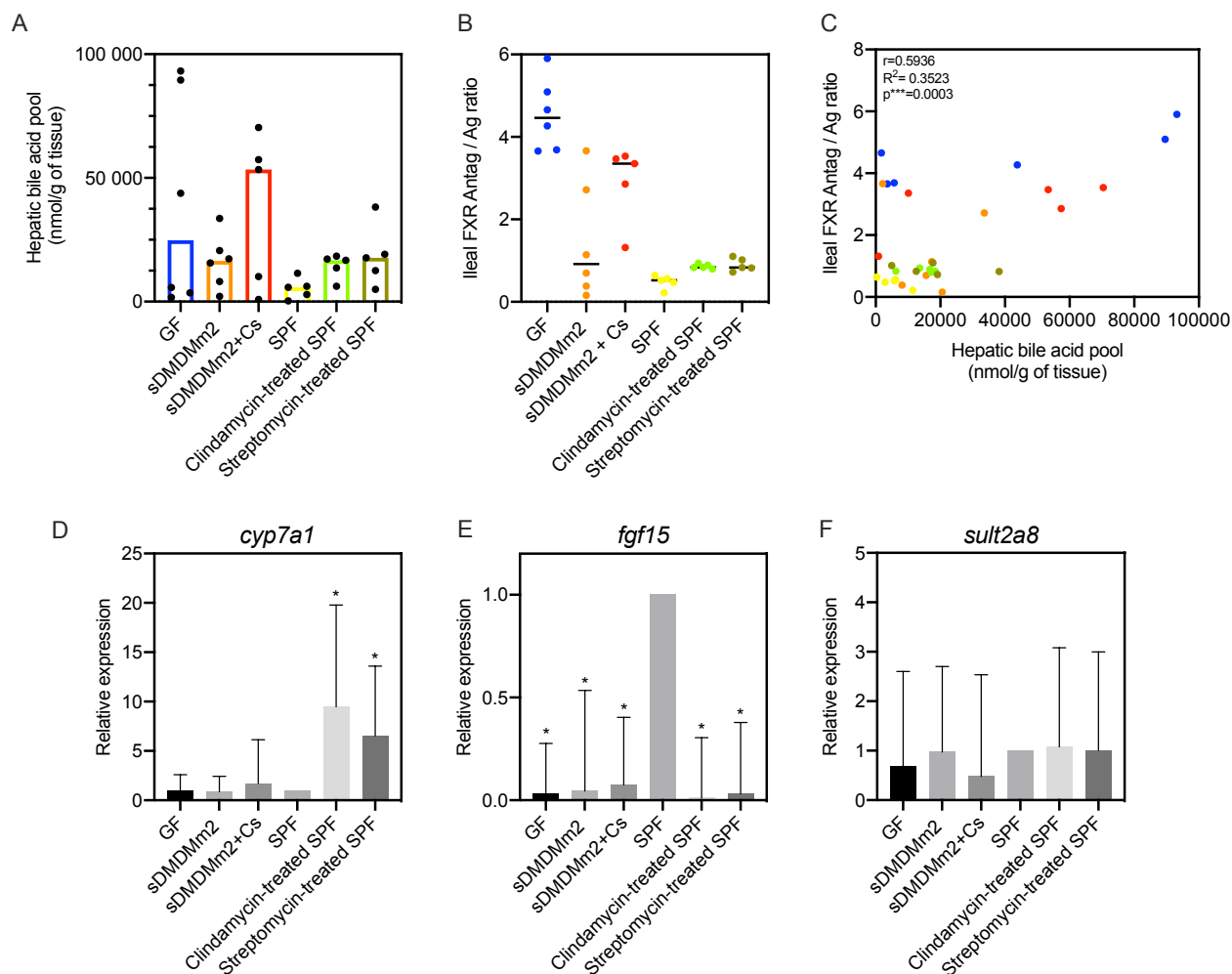


**Figure 4.7 | Probing the influence of the gut microbiota on BA synthesis and detoxification.** A) Hepatic bile acid pool. Each dot corresponds to an individual mouse. Histograms show the medians of the hepatic bile acid pool for the mouse models considered. B) ileal FXR antagonist/agonist ratio. T $\alpha$ MCA, T $\beta$ MCA were considered to be FXR antagonists and CDCA, CA, DCA, LCA, TCDCA, TCA, TDCA and TLCA, FXR agonists according to Parks *et al.* (1999)<sup>200</sup>. Each dot corresponds to an individual mouse. The horizontal bar on the scatter dot plot indicates the median for the mouse models considered. C) Correlation between the hepatic bile acid pool and the ileal FXR antagonist/agonist ratio. Each dot corresponds to an individual mouse. Pearson correlation analysis was computed with GraphPad Prism. D, E, F) Gene expression of *cyp7a1*, *fgf15* and *sult2a8* relative to SPF mice. A value of 1 is attributed to SPF mice. \* indicates a  $p$  value  $< 0.05$ .

The ileal ratio of FXR antagonists (TMCAs) over FXR agonists<sup>200</sup> (CDCA+CA+TCDCA+TCA+DCA+LCA+TDCA+TLCA) reflects the size of the hepatic bile acid pool (Figures 4.7a and 4.7b). We observed a significant correlation between the two variables (Figure 4.7c). Indeed, this relationship offers an explanation as to why *C. scindens*-colonized sDMDMm2 mice have a higher hepatic bile acid pool size compared to sDMDMm2 mice (Figure 4.7a). This higher pool size is due to the increased FXR antagonist/agonist ratio in those mice relative to mice lacking *C. scindens* (Figure 4.7b), explaining the higher bile acid synthesis. The increased ratio is likely due to reduced BSH activity in the small intestine, as reflected in the metaproteomic data, with no BSH activity detected in the small intestine (Figure 4.4). The reduced BSH activity leads to an increased concentration of FXR antagonists (particularly TMCAs) in the ileum. Indeed, T $\beta$ MCA level is 3-fold greater in the ileum of *C. scindens*-colonized cohort compared to that in the sDMDMm2 animals (Figure 4.3). Similarly to the hepatic BA pool, there is a large inter-individual variability in the ileal FXR antagonist/agonist ratio in germ-free and gnotobiotic cohorts compared to that in SPF and antibiotic-treated SPF mice (Figure 4.7b).

Antibiotic treatment also affects BA deconjugating activity, and most likely FXR signaling, leading to increased bile acid synthesis (Figure 4.7). In order to better understand the FXR-mediated regulation of bile acid synthesis by the gut microbiota, we measured

the ileal expression of *fgf15* and hepatic expression of *cyp7a1* in our mice models. Mice models with no or a reduced microbiota (GF, gnotobiotic and antibiotic-treated SPF) show a significantly reduced ileal expression of *fgf15* (more than 10-fold) relative to SPF mice.

The expression of *cyp7a1* is significantly increased in antibiotic-treated mice compared to untreated ones (Figure 4.7d). In contrast, we did not detect a significant difference in *cyp7a1* expression between GF and SPF as previously reported by Sayin *et al.* (2013). However, the increase reported by Sayin *et al.* (2013) is only 2-fold and could be considered minor when discussing gene expression. In line with our observation, a recent thesis, reported no difference in *cyp7a1* mRNA expression between GF and SPF with a chow diet<sup>202</sup>. Although not statistically significant, *C. scindens*-colonized mice show an increased *cyp7a1* expression compared to sDMDMm2 and GF mice which is consistent to the higher bile acid pool (Figure 4.7d).

Altogether, these data show that having a reduced microbiota impacts FXR signalling (via the downregulation of *fgf15*). Bile acid synthesis was mostly impacted by the antibiotic-mediated dysbiosis. There is a large inter-individual variation in the hepatic BA pool and ileal FXR antagonist / agonist ratio in germ-free and gnotobiotic mice (Figure 4.7a, b, c) which is not observed in SPF and antibiotic-treated mice. This suggests that the bile acid pool synthesis is more tightly regulated in mice harboring a more diverse microbial community.

#### 4.3.4 Bile acid detoxification

Intestinal sulfated bile acids were measured in this study. Bile acid sulfation is a major host metabolic pathway to detoxify and eliminate bile acids. Sulfotransferases (e.g., Sult2a1) catalyze the sulfation (or sulfonation) of bile acids in the liver. Sulfation of BAs increases their solubility, reduces the intestinal absorption, and consequently fosters their urinary and fecal elimination. In humans, about 70% of the bile acid pool in the urine is sulfated but under pathological conditions (e.g., cholestatic diseases), the fraction of sulfated bile acid increases<sup>25</sup>.

Sulfation in SPF mice is low compared to the germ-free, gnotobiotic and antibiotic-treated mouse models (Figures 4.3 and 4.5). In SPF mice, sulfated bile acids are not detected in the liver and the amount of sulfated BAs in the intestine are 2-fold smaller than those of the mouse models with a reduced microbial community (Figure 4.3 and 4.5). Miyata *et al.* (2006), reported that Sult2a1 is negatively regulated through FXR in mice and humans<sup>203</sup>. We analyzed the expression of *sult2a8*, recently identified as a major hepatic bile acid sulfotransferase in mice<sup>204</sup>. Expression of *sult2a8* was comparable between the various mouse models, suggesting that Sult2a8 is not regulated through FXR or influenced by gut microbiota (Figure 4.7f).



## 4.4 Conclusion

Bile acids exert crucial functions in the host that go beyond their role as lipid detergents and gut microbes play a central role in the bile acid metabolism. By modifying the structure of the bile acid, microorganisms influence their affinity to host bile acid receptors. In this study, we characterized the biogeography of bile acid transformation in gnotobiotic mice. We identify the main components in bile acid metabolism in a gnotobiotic mouse model and the localization of their activity in the gut. Furthermore, by comparing the bile acid profiles of mouse models with either reduced or more complex microbiota, we emphasized the profound influence of the gut microbial community on the regulation of the bile acid pool size and composition. Furthermore, by measuring expression of *fgf15*, *cyp7a1* and *sult2a8*, we demonstrated that a reduced microbiota affects FXR signaling but not necessarily bile acid synthesis. The later was mainly impacted by antibiotic-mediated dysbiosis. Finally, we report that bile acid sulfonation by Sult2a8, the major BA sulfotransferase in mice, does not seem to be FXR mediated, neither influenced by the gut microbiota.

### Aknowledgements

This research was funded by the Swiss National Science Foundation (Sinergia grants #CRSII3\_147603 and #CRSII5\_180317). We thank Dr. Gilbert Greub and Dr. Guy Prod'Hom from the Microbiology Institute at CHUV for their help with the antimicrobial susceptibility testing.

### Conflict of interest

The authors declare that they have no conflict of interest.

# Chapter 5 Conclusions and perspectives

This chapter summarizes the findings of this thesis. Additionally, it provides recommendations for future research and describes potential approaches to address remaining questions.

Host-microbe interactions often involve small molecules synthesized by the gut microbes that can target host receptors. Bile acids are one example of these small molecules. By interacting with host receptors TGR5 and FXR, they have a broad impact on the host physiology. Because they synthesize the major fraction of the secondary bile acid pool, bile acid 7-dehydroxylating bacteria represent a promising target for the therapeutic management of diseases associated with an abnormal bile acid pool. Despite their clear impact on the host health, this group of commensals remains overlooked.

This thesis provides insights into the microbiology of bile acid 7-dehydroxylating organisms but also into other bile acid-transforming microorganisms. By comparing the bile acid profile of mice with no microbiota, a reduced, or a more diverse microbiota, we emphasized the profound influence of gut microbes on the bile acid pool homeostasis. We showed that antibiotics have a dramatic impact on the bile acid pool and increase bile acid synthesis in the liver via the bile acid-mediated down-regulation of FXR signaling. Interestingly, clindamycin completely abolished 7-dehydroxylation in conventional mice. Colonization-resistance against *C. difficile* is conferred by 7-dehydroxylated secondary bile acids (DCA, LCA), thus clindamycin must impair colonization-resistance against this pathogen. This finding is in line with the fact that clindamycin is the antibiotic the most associated with CDI<sup>191,196</sup>.

The diversity of the gut microbiota appeared to be crucial for a tight regulation of the bile acid pool. In mice lacking microbes (germ-free) and gnotobiotic mice (only 12-13 bacterial species), major inter-individual variability is observed compared to conventional mice and antibiotic-treated mice, which harbor a more complex and diverse microbiota. However, the underlying mechanism is unclear and further research should be conducted to better understand the role of microorganisms in the regulation of bile acid pool and the inter-individual variability observed in GF and gnotobiotic mice.

sDMDMm2 mice have a simplified microbiota containing 12 bacterial species lacking 7-dehydroxylating activity. Gnotobiotic mice constitute a good approach to study the microbial transformation of the bile acids and to identify the main players. Using metabolomic and metaproteomic analysis of sDMDMm2 mice and *C. scindens*-colonized mice, we defined the biogeography of the major bile acid transformations including deconjugation, dehydrogenation and 7-dehydroxylation and identified the bacterial species responsible for each transformation. Interestingly, while all of the 12 species carry BSH- or HSDH-encoding genes, only 6 of them expressed these enzymes that contribute to the diversification of the bile acid pool. Active BSH producers were *M. intestinale* YL27, *B. caecimuris* I48. Active 3 $\alpha$ -HSDH producers were: *B. caecimuris* I48, *A. muris* KB18 and *A. muciniphila* YL44. Active 7 $\alpha$ -HSDH producers were *C. innocuum* I46, *M. intestinale* YL27, *C. clostridioforme* YL32, *B. caecimuris* I48, *B. animalis* YL2. Furthermore, we observed that most bile acid-metabolizing enzymes were expressed in the large intestine of the mice. Deconjugating activity in the small intestine of the gnotobiotic mice was low, explaining the predominance of conjugated bile acid in the bile acid pool. Several questions were raised from this study: what is triggering the expression of bile acid-metabolizing enzymes? Are conjugated bile acids sensed by bacteria triggering the expression of BSH? If so, why did only a few bacteria carrying a BSH encoding gene express the enzyme? What are the factors controlling *in vivo* activity? For 7-dehydroxylation, previous research has shown that CA induces the expression of the *bai* operon<sup>1</sup>. Additionally, pH, oxygen, and cofactors are also known to influence 7-dehydroxylation activity. In contrast, much remains to be deciphered for bile salt hydrolases and hydroxysteroid dehydrogenases activity.

In humans, bile acid 7-dehydroxylation is considered the most relevant microbial BA transformation taking place in the intestinal tract because it converts primary bile acids to 7-dehydroxylated bile acids which represent the major fraction of the human large intestine bile acid pool, are potent agonists of the host receptors TGR5 and FXR, and provide colonization resistance against *C. difficile*<sup>7</sup> and *Entamoeba histolytica*<sup>9</sup>. In this thesis, we studied bile acid 7-dehydroxylation at the intestinal scale, at the cell scale and also at molecular scale.

We studied bile acid 7-dehydroxylation at the intestinal scale by amending *C. scindens* to gnotobiotic mice lacking 7-dehydroxylating activity. Using metabolomics and NanoSIMS, we demonstrated that the large intestine constitutes the ecological niche for 7-dehydroxylating bacteria and it is where bile acid 7-dehydroxylation occurs. We detected a minor colonization of the ileum by *C. scindens* but no 7-dehydroxylation in that compartment. We hypothesized that *C. scindens* colonize primarily the large intestine because it is where it can be active and where CA is present to induce expression of *Bai* enzymes. As mentioned before, the small intestine bile acid pool is mostly conjugated in these gnotobiotic mice, thus *C. scindens* cannot be active because CA is present in too low a concentration to induce bile acid 7-dehydroxylation. Several questions can be raised from this study: Would *C. scindens* colonize and actively perform 7-dehydroxylation in the small intestine if CA concentration were higher in that compartment? Is the level of unconjugated primary bile acid the only trigger for inducing bile acid 7-dehydroxylation *in vivo*? Diseases such as *C. difficile* infection and inflammatory bowel disease (IBD) are associated with low levels of secondary bile acid and an under-representation of 7-dehydroxylating bacteria. Would the administration of unconjugated CA be sufficient to stimulate growth of the 7-dehydroxylating community and to restore the secondary BA pool by inducing the expression of *bai* genes? Another approach and promising research area would be to develop molecules with low cytotoxicity (such as UDCA) capable of inducing expression of the *bai* operon. But first, regions of the bile acid structure that are recognized by proteins involved in regulating expression of the *bai* genes must be identified. From this thesis and previous research, we know that a free 7 $\alpha$ -hydroxyl group is required to induce 7-dehydroxylation. Presence of the 12 $\alpha$ -hydroxyl group (e.g., CA) strongly induces 7-dehydroxylation. In absence of the 12 $\alpha$ -hydroxyl (e.g., CDCA) or with the saturated C12 (e.g., 12-oxoCDCA)<sup>97,160</sup>, 7-dehydroxylation is induced but to a lesser extent than with the 12 $\alpha$ -hydroxyl group. Both 5 $\alpha$ - (e.g., allo-CA) and 5 $\beta$ -H group can induce 7-dehydroxylation. In contrast, 7 $\beta$ -hydroxyl (e.g., UDCA), the 6 $\beta$ -hydroxyl group ( $\alpha$ MCA and  $\beta$ MCA), and a side chain conjugation<sup>20</sup> do not induce 7-dehydroxylation. However, we do not know whether the 3-hydroxyl is also an important functional group for the induction of 7-dehydroxylation. This could be tested by comparing the expression of *bai* genes in presence of CA versus 7 $\alpha$ ,12 $\alpha$ -cholanic acid (Figure 1.1, Steraloids ref. C1170-000). Additionally, with the advantage of not being (re)conjugated, Norcholic acid (norCA) appears to be a good candidate to investigate for the induction of *bai* genes (Figure 5.1). Such compound could be used to stimulate 7-dehydroxylation *in vivo*.

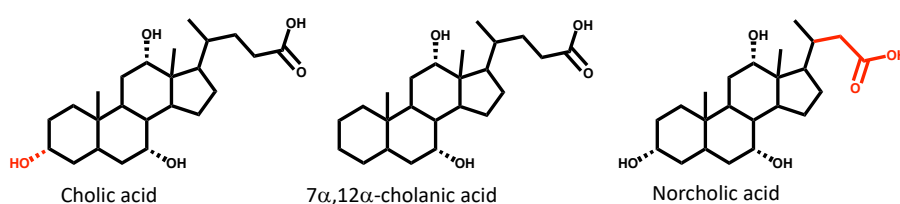
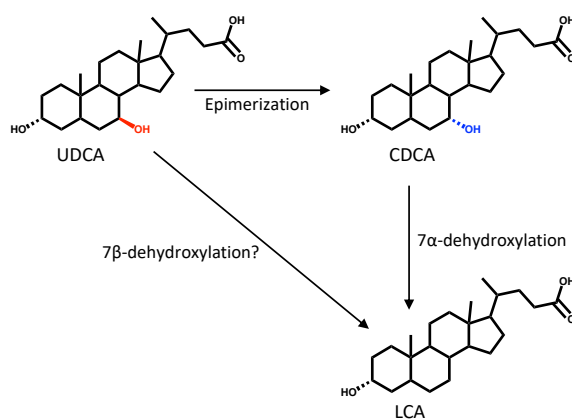


Figure 5.1 | Structure of cholic acid and 7 $\alpha$ , 12 $\alpha$ -cholanic acid and Norcholic acid.

At the cell scale, we studied the *in vitro* and *in vivo* 7-dehydroxylation activity of *C. scindens* ATCC 35704. We now have a global view of all BA transformations performed by this strain on human and murine primary bile acids (CA, CDCA, UDCA,  $\alpha$ MCA,  $\beta$ MCA). We observed that *C. scindens* ATCC 35704 metabolized only the human and murine primary bile acids CA and CDCA. The rodent-specific primary bile acids (UDCA,  $\alpha$ MCA,  $\beta$ MCA) were not transformed by *C. scindens*. Furthermore, we showed that DCA and LCA are products of primary bile acid metabolism by *C. scindens* but that other 7-dehydroxylated species were formed (e.g., 3-oxoLCA, 12-oxoLCA, isoDCA and isoLCA) and should be accounted for when quantifying the extent of bile acid 7-dehydroxylation. Another salient finding is the partitioning of the most hydrophobic bile acids (e.g., LCA) into the cell envelope. This partitioning should also be considered for bile acid mass balance purposes. This is important as in most publications, bile acids are only measured in the supernatant and the

focus is often solely on DCA and LCA. This thesis emphasizes the importance of analyzing other 7-dehydroxylated bile acids (such as 12-oxoLCA, 3-oxoLCA, isoDCA, isoLCA) to accurately quantify the extent of 7-dehydroxylation.

Such extensive characterization of 7-dehydroxylating activity with different substrates should be undertaken with other 7-dehydroxylating strains. *C. scindens* ATCC 35704 was not capable of using the murine specific bile acid as a substrate for bile acid 7-dehydroxylation. One hypothesis could be host specificity as this strain was isolated from human feces, therefore it did not evolve in the presence of murine primary bile acids. In order to test this hypothesis, one could determine whether 7-dehydroxylating strains isolated from rodents (e.g., *Extibacter muris*) are able to 7-dehydroxylate the murine specific primary bile acid (UDCA,  $\alpha$ MCA,  $\beta$ MCA). Furthermore, bile acid 7 $\beta$ -dehydroxylation remains to be clarified. As discussed in Chapter 1, 7 $\beta$ -dehydroxylation of UDCA has been reported *in vitro* for a few strains and genes of the 7 $\alpha$ -dehydroxylation pathway show activity for 7 $\beta$ -hydroxy bile acids (e.g. BaiH). However, it is intriguing that all those 7 $\beta$ -dehydroxylating strains also harbor 7 $\alpha$ -dehydroxylating activity. It could be hypothesized that 7 $\beta$ -dehydroxylation is not a specific pathway *per se*, but a two-step process including a first epimerization step (conversion of 7 $\beta$ -OH to 7 $\alpha$ -OH by 7 $\alpha$ -HSDH) followed 7 $\alpha$ -dehydroxylation (Figure 5.2).



**Figure 5.2| Bile acid 7 $\beta$ -dehydroxylation.** The 7 $\beta$ -hydroxyl and 7 $\alpha$ -hydroxyl groups are indicated in red and blue respectively.

An investigation of the transformation of UDCA by other 7-dehydroxylating strains (including known 7 $\beta$ -dehydroxylating strains such as *C. scindens* VPI 12708) could provide insight into the 7-dehydroxylation of 7 $\beta$ -bile acids. If CDCA is formed during the 7-dehydroxylation of UDCA to LCA, this will prove that 7 $\beta$ -dehydroxylation occurs via epimerization of the 7 $\beta$ -hydroxyl and subsequent 7 $\alpha$ -dehydroxylation.

Studying bile acid *in vitro* transformations can also lead to the discovery of new intermediates and subsequently new biosynthetic pathways. In this thesis, we uncovered the transient formation of 12-oxoLCA during 7-dehydroxylation of CA by *C. scindens* ATCC 35704. This finding led us to the hypothesis of the presence of an alternative 7-dehydroxylation taking place vertically on the steroid core and which would involve the oxidation of the 12 $\alpha$ -hydroxyl group. Using purified enzymes, we probed this novel vertical pathway (via C12) alongside with the known horizontal pathway (via C3). We demonstrated the co-existence of these two separate pathways and identified the core of enzymes involved in each. This finding is significant as it allows the delineation of separate pathways for the transformation of BAs bearing a C12 hydroxyl (i.e., CA) and BAs bearing only C3 hydroxyls (i.e., CDCA). Further experiments are needed to answer the questions that raised from this discovery: Which of the two pathways (vertical and horizontal) is the major

one? How bacteria regulate these two pathways? Why did 7-dehydroxylating bacteria develop this two-routes pathway? Is it to cope with their low abundance and increase the yield of 7-dehydroxylation?

Natural products and derived compounds, including steroid molecules, are used as frontline treatments for many diseases and often inspire the development of new chemically-synthesized therapeutics<sup>205</sup>. The discovery a dual-route bile acid 7-dehydroxylation pathway is a major achievement of this thesis. We believe key features of this dual-route-pathway in 7-dehydroxylating bacteria might serve as model for other microbial pathway producing high concentration metabolites in the gut. It can also inspire the development of new strategies for engineering microbial pathways in heterologous hosts, which is considered as the future of pharmaceutical production.



# References

1. Ridlon, J. M., Harris, S. C., Bhowmik, S., Kang, D.-J. J. & Hylemon, P. B. Consequences of bile salt biotransformations by intestinal bacteria. *Gut Microbes* **7**, 22–39 (2016).
2. Hofmann, A. F. The continuing importance of bile acids in liver and intestinal disease. *Arch. Intern. Med.* **159**, 2647–2658 (1999).
3. Van Nierop, F. S. *et al.* Clinical relevance of the bile acid receptor TGR5 in metabolism. *The Lancet Diabetes and Endocrinology* vol. 5 224–233 (2017).
4. Kuipers, F., Bloks, V. W. & Groen, A. K. Beyond intestinal soap--bile acids in metabolic control. *Nat Rev Endocrinol* **10**, 488–498 (2014).
5. Sayin, S. I. *et al.* Gut microbiota regulates bile acid metabolism by reducing the levels of tauro-beta-muricholic acid, a naturally occurring FXR antagonist. *Cell Metab.* **17**, 225–235 (2013).
6. Wahlström, A. *et al.* Intestinal Crosstalk between Bile Acids and Microbiota and Its Impact on Host Metabolism. *Cell Metab* **24**, 41–50 (2016).
7. Buffie, C. G. *et al.* Precision microbiome reconstitution restores bile acid mediated resistance to *Clostridium difficile*. *Nature* **517**, 205–8 (2015).
8. Weingarden, A. R. *et al.* Changes in Colonic Bile Acid Composition following Fecal Microbiota Transplantation Are Sufficient to Control *Clostridium difficile* Germination and Growth. *PLoS One* **11**, (2016).
9. Burgess, S. L. *et al.* Gut microbiome communication with bone marrow regulates susceptibility to amebiasis. *bioRxiv* 487652 (2019) doi:10.1101/487652.
10. Thomas, C., Pellicciari, R., Pruzanski, M., Auwerx, J. & Schoonjans, K. Targeting bile-acid signalling for metabolic diseases. *Nat. Rev. Drug Discov.* **7**, 678–693 (2008).
11. Ajouz, H., Mukherji, D. & Shamseddine, A. Secondary bile acids: an underrecognized cause of colon cancer. *World J. Surg. Oncol.* **12**, 164 (2014).
12. Yoshimoto, S. *et al.* Obesity-induced gut microbial metabolite promotes liver cancer through senescence secretome. *Nature* **499**, 97–101 (2013).
13. Taur, Y. & Pamer, E. G. Harnessing microbiota to kill a pathogen: Fixing the microbiota to treat *Clostridium difficile* infections. *Nature Medicine* vol. 20 246–247 (2014).
14. Lopez, A. D., Mathers, C. D., Ezzati, M., Jamison, D. T. & Murray, C. J. L. Global and regional burden of disease and risk factors, 2001: systematic analysis of population health data. *Lancet* **367**, 1747–57 (2006).
15. Golden, S. H., Robinson, K. A., Saldanha, I., Anton, B. & Ladenson, P. W. Clinical review: Prevalence and incidence of endocrine and metabolic disorders in the United States: a comprehensive review. *J. Clin. Endocrinol. Metab.* **94**, 1853–78 (2009).
16. Lessa FC *et al.* Burden of *Clostridium difficile* infection in the United States. *N Engl J Med* **372**, 825–834 (2015).
17. Schroeder, B. O. & Bäckhed, F. Signals from the gut microbiota to distant organs in physiology and disease. *Nature Medicine* vol. 22 1079–1089 (2016).
18. Song, Z. *et al.* Taxonomic profiling and populational patterns of bacterial bile salt hydrolase (BSH) genes based on worldwide human gut microbiome. *Microbiome* (2019) doi:10.1186/s40168-019-0628-3.
19. Edenharder, R. Dehydroxylation of cholic acid at C12 and epimerization at C5 and C7 by *Bacteroides* species. *J. Steroid*



- Biochem.* **21**, 413–20 (1984).
20. Batta, A. K. *et al.* Side chain conjugation prevents bacterial 7-dehydroxylation of bile acids. *J. Biol. Chem.* **265**, 10925–10928 (1990).
  21. Pacini, N. *et al.* Transformation of sulfated bile acids by human intestinal microflora. *Arzneimittelforschung.* **37**, 983–7 (1987).
  22. Ridlon, J. M., Kang, D. J. & Hylemon, P. B. Bile salt biotransformations by human intestinal bacteria. *J. Lipid Res.* **47**, 241–59 (2006).
  23. Hamilton, J. P. *et al.* Human cecal bile acids: concentration and spectrum. *Am. J. Physiol. Gastrointest. Liver Physiol.* **293**, G256–G263 (2007).
  24. Devlin, A. S. & Fischbach, M. A. A biosynthetic pathway for a prominent class of microbiota-derived bile acids. *Nat. Chem. Biol.* **11**, 685–690 (2015).
  25. Alnouti, Y. Bile Acid Sulfation: A Pathway of Bile Acid Elimination and Detoxification. *Toxicol. Sci.* **108**, 225–246 (2009).
  26. Marschall, H. U. *et al.* Human liver class I alcohol dehydrogenase gammagamma isozyme: the sole cytosolic 3beta-hydroxysteroid dehydrogenase of iso bile acids. *Hepatology* **31**, 990–996 (2000).
  27. Dawson, P. A. & Karpen, S. J. Intestinal transport and metabolism of bile acids. *J. Lipid Res.* **56**, 1085–1099 (2015).
  28. Doden, H. *et al.* Metabolism of oxo-bile acids and characterization of recombinant 12 $\alpha$ -hydroxysteroid dehydrogenases from bile acid 7 $\alpha$ -dehydroxylating human gut bacteria *Clostridium scindens* ATCC 35704, *Clostridium hylemonae* DSM 15053 and *Clostridium hiranonis* DSM 13275. *Appl. Environ. Microbiol.* (2018) doi:10.1128/AEM.00235-18.
  29. Marion, S. *et al.* In vitro and in vivo characterization of *Clostridium scindens* bile acid transformations. *Gut Microbes* 1–23 (2018) doi:10.1080/19490976.2018.1549420.
  30. Kollerov, V. V *et al.* Deoxycholic acid transformations catalyzed by selected filamentous fungi. *Steroids* **107**, 20–29 (2016).
  31. Kollerov, V. V *et al.* Hydroxylation of lithocholic acid by selected actinobacteria and filamentous fungi. *Steroids* **78**, 370–378 (2013).
  32. Hagey, L. R., Vidal, N., Hofmann, A. F. & Krasowski, M. D. Evolutionary diversity of bile salts in reptiles and mammals, including analysis of ancient human and extinct giant ground sloth coprolites. *BMC Evol Biol* **10**, 133 (2010).
  33. Hofmann, A. F., Hagey, L. R. & Krasowski, M. D. Bile salts of vertebrates: structural variation and possible evolutionary significance. *J. Lipid Res.* **51**, 226–246 (2010).
  34. Midtvedt, T. & Norman, A. Anaerobic, bile acid transforming microorganisms in rat intestinal content. *Acta Pathol. Microbiol. Scand.* **72**, 337–344 (1968).
  35. Doerner, K. C., Takamine, F., LaVoie, C. P., Mallonee, D. H. & Hylemon, P. B. Assessment of fecal bacteria with bile acid 7 $\alpha$ -dehydroxylating activity for the presence of bai-like genes. *Appl. Environ. Microbiol.* **63**, 1185–1188 (1997).
  36. Wells, J. E., Berr, F., Thomas, L. A., Dowling, R. H. & Hylemon, P. B. Isolation and characterization of cholic acid 7 $\alpha$ -dehydroxylating fecal bacteria from cholesterol gallstone patients. *J. Hepatol.* **32**, 4–10 (2000).
  37. Lagkouvardos, I. *et al.* The Mouse Intestinal Bacterial Collection (miBC) provides host-specific insight into cultured diversity and functional potential of the gut microbiota. *Nat Microbiol* **1**, 16131 (2016).
  38. Tawthep, S. *et al.* Isolation of six novel 7-oxo- or urso-type secondary bile acid-producing bacteria from rat cecal contents. *J. Biosci. Bioeng.* **124**, 514–522 (2017).
  39. Eyssen, H. J., De Pauw, G. & Van Eldere, J. Formation of hyodeoxycholic acid from muricholic acid and hyocholic acid by an unidentified gram-positive rod termed HDCA-1 isolated from rat intestinal microflora. *Appl. Environ. Microbiol.* **65**, 3158–3163 (1999).
  40. Bokkenheuser, V., Hoshita, T. & Mosbach, E. H. Bacterial 7-dehydroxylation of cholic acid and allocholic acid. *J. Lipid Res.* **10**, 421–6 (1969).
  41. Hirano, S., Nakama, R., Tamaki, M. & Oda, H. Isolation and characterization of thirteen intestinal microorganisms capable of

- 7 $\alpha$ -Dehydroxylating Bile Acids. *Appl. Environ. Microbiol.* **41**, 737–745 (1981).
42. Alou, M. T., Fournier, P.-E. & Raoult, D. *Africanella massiliensis*, a new bacterial genus isolated from human gut microbiota. *New microbes new Infect.* **12**, 99–100 (2016).
  43. Pikuta, E. V. *et al.* *Proteocatella spheonisci* gen. nov., sp. nov., a psychrotolerant, spore-forming anaerobe isolated from penguin guano. *Int. J. Syst. Evol. Microbiol.* **59**, 2302–2307 (2009).
  44. Takamine, F. & Imamura, T. Isolation and characterization of bile acid 7-dehydroxylating bacteria from human feces. *Microbiol. Immunol.* **39**, 11–18 (1995).
  45. Kitahara, M., Takamine, F., Imamura, T. & Benno, Y. Assignment of *Eubacterium* sp. VPI 12708 and related strains with high bile acid 7 $\alpha$ -dehydroxylating activity to *Clostridium scindens* and proposal of *Clostridium hylemonae* sp. nov., isolated from human faeces. *Int. J. Syst. Evol. Microbiol.* **50**, 971–978 (2000).
  46. Hirano, S., Nakama, R., Tamaki, M., Masuda, N. & Oda, H. Isolation and characterization of thirteen intestinal microorganisms capable of 7 $\alpha$ -dehydroxylating bile acids. *Appl. Environ. Microbiol.* **41**, 737–745 (1981).
  47. Rajilić-Stojanović, M. & de Vos, W. M. The first 1000 cultured species of the human gastrointestinal microbiota. *FEMS Microbiol. Rev.* **38**, 996–1047 (2014).
  48. Yutin, N. & Galperin, M. Y. A genomic update on clostridial phylogeny: Gram-negative spore formers and other misplaced clostridia. *Environ. Microbiol.* **15**, 2631–2641 (2013).
  49. Galperin, M. Y., Brover, V., Tolstoy, I. & Yutin, N. Phylogenomic analysis of the family peptostreptococcaceae (*Clostridium* cluster xi) and proposal for reclassification of *Clostridium litorale* (Fendrich *et al.* 1991) and *Eubacterium acidaminophilum* (Zindel *et al.* 1989) as *peptoclostridium litorale* gen. nov. *Int. J. Syst. Evol. Microbiol.* **66**, 5506–5513 (2016).
  50. Hirano, S. & Masuda, N. Enhancement of the 7  $\alpha$ -dehydroxylase activity of a gram-positive intestinal anaerobe by *Bacteroides* and its significance in the 7-dehydroxylation of ursodeoxycholic acid. *J. Lipid Res.* **23**, 1152–8 (1982).
  51. Midtvedt, T. & Norman, A. Bile acid transformations by microbial strains belonging to genera found in intestinal contents. *Acta Pathol. Microbiol. Scand.* **71**, 629–638 (1967).
  52. Gustafsson, B. E., Midtvedt, T. & Norman, A. Isolated fecal microorganisms capable of 7- $\alpha$ -dehydroxylating bile acids. *J. Exp Med* **123**, 413–432 (1966).
  53. Vital, M., Rud, T., Rath, S., Pieper, D. H. & Schlüter, D. Diversity of Bacteria Exhibiting Bile Acid-inducible 7 $\alpha$ -dehydroxylation Genes in the Human Gut. *Comput. Struct. Biotechnol. J.* **17**, 1016–1019 (2019).
  54. White, B. A., Fricke, R. J. & Hylemon, P. B. 7  $\beta$ -Dehydroxylation of ursodeoxycholic acid by whole cells and cell extracts of the intestinal anaerobic bacterium, *Eubacterium* species V.P.I. 12708. *J. Lipid Res* **23**, 145–153 (1982).
  55. Takamine, F. & Imamura, T. 7  $\beta$ -dehydroxylation of 3,7-dihydroxy bile acids by a *Eubacterium* species strain C-25 and stimulation of 7  $\beta$ -dehydroxylation by *Bacteroides distasonis* strain K-5. *Microbiol Immunol* **29**, 1247–1252 (1985).
  56. Kang, D.-J., Ridlon, J. M., Moore, D. R., Barnes, S. & Hylemon, P. B. *Clostridium scindens* baiCD and baiH genes encode stereospecific 7 $\alpha$ /7 $\beta$ -hydroxy-3-oxo- $\Delta^4$ -cholenoic acid oxidoreductases. *Biochim. Biophys. Acta* **1781**, 16–25 (2008).
  57. Kageyama, A., Benno, Y. & Nakase, T. Phylogenetic evidence for the transfer of *Eubacterium lentum* to the genus *Eggerthella* as *Eggerthella lenta* gen. nov., comb. nov. *Int. J. Syst. Bacteriol.* (1999) doi:10.1099/00207713-49-4-1725.
  58. Doerner, K. C., Takamine, F., Voie, C. P. L. A. & Mallonee, D. H. Assessment of Fecal Bacteria with Bile Acid 7 $\alpha$ -Dehydroxylating Activity for the Presence of bai -Like Genes. *Appl. Environ. Microbiol.* **63**, 1185–1188 (1997).
  59. Narushima, S. *et al.* Deoxycholic acid formation in gnotobiotic mice associated with human intestinal bacteria. *Lipids* **41**, 835–843 (2006).
  60. Narushima, S., Itoh, K., Takamine, F. & Uchida, K. Absence of cecal secondary bile acids in gnotobiotic mice associated with two human intestinal bacteria with the ability to dehydroxylate bile acids in vitro. *Microbiol. Immunol.* **43**, 893–897 (1999).
  61. Hirano, S., Masuda, N., Oda, H. & Imamura, T. Transformation of Bile Acids by Mixed Microbial Cultures from Human Feces and Bile Acid Transforming Activities of Isolated Bacterial Strains. *Microbiol. Immunol.* **25**, 271–282 (1981).
  62. Stellwag, E. J. & Hylemon, P. B. 7 $\alpha$ -Dehydroxylation of cholic acid and chenodeoxycholic acid by *Clostridium leptum*. *J. Lipid*

- Res.* **20**, 325–333 (1979).
63. Narushima, S., Itoh, K., Kuruma, K. & Uchida, K. Caecal bile acid compositions in gnotobiotic mice associated with human intestinal bacteria with the ability to transform bile acids in vitro. *Microb. Ecol. Health Dis.* **11**, 55–60 (1999).
  64. Dickinson, A. B., Gustafsson, B. E. & Norman, A. Determination of bile acid conversion potencies of intestinal bacteria by screening in vitro and subsequent establishment in germfree rats. *Acta Pathol. Microbiol. Scand. Sect. B Microbiol. Immunol.* **79 B**, 691–698 (1971).
  65. Sender, R., Fuchs, S. & Milo, R. Revised Estimates for the Number of Human and Bacteria Cells in the Body. *PLoS Biol.* **14**, (2016).
  66. Kitahara, M., Sakata, S., Sakamoto, M. & Benno, Y. Comparison among fecal secondary bile acid levels, fecal microbiota and *Clostridium scindens* cell numbers in Japanese. *Microbiol. Immunol.* **48**, 367–375 (2004).
  67. Qin, J. *et al.* A human gut microbial gene catalogue established by metagenomic sequencing. *Nature* **464**, 59–65 (2010).
  68. Kurakawa, T. *et al.* Diversity of intestinal *Clostridium coccoides* group in the Japanese population, as demonstrated by reverse transcription-quantitative PCR. *PLoS One* **10**, (2015).
  69. Wang, D. Y. The isolation of novel Lachnospiraceae strains and the evaluation of their potential roles in colonization resistance against *Clostridium difficile*. (University of Michigan, Ann Arbor, 2014).
  70. Browne, H. P., Neville, B. A., Forster, S. C. & Lawley, T. D. *Transmission of the gut microbiota: Spreading of health.* *Nature Reviews Microbiology* vol. 15 531–543 (Europe PMC Funders, 2017).
  71. Jönsson, G., Midtvedt, A. C., Norman, A. & Midtvedt, T. Intestinal microbial bile acid transformation in healthy infants. *J. Pediatr. Gastroenterol. Nutr.* **20**, 394–402 (1995).
  72. Tanaka, M. & Nakayama, J. Development of the gut microbiota in infancy and its impact on health in later life. *Allergol. Int.* **66**, 515–522 (2017).
  73. Solbach, P. *et al.* BaiCD gene cluster abundance is negatively correlated with *Clostridium difficile* infection. *PLoS One* **13**, e0196977 (2018).
  74. Samuelsson, B. Bile Acids and Steroids. 96. On the mechanism of the biological formation of deoxycholic acid from cholic acid. *J Biol Chem* **235**, 261–266 (1960).
  75. Mallonee, D. H., White, W. B. & Hylemon, P. B. Cloning and sequencing of a bile acid-inducible operon from *Eubacterium* sp. strain VPI 12708. *J. Bacteriol.* **172**, 7011–7019 (1990).
  76. Mallonee, D. H., Adams, J. L. & Hylemon, P. B. The bile acid-inducible baiB gene from *Eubacterium* sp. strain VPI 12708 encodes a bile acid-coenzyme A ligase. *J. Bacteriol.* **174**, 2065–2071 (1992).
  77. Mallonee, D. H., Lijewski, M. A. & Hylemon, P. B. Expression in *Escherichia coli* and characterization of a bile acid-inducible 3 $\alpha$ -hydroxysteroid dehydrogenase from *Eubacterium* sp. strain VPI 12708. *Curr. Microbiol.* **30**, 259–263 (1995).
  78. Mallonee, D. H. & Hylemon, P. B. Sequencing and expression of a gene encoding a bile acid transporter from *Eubacterium* sp. strain VPI 12708. *J. Bacteriol.* **178**, 7053–8 (1996).
  79. Ye, H. Q., Mallonee, D. H., Wells, J. E., Björkhem, I. & Hylemon, P. B. The bile acid-inducible baiF gene from *Eubacterium* sp. strain VPI 12708 encodes a bile acid-coenzyme A hydrolase. *J. Lipid Res.* **40**, 17–23 (1999).
  80. White, W. B., Franklund, C. V., Coleman, J. P. & Hylemon, P. B. Evidence for a multigene family involved in bile acid 7-dehydroxylation in *Eubacterium* sp. strain VPI 12708. *J. Bacteriol.* **170**, 4555–61 (1988).
  81. Dawson, J. A., Mallonee, D. H., Björkhem, I. & Hylemon, P. B. Expression and characterization of a C24 bile acid 7 $\alpha$ -dehydratase from *Eubacterium* sp. strain VPI 12708 in *Escherichia coli*. *J. Lipid Res.* **37**, 1258–67 (1996).
  82. Baron, S. F., Franklund, C. V. & Hylemon, P. B. Cloning, sequencing, and expression of the gene coding for bile acid 7  $\alpha$ -hydroxysteroid dehydrogenase from *Eubacterium* sp. strain VPI 12708. *J. Bacteriol.* **173**, 4558–4569 (1991).
  83. Baron, S. F. & Hylemon, P. B. Expression of the bile acid-inducible NADH:flavin oxidoreductase gene of *Eubacterium* sp. VPI 12708 in *Escherichia coli*. *Biochim. Biophys. Acta* **1249**, 145–154 (1995).

84. Franklund, C. V., Baron, S. F. & Hylemon, P. B. Characterization of the baiH gene encoding a bile acid-inducible NADH:flavin oxidoreductase from Eubacterium sp. strain VPI 12708. *J. Bacteriol.* **175**, 3002–3012 (1993).
85. Gopal-Srivastava, R., Mallonee, D. H., White, W. B. & Hylemon, P. B. Multiple copies of a bile acid-inducible gene in Eubacterium sp. strain VPI 12708. *J. Bacteriol.* **172**, 4420–4426 (1990).
86. Bhowmik, S. *et al.* Structural and functional characterization of BaiA, an enzyme involved in secondary bile acid synthesis in human gut microbe. *Proteins* **82**, 216–29 (2014).
87. Bhowmik, S. *et al.* Structure and functional characterization of a bile acid 7 $\alpha$  dehydratase BaiE in secondary bile acid synthesis. *Proteins* **84**, 316–331 (2016).
88. Ridlon, J. M. J. & Hylemon, P. B. P. Identification and characterization of two bile acid coenzyme A transferases from *Clostridium scindens*, a bile acid 7 $\alpha$ -dehydroxylating intestinal bacterium. *J. Lipid Res.* **53**, 66–76 (2012).
89. Harris, S. C. *et al.* Identification of a gene encoding a flavoprotein involved in bile acid metabolism by the human gut bacterium *Clostridium scindens* ATCC 35704. *Biochim. Biophys. Acta - Mol. Cell Biol. Lipids* **1863**, 276–283 (2018).
90. Funabashi, M. *et al.* A metabolic pathway for bile acid dehydroxylation by the gut microbiome. *bioRxiv* 758557 (2019) doi:10.1101/758557.
91. Heinken, A. *et al.* Systematic assessment of secondary bile acid metabolism in gut microbes reveals distinct metabolic capabilities in inflammatory bowel disease. *Microbiome* **7**, (2019).
92. Donaldson, G. P., Lee, S. M. & Mazmanian, S. K. Gut biogeography of the bacterial microbiota. *Nat. Rev. Microbiol.* **14**, 20–32 (2015).
93. Begley, M. M., Gahan, C. G. M. M. & Hill, C. The interaction between bacteria and bile. *FEMS Microbiology Reviews* vol. 29 625–651 (2005).
94. Hofmann, a F. & Mysels, K. J. Bile acid solubility and precipitation in vitro and in vivo: the role of conjugation, pH, and Ca<sup>2+</sup> ions. *J. Lipid Res.* **33**, 617–26 (1992).
95. Dalla Vecchia, E., Suvorova, E. I., Maillard, J. & Bernier-Latmani, R. Fe(III) reduction during pyruvate fermentation by *Desulfotomaculum reducens* strain MI-1. *Geobiology* **12**, 48–61 (2014).
96. Midtvedt, T. & Norman, A. Parameters in 7- $\alpha$ -dehydroxylation of bile acids by anaerobic lactobacilli. *Acta Pathol. Microbiol. Scand.* **72**, 313–329 (1968).
97. White, B. A., Lipsky, R. L., Fricke, R. J. & Hylemon, P. B. Bile acid induction specificity of 7 $\alpha$ -dehydroxylase activity in an intestinal Eubacterium species. *Steroids* **35**, 103–109 (1980).
98. Ridlon, J. M., Kang, D. J. & Hylemon, P. B. Isolation and characterization of a bile acid inducible 7 $\alpha$ -dehydroxylating operon in *Clostridium hylemonae* TN271. *Anaerobe* **16**, 137–146 (2010).
99. Van Eldere, J., Celis, P., De Pauw, G., Lesaffre, E. & Eyssen, H. Tauroconjugation of cholic acid stimulates 7 $\alpha$ -dehydroxylation by fecal bacteria. *Appl. Environ. Microbiol.* **62**, 656–661 (1996).
100. Masuda, N., Oda, H., Hirano, S. & Hiromitsu, A. Enhancement of the 7 $\alpha$ -Dehydroxylase Activity of a Gram- Positive Intestinal Anaerobe by Flavins. *Appl. Environ. Microbiol.* **45**, 308–309 (1983).
101. Mar Rodríguez, M. *et al.* Obesity changes the human gut mycobiome. *Sci. Rep.* **5**, 14600 (2015).
102. Joyce, S. A. & Gahan, C. G. M. Bile Acid Modifications at the Microbe-Host Interface: Potential for Nutraceutical and Pharmaceutical Interventions in Host Health. in *Annual Review of Food Science and Technology, Vol 7* (eds. Doyle, M. P. & Klaenhammer, T. R.) vol. 7 313–333 (2016).
103. Ridlon, J. M. & Bajaj, J. S. The human gut sterolbiome: Bile acid-microbiome endocrine aspects and therapeutics. *Acta Pharm. Sin. B* **5**, 99–105 (2015).
104. McMillin, M. & DeMorrow, S. Effects of bile acids on neurological function and disease. *FASEB J.* **30**, 3658–3668 (2016).
105. Schaap, F. G., Trauner, M. & Jansen, P. L. M. Bile acid receptors as targets for drug development. *Nat. Rev. Gastroenterol. Hepatol.* **11**, 1–13 (2013).

106. Trabelsi, M. S. *et al.* Farnesoid X receptor inhibits glucagon-like peptide-1 production by enteroendocrine L cells. *Nat. Commun.* **6**, (2015).
107. Sinal, C. J. *et al.* Targeted disruption of the nuclear receptor FXR/BAR impairs bile acid and lipid homeostasis. *Cell* **102**, 731–744 (2000).
108. Inagaki, T. *et al.* Fibroblast growth factor 15 functions as an enterohepatic signal to regulate bile acid homeostasis. *Cell Metab* **2**, 217–225 (2005).
109. Holt, J. A. *et al.* Definition of a novel growth factor-dependent signal cascade for the suppression of bile acid biosynthesis. *Genes Dev.* (2003) doi:10.1101/gad.1083503.
110. Johansson, M. E. V., Sjövall, H. & Hansson, G. C. The gastrointestinal mucus system in health and disease. *Nat. Rev. Gastroenterol. Hepatol.* **10**, 352–361 (2013).
111. Barcelo, A. *et al.* Effect of Bile Salts on Colonic Mucus Secretion in Isolated Vascularly Perfused Rat Colon. *Dig. Dis. Sci.* **46**, 1223–1231 (2001).
112. Lewin, M. R., El Masri, S. H. & Clark, C. G. Effects of Bile Acids on Mucus Secretion in the Dog Colon. *Eur. Surg. Res.* **11**, 392–398 (1979).
113. Van Den Abbeele, P. *et al.* Butyrate-producing Clostridium cluster XIVa species specifically colonize mucins in an in vitro gut model. *ISME J.* **7**, 949–961 (2013).
114. Ward, J. B. J. *et al.* Ursodeoxycholic acid and lithocholic acid exert anti-inflammatory actions in the colon. *Am. J. Physiol. Liver Physiol.* **312**, G550–G558 (2017).
115. Duboc, H. *et al.* Connecting dysbiosis, bile-acid dysmetabolism and gut inflammation in inflammatory bowel diseases. *Gut* **62**, 531–539 (2013).
116. Nagao-Kitamoto, H. & Kamada, N. Host-microbial Cross-talk in Inflammatory Bowel Disease. *Immune Netw.* **17**, 1–12 (2017).
117. Wang, S. *et al.* Diet-induced remission in chronic enteropathy is associated with altered microbial community structure and synthesis of secondary bile acids. *Microbiome* (2019) doi:10.1186/s40168-019-0740-4.
118. Li, T., Jahan, A. & Chiang, J. Y. L. Bile acids and cytokines inhibit the human cholesterol 7 $\alpha$ -hydroxylase gene via the JNK/c-Jun pathway in human liver cells. *Hepatology* (2006) doi:10.1002/hep.21183.
119. Ridlon, J. M., Alves, J. M., Hylemon, P. B. & Bajaj, J. S. Cirrhosis, bile acids and gut microbiota: unraveling a complex relationship. *Gut Microbes* **4**, 382–387 (2013).
120. Wunsch, E. *et al.* Expression of hepatic Fibroblast Growth Factor 19 is enhanced in Primary Biliary Cirrhosis and correlates with severity of the disease. *Sci. Rep.* (2015) doi:10.1038/srep13462.
121. Chen, Y. *et al.* Characterization of fecal microbial communities in patients with liver cirrhosis. *Hepatology* (2011) doi:10.1002/hep.24423.
122. Musso, G., Cassader, M. & Gambino, R. Non-alcoholic steatohepatitis: emerging molecular targets and therapeutic strategies. *Nat. Rev. Drug Discov.* **15**, 249–274 (2016).
123. Guohong-Liu, Qingxi-Zhao & Hongyun-Wei. Characteristics of intestinal bacteria with fatty liver diseases and cirrhosis. *Annals of Hepatology* (2019) doi:10.1016/j.aohep.2019.06.020.
124. Wang, L. & Wan, Y. J. Y. The role of gut microbiota in liver disease development and treatment. *Liver Research* vol. 3 3–18 (2019).
125. Jiao, N. *et al.* Suppressed hepatic bile acid signalling despite elevated production of primary and secondary bile acids in NAFLD. *Gut* **67**, (2018).
126. Katsuma, S., Hirasawa, A. & Tsujimoto, G. Bile acids promote glucagon-like peptide-1 secretion through TGR5 in a murine enteroendocrine cell line STC-1. *Biochem. Biophys. Res. Commun.* (2005) doi:10.1016/j.bbrc.2005.01.139.
127. Thomas, C. *et al.* TGR5-Mediated Bile Acid Sensing Controls Glucose Homeostasis. *Cell Metab.* (2009) doi:10.1016/j.cmet.2009.08.001.

128. Leffler, D. A. & Lamont, J. T. Clostridium difficile infection. *N. Engl. J. Med.* **372**, 1539–48 (2015).
129. Studer, N. *et al.* Functional Intestinal Bile Acid 7 $\alpha$ -Dehydroxylation by Clostridium scindens Associated with Protection from Clostridium difficile Infection in a Gnotobiotic Mouse Model. *Front. Cell. Infect. Microbiol.* **6**, 191 (2016).
130. Thanissery, R., Winston, J. A. & Theriot, C. M. Inhibition of spore germination, growth, and toxin activity of clinically relevant C. difficile strains by gut microbiota derived secondary bile acids. *Anaerobe* **45**, 86–100 (2017).
131. Francis, M. B., Allen, C. A. & Sorg, J. A. Muricholic Acids Inhibit Clostridium difficile Spore Germination and Growth. *PLoS One* **8**, 1–7 (2013).
132. Khurana, S., Raufman, J.-P. P. & Pallone, T. L. *Bile acids regulate cardiovascular function. Clinical and Translational Science* vol. 4 210–218 (Blackwell Publishing Inc, 2011).
133. Adhikari, A. A. *et al.* Development of a covalent inhibitor of gut bacterial bile salt hydrolases. *Nat. Chem. Biol.* (2020) doi:10.1038/s41589-020-0467-3.
134. Swann, J. R. *et al.* Systemic gut microbial modulation of bile acid metabolism in host tissue compartments. *Proc. Natl. Acad. Sci.* **108**, 4523–4530 (2011).
135. Wahlström, A., Sayin, S. I., Marschall, H. U. & Bäckhed, F. Intestinal Crosstalk between Bile Acids and Microbiota and Its Impact on Host Metabolism. *Cell Metabolism* vol. 24 41–50 (2016).
136. Buffie, C. G. *et al.* Precision microbiome restoration of bile acid-mediated resistance to Clostridium difficile. *Nature* **517**, 205–208 (2015).
137. Bernstein, H., Bernstein, C., Payne, C. M., Dvorakova, K. & Garewal, H. Bile acids as carcinogens in human gastrointestinal cancers. *Mutat Res* **589**, 47–65 (2005).
138. Joyce, S. A. *et al.* Regulation of host weight gain and lipid metabolism by bacterial bile acid modification in the gut. *Proc. Natl. Acad. Sci.* **111**, 7421–7426 (2014).
139. Tropini, C., Earle, K. A., Huang, K. C. & Sonnenburg, J. L. The Gut Microbiome: Connecting Spatial Organization to Function. *Cell Host Microbe* **21**, 433–442 (2017).
140. Kitahara, M., Takamine, F., Imamura, T. & Benno, Y. Clostridium hiranonis sp. nov., a human intestinal bacterium with bile acid 7 $\alpha$ -dehydroxylating activity. *Int. J. Syst. Evol. Microbiol.* **51**, 39–44 (2001).
141. Morris, G. N., Winter, J., Cato, E. P., Ritchie, A. E. & Bokkenheuser, V. D. Clostridium scindens sp. nov., a Human Intestinal Bacterium with Desmolytic Activity on Corticoids. *Int. J. Syst. Bacteriol.* **35**, 478–481 (1985).
142. Shen, A. *et al.* A Gut Odyssey: The Impact of the Microbiota on Clostridium difficile Spore Formation and Germination. *PLoS Pathog.* **11**, (2015).
143. Greathouse, K. L., Harris, C. C. & Bultman, S. J. *Dysfunctional families: Clostridium scindens and secondary bile acids inhibit the growth of clostridium difficile. Cell Metabolism* vol. 21 9–10 (2015).
144. Hoppe, P., Cohen, S. & Meibom, A. NanoSIMS: Technical Aspects and Applications in Cosmochemistry and Biological Geochemistry. *Geostand. Geoanalytical Res.* (2013) doi:10.1111/j.1751-908X.2013.00239.x.
145. Brugiroux, S. *et al.* Genome-guided design of a defined mouse microbiota that confers colonization resistance against Salmonella enterica serovar Typhimurium. *Nat Microbiol* **2**, 16215 (2016).
146. Macdonald, I. A. & Hutchison, D. M. Epimerization versus dehydroxylation of the 7 $\alpha$ -hydroxyl- group of primary bile acids: Competitive studies with Clostridium absonum and 7 $\alpha$ -dehydroxylating bacteria (Eubacterium SP.). *J. Steroid Biochem.* **17**, 287–293 (1982).
147. Zhang, Y. & Klaassen, C. D. Effects of feeding bile acids and a bile acid sequestrant on hepatic bile acid composition in mice. *J Lipid Res* **51**, 3230–3242 (2010).
148. Hirano, S. & Masuda, N. Transformation of bile acids by Eubacterium lentum. *Appl. Environ. Microbiol.* **42**, 912–5 (1981).
149. Wells, J. E. & Hylemon, P. B. Identification and characterization of a bile acid 7 $\alpha$ -dehydroxylation operon in Clostridium sp. strain TO-931, a highly active 7 $\alpha$ -dehydroxylating strain isolated from human feces. *Appl. Environ. Microbiol.* **66**, 1107–1113 (2000).

150. Hofmann, A. F. & Eckmann, L. How bile acids confer gut mucosal protection against bacteria. *Proc. Natl. Acad. Sci.* **103**, 4333–4334 (2006).
151. Islam, K. B. M. S. *et al.* Bile Acid Is a Host Factor That Regulates the Composition of the Cecal Microbiota in Rats. *Gastroenterology* **141**, 1773–1781 (2011).
152. Inagaki, T. *et al.* Regulation of antibacterial defense in the small intestine by the nuclear bile acid receptor. *Proc. Natl. Acad. Sci.* **103**, 3920–3925 (2006).
153. Shapiro, H., Kolodziejczyk, A. A., Halstuch, D. & Elinav, E. Bile acids in glucose metabolism in health and disease. *J. Exp. Med.* **20171965** (2018) doi:10.1084/jem.20171965.
154. Sacquet, E. C., Gadelle, D. P., Riottot, M. J. & Raibaud, A. P. M. Absence of Transformation of  $\beta$ -Muricholic Acid by Human Microflora Implanted in the Digestive Tracts of Germfree Male Rats. *Appl. Environ. Microbiol.* **47**, 1167–1168 (1984).
155. Winter, J. *et al.* Mode of action of steroid desmolase and reductases synthesized by *Clostridium 'scindens'* (formerly *Clostridium* strain 19). *J. Lipid Res.* **25**, 1124–31 (1984).
156. Gerard, P. & Gérard, P. Metabolism of cholesterol and bile acids by the gut microbiota. *Pathogens* **3**, 14–24 (2013).
157. Musat, N., Musat, F., Weber, P. K. & Pett-Ridge, J. Tracking microbial interactions with NanoSIMS. (2016).
158. Neufeld, J. D., Wagner, M. & Murrell, J. C. Who eats what, where and when? Isotope-labelling experiments are coming of age. *ISME Journal* vol. 1 103–110 (2007).
159. Gibbin, E. *et al.* Using NanoSIMS coupled with microfluidics to visualize the early stages of coral infection by *Vibrio coralliilyticus*. *BMC Microbiol.* **18**, 39 (2018).
160. Ridlon, J. M., Kang, D. J. & Hylemon, P. B. Isolation and characterization of a bile acid inducible 7 $\alpha$ -dehydroxylating operon in *Clostridium hylemonae* TN271. *Anaerobe* **16**, 137–146 (2010).
161. Ridlon, J., Alves, J., Hylemon, P. & Bajaj, J. Cirrhosis, bile acids and gut microbiota. *Jhep* **4**, 382–387 (2013).
162. Gasteiger, E. *et al.* Protein Identification and Analysis Tools on the ExPASy Server. in *The Proteomics Protocols Handbook* (2005). doi:10.1385/1-59259-890-0:571.
163. Kang, D.-J. *et al.* *Clostridium scindens* baiCD and baiH genes encode stereo- specific 7 $\alpha$ /7 $\beta$ -hydroxy-3-oxo- $\Delta$  4 -cholenoic acid oxidoreductases. *Biochim Biophys Acta* **1781**, 16–25 (2008).
164. Zhabinskii, V. N., Khripach, N. B. & Khripach, V. A. Steroid plant hormones: Effects outside plant kingdom. *Steroids* (2015) doi:10.1016/j.steroids.2014.08.025.
165. Sultan, A. Steroids: A Diverse Class of Secondary Metabolites. *Med. Chem. (Los. Angeles)*. (2015) doi:10.4172/2161-0444.1000279.
166. Chen, W. *et al.* Promiscuous enzymatic activity-aided multiple-pathway network design for metabolic flux rearrangement in hydroxytyrosol biosynthesis. *Nat. Commun.* (2019) doi:10.1038/s41467-019-08781-2.
167. Ridlon, J. J. M., Kang, D. J. D., Hylemon, P. B. P. & Bajaj, J. J. S. Bile acids and the gut microbiome. *Curr. Opin. Gastroenterol.* **30**, 332–8 (2014).
168. Edenharder, R. Dehydroxylation of cholic acid at C12 and epimerization at C5 and C7 by *Bacteroides* species. *J. Steroid Biochem.* **21**, 413–420 (1984).
169. Huijghebaert, S., Parmentier, G. & Eyssen, H. *Specificity of bile salt sulfatase activity in man, mouse and rat intestinal microflora.* *J. steroid Biochem* vol. 20 [https://ac-els-cdn-com.docelec.univ-lyon1.fr/0022473184904047/1-s2.0-0022473184904047-main.pdf?\\_tid=8752ccb1-d2a7-44ad-8440-2a4e0a742cba&acdnat=1535022486\\_0e224ae7d784c97b3ee4754aea2ba9b1](https://ac-els-cdn-com.docelec.univ-lyon1.fr/0022473184904047/1-s2.0-0022473184904047-main.pdf?_tid=8752ccb1-d2a7-44ad-8440-2a4e0a742cba&acdnat=1535022486_0e224ae7d784c97b3ee4754aea2ba9b1) (1984).
170. Kelsey, M. I., Molina, J. E., Huang, S. K. & Hwang, K. K. The identification of microbial metabolites of sulfolithocholic acid. *J. Lipid Res.* **21**, 751–9 (1980).
171. Macdonald, I. A., Bokkenheuser, V. D., Winter, J., McLernon, A. M. & Mosbach, E. H. Degradation of steroids in the human gut. *J. Lipid Res.* **24**, 675–700 (1983).

172. Prabha, V. & Ohri, M. Review: Bacterial transformations of bile acids. *World J. Microbiol. Biotechnol.* **22**, 191–196 (2006).
173. Quinn, R. A. *et al.* Global chemical effects of the microbiome include new bile-acid conjugations. *Nature* (2020) doi:10.1038/s41586-020-2047-9.
174. Huijghebaert, S. M., Mertens, J. A. & Eyssen, H. J. Isolation of a bile salt sulfatase-producing *Clostridium* strain from rat intestinal microflora. *Appl. Environ. Microbiol.* **43**, 185–92 (1982).
175. Harris, S. C. *et al.* Bile acid oxidation by *Eggerthella lenta* strains C592 and DSM 2243 T. *Gut Microbes* **9**, 523–539 (2018).
176. Urdaneta, V. *et al.* Interactions between Bacteria and Bile Salts in the Gastrointestinal and Hepatobiliary Tracts. *Front. Med.* **4**, 163 (2017).
177. Foley Id, M. H., O'flaherty Id, S., Id, R. B. & Theriot Id, C. M. Bile salt hydrolases: Gatekeepers of bile acid metabolism and host-microbiome crosstalk in the gastrointestinal tract. (2019) doi:10.1371/journal.ppat.1007581.
178. Devendran, S. *et al.* *Clostridium scindens* ATCC 35704: Integration of Nutritional Requirements, the Complete Genome Sequence, and Global Transcriptional Responses to Bile Acids. *Appl. Environ. Microbiol.* **85**, e00052-19 (2019).
179. Selwyn, F. P., Csanaky, I. L., Zhang, Y. & Klaassen, C. D. Importance of large intestine in regulating bile acids and glucagon-like peptide-1 in germ-free mice. *Drug Metab. Dispos.* **43**, 1544–1556 (2015).
180. Garzetti, D. *et al.* High-Quality Whole-Genome Sequences of the Oligo-Mouse-Microbiota Bacterial Community. *Genome Announc.* **5**, e00758-17 (2017).
181. Hyatt, D. *et al.* Prodigal: prokaryotic gene recognition and translation initiation site identification. *BMC Bioinformatics* **11**, 119 (2010).
182. Patnode, M. L. *et al.* Interspecies Competition Impacts Targeted Manipulation of Human Gut Bacteria by Fiber-Derived Glycans. (2019) doi:10.1016/j.cell.2019.08.011.
183. Clarkson, S. M. *et al.* Construction and Optimization of a Heterologous Pathway for Protocatechuate Catabolism in *Escherichia coli* Enables Bioconversion of Model Aromatic Compounds. *Appl. Environ. Microbiol.* **83**, e01313-17 (2017).
184. Elias, J. E. & Gygi, S. P. Target-decoy search strategy for increased confidence in large-scale protein identifications by mass spectrometry. *Nat. Methods* **4**, 207–214 (2007).
185. Diamant, B. J. & Noble, W. S. Faster SEQUEST Searching for Peptide Identification from Tandem Mass Spectra. *J. Proteome Res.* **10**, 3871–3879 (2011).
186. Käll, L., Canterbury, J. D., Weston, J., Noble, W. S. & MacCoss, M. J. Semi-supervised learning for peptide identification from shotgun proteomics datasets. *Nat. Methods* **4**, 923–5 (2007).
187. Argentini, A. *et al.* moFF: a robust and automated approach to extract peptide ion intensities. *Nat. Methods* **13**, 964–966 (2016).
188. Polpitiya, A. D. *et al.* DANTE: a statistical tool for quantitative analysis of -omics data. *Bioinformatics* **24**, 1556–8 (2008).
189. Watanabe, M., Fukiya, S. & Yokota, A. Comprehensive evaluation of the bactericidal activities of free bile acids in the large intestine of humans and rodents. *J. Lipid Res.* (2017) doi:10.1194/jlr.M075143.
190. Winter, S. E., Lopez, C. A. & Bäuml, A. J. The dynamics of gut-associated microbial communities during inflammation. *EMBO Reports* (2013) doi:10.1038/embor.2013.27.
191. Deshpande, A. *et al.* Community-associated *clostridium difficile* infection antibiotics: A meta-analysis. *Journal of Antimicrobial Chemotherapy* vol. 68 1951–1961 (2013).
192. Brown, K. A., Khanafer, N., Daneman, N. & Fisman, D. N. Meta-analysis of antibiotics and the risk of community-associated *Clostridium difficile* infection. *Antimicrob. Agents Chemother.* **57**, 2326–2332 (2013).
193. Slimings, C. & Riley, T. V. Antibiotics and hospital-acquired *Clostridium difficile* infection: Update of systematic review and meta-analysis. *Journal of Antimicrobial Chemotherapy* vol. 69 881–891 (2014).
194. Pear, S. M., Williamson, T. H., Bettin, K. M., Gerding, D. N. & Galgiani, J. N. Decrease in nosocomial *Clostridium difficile*-associated diarrhea by restricting clindamycin use. *Ann. Intern. Med.* **120**, 272–7 (1994).



195. Climo, M. W. *et al.* Hospital-wide restriction of clindamycin: effect on the incidence of *Clostridium difficile*-associated diarrhea and cost. *Ann. Intern. Med.* **128**, 989–95 (1998).
196. Buffie, C. G. *et al.* Profound alterations of intestinal microbiota following a single dose of clindamycin results in sustained susceptibility to *Clostridium difficile*-induced colitis. *Infect. Immun.* **80**, 62–73 (2012).
197. Houten, S. M., Volle, D. H., Cummins, C. L., Mangelsdorf, D. J. & Auwerx, J. In Vivo Imaging of Farnesoid X Receptor Activity Reveals the Ileum as the Primary Bile Acid Signaling Tissue. *Mol. Endocrinol.* **21**, 1312–1323 (2007).
198. Chiang, J. Y. L. Bile acids: regulation of synthesis. *J. Lipid Res.* **50**, 1955–1966 (2009).
199. Wang, H., Chen, J., Hollister, K., Sowers, L. C. & Forman, B. M. Endogenous Bile Acids are Ligands for the Nuclear Receptor FXR/BAR. *Mol. Cell* **3**, 543–553 (1999).
200. Parks, D. J. *et al.* Bile acids: Natural ligands for an orphan nuclear receptor. *Science (80-. ).* **284**, 1365–1368 (1999).
201. Li, F. *et al.* Microbiome remodelling leads to inhibition of intestinal farnesoid X receptor signalling and decreased obesity. *Nat. Commun.* **4**, 2384 (2013).
202. Just, S. Impact of the interplay between bile acids , lipids , intestinal Coriobacteriaceae and diet on host metabolism. *These* (2017).
203. Miyata, M. *et al.* Chenodeoxycholic acid-mediated activation of the farnesoid X receptor negatively regulates hydroxysteroid sulfotransferase. *Drug Metab. Pharmacokinet.* **21**, 315–23 (2006).
204. Dawson, P. A. & Setchell, K. D. R. Will the real bile acid sulfotransferase please stand up? Identification of Sult2a8 as a major hepatic bile acid sulfonating enzyme in mice1. *Journal of Lipid Research* (2017) doi:10.1194/jlr.C077420.
205. Pickens, L. B., Tang, Y. & Chooi, Y.-H. Metabolic Engineering for the Production of Natural Products. *Annu. Rev. Chem. Biomol. Eng.* (2011) doi:10.1146/annurev-chembioeng-061010-114209.
206. The European Committee on Antimicrobial Susceptibility Testing. *Breakpoint tables for interpretation of MICs and zone diameters Version 9.0, 2019.* (2019).

# Annex 1 | Supplementary information for Chapter 1.

**Table S1 | Bile acid 7-dehydroxylating bacteria isolated from other mammals.**

A green cell indicates that the strain could 7-dehydroxylate the bile acid substrate tested. If for a strain the bile acid 7-dehydroxylation was not tested, the cell is white.

Organism	Strain	Family	Isolated from	7-dehydroxylation of			References
				CA	CDCA	MCAs	
<i>Extibacter muris</i>	DSM 28560	Lachnospiraceae	Mouse faeces				37
	DSM 28561						
<i>Proteocatella sphenisci</i>	DSM 23131	Peptostreptococcaeae	Penguins guano				43
<i>Clostridium scindens</i>	G10	Lachnospiraceae	Rat feces				38
Not assigned	HDCA-1	Not assigned	Rat feces				39
Not assigned	FA 1/146	<i>Bacteroides sp.</i>	Rabbit feces				40
Not assigned	Strain II	<i>Clostridium</i> genus	Rat feces				52,96
Not assigned	Strain III	<i>Clostridium</i> genus	Rat feces				52
Not assigned	Strain V	<i>Clostridium</i> genus	Rat feces				52
Not assigned	Strain VI	<i>Clostridium</i> genus	Rat feces				52
Not assigned	Strain VII	<i>Clostridium</i> genus	Rat feces				52
Not assigned	Strain VIII	<i>Clostridium</i> genus	Rat feces				52

**Table S2 | Bile acid 7-dehydroxylating bacteria and sporulation.**

A green cell indicates that sporulation was observed for the strain tested. A red cell indicates that sporulation was not observed. If for a strain sporulation was not investigated, the cell is white. An orange cell indicates a situation where it is not clear whether the strain sporulates or not.

\* Conflicting results between two studies for the same strain tested.

\*\* Terminal swelling of the bacterial cells resembling spores were observed. However, these swellings did not take spore stains and released spores could not be demonstrated.

Organism	Strain	Isolated from	Sporulation	References
<i>Clostridium scindens</i>	ATCC 35704 = JCM 6567	Humans		45
<i>Clostridium scindens</i>	VPI 12708	Humans		44,45
<i>Clostridium scindens</i>	Y-1113	Humans		44,45
<i>Clostridium scindens</i>	I-10	Humans		45
<i>Clostridium scindens</i>	M-18	Humans		44,45
<i>Clostridium scindens</i>	TH-82	Humans		45
<i>Clostridium scindens</i>	36S	Humans		44,45
<i>Clostridium hylemonae</i>	TN-271	Humans		45
<i>Clostridium hylemonae</i>	TN-272	Humans		45
<i>Clostridium hiranonis</i>	TO-931 = JCM 10541	Humans		140
<i>Clostridium hiranonis</i>	HD-17 = JCM 10542	Humans	*	41,140
<i>Clostridium sordellii</i>	4709	?		41
<i>Clostridium sordellii</i>	Y-67	Humans		44
<i>Eggerthella lenta</i> like sp.	c-25	Humans		41
<i>Eggerthella lenta</i> like sp.	b-8	Humans		41
<i>Clostridium</i> sp.	S-11	Sewage		41
<i>Clostridium</i> sp.	HU-2	Humans		41
<i>Clostridium</i> sp.	HU-6	Humans		41
<i>Clostridium</i> sp.	N-9-2	Humans		41
<i>Clostridium</i> sp.	N-9-4	Humans		41
<i>Clostridium</i> sp.	N-9-10	Humans		41
<i>Clostridium</i> sp.	I-55	Humans		41
<i>Clostridium</i> sp.	I-B6	Sewage		41
<i>Clostridium</i> sp.	I-102	Humans		41
<i>Clostridium</i> sp.	II-27	Sewage		41
<i>Eubacterium</i> sp.	Y-1112	Humans		44
<i>Eubacterium</i> sp.	Y-98	Humans		44
<i>Eubacterium</i> sp.	O-51	Humans		44
<i>Eubacterium</i> sp.	O-52	Humans		44
<i>Eubacterium</i> sp.	O-71	Humans		44
<i>Eubacterium</i> sp.	O-72	Humans		44
<i>Eubacterium</i> sp.	M-2	Humans		44
<i>Eubacterium</i> sp.	M-17	Humans		44
<i>Eubacterium</i> sp.	10	Humans		44
<i>Eubacterium</i> sp.	12	Humans		44
<i>Proteocatella sphenisci</i>	DSM 23131	Penguins		43
<i>Bacteroides</i> sp.	FA 1/146	Rabbit		40
<i>Clostridium</i> genus	Strain II	Rat	**	52
<i>Clostridium</i> genus	Strain III	Rat	**	52
<i>Clostridium</i> genus	Strain V	Rat	**	52
<i>Clostridium</i> genus	Strain VI	Rat	**	52
<i>Clostridium</i> genus	Strain VII	Rat	**	52
<i>Clostridium</i> genus	Strain VIII	Rat	**	52

# Annex 2| Supplementary information for Chapter 2.

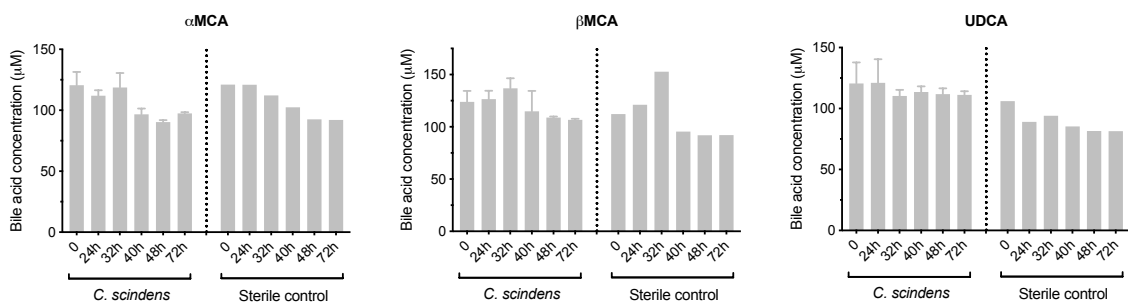


**Figure S1| Primary bile acids that were not metabolized by *Clostridium scindens* in vitro.** *C. scindens* was grown in BHIS-S containing one primary bile acid (UDCA, αMCA and βMCA) in triplicate. Six time points were selected along the growth curves for bile acid analyses. Histograms combined bile acids analyzed in the supernatants and the biomass (SUP + PEL). The analyses were carried out in triplicate, collected from triplicate cultures of *C. scindens*. Histograms indicate the mean and the standard deviation.

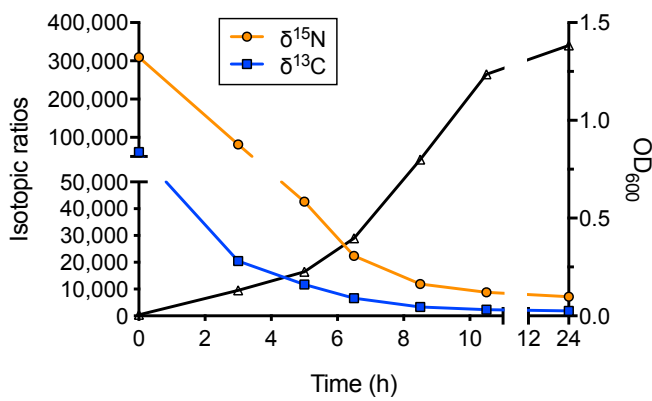


**Figure S2| The isotopic labeling of *C. scindens* decreases as cells grow.** Isotopically labeled *C. scindens* cells were transferred into a BHIS-S medium. The growth was measured with OD<sub>600</sub> and isotopic ratios of the cells quantified using NanoSIMS. Each symbol represents an average of the isotopic ratio of all cells (n≥50) present on one NanoSIMS image.

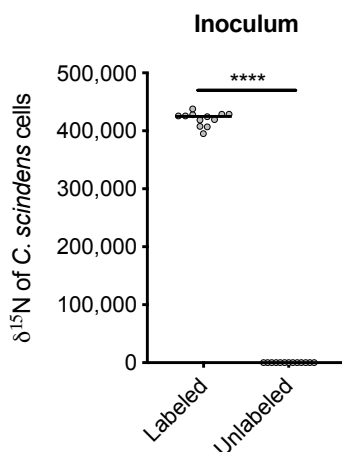


**Figure S3 | Nitrogen isotopic ratios of *C. scindens* labeled and unlabeled (control) inoculum.** *C. scindens* was isotopically labeled *in vitro* in a medium containing  $^{15}\text{N}$  labeled nutrients prior to inoculation into mice. A control culture of *C. scindens* (unlabeled) was prepared in a medium deprived of labeled nutrients. The nitrogen isotopic ratios of the two *C. scindens* inoculum (labeled and unlabeled) were determined on the NanoSIMS. Each symbol corresponds to the average  $\delta^{15}\text{N}$  of one NanoSIMS image ( $\geq 50$  cells). Statistical analysis used Mann-Whitney-U tests to compare *C. scindens* isotopic ratios. Ns, not statistically significant ( $p \geq 0.05$ ), \*\*\*\* $p < 0.0001$ .

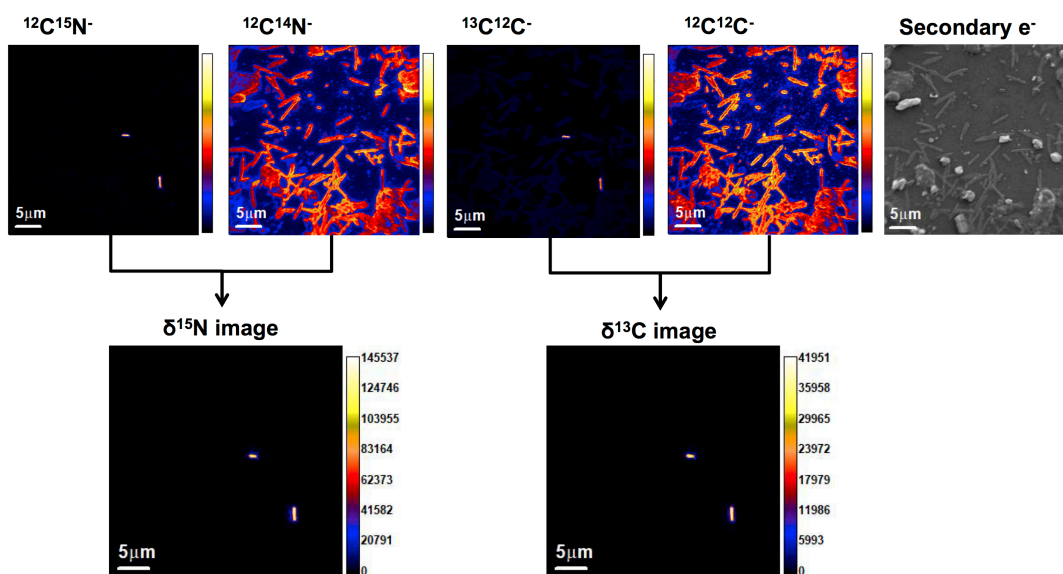
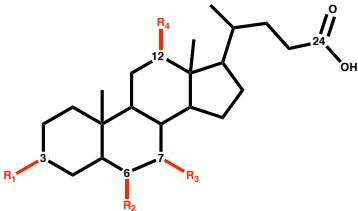


**Figure S4 | NanoSIMS and ratio images obtained from a cecum sample (t=6h) collected from a mouse colonized with isotopically labeled cells of *C. scindens*.** The isotopically-labeled cells of *C. scindens* from a cecum sample emerge on the ratio images. *Clostridium scindens* cells labeled with  $^{15}\text{N}$  and  $^{13}\text{C}$  were inoculated into sDMDMm2 mice, a gnotobiotic mouse model with a reduced microbiota. On the NanoSIMS  $^{12}\text{C}^{14}\text{N}^-$  and  $^{12}\text{C}^{12}\text{C}^-$  images, we observe the entire gut microbial community of the mouse, as  $^{14}\text{N}$  and  $^{12}\text{C}$  account for the vast majority of the nitrogen and carbon. In contrast,  $^{15}\text{N}$  and  $^{13}\text{C}$  are rare isotopes. Within the microbial community of sDMDMm2 mice, only *C. scindens* cells, enriched in  $^{15}\text{N}$  and  $^{13}\text{C}$ , are visible on the images of the secondary ions species  $^{12}\text{C}^{15}\text{N}^-$  and  $^{12}\text{C}^{13}\text{C}^-$ , and consequently on the two ratio images. The secondary electron image gives an overview of the sample. Nitrogen and carbon ratio images were obtained by taking the ratio between the drift-corrected, cumulative  $^{12}\text{C}^{15}\text{N}^-$ ,  $^{12}\text{C}^{14}\text{N}^-$  and  $^{12}\text{C}^{13}\text{C}^-$ ,  $^{12}\text{C}^{12}\text{C}^-$  images.

Table S1| Structure of common human and murine bile acids.

Bile Acid Name	Abbreviations	R1	R2	R3	R4	ketone group	conjugate
Cholic acid	CA	3 $\alpha$		7 $\alpha$	12 $\alpha$	-	-
Chenodeoxycholic acid	CDCA	3 $\alpha$		7 $\alpha$		-	-
$\alpha$ -Muricholic acid	$\alpha$ MCA	3 $\alpha$	6 $\beta$	7 $\alpha$		-	-
$\beta$ -Muricholic acid	$\beta$ MCA	3 $\alpha$	6 $\beta$	7 $\beta$		-	-
$\omega$ -Muricholic acid	$\omega$ MCA	3 $\alpha$	6 $\alpha$	7 $\beta$		-	-
Ursodeoxycholic acid	UDCA	3 $\alpha$		7 $\beta$		-	-
Deoxycholic acid	DCA	3 $\alpha$			12 $\alpha$	-	-
Lithocholic acid	LCA	3 $\alpha$				-	-
3-oxodeoxycholic acid	3-oxoDCA				12 $\alpha$	C3	
3-oxocholic acid	3-oxoCA			7 $\alpha$	12 $\alpha$	C3	
3-oxolithocholic acid	3-oxoLCA					C3	
3-oxochenodeoxycholic acid	3-oxoCDCA			7 $\alpha$		C3	
7-oxodeoxycholic acid	7-oxoDCA	3 $\alpha$			12 $\alpha$	C7	
7-oxolithocholic acid	7-oxoLCA	3 $\alpha$				C7	
Isoodeoxycholic acid	isoDCA	3 $\beta$			12 $\alpha$	-	
Isolithocholic acid	isoLCA	3 $\beta$				-	
12-oxolithocholic acid	12-oxoLCA	3 $\alpha$				C12	
Taurocholic acid	TCA	3 $\alpha$		7 $\alpha$	12 $\alpha$	-	taurine
Taurochenodeoxycholic acid	TCDCa	3 $\alpha$		7 $\alpha$		-	taurine
Tauroursodeoxycholic acid	TUDCA	3 $\alpha$		7 $\beta$		-	taurine
Tauro- $\alpha$ -muricholic acid	T $\alpha$ MCA	3 $\alpha$	6 $\beta$	7 $\alpha$		-	taurine
Tauro- $\beta$ -muricholic acid	T $\beta$ MCA	3 $\alpha$	6 $\beta$	7 $\beta$		-	taurine
Taurocholic acid 7-sulfate	TCA7S			7-sulfate	12 $\alpha$	-	taurine
Cholic acid 7-sulfate	CA7S	3 $\alpha$		7-sulfate	12 $\alpha$	-	
Chenodeoxycholic acid 3-sulfate	CDCA3S			7-sulfate		-	

Structure of unconjugated bile acids



Structure of tauro-conjugated bile acids

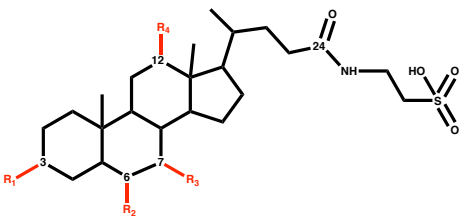
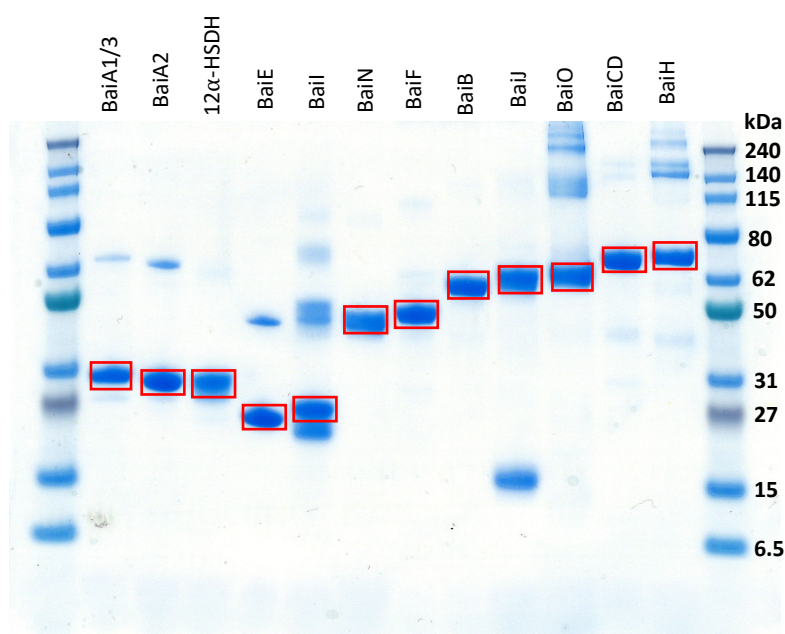


Table S2 | Bile acid standards used in this study.

	Name	Abbreviation	Position of hydroxyl group(s)	Position of ketone group(s)	[M-H] <sup>-</sup>	LOD (nM)	Note
					theoretical		
External standards	3-oxolithocholic acid	3-oxoLCA	-	C3	373.2748	2.2	
	allolithocholic acid	alloLCA	3α	-	375.2905	3.9	
	isolithocholic acid	isoLCA	3β	-	375.2905	6.7	
	lithocholic acid	LCA	3α	-	375.2905	1.4	
	6-oxo-allolithocholic acid	6-oxo-alloLCA	3α	C6	389.2697	7.7	
	6-oxolithocholic acid	6-oxoLCA	3α	C6	389.2697	28.1	
	7-oxolithocholic acid	7-oxoLCA	3α	C7	389.2697	5.1	
	12-oxolithocholic acid	12-oxoLCA	3α	C12	389.2697	15.9	
	3-oxodeoxycholic acid	3-oxoDCA	12α	C3	389.2697	6.7	
	3-oxochenodeoxycholic acid	3-oxoCDCA	7α	C3	389.2697	4.9	
	murideoxycholic acid	MDCA	3α, 6β	-	391.2854	14.6	
	ursodeoxycholic acid	UDCA	3α, 7β	-	391.2854	4.3	
	hyodeoxycholic acid	HDCA	3α, 6α	-	391.2854	17.1	
	chenodeoxycholic acid	CDCA	3α, 7α	-	391.2854	12.7	
	deoxycholic acid	DCA	3α, 12α	-	391.2854	3.2	
	isodeoxycholic acid	isoDCA	3β, 12α	-	391.2854	13.1	
	7, 12-dioxolithocholic acid	7, 12-dioxoLCA	3α	C7, C12	403.54	27.3	
	7-oxodeoxycholic acid	7-oxoDCA	3α, 12α	C7	405.2647	3.7	
	3-dehydrocholic acid	3-oxoCA	7α, 12α	C3	405.2647	1.8	
	12-oxochenodeoxycholic acid	12-oxoCDCA	3α, 7α	C12	405.2647	467.8	
	ω-muricholic acid	ωMCA	3α, 6α, 7β	-	407.2803	14.9	
	α-muricholic acid	αMCA	3α, 6β, 7α	-	407.2803	19.1	
	β-muricholic acid	βMCA	3α, 6β, 7β	-	407.2803	12.1	
	hyocholic acid	HCA	3α, 6α, 7α	-	407.2803	22.4	
	cholic acid	CA	3α, 7α, 12α	-	407.2803	3.9	
	chenodeoxycholic acid 3-sulfate	CDCA3S	7α	-	471.2422	20.3	
	taurolithocholic acid	TLCA	3α	-	482.2946	2.0	
	cholic acid 7-sulfate	CA7S	3α, 12α	-	487.23711	32.1	
	tauroursodeoxycholic acid	TUDCA	3α, 7β	-	498.2895	10.6	
	taurohyodeoxycholic acid	THDCA	3α, 6α	-	498.2895	3.9	
	taurumurideoxycholic acid	TMDCA	3α, 6β	-	498.2895	11.2	
	taurochenodeoxycholic acid	TCDCa	3α, 7α	-	498.2895	2.4	
	taurodeoxycholic acid	TDCA	3α, 12α	-	498.2895	2.1	
	tauro-ω-muricholic acid	TωMCA	3α, 6α, 7β	-	514.2844	1423.1	
	tauro-α-muricholic acid	TαMCA	3α, 6β, 7α	-	514.2844	175.5	
	tauro-β-muricholic acid	TβMCA	3α, 6β, 7β	-	514.2844	214.0	
	taurohyocholic acid	THCA	3α, 6α, 7α	-	514.2844	192.4	
	taurocholic acid	TCA	3α, 7α, 12α	-	514.2844	121.0	
	taurolithocholic acid 3-sulfate	TLCA3S	3α	-	562.25138	34.7	
	taurocholic acid 3-sulfate	TCA3S	7α, 12α	-	594.24121	85.3	TCA3S standard was used to quantify TCA7S in the <i>in vivo</i> samples as 7-sulfated bile acids are predominant in mice
Internal standards	deuterated chenodeoxycholic acid	CDCA-D4	3α, 7α	-	395.3105		
	deuterated deoxycholic acid	DCA-D4	3α, 12α	-	395.3105		
	deuterated lithocholic acid	LCA-D4	3α	-	379.3156		
	deuterated cholic acid	CA-D4	3α, 7α, 12α	-	411.3054		
	deuterated tauroursodeoxycholic acid	TUDCA-D4	3α, 7β	-	502.3146		
	deuterated taurocholic acid	TCA-D4	3α, 7α, 12α	-	518.3095		

## Annex 3| Supplemental information of Chapter 3



**Figure S1|** Picture of the gel with all the purified enzymes used in this study. The red rectangles indicate the purified enzymes. The other bands either can be dimers, trimers of the protein or degradation products



**Table S1 | Primers, restriction sites and expression strain used for the cloning of *bai* genes.**

The 12 $\alpha$ -HSDH construct in pET51b+ was kindly provided by Heidi Doden and Jason Ridlon from University of Illinois, Urbana-Champaign, US.

Gene	Primers (F, R)	Vector	Tag	Restriction sites used for cloning	Protein expression strain
12 $\alpha$ HSDH	N/A	pET51b+	N-ter Strep	N/A	BL21-CodonPlus(DE3)-RIPL
BaiA1/3	GCA GTT CGA AAA GGG ATC CGG ATC CAT GAA ACT TGT ACA GGA CAA A	m-pET28b+	N-ter Strep	BamHI - NotI	BL21-CodonPlus(DE3)-RIPL
	GGT GCT CGA GTG CGG CCG CCT ACT ATG GCC TGT AAG CCC CAT C				
BaiA2	GCA GTT CGA AAA GGG ATC CGG ATC CAT GAA TCT CGT ACA AGA CAA G	m-pET28b+	N-ter Strep	BamHI - NotI	BL21-CodonPlus(DE3)-RIPL
	GGT GCT CGA GTG CGG CCG CCT ATT ATG GTC TGT AAG CTC CGT C				
BaiCD	GCA GTT CGA AAA GGG ATC CAT GAG TTA CGA AGC ACT TTT T	m-pET28b+	N-ter Strep	NcoI - NotI	BL21-CodonPlus(DE3)-RIPL
	GGT GCT CGA GTG CGG CCG CCT ACT AGA TTG CCA TTC CTG C				
BaiH	GCA GTT CGA AAA GGG ATC CAT GGA TAT GAA ACA TTC CAG A	m-pET28b+	N-ter Strep	NcoI - NotI	BL21-CodonPlus(DE3)-RIPL
	GGT GCT CGA GTG CGG CCG CCT ATT ACA GGC TGT ATG CCT T				
BaiB	GCA GTT CGA AAA GGG ATC CGG ATC CAT GCA CAA AAA ATC AAC GTG T	m-pET28b+	N-ter Strep	BamHI - NotI	BL21-CodonPlus(DE3)-RIPL
	GGT GCT CGA GTG CGG CCG CCT ATC ATA CCC CGC GGG CAA TAC A				
BaiF	GCA GTT CGA AAA GGG ATC CGG ATC CAT GGC TGG ATT AAA AGA TTT T	m-pET28b+	N-ter Strep	BamHI - NotI	BL21-CodonPlus(DE3)-RIPL
	GGT GCT CGA GTG CGG CCG CCT ATT ACT CCT CTT TCT TTC TCA T				
BaiE	GCA GTT CGA AAA GGG ATC CAT GAT ACA TAT GAC ATT AGA A	m-pET28b+	N-ter Strep	NcoI - NotI	BL21-CodonPlus(DE3)-RIPL
	GGT GCT CGA GTG CGG CCG CCT ATT ATT TGT GCA TGT TCA T				
BaiI	GCA GTT CGA AAA GGG ATC CAT GGC AGT GAA GGC AAT CTC A	m-pET28b+	N-ter Strep	NcoI - NotI	BL21-CodonPlus(DE3)-RIPL
	GGT GCT CGA GTG CGG CCG CCT ATT AAA AAT CAC ATG TAT C				
BaiJ	GCA GTT CGA AAA GGG ATC CGG ATC CAT GGC AAG TTA TAC ACC CGG G	m-pET28b+	N-ter Strep	BamHI - NotI	BL21-CodonPlus(DE3)-RIPL
	GGT GCT CGA GTG CGG CCG CCT ATT ACA GCA TCT CTC TCT G				
BaiO	GCA GTT CGA AAA GGG ATC CGG ATC CAT GAT ATC TAT GAT TCG GAT C	m-pET28b+	N-ter Strep	BamHI - NotI	BL21-CodonPlus(DE3)-RIPL
	GGT GCT CGA GTG CGG CCG CCT ATT AAA AAT TTC TTA AGC CTT T				
BaiN	CTT TAA GAA GGA GAT ATA CCA TGA ATC GGA TTG GAA TCA TCG GAG G	pET28b+	C-ter His	XhoI - NcoI	BL21-CodonPlus(DE3)-RIPL
	TGG TGG TGG TGG TGC GCG GGT CTT TCC GCC GCC GC				

**Table S2 | Bile acid standards used for the UHPLC-HRMS bile acid analysis.** For each bile acid standard, its commonly used abbreviation, partial name, molecular formula, theoretical [M-H]<sup>-</sup>, supplier and catalogue number are indicated.

All CoA conjugates standard were synthesized in the laboratory by incubating the bile acid with purified BaiB (CoA ligase) in 50mM Hepes 50mM KCl pH7.5 buffer containing 500uM ATP and 500uM Coenzyme A.

Abbreviations	Partial Name	Molecular Formula	Theoretical [M-H] <sup>-</sup>	Supplier	Catalogue Nb
CA	3 $\alpha$ ,7 $\alpha$ ,12 $\alpha$ -trihydroxy-5 $\beta$ -cholan-24-oic acid	C <sub>24</sub> H <sub>40</sub> O <sub>5</sub>	407.2803	VWR	A11257.14
3-oxoCA	7 $\alpha$ ,12 $\alpha$ -dihydroxy-3-oxo-5 $\beta$ -cholan-24-oic acid	C <sub>24</sub> H <sub>38</sub> O <sub>5</sub>	405.2647	Steraloids	C1272-000
7-oxoDCA	3 $\alpha$ ,12 $\alpha$ -dihydroxy-7-oxo-5 $\beta$ -cholan-24-oic acid	C <sub>24</sub> H <sub>38</sub> O <sub>5</sub>	405.2647	Steraloids	C1250-000
12-oxoCDCA	3 $\alpha$ ,7 $\alpha$ -dihydroxy-12-oxo-5 $\beta$ -cholan-24-oic acid	C <sub>24</sub> H <sub>38</sub> O <sub>5</sub>	405.2647	Merck	T154083
7,12-dioxoLCA	7,12-dioxo-5 $\beta$ -cholan-24-oic acid	C <sub>24</sub> H <sub>36</sub> O <sub>5</sub>	403.249	Steraloids	C1500-000
3,7,12-trioxoCA	3,7,12-trioxo-5 $\beta$ -cholan-24-oic acid	C <sub>24</sub> H <sub>34</sub> O <sub>5</sub>	401.2333	Merck	30830
3-oxoDCA	12 $\alpha$ -hydroxy-3-oxo-cholan-24-oic acid	C <sub>24</sub> H <sub>38</sub> O <sub>4</sub>	389.2697	Steraloids	C1725-000
12oxoLCA	3 $\alpha$ -hydroxy-12-oxo-5 $\beta$ -cholan-24-oic acid	C <sub>24</sub> H <sub>38</sub> O <sub>4</sub>	389.2697	Steraloids	C1650-000
12-oxo- $\Delta^9$ -LCA	12-oxo-9-cholen-24-oic acid	C <sub>24</sub> H <sub>36</sub> O <sub>4</sub>	387.2541	Steraloids	C2670-000
DCA	3 $\alpha$ ,12 $\alpha$ -dihydroxy-5 $\beta$ -cholan-24-oic acid	C <sub>24</sub> H <sub>40</sub> O <sub>4</sub>	391.2854	Steraloids	C1070-000
CA-CoA	3 $\alpha$ ,7 $\alpha$ ,12 $\alpha$ -trihydroxy-5 $\beta$ -cholanyl-CoA	C <sub>45</sub> H <sub>74</sub> N <sub>7</sub> O <sub>20</sub> P <sub>3</sub> S	1156.3849	NA	NA
3-oxoCA-CoA	7 $\alpha$ ,12 $\alpha$ -dihydroxy-3-oxo-5 $\beta$ -cholanyl-CoA	C <sub>45</sub> H <sub>72</sub> N <sub>7</sub> O <sub>20</sub> P <sub>3</sub> S	1154.3693	NA	NA
12-oxoCDCA-CoA	3 $\alpha$ ,7 $\alpha$ -dihydroxy-12-oxo-5 $\beta$ -cholanyl-CoA	C <sub>45</sub> H <sub>72</sub> N <sub>7</sub> O <sub>20</sub> P <sub>3</sub> S	1154.3693	NA	NA
3-oxoDCA-CoA	12 $\alpha$ -hydroxy-3-oxo-5 $\beta$ -cholanyl-CoA	C <sub>45</sub> H <sub>72</sub> N <sub>7</sub> O <sub>19</sub> P <sub>3</sub> S	1138.3744	NA	NA
12-oxoLCA-CoA	3 $\alpha$ -hydroxy-12-oxo-5 $\beta$ -cholanyl-CoA	C <sub>45</sub> H <sub>72</sub> N <sub>7</sub> O <sub>19</sub> P <sub>3</sub> S	1138.3744	NA	NA
12-oxo- $\Delta^9$ -LCA-CoA	12-oxo-9-cholanyl-CoA	C <sub>45</sub> H <sub>70</sub> N <sub>7</sub> O <sub>19</sub> P <sub>3</sub> S	1136.3587	NA	NA



## Annex 4| Supplemental information for Chapter 4

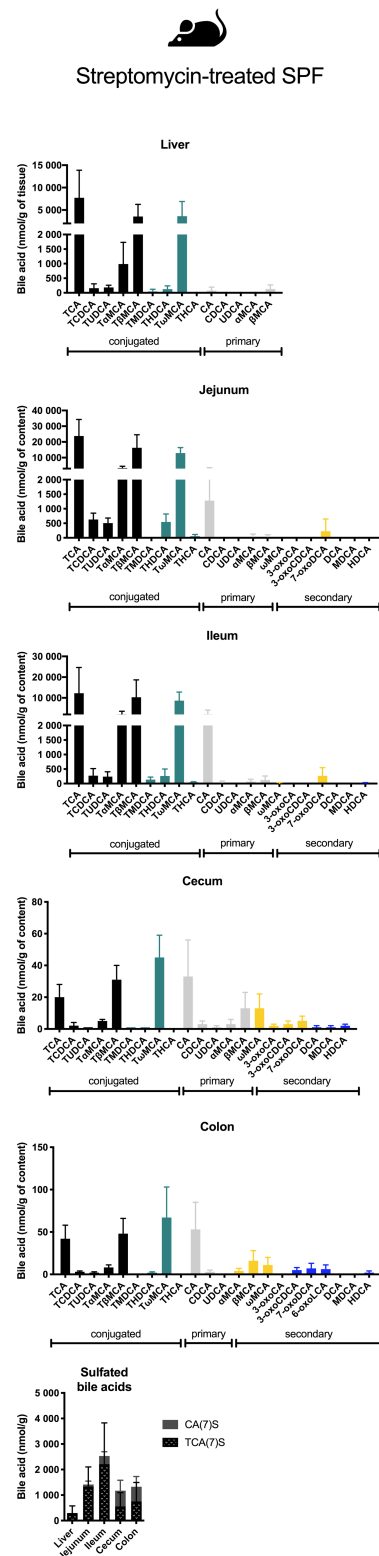


**Figure S1 | Bile acid composition along the intestinal tract in streptomycin-treated SPF mice based on LC-MS/MS analysis.** SPF mice were pre-treated with streptomycin 24h before sacrifice. Intestinal content samples were harvested from streptomycin-treated SPF mice (n=5). Samples were processed for bile acid LC-MS/MS measurements. Values indicate measured bile acid concentrations in nmol / g of tissue or intestinal content. Black bars indicate primary conjugated bile acids, teal bars secondary conjugated BAs, gray bars primary deconjugated BAs, yellow bars secondary BAs (all but 7-dehydroxylated), and blue bars represent 7-dehydroxylated BAs.

**Table S1 | Oligo-MM12 microbiota composition.** sDMDMm2 mice are colonized with a mouse-intestine derived 12-species mouse microbiota (Oligo- MM12). All Oligo-MM12 strains are available at <http://www.dsmz.de/miBC>.

Strain	Culture collection n°	Phylum	Family	Genus
<i>Bifidobacterium animalis</i> subsp. <i>animalis</i> YL2	<a href="#">DSM 26074</a>	Actinobacteria	Bifidobacteriaceae	<i>Bifidobacterium</i>
<i>Bacteroides caecimuris</i> I48	<a href="#">DSM 26085</a>	Bacteroidetes	Bacteroidaceae	<i>Bacteroides</i>
<i>Muribaculum intestinale</i> YL27	<a href="#">DSM 28989</a>	Bacteroidetes	Muribaculaceae	<i>Muribaculum</i>
<i>Clostridium clostridioforme</i> YL32	<a href="#">DSM 26114</a>	Firmicutes	Clostridiaceae	<i>Clostridium</i>
<i>Acutalibacter muris</i> KB18	<a href="#">DSM 26090</a>	Firmicutes	Ruminococcaceae	<i>Acutalibacter</i>
<i>Clostridium innocuum</i> I46	<a href="#">DSM 26113</a>	Firmicutes	Clostridiaceae	<i>Clostridium</i>
<i>Blautia coccoides</i> YL58	<a href="#">DSM 26115</a>	Firmicutes	Lachnospiraceae	<i>Blautia</i>
<i>Flavonifractor plautii</i> YL31	<a href="#">DSM 26117</a>	Firmicutes	Clostridia, not assigned to family	<i>Flavonifractor</i>
<i>Lactobacillus reuteri</i> I49	<a href="#">DSM 32035</a>	Firmicutes	Lactobacillaceae	<i>Lactobacillus</i>
<i>Enterococcus faecalis</i> KB1	<a href="#">DSM 32036</a>	Firmicutes	Enterococcaceae	<i>Enterococcus</i>
<i>Turicimonas muris</i> YL45	<a href="#">DSM 26109</a>	Proteobacteria	Sutterellaceae	<i>Turicimonas</i>
<i>Akkermansia muciniphila</i> YL44	<a href="#">DSM 26127</a>	Verrucomicrobia	Akkermansiaceae	<i>Akkermansia</i>

**Table S2 | Bile acid standards used for the UHPLC-HRMS bile acid analysis.** For each bile acid standard, its commonly used abbreviation, trivial name, partial name, molecular formula, theoretical [M-H]<sup>-</sup>, and retention time (R<sub>t</sub>) are indicated.

Abbreviations	Trivial Name	Partial Name	Molecular Formula	[M-H] <sup>-</sup>	R <sub>t</sub> (min)	LOD (nM)
3-oxoLCA	3-oxo-lithocholic acid <sup>1</sup>	3-oxo-5β-cholan-24-oic acid	C <sub>24</sub> H <sub>38</sub> O <sub>3</sub>	373.2748	20.09	2
alloLCA	allolithocholic acid <sup>1</sup>	3α-hydroxy-5α-cholan-24-oic acid	C <sub>24</sub> H <sub>40</sub> O <sub>3</sub>	375.2905	18.94	4
isoLCA	isolithocholic acid <sup>1</sup>	3β-hydroxy-5β-cholan-24-oic acid	C <sub>24</sub> H <sub>40</sub> O <sub>3</sub>	375.2905	19.31	7
LCA	lithocholic acid <sup>1</sup>	3α-hydroxy-5β-cholan-24-oic acid	C <sub>24</sub> H <sub>40</sub> O <sub>3</sub>	375.2905	19.93	1
6-oxoLCA	6-oxolithocholic acid <sup>4</sup>	3α-hydroxy-6-oxo-5β-cholan-24-oic acid	C <sub>24</sub> H <sub>38</sub> O <sub>4</sub>	389.2697	12.58	28
6-oxo- alloLCA	6-oxo-allolithocholic acid <sup>1</sup>	3α-hydroxy-6-oxo-5α-cholan-24-oic acid	C <sub>24</sub> H <sub>38</sub> O <sub>4</sub>	389.2697	13.86	8
7-oxoLCA	7-oxolithocholic acid <sup>1</sup>	3α-hydroxy-7-oxo-5β-cholan-24-oic acid	C <sub>24</sub> H <sub>38</sub> O <sub>4</sub>	389.2697	14.39	5
12-oxoLCA	12-oxo-lithocholic acid <sup>1</sup>	3α-hydroxy-12-oxo-5β-cholan-24-oic acid	C <sub>24</sub> H <sub>38</sub> O <sub>4</sub>	389.2697	14.90	16
3-oxo- CDCA	3-oxo-chenodeoxycholic acid <sup>4</sup>	7α-dihydroxy-3-oxo-5β-cholan-24-oic acid	C <sub>24</sub> H <sub>38</sub> O <sub>4</sub>	389.2697	16.67	5
MDCA	murideoxycholic acid <sup>1</sup>	3α,6β-dihydroxy-5β-cholan-24-oic acid	C <sub>24</sub> H <sub>40</sub> O <sub>4</sub>	391.2854	9.69	15
UDCA	ursodeoxycholic acid <sup>2</sup>	3α,7β-dihydroxy-5β-cholan-24-oic acid	C <sub>24</sub> H <sub>40</sub> O <sub>4</sub>	391.2854	12.12	4
HDCA	hyodeoxycholic acid <sup>3</sup>	3α,6α-dihydroxy-5β-cholan-24-oic acid	C <sub>24</sub> H <sub>40</sub> O <sub>4</sub>	391.2854	12.78	17
CDCA	chenodeoxycholic acid <sup>1</sup>	3α,7α-dihydroxy-5β-cholan-24-oic acid	C <sub>24</sub> H <sub>40</sub> O <sub>4</sub>	391.2854	16.70	13
DCA	deoxycholic acid <sup>1</sup>	3α,12α-dihydroxy-5β-cholan-24-oic acid	C <sub>24</sub> H <sub>40</sub> O <sub>4</sub>	391.2854	16.92	3
7-oxo- oDCA	7-oxodeoxycholic acid <sup>1</sup>	3α,12α-dihydroxy-7-oxo-5β-cholan-24-oic acid	C <sub>24</sub> H <sub>38</sub> O <sub>5</sub>	405.2647	7.63	4
3-oxo- oCA	3-dehydrocholic acid <sup>1</sup>	7α,12α-dihydroxy-3-oxo-5β-cholan-24-oic acid	C <sub>24</sub> H <sub>38</sub> O <sub>5</sub>	405.2647	10.75	2
ωMCA	ω-muricholic acid <sup>1</sup>	3α,6α,7β-trihydroxy-5β-cholan-24-oic acid	C <sub>24</sub> H <sub>40</sub> O <sub>5</sub>	407.2803	6.46	15
αMCA	α-muricholic acid <sup>1</sup>	3α,6β,7α-trihydroxy-5β-cholan-24-oic acid	C <sub>24</sub> H <sub>40</sub> O <sub>5</sub>	407.2803	7.05	19
βMCA	β-muricholic acid <sup>1</sup>	3α,6β,7β-trihydroxy-5β-cholan-24-oic acid	C <sub>24</sub> H <sub>40</sub> O <sub>5</sub>	407.2803	7.49	12
HCA	hyocholic acid <sup>1</sup>	3α,6α,7α-trihydroxy-5β-cholan-24-oic acid	C <sub>24</sub> H <sub>40</sub> O <sub>5</sub>	407.2803	10.17	22
CA	cholic acid <sup>3</sup>	3α,7α,12α-trihydroxy-5β-cholan-24-oic acid	C <sub>24</sub> H <sub>40</sub> O <sub>5</sub>	407.2803	12.18	4
CDCA3S	chenodeoxycholic acid 3-sulfate <sup>5</sup>	7α-hydroxy-3α-sulfooxy,5β-cholan-24-oic acid	C <sub>24</sub> H <sub>40</sub> O <sub>7</sub> S	471.2422	10.93	20
TLCA	taurolithocholic acid <sup>1</sup>	(tauro)-3α-hydroxy-5β-cholan-24-oic acid	C <sub>26</sub> H <sub>45</sub> NO <sub>5</sub> S	482.2946	17.52	2
CA7S	cholic acid 7-sulfate <sup>6</sup>	3α,12α-dihydroxy-7α-sulfooxy-5β-cholan-24-oic acid	C <sub>24</sub> H <sub>40</sub> O <sub>8</sub> S	487.2371	5.07	32
TMDCA	taumurideoxycholic acid <sup>4</sup>	(tauro)-3α,6β-dihydroxy-5β-cholan-24-oic acid	C <sub>26</sub> H <sub>45</sub> NO <sub>6</sub> S	498.2895	7.66	11
TUDCA	tauroursodeoxycholic acid <sup>1</sup>	(tauro)-3α,7β-dihydroxy-5β-cholan-24-oic acid	C <sub>26</sub> H <sub>45</sub> NO <sub>6</sub> S	498.2895	10.72	11
THDCA	taurohyodeoxycholic acid <sup>1</sup>	(tauro)-3α,6α-dihydroxy-5β-cholan-24-oic acid	C <sub>26</sub> H <sub>45</sub> NO <sub>6</sub> S	498.2895	11.35	4
TDCA	taurodeoxycholic acid <sup>2</sup>	(tauro)-3α,12α-dihydroxy-5β-cholan-24-oic acid	C <sub>26</sub> H <sub>45</sub> NO <sub>6</sub> S	498.2895	16.12	2
TCDCa	taurochenodeoxycholic acid <sup>2</sup>	(tauro)-3α,7α-dihydroxy-5β-cholan-24-oic acid	C <sub>26</sub> H <sub>45</sub> NO <sub>6</sub> S	498.2895	15.91	2
TωMCA	tauro-ω-muricholic acid <sup>1</sup>	(tauro)-3α,6α,7β-trihydroxy-5β-cholan-24-oic acid	C <sub>26</sub> H <sub>45</sub> NO <sub>7</sub> S	514.2844	5.18	1423
TαMCA	tauro-α-muricholic acid <sup>1</sup>	(tauro)-3α,6β,7α-trihydroxy-5β-cholan-24-oic acid	C <sub>26</sub> H <sub>45</sub> NO <sub>7</sub> S	514.2844	5.84	176
TβMCA	tauro-β-muricholic acid <sup>1</sup>	(tauro)-3α,6β,7β-trihydroxy-5β-cholan-24-oic acid	C <sub>26</sub> H <sub>45</sub> NO <sub>7</sub> S	514.2844	6.12	214
THCA	taurohyocholic acid <sup>1</sup>	(tauro)-3α,6α,7α-trihydroxy-5β-cholan-24-oic acid	C <sub>26</sub> H <sub>45</sub> NO <sub>7</sub> S	514.2844	8.80	192
TCA	taurocholic acid <sup>2</sup>	(tauro)-3α,7α,12α-trihydroxy-5β-cholan-24-oic acid	C <sub>26</sub> H <sub>45</sub> NO <sub>7</sub> S	514.2844	11.74	121
TLCA3S	taurolithocholic acid 3-sulfate <sup>2</sup>	(tauro)-3α-sulfooxy-5β-cholan-24-oic acid	C <sub>26</sub> H <sub>45</sub> NO <sub>8</sub> S <sub>2</sub>	562.2514	11.98	35
TCA3S	taurocholic acid 3-sulfate <sup>6</sup>	(tauro)-7α,12α-dihydroxy-3α-sulfooxy-5β-cholan-24-oic acid	C <sub>26</sub> H <sub>45</sub> NO <sub>10</sub> S <sub>2</sub>	594.2412	3.52	85
DCA-D4	deuterated deoxycholic acid <sup>1</sup>	deoxycholic acid -2,2,4,4-d4 acid	C <sub>24</sub> D <sub>4</sub> H <sub>36</sub> O <sub>4</sub>	395.3105	16.87	
CDCA-D4	deuterated chenodeoxycholic acid <sup>1</sup>	chenodeoxycholic-2,2,4,4-d4 acid	C <sub>24</sub> D <sub>4</sub> H <sub>36</sub> O <sub>4</sub>	395.3105	16.69	

Suppliers: <sup>1</sup> Steraloids (Newport, RI, US), <sup>2</sup> Sigma-Aldrich (Switzerland), <sup>3</sup> VWR (Switzerland), <sup>4</sup> L. Hagey (UCSD, CA, USA), <sup>5</sup> Alsachim (France), <sup>6</sup> Cayman Chemicals (Ann Harbor, MI, USA).

Bile acid highlighted in red correspond to the recovery standards used in the study.

**Table S3 | Reference protein sequences for each bile acid metabolizing enzyme.**

Reference sequences for each type of bile acid metabolizing enzymes (BSH, 3 $\alpha$ -HSDH, 3 $\beta$ -HSDH, 7 $\alpha$ -HSDH, 7 $\beta$ -HSDH and 12 $\alpha$ -HSDH) that were selected on the NCBI database.

Enzyme	Reference sequence annotation	Accession n°
BSH	choloylglycine hydrolase family protein [Enterococcus faecalis]	<a href="#">WP_016632767.1</a>
3 $\alpha$ -HSDH	3-alpha hydroxysteroid dehydrogenase [[Clostridium] scindens]	<a href="#">AAC45414.1</a>
3 $\beta$ -HSDH	3-beta hydroxysteroid dehydrogenase [Clostridium botulinum]	<a href="#">AUM86449.1</a>
7 $\alpha$ -HSDH	7-alpha-hydroxysteroid dehydrogenase [[Clostridium] sordellii]	<a href="#">AAA53556.1</a>
7 $\beta$ -HSDH	7-beta-hydroxysteroid dehydrogenase [[Ruminococcus] gnavus]	<a href="#">AGN52919.1</a>
12 $\alpha$ -HSDH	oxidoreductase, short chain dehydrogenase/reductase family protein [[Clostridium] scindens ATCC 35704]	<a href="#">EDS06338.1</a>



**Table S4 | Bile acid metabolizing enzymes in the OligoMM12 community and *Clostridium scindens* ATCC 35704.**

Enzyme	Organism / Strain	Annotation
BaiG	C. scindens ATCC 35704	>Multidrug resistance protein 3 [Clostridium] scindens ATCC 35704 QBF74039.1
BaiB	C. scindens ATCC 35704	>Bile acid-coenzyme A ligase [Clostridium] scindens ATCC 35704 QBF74034.1
BaiA1	C. scindens ATCC 35704	>Bile acid 7-dehydroxylase 1/3 [Clostridium] scindens ATCC 35704 QBF75061.1
BaiA2	C. scindens ATCC 35704	>Bile acid 7-dehydroxylase 2 [Clostridium] scindens ATCC 35704 QBF74037.1
BaiCD	C. scindens ATCC 35704	>NADH oxidase [Clostridium] scindens ATCC 35704 QBF74035.1
BaiH	C. scindens ATCC 35704	>NADH oxidase [Clostridium] scindens ATCC 35704 QBF74040.1
BaiE	C. scindens ATCC 35704	>Bile acid 7-alpha dehydratase [Clostridium] scindens ATCC 35704 QBF74036.1
BaiI	C. scindens ATCC 35704	>hypothetical protein [Clostridium] scindens ATCC 35704 QBF74041.1
BaiN	C. scindens ATCC 35704	>hypothetical protein [Clostridium] scindens ATCC 35704 QBF75607.1
BaiF	C. scindens ATCC 35704	>Bile acid-CoA transferase [Clostridium] scindens ATCC 35704 QBF74038.1
BSH	Bifidobacterium_animalis_subsp._animalis_YL2	>linear amide C-N hydrolase Bifidobacterium animalis subsp. animalis PHQ54582.1
BSH	[Clostridium] clostridioforme strain YL32	>penicillin amidase [Clostridium] clostridioforme OXE67266.1
BSH	Acutalibacter muris strain KB18	>linear amide C-N hydrolase Acutalibacter muris ASB39560.1
BSH	Lactobacillus_reuteri_I49	>chologylglycine hydrolase Lactobacillus reuteri OXE59352.1
BSH	Enterococcus faecalis KB1	>chologylglycine hydrolase Enterococcus faecalis ASU26830.1
BSH	Bacteroides caecimuris_I48	>chologylglycine hydrolase Bacteroides caecimuris OXE65892.1
BSH	Muribaculum_intestinale_YL27	>hypothetical protein Muribaculum intestinale ASB37608.1
3α-HSDH	Bacteroides caecimuris_I48	>beta-ketoacyl-ACP reductase Bacteroides caecimuris OXE63766.1
3α-HSDH	Acutalibacter muris strain KB18	>3-oxoacyl-[acyl-carrier-protein] reductase Acutalibacter muris ASB42640.1
3α-HSDH	Clostridium innocuum I46	>beta-ketoacyl-ACP reductase [Clostridium] innocuum ASU20943.1
3α-HSDH	Blautia coccoides YL58	>3-oxoacyl-[acyl-carrier-protein] reductase Blautia coccoides ASU27717.1
3α-HSDH	Akkermansia_muciniphila_YL44	>beta-ketoacyl-ACP reductase Akkermansia muciniphila ASB35689.1
3α-HSDH	Muribaculum_intestinale_YL27	>3-oxoacyl-[acyl-carrier-protein] reductase Muribaculum intestinale ASB38106.1
3α-HSDH	[Clostridium] clostridioforme strain YL32	>3-oxoacyl-[acyl-carrier-protein] reductase [Clostridium] clostridioforme OXE62956.1
3α-HSDH	Flavonifractor_plautii_YL31	>beta-ketoacyl-ACP reductase Flavonifractor plautii OXE49040.1
3β-HSDH	Lactobacillus_reuteri_I49	>NADH-flavin reductase Lactobacillus reuteri OXE60106.1
3β-HSDH	Lactobacillus_reuteri_I49	>NADH-flavin reductase Lactobacillus reuteri OXE59907.1
3β-HSDH	Enterococcus faecalis KB1	>NAD(P)-dependent oxidoreductase Enterococcus faecalis ASU26092.1
3β-HSDH	Turicimonas muris YL45	>3-beta hydroxysteroid dehydrogenase Turicimonas muris OXE47272.1
7α-HSDH	Bacteroides caecimuris_I48	>NAD(P)-dependent oxidoreductase Bacteroides caecimuris OXE65616.1
7α-HSDH	Bacteroides caecimuris_I48	>beta-ketoacyl-ACP reductase Bacteroides caecimuris OXE63766.1
7α-HSDH	Muribaculum_intestinale_YL27	>3-oxoacyl-[acyl-carrier-protein] reductase Muribaculum intestinale ASB38106.1
7α-HSDH	Acutalibacter muris strain KB18	>3-oxoacyl-[acyl-carrier-protein] reductase Acutalibacter muris ASB42640.1
7α-HSDH	Flavonifractor_plautii_YL31	>NAD(P)-dependent oxidoreductase Flavonifractor plautii OXE46436.1
7α-HSDH	[Clostridium] clostridioforme strain YL32	>3-oxoacyl-ACP reductase [Clostridium] clostridioforme OXE67815.1
7α-HSDH	Clostridium innocuum I46	>beta-ketoacyl-ACP reductase [Clostridium] innocuum ASU20943.1
7α-HSDH	Akkermansia_muciniphila_YL44	>beta-ketoacyl-ACP reductase Akkermansia muciniphila ASB35689.1
7α-HSDH	C. scindens ATCC 35704	>NADP-dependent 7-alpha-hydroxysteroid dehydrogenase [Clostridium] scindens ATCC 35704 QBF73869.1
7β-HSDH	Bifidobacterium_animalis_subsp._animalis_YL2	>short-chain dehydrogenase Bifidobacterium animalis subsp. animalis PHQ54437.1
7β-HSDH	[Clostridium] clostridioforme strain YL32	>SDR family oxidoreductase [Clostridium] clostridioforme OXE69155.1
7β-HSDH	[Clostridium] clostridioforme strain YL32	>NAD(P)-dependent oxidoreductase [Clostridium] clostridioforme OXE67288.1
7β-HSDH	Clostridium innocuum I46	>ketoacyl reductase [Clostridium] innocuum ASU19348.1
7β-HSDH	Lactobacillus_reuteri_I49	>NAD(P)-dependent oxidoreductase Lactobacillus reuteri OXE59909.1
12α-HSDH	Bacteroides caecimuris_I48	>beta-ketoacyl-ACP reductase Bacteroides caecimuris OXE63766.1
12α-HSDH	Muribaculum_intestinale_YL27	>3-oxoacyl-[acyl-carrier-protein] reductase Muribaculum intestinale ASB38106.1
12α-HSDH	Flavonifractor_plautii_YL31	>beta-ketoacyl-ACP reductase Flavonifractor plautii OXE49040.1
12α-HSDH	Flavonifractor_plautii_YL31	>NAD(P)-dependent oxidoreductase Flavonifractor plautii OXE46310.1
12α-HSDH	Akkermansia_muciniphila_YL44	>beta-ketoacyl-ACP reductase Akkermansia muciniphila ASB35689.1
12α-HSDH	C. scindens ATCC 35704	>3-oxoacyl-[acyl-carrier-protein] reductase FabG [Clostridium] scindens ATCC 35704 QBF73369.1

**Table S5 | Abundance of the bile acid-metabolizing enzymes detected in the metaproteome of the two gnotobiotic mice.** Proteins detected in the metaproteomes for the different intestinal compartment (small intestine, cecum and colon) in sDMDMm2 and *C. scindens*-colonized sDMDMm2 mice. The values correspond to the log2-transformed MS normalized protein intensities.

Enzymes	Organisms	Identifier	Small intestine					
			sDMDMm2 + <i>C. scindens</i>			sDMDMm2		
			Mouse 1	Mouse 2	Mouse 3	Mouse 1	Mouse 2	Mouse 3
BSH	Bacteroides caecimuris I48	<a href="#">OXE65892.1</a>						
BSH	Muribaculum intestinale YL27	<a href="#">ASB37608.1</a>				21.39	24.17	20.55
BaiCD	Clostridium scindens ATCC 35704	<a href="#">QBF74035.1</a>						
7β-HSDH	Bifidobacterium animalis subsp animalis YL2	<a href="#">PHQ54437.1</a>						
7β-HSDH	Clostridium clostridioforme YL32	<a href="#">OXE69155.1</a>						
7β-HSDH	Clostridium innocuum I46	<a href="#">ASU19348.1</a>				19.22	19.07	19.36
7α-HSDH	Bacteroides caecimuris I48	<a href="#">OXE65616.1</a>						
7α-HSDH	Clostridium scindens ATCC 35704	<a href="#">QBF73869.1</a>						
7α-HSDH	Muribaculum intestinale YL27	<a href="#">ASB38106.1</a>						
3α-HSDH	Acutalibacter muris KB18	<a href="#">ASB42640.1</a>						
3α-HSDH	Akkermansia muciniphila YL44	<a href="#">ASB35689.1</a>						
3α-HSDH	Bacteroides caecimuris I48	<a href="#">OXE63766.1</a>	21.62	17.44				

Enzymes	Organisms	Identifier	Cecum					
			sDMDMm2 + <i>C. scindens</i>			sDMDMm2		
			Mouse 1	Mouse 2	Mouse 3	Mouse 1	Mouse 2	Mouse 3
BSH	Bacteroides caecimuris I48	<a href="#">OXE65892.1</a>						
BSH	Muribaculum intestinale YL27	<a href="#">ASB37608.1</a>	19.66	18.00	18.44	20.28	17.92	20.93
BaiCD	Clostridium scindens ATCC 35704	<a href="#">QBF74035.1</a>						
7β-HSDH	Bifidobacterium animalis subsp animalis YL2	<a href="#">PHQ54437.1</a>						
7β-HSDH	Clostridium clostridioforme YL32	<a href="#">OXE69155.1</a>	20.46	21.65	21.44	20.08	20.53	19.20
7β-HSDH	Clostridium innocuum I46	<a href="#">ASU19348.1</a>						
7α-HSDH	Bacteroides caecimuris I48	<a href="#">OXE65616.1</a>						
7α-HSDH	Clostridium scindens ATCC 35704	<a href="#">QBF73869.1</a>						
7α-HSDH	Muribaculum intestinale YL27	<a href="#">ASB38106.1</a>				20.08	21.14	19.20
3α-HSDH	Acutalibacter muris KB18	<a href="#">ASB42640.1</a>				20.86	20.26	21.19
3α-HSDH	Akkermansia muciniphila YL44	<a href="#">ASB35689.1</a>						
3α-HSDH	Bacteroides caecimuris I48	<a href="#">OXE63766.1</a>	26.91	27.64	29.31	27.41	28.21	28.04

Enzymes	Organisms	Identifier	Colon					
			sDMDMm2 + <i>C. scindens</i>			sDMDMm2		
			Mouse 1	Mouse 2	Mouse 3	Mouse 1	Mouse 2	Mouse 3
BSH	Bacteroides caecimuris I48	<a href="#">OXE65892.1</a>	21.98	20.92	20.48	20.05	20.50	16.95
BSH	Muribaculum intestinale YL27	<a href="#">ASB37608.1</a>	24.23	24.04	23.69	22.68	22.48	22.60
BaiCD	Clostridium scindens ATCC 35704	<a href="#">QBF74035.1</a>	18.06	20.02	19.65			
7β-HSDH	Bifidobacterium animalis subsp animalis YL2	<a href="#">PHQ54437.1</a>	17.21	19.21	19.03			
7β-HSDH	Clostridium clostridioforme YL32	<a href="#">OXE69155.1</a>						
7β-HSDH	Clostridium innocuum I46	<a href="#">ASU19348.1</a>						
7α-HSDH	Bacteroides caecimuris I48	<a href="#">OXE65616.1</a>	20.59	20.65	23.56	18.98	19.83	18.13
7α-HSDH	Clostridium scindens ATCC 35704	<a href="#">QBF73869.1</a>	20.85	25.25	23.25			
7α-HSDH	Muribaculum intestinale YL27	<a href="#">ASB38106.1</a>	20.19	20.35	19.37	22.08	22.55	20.98
3α-HSDH	Acutalibacter muris KB18	<a href="#">ASB42640.1</a>						
3α-HSDH	Akkermansia muciniphila YL44	<a href="#">ASB35689.1</a>				21.80	20.89	22.45
3α-HSDH	Bacteroides caecimuris I48	<a href="#">OXE63766.1</a>	27.80	26.25	24.21	23.46	22.42	25.49

**Table S6 | Antibiotic susceptibility of three major bile acid 7 $\alpha$ -dehydroxylating strains.** Antibiotic susceptibility testing was performed for three major bile acid 7 $\alpha$ -dehydroxylating strains (*Clostridium scindens* ATCC 35704, *Clostridium hylemonae* DSM 15053, and *Clostridium hiranonis* DSM 13275). For each antimicrobial agent, the minimal inhibitory concentration (MIC) was determined with Etest® (bioMérieux, France). The MIC results were interpreted according to the breakpoints described by the European Committee on Antimicrobial Susceptibility Testing (EUCAST) for Gram- positive anaerobes<sup>206</sup>. If the MIC value is  $\leq$  to the EUCAST breakpoint the strain is considered sensitive to the antimicrobial (green cell). If the MIC value is  $>$  to the EUCAST breakpoint, the strain is considered resistant to the antimicrobial (red cell). For some antimicrobial, EUCAST breakpoints are not available (white cell).

Class	Antimicrobial agent	<i>C. scindens</i> ATCC 35704	<i>C. hylemonae</i> DSM 15053	<i>C. hiranonis</i> DSM 13275
		MIC (mg/L)	MIC (mg/L)	MIC (mg/L)
Penicillins	Amoxicillin	0.06	0.094	<0.016
	Amoxicillin + clavulanic acid	0.12	0.094	0.016
	Ampicillin	0.12	0.125	<0.016
	Ampicillin + sulbactam	0.094	0.094	<0.016
	Piperacillin + tazobactam	0.25	0.75	0.19
	Ticarcillin + clavulanic acid	0.38	0.5	0.5
Carbapenems	Imipenem	0.5	0.38	0.25
Fluoroquinolones	Ciprofloxacin	>32	>32	0.25
	Levofloxacin	>32	>32	0.125
	Moxifloxacin	>32	4	0.002
Cephalosporins	Cefuroxime	<0.016	1.5	0.38
	Ceftriaxone	1	0.5	0.38
	Cefixime	0.75	1.5	0.125
Macrolides	Erythromycin	>256	8	32
Aminoglycosides	Amikacin	>256	>256	16
	Streptomycin	>1024	48	0.25
Tetracyclines	Doxycyclin	3	0.094	0.75
Lincosamides	Clindamycin	1	3	>256
Glycopeptides	Vancomycin	0.5	1	0.25
Nitroimidazole	Metronidazole	0.06	0.38	0.25

**Table S7 | Primers sequence used for RT-qPCR analysis.**

Gene	F/R	Primer sequence (5'-3')
<i>Rpl32</i>	Forward	ATC AGG CAC CAG TCA GAC CGA T
	Reverse	GTT GCT CCC ATA ACC GAT GTT GG
<i>Fgf15</i>	Forward	GAG GAC CAA AAC GAA CGA AAT T
	Reverse	ACG TCC TTG ATG GCA ATC G
<i>Cyp7a1</i>	Forward	AGC AAC TAA ACA ACC TGC CAG TAC TA
	Reverse	GTC CGG ATA TTC AAG GAT GCA
<i>Sult2a8</i>	Forward	ATG ACA GAT GAA TTT CTG TGG
	Reverse	ACT ATG ATC GTG TCT TCA TCC

# Solenne Marion

## Curriculum Vitae

Avenue du Tir-Fédéral 16  
1024 Ecublens, Switzerland  
☎ (+41) 76 690 71 57  
✉ solenne.marion1@gmail.com  
🌐 solenne.marion



### Personal Information

Nationality French  
Date of Birth October 28th, 1991.  
Marital status Single, without children.  
Driving Licence Category B.  
Swiss Permit B.

### Education

- 2015-2020 **Ph.D. in Microbiology**, *Ecole Polytechnique Federale de Lausanne*, Switzerland.  
Thesis: "Biogeography and biochemistry of bile acid 7-dehydroxylation in the mammalian gut"  
Advisor: Prof. R. Bernier-Latmani
- 2014 - 2015 **M.Sc. in Infectiology with major in Microbiology**, *Université Paris Descartes*, France.  
Thesis: "Deciphering the role of the tick gut microbiota on Lyme Disease"  
Advisor: Prof. E. Fikrig (Yale University, USA)
- 2009-2015 **Pharm.D.**, *Faculty of Pharmacy, Université Claude Bernard Lyon 1*, France.  
Thesis: "Study of the diversity of *Staphylococcus aureus* strains in Cystic Fibrosis Patients"  
Advisor: Dr. A. Doleans-Jordheim

### Awards

- 2015 **Outstanding Student Research Award of the Promotion 2009-2015**, Faculty of Pharmacy, Université Claude Bernard Lyon 1, France.

### Experience

- 2015 **Master Internship (6 months)**, *Department of Internal Medicine, Yale University*, New Haven, USA.  
Investigation of the influence of the tick gut microbiota on transmission of *Borrelia burgdorferi* to mice.  
Advisors: **Prof. E. Fikrig and Dr. S. Narashiman**
- 2013-2014 **Internship (6 months)**, *Laboratoire de Bactériologie du Groupement Hospitalier Est*, Lyon, France.  
- Evaluation of two rapid diagnostic tests performance (bioMérieux and NG Biotech) for the detection of urinary antigens of *Legionella pneumophila* in collaboration with Legionella National Reference Center.  
- Evaluation of two diagnostic tests performance (Meridian and Alere) for the detection of *Clostridium difficile* toxins.  
- Participation to PIRLA clinical study on Osteoarticular Infections.
- 2013 **Internship (4 months)**, *UMR 5557 Écologie Microbienne, Université Claude Bernard Lyon 1*, Lyon, France.  
Characterization of *Staphylococcus aureus* strains isolated from Cystic Fibrosis patients: antibiotic resistance (mecA/mecC genes), Agr typing (agrI, agrII, agrIII, agrIV genes) and virulence (pvl gene).  
Advisor: **Dr. A. Doléans-Jordheim**
- 2011 – 2013 **Pharmacy Student employee**, *Pharmacie des Gratte-ciels, Pharmacie du Vieux-Lyon*, Lyon, France.
- 2012 **Internship (1 month)**, *Laboratoire de Bactériologie, Virologie et Microbiologie Industrielle, Université Paul Sabatier Toulouse III*, Toulouse, France.  
Research project on *Pseudomonas aeruginosa* biofilms grown under anaerobic conditions.  
Advisors: **Prof. C. Roques and A. Furiga**

---

## Publications

- 2018 Marion S., Studer N., Desharnais L., Menin L., Escrig, S., Meibom A., Hapfelmeier S., Bernier-Latmani R. (2018) In vitro and in vivo characterization of *Clostridium scindens* bile acid transformations. Gut Microbes, DOI:10.1080/19490976.2018.1549420.
- 2019 Marion S., Desharnais L., Studer N., Notter D. M., Poudel S., Menin L., Janowczyk A., Hettich R., Hapfelmeier S., Bernier-Latmani R. Biogeography of microbial bile acid transformations along the murine gut. *Submitted to Journal of Lipid Research*.
- 2020 Marion S., Reeves M., Meibom K., Lau K., Pojer F., Menin L, Bernier-Latmani R. The bile acid 7-dehydroxylation pathway revamped. *In preparation*.

## Oral presentations

- 2019 Marion S., Studer N., Desharnais L., Menin L., Escrig, S., Meibom A., Hapfelmeier S., Bernier-Latmani R., Microbial Bile Acid Transformations in vitro and in vivo . Keystone Symposia "Microbiome: Chemical Mechanisms and Biological Consequences", March 10-14, Montreal, QC, Canada.

---

## Skills

- Expertise Pharmacology, ADME, Clinical studies, Microbiology, GLP, Animal experiment, Analytical chemistry (LC-MS/MS, NanoSIMS, Metaproteomics), Molecular biology (Cloning, Protein expression and purification).
- Soft skills Communication, Teamwork, Adaptability, Creativity, Problem-solving.

---

## Languages

- French** Native Speaker
- English** Professional Proficiency
- Italian** Intermediate
- German** Beginner

---

## Interests

- Mountaineering
- Cycling
- Gardening
- DIY activities